Nuclear Science
NEA/NSC/R(2019)1
February 2019
www.oecd-nea.org

A Code-to-Code Benchmark for High-Temperature Gas-Cooled Reactor Fuel Element Depletion

OECD
BETTER POLICIES FOR BETTER LIVES

NEA
NUCLEAR ENERGY AGENCY

Nuclear Energy Agency

NEA/NSC/R(2019)1

Unclassified

English text only

14 February 2019

NUCLEAR ENERGY AGENCY
NUCLEAR SCIENCE COMMITTEE

A Code-to-Code Benchmark for High-Temperature Gas-Cooled Reactor Fuel Element Depletion

This document exists only in PDF.

JT03443140

ORGANISATION FOR ECONOMIC CO-OPERATION AND DEVELOPMENT

The OECD is a unique forum where the governments of 36 democracies work together to address the economic, social and environmental challenges of globalisation. The OECD is also at the forefront of efforts to understand and to help governments respond to new developments and concerns, such as corporate governance, the information economy and the challenges of an ageing population. The Organisation provides a setting where governments can compare policy experiences, seek answers to common problems, identify good practice and work to co-ordinate domestic and international policies.

The OECD member countries are: Australia, Austria, Belgium, Canada, Chile, the Czech Republic, Denmark, Estonia, Finland, France, Germany, Greece, Hungary, Iceland, Ireland, Israel, Italy, Japan, Korea, Latvia, Lithuania, Luxembourg, Mexico, Netherlands, New Zealand, Norway, Poland, Portugal, Slovak Republic, Slovenia, Spain, Sweden, Switzerland, Turkey, the United Kingdom and the United States. The European Commission takes part in the work of the OECD.

OECD Publishing disseminates widely the results of the Organisation's statistics gathering and research on economic, social and environmental issues, as well as the conventions, guidelines and standards agreed by its members.

NUCLEAR ENERGY AGENCY

The OECD Nuclear Energy Agency (NEA) was established on 1 February 1958. Current NEA membership consists of 33 countries: Argentina, Australia, Austria, Belgium, Canada, the Czech Republic, Denmark, Finland, France, Germany, Greece, Hungary, Iceland, Ireland, Italy, Japan, Korea, Luxembourg, Mexico, the Netherlands, Norway, Poland, Portugal, Romania, Russia, the Slovak Republic, Slovenia, Spain, Sweden, Switzerland, Turkey, the United Kingdom and the United States. The European Commission also takes part in the work of the Agency.

The mission of the NEA is:

– to assist its member countries in maintaining and further developing, through international co-operation, the scientific, technological and legal bases required for a safe, environmentally sound and economical use of nuclear energy for peaceful purposes;

– to provide authoritative assessments and to forge common understandings on key issues as input to government decisions on nuclear energy policy and to broader OECD analyses in areas such as energy and the sustainable development of low-carbon economies.

Specific areas of competence of the NEA include the safety and regulation of nuclear activities, radioactive waste management and decommissioning, radiological protection, nuclear science, economic and technical analyses of the nuclear fuel cycle, nuclear law and liability, and public information. The NEA Data Bank provides nuclear data and computer program services for participating countries.

Corrigenda to OECD publications may be found online at: *www.oecd.org/publishing/corrigenda*.

Foreword

The Nuclear Energy Agency (NEA) Working Party on Scientific Issues of Reactor Systems (WPRS) was established in 2004 and reports to the NEA Nuclear Science Committee (NSC). Its focus is the study of reactor physics, fuel performance and radiation transport and shielding in present and future nuclear power systems. The Working Party also studies the uncertainties associated with modelling of these phenomena, particularly the modelling of reactor transient events. Within the WPRS, the Expert Group on Reactor Physics and Advanced Nuclear Systems (EGRPANS) was formed to provide expert advice to the WPRS and the nuclear community on the development needs (data and methods, validation experiments, scenario studies) for different reactor systems. Reactor types considered by EGRPANS include, but are not limited to, present generation light water reactors (LWRs) and heavy water reactors (HWRs) with advanced and innovative fuels, evolutionary and innovative.

LWRs and HWRs, high-temperature reactors (HTRs), fast spectrum systems and advanced reactor systems, and accelerator-driven (subcritical) and critical systems for waste transmutation. The present report has been prepared to summarise the results of a benchmark that was developed as the first, simplest phase in a planned series of increasingly complex set of code-to-code benchmarks. The intent of this benchmark was to encourage contribution of a wide range of computational results for depletion calculations in a set of basic fuel cell models. This report summarised the results provided in 21 sets of results that were submitted by 12 participants internationally. The benchmark specification and the results provided here provide the necessary data for comparative studies by future researchers.

Acknowledgements

This benchmark is a result of several years of effort in preparation and distribution of the problem specifications, participant analyses and collection and evaluation of the results. The benchmark organisers express their sincere gratitude to the participants who devoted their time and effort to this benchmark. Special thanks go to Mark D. DeHart (Idaho National Laboratory) and Anthony P. Ulses (International Atomic Energy Agency). This work has been performed under the auspices of NEA Working Party on Scientific Issues of Reactor Systems (WPRS) and was sponsored by Oak Ridge National Laboratory, Idaho National Laboratory and the NEA.

Table of contents

List of figures

List of tables

List of abbreviations and acronyms

AVR	Arbeitsgemeinschaft Versuchsreaktor (Germany)
BOL	Beginning of life
CE	Continuous energy
DH	Doubly heterogeneous
EOL	End of life
EGRPANS	Expert Group on Reactor Physics and Advanced Nuclear Systems (NEA)
ENDF	Evaluated Nuclear Data File
HWR	Heavy water reactor
HTR	High-temperature reactor
HTTR	High-temperature test reactor
HTGR	High-temperature gas reactor
IAEA	International Atomic Energy Agency
INL	Idaho National Laboratory (United States)
LWR	Light water reactor
MHTGR	Modular high-temperature gas-cooled reactor
MG	Multi-group
NEA	Nuclear Energy Agency
NSC	Nuclear Science Committee (NEA)
NGNP	Next generation nuclear plant
ORNL	Oak Ridge National Laboratory (United States)
PBR	Pebble bed reactor
PBMR	Pebble bed modular reactor
RPT	Reactivity-equivalent physical transformation

TRISO	Tristructural-isotropic
VHTR	Very-high-temperature reactor
WPRS	Working Party on Scientific Issues of Reactor Systems (NEA)

I. Introduction

The high-temperature gas reactor (HTGR) is a Generation IV reactor concept that uses a graphite-moderated gas-cooled nuclear reactor with a once-through uranium fuel cycle. This design permits a very high outlet temperature in the order of 1 000°C. The first HTGR design was proposed at the Clinton Laboratories (now Oak Ridge National Laboratory) in 1947. Germany also played a significant role in HTGR development over the next decade. The Peach Bottom reactor in the United States (US) was the first HTGR to produce electricity, with operation from 1966 through 1974 as a 150 MW(th) demonstration plant. The Fort St. Vrain plant was the first commercial power design, operating from 1979 to 1989 with a power rating of 842 MW(th). Even though the reactor was beset by operational issues that led to its decommissioning due to economic factors, it served as proof of the HTGR concept in the United States. HTGRs have also existed in the United Kingdom (the Dragon reactor) and Germany (AVR and THTR-300), and currently exist in Japan (the HTTR using prismatic fuel with 30 MWth of capacity) and the People's Republic of China (the HTR-10, a pebble bed design with 10 MWe of generation). Two full-scale pebble bed HTGRs, each with 100-195 MWe of electrical production capacity are under construction in China, and are promoted in several countries by reactor designers. The US Department of Energy (DOE) Next Generation Nuclear Plant (NGNP) represents a significant and growing activity in the United States.

HTGR designs utilise graphite-moderated fuel forms and helium gas as a coolant. There are two main forms of HTGR fuels: pebbles are used in the pebble bed reactor (PBR), while cylindrical rods (or compacts) are used in the modular high-temperature gas-cooled reactor (MHTGR). In PBRs, fuel elements are ~6-cm-diameter spheres; in MHTGRs, the fuel elements are graphite rods that are inserted into graphite hexagonal blocks. In both systems, fuel elements (spheres and rods) are comprised of tristructural-isotropic (TRISO) fuel particles (early designs used bistructural-isotropic, or BISO, fuel particles). The TRISO particles are either dispersed in the matrix of a graphite pebble for the pebble bed design or moulded into compacts/rods that are then inserted into hexagonal graphite blocks in prismatic cores. In general, fuel grains have a density of a few hundred grains per cm^3.

The HTGR concept is a significant departure from LWR designs, showing promise for improved thermal efficiency due to high outlet temperatures. The nature of chemical interactions in gas-cooled graphite will also allow for significantly higher fuel burn-ups than is available in LWRs. However, because of the significant differences in the physics between HTGR and LWR designs, existing reactor analysis methods and data will be confronted by significant changes in the physics of neutron slowing down, absorption and scattering. Furthermore, the use of localised fuel grains within a larger fuel element results in two levels of heterogeneity that will challenge many existing lattice physics methods. Hence, there is a need for advanced methods for treatment of both levels of heterogeneity effects. In doubly heterogeneous (DH) systems, heterogeneous fuel particles in a moderator matrix form the fuel region of the fuel element (pebble or rod) and thus constitute the first level of heterogeneity. Fuel elements themselves are also heterogeneous with fuel and moderator or reflector regions, forming the second level of heterogeneity. The fuel elements may also form regular or irregular lattices.

Continuous energy (CE) methods are able to explicitly represent the dynamics of neutron slowing down in a heterogeneous environment with randomised grain distributions, but traditional tracking simulations can be extremely slow and the large number of grains in a fuel element may often represent an extreme burden on computational resources. A number of approximations or simplifying assumptions have been developed to simplify the computational process and reduce the effort. Multi-group (MG) methods, on the other hand, require special treatment of DH fuels in order to properly capture resonance effects, and generally cannot explicitly represent a random distribution of grains due to the excessive computational burden resulting from the spatial grain distribution. The effect of such approximations may be important and has potential to misrepresent the spectrum within a fuel grain or element.

Depletion methods utilised in lattice calculations typically rely on point depletion methods, based on the isotopic inventory of fuel depleted, assuming a single localised neutron flux. This flux is generally determined using either a CE or MG transport solver. Hence, in application to DH fuels, the primary factor influencing the accuracy of a depletion calculation will be the accuracy of the local flux calculated within the transport solution and the cross-sections collapsed using these fluxes.

Although thousands of kilograms of spent fuel assemblies are available from the operation of US and German reactors, the detailed information required for modelling the depletion of such fuel (local power density, environment, temperatures, cycle histories, etc.) was not recorded or is no longer available. The current lack of well-qualified experimental measurements for spent HTGR fuel elements limits the validation of advanced DH depletion method. Because of this shortage of data, this benchmark has been developed as the first, simplest phase in a planned series of increasingly complex set of code-to-code benchmarks. The intent of this benchmark is to encourage submission of a wide range of computational results for depletion calculations in a set of basic fuel cell models. Comparison of results using independent methods and data should provide insight into potential limitations in various modelling approximations. The benchmark seeks to provide the simplest possible models, in order to minimise the effect of competing and potentially offsetting phenomena that might mask weaknesses in given methods.

Twenty-one sets of results have been submitted by twelve participants internationally. Various approaches were used for the treatment of microscopic grains dispersed in fuel elements in the second and third parts of the benchmark, including explicit treatment of grains distributed within a regular lattice, a randomised distribution of explicit grains, reactivity-equivalent physical transformation (RPT) and a two-pass homogenisation with disadvantage factors. The broad agreement appears to validate each of the double heterogeneity treatments. The following section provides the benchmark specification itself, for three different fuel types. This is followed by a discussion of results in terms of trends, commonalities and outliers for the three fuel depletion types. Information on the various submissions, participants, compiled results and plots of those results are provided in a number of appendices.

II. Benchmark specification

This benchmark consists of three parts – a calculation of depletion in an infinite lattice of TRISO fuel grains, a depletion calculation for pebbles representative of pebble bed modular reactor (PBMR) fuel, and a similar calculation for an infinite lattice supercell representative of a prismatic MHTGR assembly lattice. The grain and pebble calculations may be performed in one or three dimensions; the prismatic lattice calculation is essentially a two-dimensional, infinite height model suitable for two- and three-dimensional methods. Participants are urged to perform and submit calculations for any or all configurations, based on available code capabilities. Participants are also encouraged to provide multiple submissions using different codes or data, where available.

II.A. Fuel specifications

This benchmark consists of depletion calculations for three different configurations – the first an infinite lattice of grains, the second representative of a generic pebble bed configuration and the third based on the characteristics of an MHTGR prismatic fuel element. For simplicity, all models will be based on a single TRISO fuel element type design, although with different particle densities within the fuel element types (the density of the infinite grain lattice model is based on the density of grains in the pebble design). Configurations 2 and 3 are based on an infinite lattice representation of fuel elements. Note that at 8.2 wt% enrichment, these TRISO fuel particles have a lower enrichment than anticipated for an MHTGR fuel design, which are expected to be at greater than 10% enrichment.

Data for the grain dimensions used in all three configurations are provided in Table 1. Table 2 provides isotopic concentrations for all compositions used in all configurations. Isotopic compositions and particle coating parameters have been selected based on specifications provided for a related benchmark (Hosking et al., 2005). The infinite lattice of grains and the pebble bed fuel design have also been drawn from this reference; a representative design for a prismatic fuel lattice has been developed based on specifications available in (Kim et al., 2007). For the purposes of this benchmark, all materials in all models are assumed to be at a uniform temperature of 293.6 K. Details of the three models are provided below.

1. Infinite lattice grain model

This model is intended to provide a baseline comparison on methods without requiring the complexity of a DH treatment. Effectively, it represents an infinite lattice of coated particles with a density based on that of the pebble bed fuel element described below. For straightforwardness, a cubic lattice is assumed such that a 9.043% packing fraction is attained. The fuel grains are spaced within the graphite matrix defined for both pebble bed and prismatic fuel models. Dimensions of this lattice are provided in Table 3, with grain dimensions and isotopic concentrations as provided in Tables 1 and 2, respectively.

2. Pebble bed model

The pebble bed model consists of a single fuel pebble in an infinite lattice. A cubic lattice is assumed for simplicity. Specifications for the pebble are provided in Table 4. The fuel pebble consists of a 2.5 cm radius fuel volume encased in a 3.0 cm radius (0.5 cm thick) outer coating. The fuel volume contains a random dispersion of coated fuel particles within a graphite matrix. Regions outside the pebble are filled with coolant, helium. Pebbles are assumed to be in direct contact; i.e. the pebble-to-pebble pitch is 6.0 cm. Table 4 provides the pebble-to-pebble pitch for a cubic lattice for use in three-dimensional models; however, the equivalent coolant radius is also provided for use in one-dimensional models.

3. Prismatic fuel model

The prismatic fuel model is somewhat more complicated, requiring a supercell model including both fuel and coolant channels. Figure 1 shows a portion of the repeating lattice pattern. A rectangular, triangular or hexagonal supercell may be used, taking advantage of symmetry with reflective boundary conditions. Fuel compacts are radially centred within each fuel channel; coolant channels and the fuel/channel gap are filled with helium. Because the fuel is assumed to be infinite in height, the model is essentially two-dimensional. The compact height given in Table 5 is for volume and particle density calculations only. The fuel consists of 1.245 cm diameter fuel compacts centred in a 1.270 cm diameter channel. The block also contains 1.588 cm gas flow coolant holes. Fuel and coolant channel holes are centred on a 1.880 cm triangular pitch arranged as shown in Figure 1.

Table 1. Coated particle specification

Item	Units	Value
UO_2 fuel density	g/cm^3	10.4
Uranium enrichment (by mass ^{235}U / (^{235}U+^{238}U)	%	8.2
Fuel natural boron impurity by mass	ppm	1
Outer coated particle radius	mm	0.455
Fuel kernel radius	mm	0.25
Coating materials	-	C/C/SiC/C
Coating thickness	mm	0.09 0.04/0.035/0.04
Coating densities	g/cm^3	1.05/1.9/3.18/1.9

Table 2. Material specifications

Material	Nuclide	Atoms per barn•cm
UO_2 fuel	^{238}U	2.12877e-02
	^{235}U	1.92585e-03
	O	4.64272e-02
	B-10	1.14694e-07
	B-11	4.64570e-07
Inner low-density carbon kernel coating	C (nat)	5.26449e-02
Pyro carbon kernel coatings (inner and outer)	C (nat)	9.52621e-02
Silicon carbide kernel coating	C (nat)	4.77240e-02
	Si (nat)	4.77240e-02
Pebble/compact carbon matrix	C (nat)	8.77414e-02
	B-10	9.64977e-09
	B-11	3.90864e-08
Pebble outer coating/Prismatic block	C (nat)	8.77414e-02
	B-10	9.64977e-09
	B-11	3.90864e-08
Helium coolant	He-3	3.71220e-11
	He-4	2.65156e-5

Table 3. Fuel grain lattice data

Item	Units	Value
Unit cell grain square array pitch (cubical outer boundary)	cm	0.16341
Unit cell grain outer radius (spherical outer boundary)	cm	0.10137
Grain outer radius	cm	0.0455
Packing fraction of coated particles	%	9.043
Graphite matrix density	g/cm^3	1.75
Graphite matrix natural boron impurity by mass	ppm	0.5
UO_2 fuel mass per pebble	g	6.806E-4

Table 4. Pebble bed fuel lattice data

Item	Units	Value
Unit cell pebble square array pitch (cubical outer boundary)	cm	6.0
Unit cell coolant outer radius (spherical outer boundary)	cm	3.53735
Pebble radius	cm	3.0
Radius of fuel zone	cm	2.5
Pebble outer carbon coating thickness	cm	0.5
Pebble outer carbon natural boron impurity by mass	ppm	0.5
Number of coated particles per pebble	-	15 000
Packing fraction of coated particles	%	9.043
Graphite matrix density	g/cm^3	1.75
Graphite matrix natural boron impurity by mass	ppm	0.5
Pebble outer carbon coating density	g/cm^3	1.75
UO_2 fuel mass per pebble	g	10.210

Figure 1. Prismatic assembly lattice pattern

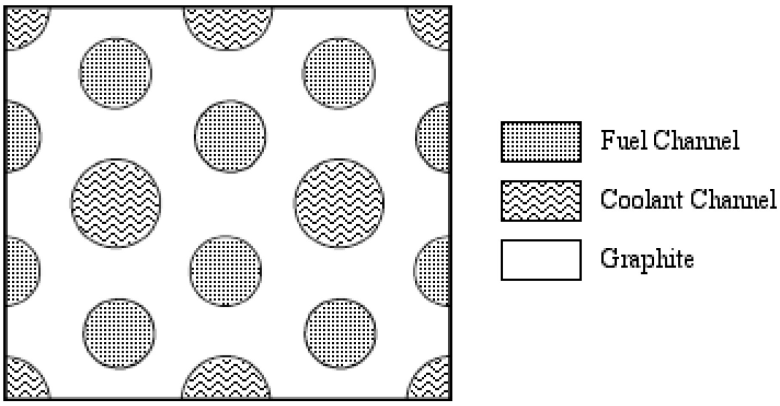

Table 5. Prismatic fuel lattice data

Item	Units	Value
Triangular pitch (coolant channel-rod channel and rod channel-rod channel)	cm	1.880
Fuel channel diameter	cm	1.270
Coolant channel diameter	cm	1.588
Fuel compact (centred in fuel channel) diameter	cm	1.245
Compact height	cm	4.93
Number of coated particles per compact	-	3 000
Packing fraction of coated particles	%	19.723
Graphite matrix density	g/cm^3	1.75
Graphite matrix natural boron impurity by mass	ppm	0.5
UO_2 fuel mass per compact	g	2.042

II.B. Depletion calculations

Depletion calculations are to be performed for each model. Results (described later) are to be reported for fresh fuel and for burn-up steps of 0.5, 5, 10, 20, 40, 80, and 120 GWd/tonne initial uranium (intermediate burn-up steps should be performed as appropriate to ensure accurate depletion). Depletion is to be performed at a constant power of 62 MW/tonne initial uranium, assuming continuous burn-up with no downtime. Both fuel and the graphite matrix (boron impurities) should be depleted.

Reported results are as follows:

- infinite multiplication factor;
- spectral indices (assuming a fast/thermal boundary at 0.625eV):
  - $\rho^{238} = {}^{238}U_{cap}(fast) / {}^{238}U_{cap}(thermal)$;
  - $\delta^{235} = {}^{235}U_{fis}(fast) / {}^{235}U_{fis}(thermal)$;
  - $\delta^{238} = {}^{238}U_{fis} / {}^{235}U_{fis}$;
  - $c/f^{235} = {}^{238}U_{cap} / {}^{235}U_{fis}$.
- nuclide concentrations (grams/tonne initial U):
  - actinides: ${}^{235}U$, ${}^{238}U$, ${}^{239}Pu$, ${}^{240}Pu$, ${}^{241}Pu$, ${}^{242}Pu$, ${}^{241}Am$, ${}^{244}Cm$ and ${}^{245}Cm$;
  - fission products: ${}^{85}Kr$, ${}^{90}Sr$, ${}^{110m}Ag$, ${}^{137}Cs$, ${}^{135}Xe$, ${}^{149}Sm$ and ${}^{151}Sm$.
- volume-averaged energy-dependent spectrum in fuel pebble/compact (using participant's own group structure).

To be able to include calculations from as many different methods as possible, depletion calculations are to be performed without a critical spectrum correction.

Reflective/mirror boundary conditions should be used where available; white boundary conditions may be used where reflection is not an option.

II.C. Reporting of results

Each submission was requested to include the following information:

- date;
- organisation;
- contact person;
- e-mail address of the contact person;
- computer code(s) used;
- description of the analysis environment, including neutron data library source, group structure and data processing method (for MG), description of code system, geometry modelling approach, convergence limit or statistical errors for the eigenvalue calculations, assumptions/ approximations in treating double heterogeneity, and any other relevant information;
- keyword GRAIN, followed by results for infinite lattice grain (if grain depletion was performed;
- keyword PEBBLE, followed by results for pebble bed fuel (if pebble bed depletion was performed);
- keyword PRISM, followed by results for prismatic fuel (if prismatic fuel depletion was performed).

III. Results

Results were submitted for 21 sets of calculations, provided by 12 individuals or teams representing ten organisations in 6 countries. A total of 11 unique computer codes systems were used. Because of the differing capabilities and limitations of the different code systems, submissions included one, two or all three fuel configurations. Overall, 8 solutions were submitted for the grain model; 15 for the pebble bed model and 18 for the prismatic fuel supercell, with a mix of deterministic and Monte Carlo approaches and both MG and CE cross-section treatment in the Monte Carlo results. Table 6 provides a summary of all participants in the benchmark exercise, codes used and the fuel configurations modelled. In plots and tables provided below and in appendices, each submission is identified by the shortened “Submission Label” listed in the last column of the table.

Detailed information on each submission (e.g. neutron library type, convergence criteria, comments on analysis approach, etc.) are provided in Appendix A. This information was taken from the spreadsheet submissions provided for each analysis type. Each of the plots provided in the body of this report is included as a full-page plot in Appendices B-D for grain, pebble and prismatic cases, respectively, to allow a more detailed examination of the plotted results.

As described earlier, for each of the three fuel types, a number of data types was requested: $k_{\text{-inf}}$, four spectral indices, nine actinide inventories and seven fission product inventories, for a fresh fuel state and for seven depletion steps. Although not all participants provided all data, a tremendous amount of data is available. Thus, the complete set of results are not presented nor discussed in full here. Complete sets of plots of all submitted data are provided in Appendices B, C and D for grain, pebble and prismatic configurations, respectively. The raw data (reported values for each of the parameters) are provided in Appendix E. Note that while the volume-averaged energy-dependent spectrum in fuel pebble/compact models was also requested, this data was provided by only three participants, making it difficult to be used to assess data trends. Hence, this data has been omitted here. The following subsections discuss trends noted for each type of data, with relevant key data plots provided.

III.A. Multiplication factor

A key factor in being able to demonstrate consistency in modelling approaches is the multiplication factor provided by each participant. Figures 2, 3 and 4 show the results for $k_{\text{-inf}}$ as a function of burn-up for the three configurations. These results are difficult to compare to each other as each contained a different sets of codes and data. However, it is clear that all methods and data provided in independent calculations are consistent within a reasonably tight band. Each figure shows the value of $k_{\text{-inf}}$ as a function of burn-up with the value of k plotted on the left hand axis. The mean value of all participants is also plotted in each figure. The right axis shows the standard deviations for the set of results.

Note that in the plots of the grain (Figure 2) and prismatic (Figure 4) results, two standard deviation curves are shown. This first (dashed turquoise line) shows the standard deviation for all plotted results. The second shows the standard deviation with the UNAM results excluded. In both sets of calculations, UNAM results are an outlier and tend to skew the results. UNAM calculations used a homogenised approach for all materials rather than explicit grain representations for both grain and prismatic models. This approach resulted in a harder spectrum and increased plutonium production (see Figures B-2, B-7 through B-10). These results are valuable in demonstrating the importance of discrete grain modelling to properly capture self-shielding effects.

Table 6. List of participants and codes used for HTGR benchmark calculations

Organisation	Country	Contact person	Code used	Configurations modelled	Submission label
Idaho National Laboratory/Studsvik Scandpower	US	William Skerjanc	HELIOS 2	☐Grain ☐Pebble ☑Prismatic	INL/Studsvik
Forschungszentrum Dresden-Rossendorf	Germany	Emil Fridman	BGCore (explicit lattice)	☑Grain ☐Pebble ☑Prismatic	FZD 1
			BGCore (RPT)	☐Grain ☐Pebble ☑Prismatic	FZD 2
			HELIOS 1.9	☑Grain ☐Pebble ☑Prismatic	FZD 3
Institut fuer Kernenergetik und Energiesysteme	Germany	Astrid Meier Johannes Bader Wolfgang Bernnat	MCNP/ Abbrand	☑Grain ☑Pebble ☑Prismatic	IKE 1
			Microx2.2/ORIGEN2.2	☑Grain ☑Pebble ☑Prismatic	IKE 2
		Janis Lapins	SCALE 6 (TRITON)	☑Grain ☑Pebble ☑Prismatic	IKE 3

Table 6. List of participants and codes used for HTGR benchmark calculations (continued)

Organisation	Country	Contact person	Code used	Configurations modelled	Submission label
Gesellschaft fuer Anlagen- und Reaktorsicherheit mbH	Germany	Winfried Zwermann	MONTEBURNS 2.0	☑Grain ☑Pebble ☑Prismatic	GRS
Lawrence Livermore National Laboratory	US	Massimiliano Fratoni	MOCUP	☑Grain ☑Pebble ☑Prismatic	LLNL
VTT Technical Research Centre of Finland	Finland	Jaakko Leppänen	Serpent 1.1.2 (dispersed fuel)	☐Grain ☑Pebble ☑Prismatic	VTT 1
VTT Technical Research Centre of Finland				☑Grain ☑Pebble ☑Prismatic	VTT 2
Oak Ridge National Laboratory	US	Mark DeHart	SCALE 6.1 β (TRITON/NEWT)	☐Grain ☑Pebble ☑Prismatic	ORNL 1
			SCALE 6.1 β (TRITON/KENO V.a)	☑Grain ☑Pebble ☑Prismatic	ORNL 2
			SCALE 6.1 β (TRITON/XSDRN)	☐Grain ☑Pebble ☐Prismatic	ORNL 3

Table 6. List of participants and codes used for HTGR benchmark calculations (continued)

Organisation	Country	Contact person	Code used	Configurations modelled	Submission label
Oak Ridge National Laboratory	US	Mark DeHart	SCALE 6.1 β (TRITON/XSDRN with RPT)	☐Grain ☑Pebble ☐Prismatic	ORNL 4
Los Alamos National Laboratory	US	Sang-Yoon Lee	MCNPX 2.7 β	☐Grain ☑Pebble ☐Prismatic	LANL
Korea Atomic Energy Research Institute	Korea	Kim Yonghee	HELIOS	☐Grain ☑Pebble ☑Prismatic	KAERI 1
			MCCARD (RPT)	☐Grain ☑Pebble ☑Prismatic	KAERI 2
			MCCARD (DH)	☐Grain ☑Pebble ☑Prismatic	KAERI 3
National Autonomous University of Mexico	Mexico	Juan-Luis Francois	MCNPX 2.6.0	☑Grain ☐Pebble ☑Prismatic	UNAM
Idaho National Laboratory and Polytechnique Montreal	US/ Canada	Mike Pope	DRAGON 4.03	☐Grain ☐Pebble ☑Prismatic	INL/ PolyMtl

Figure 2. k_{-inf} vs Burn-up for grain depletion

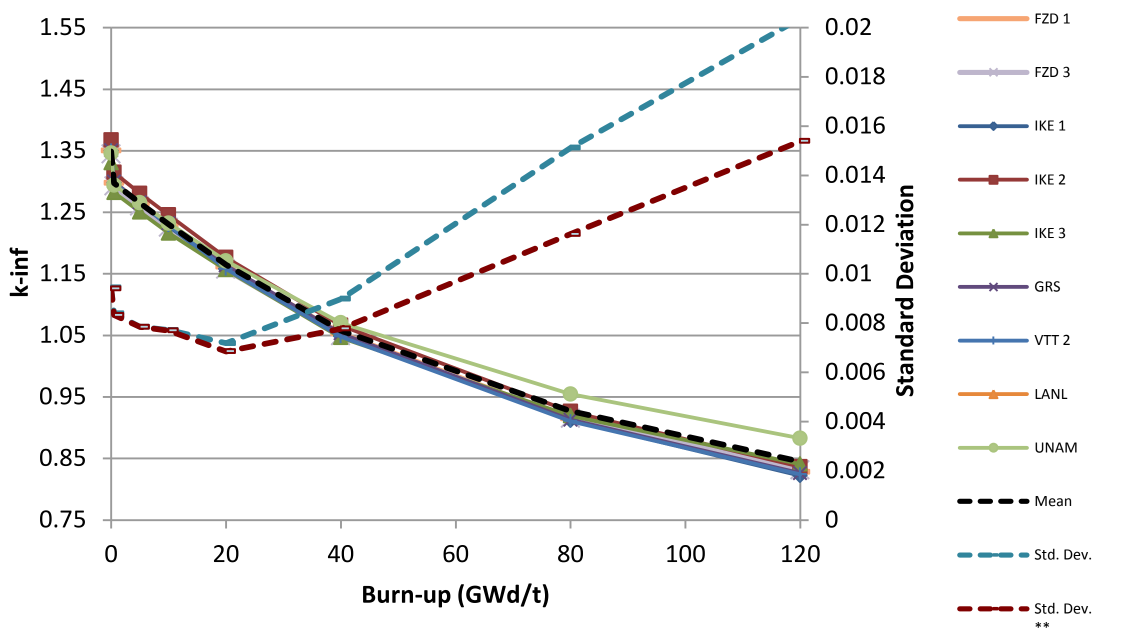

Figure 3. k_{-inf} vs Burn-up for pebble depletion

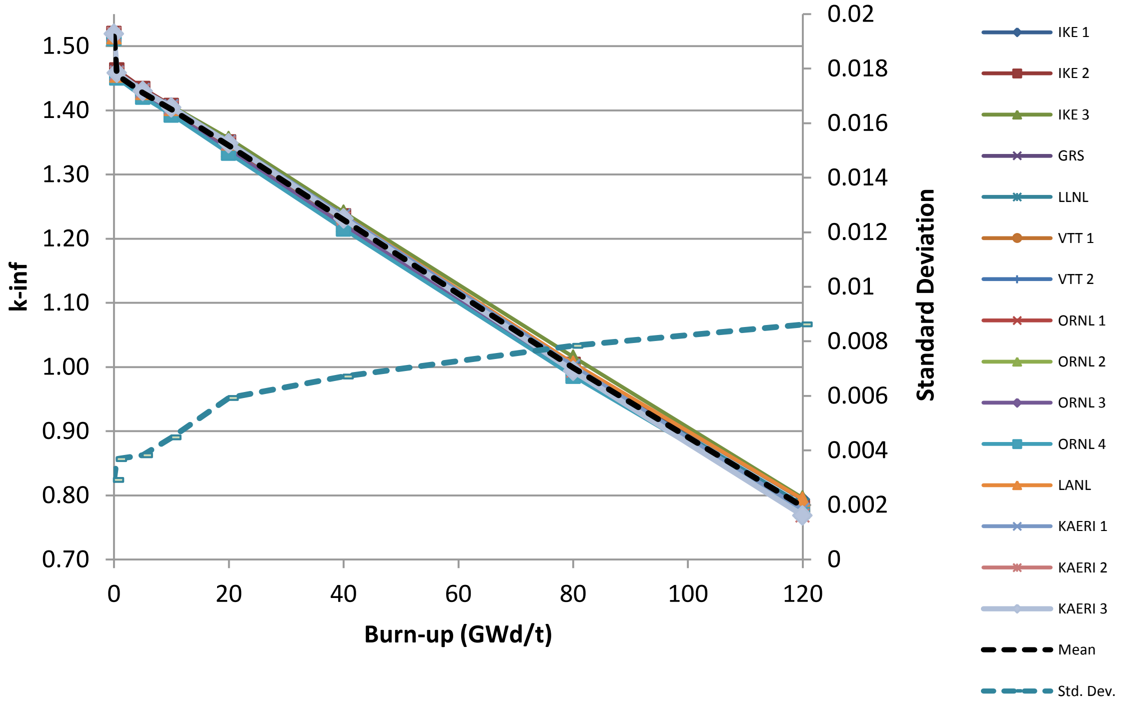

Figure 4. k_{-inf} vs burn-up for prismatic supercell depletion

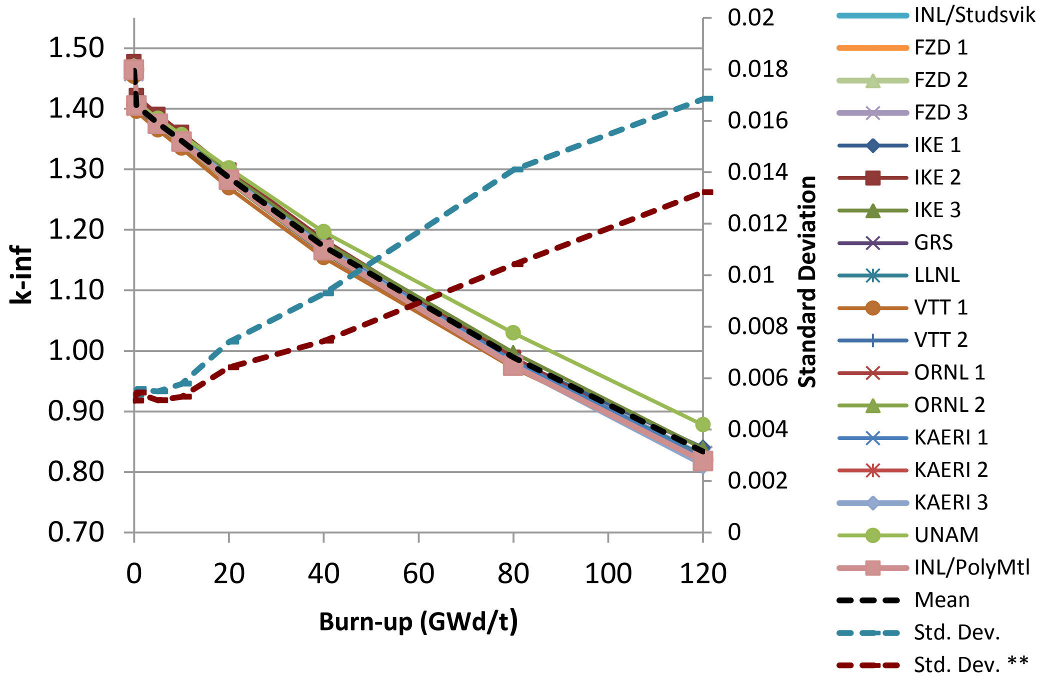

With the exclusion of UNAM results, the results are in agreement with a standard deviation of 1.5% or less, occurring at the maximum burn-up of 120 GWd/t. It is interesting to note that the pebble model shows the best overall agreement over the entire burn-up cycle, with a standard deviation of less than 1% at end-of-life (EOL). In fact, the pebble results show better agreement than the grain models, in which double heterogeneity effects are not present. This is somewhat surprising, but it is also noted that the grain solution shows a greater spread in results at beginning of life (BOL), with a standard deviation of approximately 1% for the grain models, and on the order of 0.85% for the pebble models. The reason for this trend is not clear, but it may be a result of offsetting errors in doubly heterogeneity models. In addition, the grain models are the only set of data that shows a decrease in the standard deviation with burn-up early in the burn history. Nevertheless, overall agreement is good among all participants with the exclusion of UNAM results; the results of the simplified homogeneous treatment are demonstrated in the results of these calculations.

III.B. Spectral indices

Four spectral indices were requested for each fuel configuration; however, the number of values submitted varied significantly by index type and configuration. All show consistent trends; however, each case has participant outliers that indicate a possible inconsistency in that participant's results.

III.B.1 Spectral indices for grain depletion

Plots of reported results for the four spectral indices for the grain depletion model are shown in Figures 5-8 below. The fast to thermal ratios for capture and fission in ^{238}U and ^{235}U, respectively, ρ^{238} and δ^{235}, show an increase with burn-up, indicating spectral hardening with increased rates of fast capture and fast fission rates. IKE 3 results are slightly higher only for ρ^{238}, while IKE 2 results are slightly low for both indices. As might be expected, the ^{238}U fission ratio δ^{238} shows the same trends as ρ^{238}, with IKE 3 high and IKE 2 low. IKE 1 also is somewhat higher than the mean. Given the sparsity of data, however, it is not clear if the IKE 1 and IKE 2 results are high, or other results are low. Finally, the ^{238}U capture to ^{235}U fission ratio, c/f_{235}, shows a good grouping of consistent results, but with IKE 2 slightly lower than the group and IKE 3 very slightly higher.

Figure 5. ρ_{238} for grain depletion

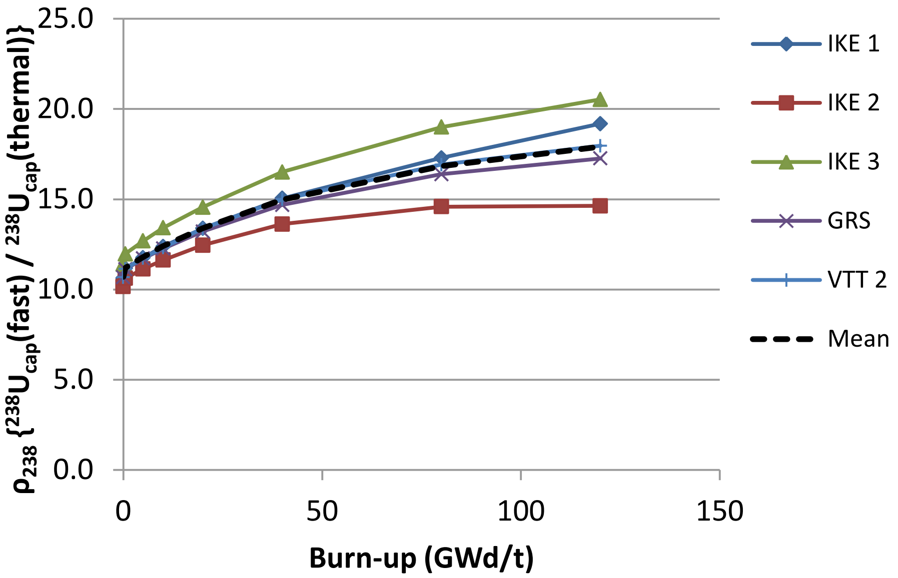

Figure 6. δ_{235} for grain depletion

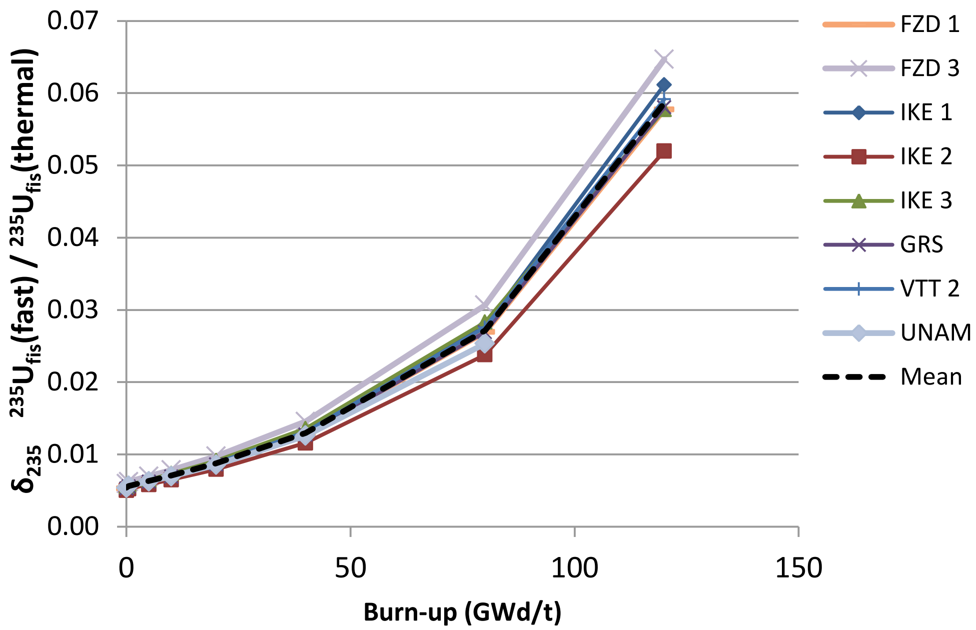

Figure 7. δ_{238} for grain depletion

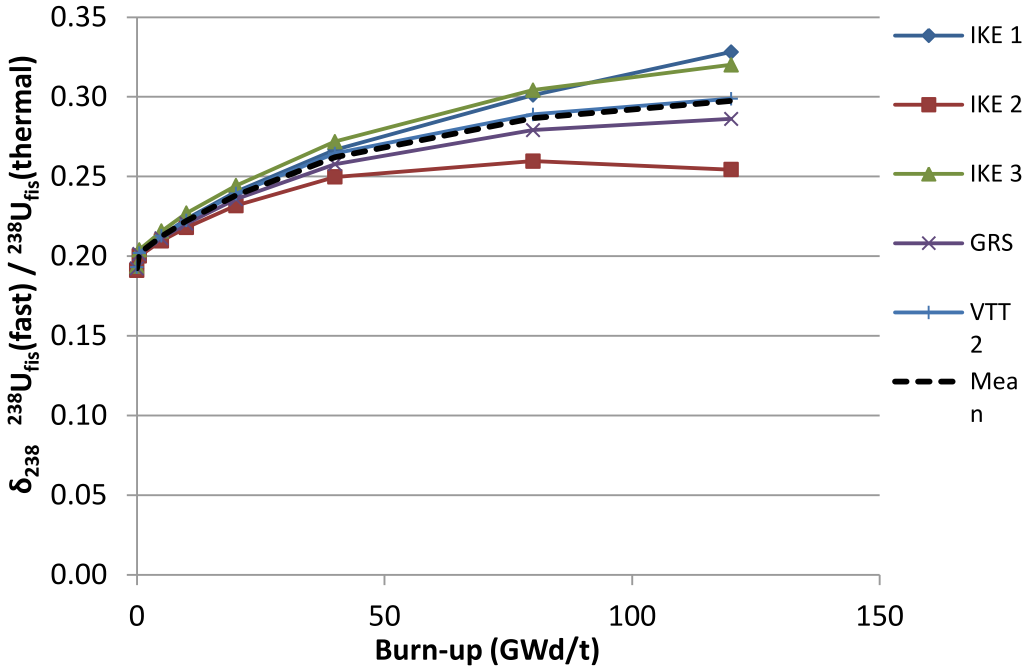

Figure 8. c/f_{235} for grain depletion

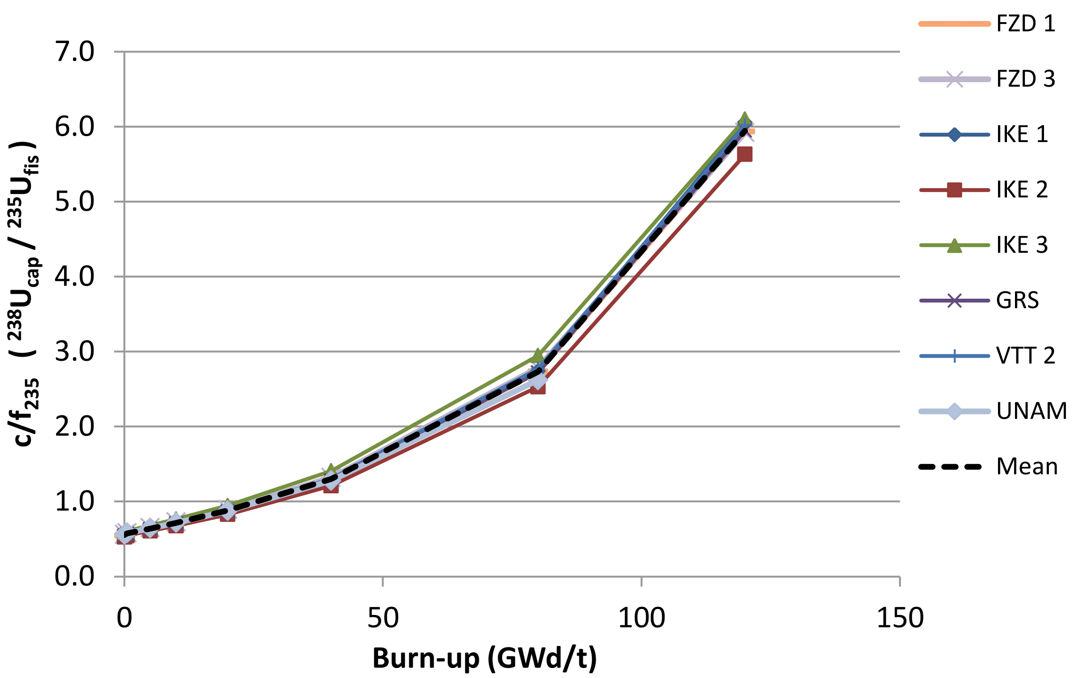

III.B.2 Spectral indices for pebble depletion

Trends seen in spectral indices for depletion within an infinite lattice of pebbles show a significant change from those of grain depletion (see Figures 9-12). Here, the indices indicate spectral softening as a function of burn-up after a slight hardening at BOL. This is likely due to the DH nature of the fuel (as will be shown later, depletion of prismatic fuel shows identical trends). With more participants in these calculations, a more representative set of results is available. Here, LANL results are clearly inconsistent with other participants for ρ^{238}, δ^{238} and c/f_{235}, but grouped with other results for δ^{235}, indicating an issue with ^{238}U. However, this spectral difference was not seen in LANL k_{-inf} results shown in Figure 3. The LANL results skew the average for all participants, however, a better grouping of results is seen with all participants than for the grain depletion results. IKE 1 does come in slightly high for δ^{235} and IKE 2 sets the lower bound for δ^{238}, but with the exception of LANL results, reported spectral indices are in good agreement.

Figure 9. ρ_{238} for pebble depletion

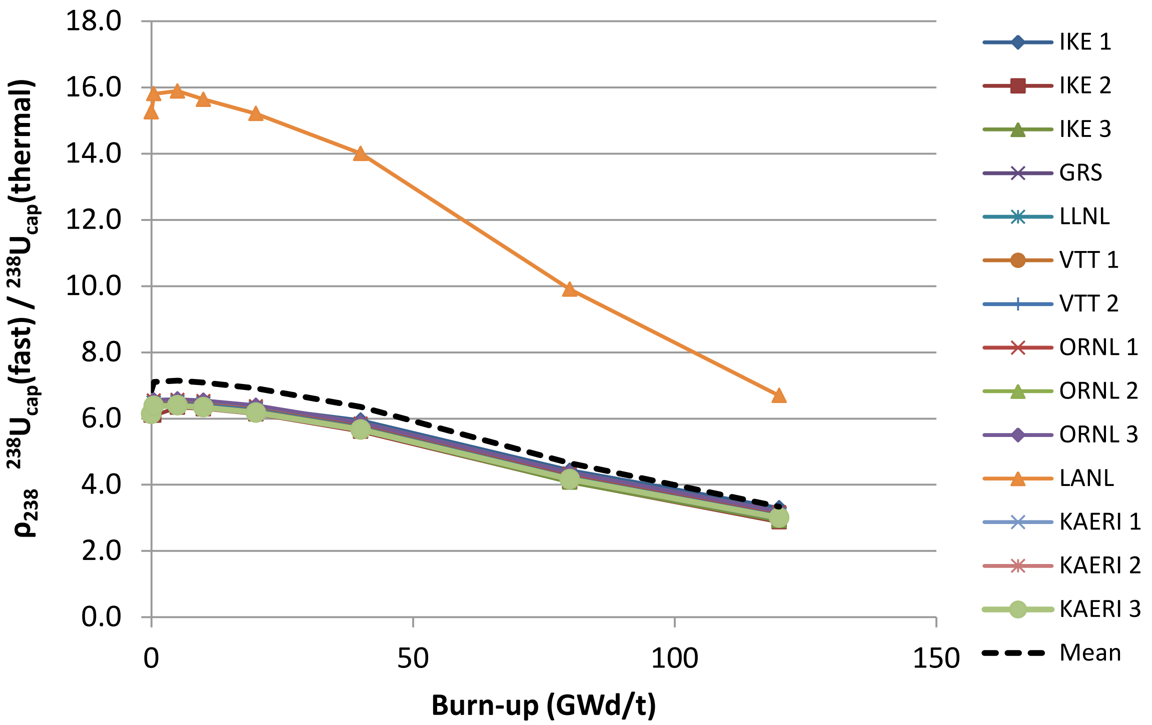

Figure 10. δ_{235} for pebble depletion

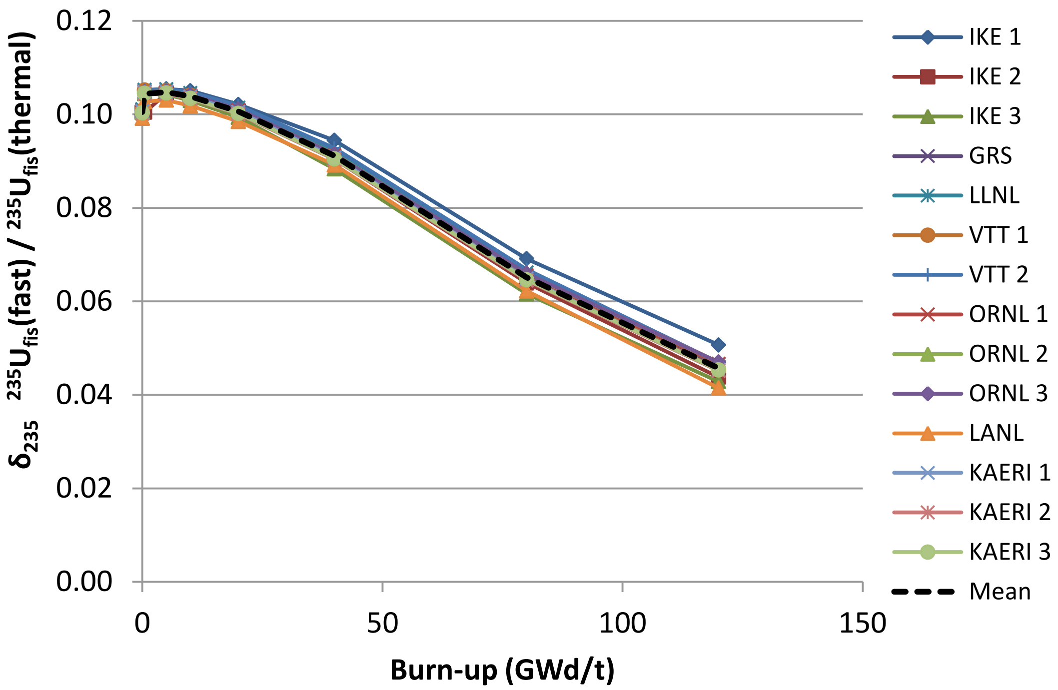

Figure 11. δ_{238} for pebble depletion

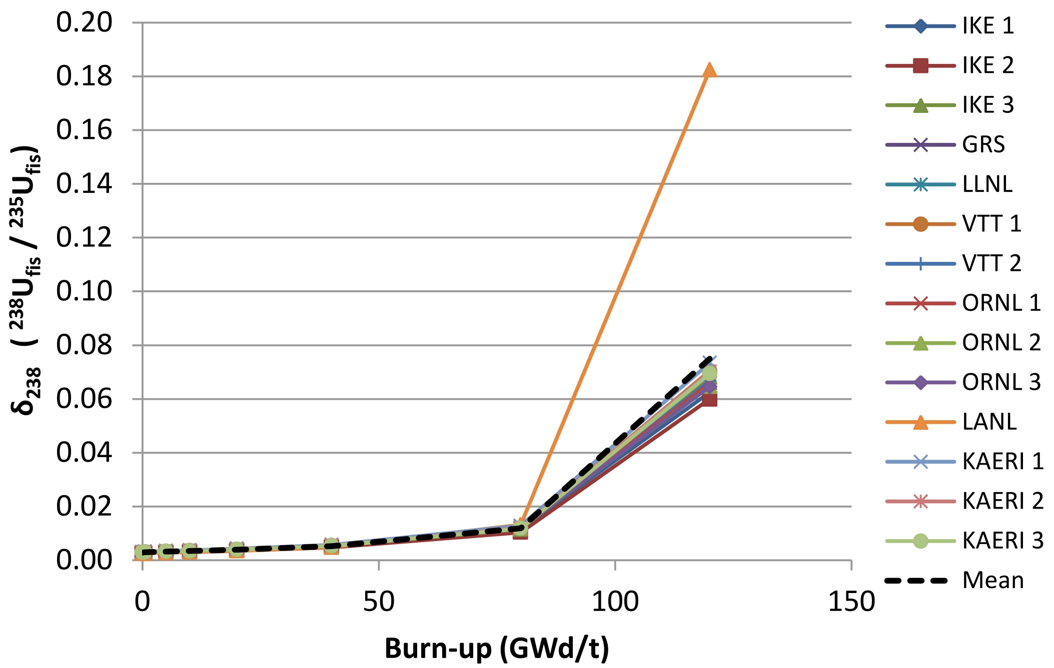

Figure 12. c/f_{235} for pebble depletion

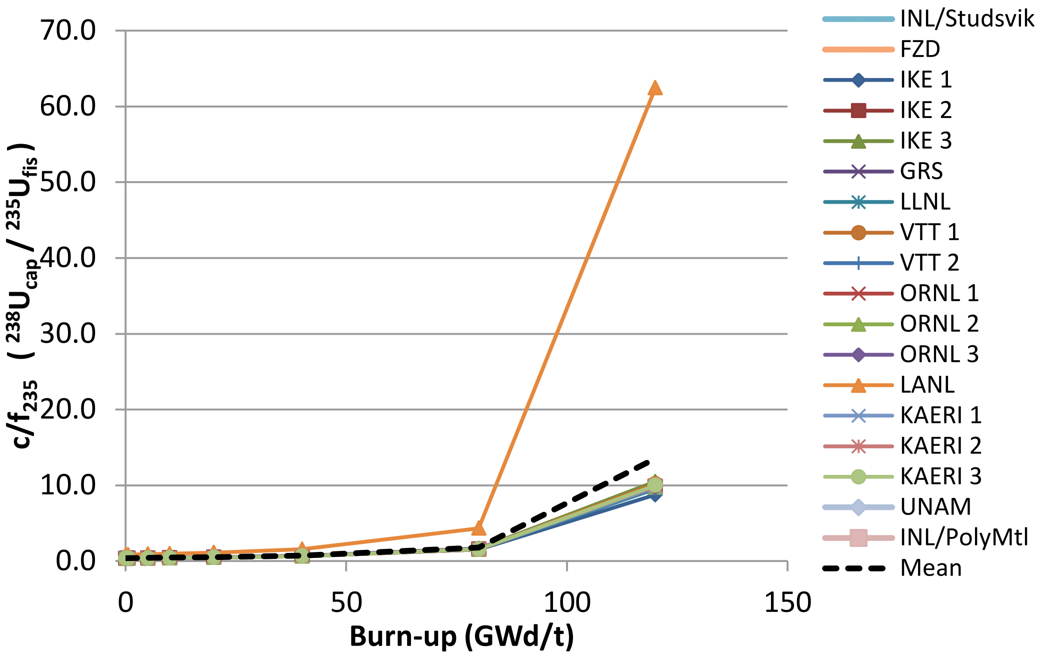

III.B.3 Spectral indices for prismatic depletion

Unlike the results of pebble depletion, prismatic depletion (Figures 13-16) shows significant spread from the mean for both ρ^{238} and δ^{235}, with IKE 2 again low, and INL/Studsvik, IKE 1, and VTT 1 somewhat high. However, for the remaining two indices there is generally good agreement, although the spread in results increases somewhat at higher burn-ups. The shape of the index profiles for the prismatic fuel is consistent with that of the pebble fuel.

Table 7 provides a summary of the shape of the spectral index curves for each of the fuel types, with an indication of the direction and curvature of the plots. Note that the general shapes of index trends for the pebble and prismatic fuels are identical, but much different from the grain depletion indices.

Figure 13. ρ_{238} for prismatic depletion

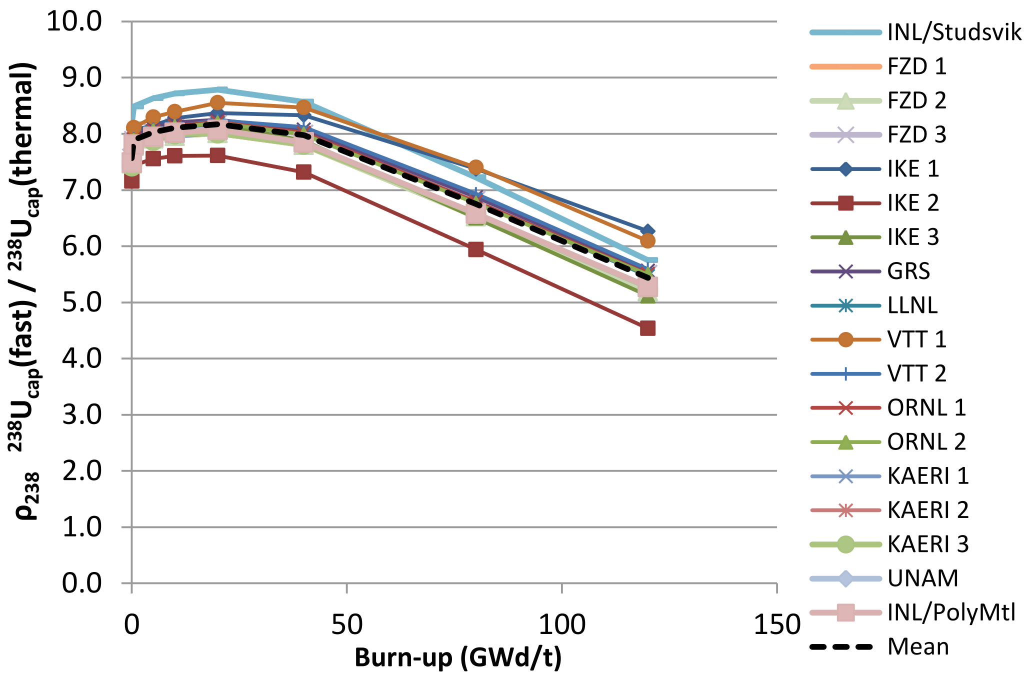

Figure 14. δ_{235} for prismatic depletion

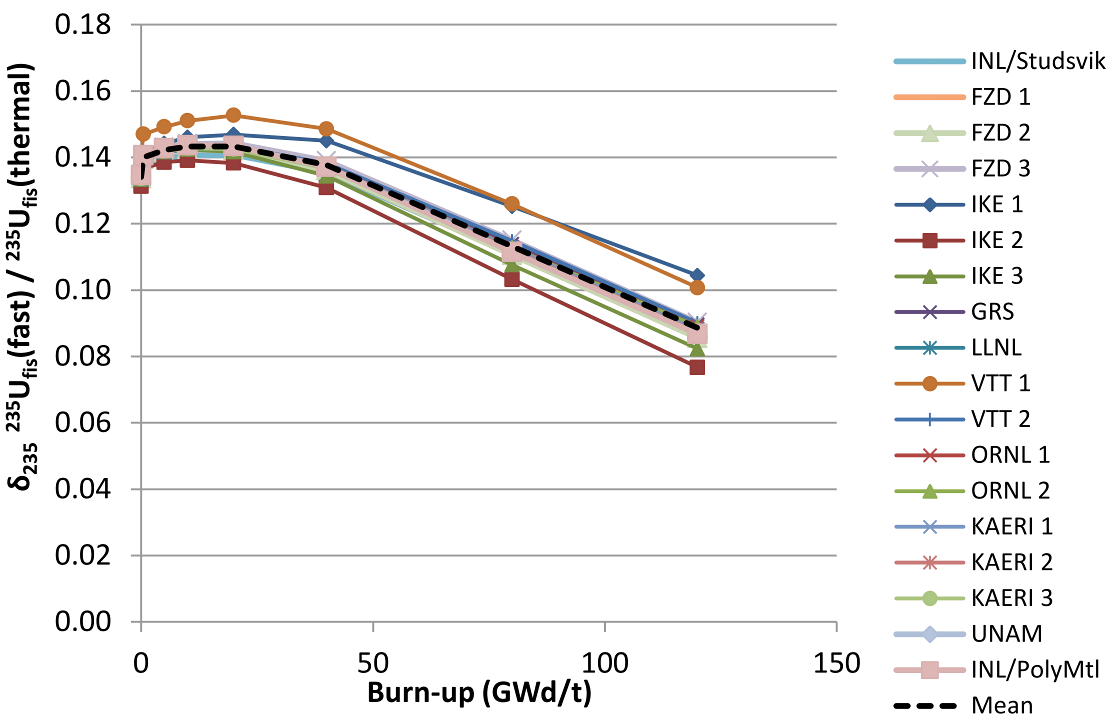

Figure 15. δ_{238} for prismatic depletion

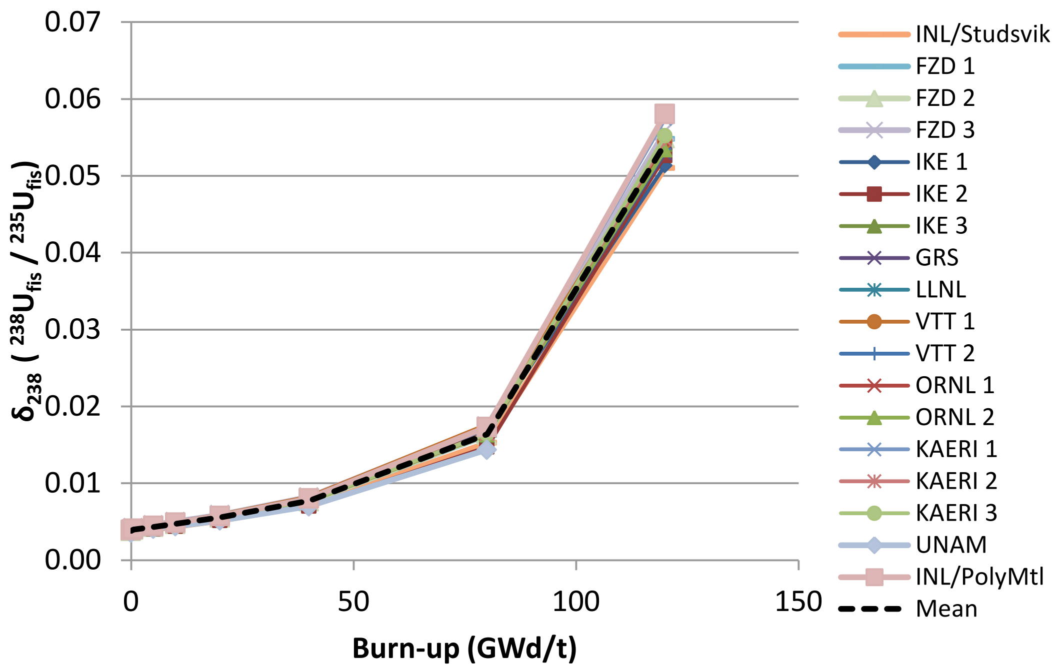

Figure 16. c/f_{235} for prismatic depletion

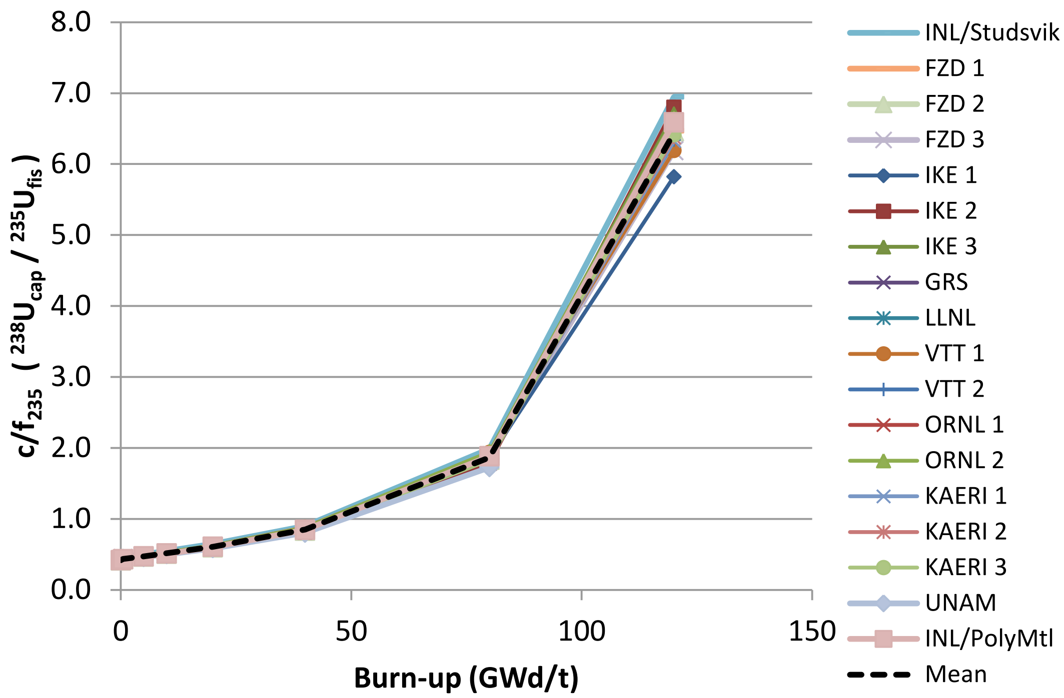

Table 7. Form of spectral index curve for three fuel types

	Grain depletion	Pebble depletion	Prismatic depletion
ρ^{238}	Increasing, concave down (Figure 5)	Initial Increase, then decreasing, concave down (Figure 9)	Initial Increase, the decreasing, concave down (Figure 13)
δ^{235}	Increasing, concave up (Figure 6)	Initial Increase, the decreasing, concave down (Figure 10)	Initial Increase, the decreasing, concave down (Figure 14)
δ^{238}	Increasing, concave down (Figure 7)	Increasing, concave up (Figure 11)	Increasing, concave up (Figure 15)
c/f_{235}	Increasing, concave up (Figure 8)	Increasing, concave up (Figure 12)	Increasing, concave up (Figure 16)

III.C. Actinide depletion

Isotopic inventories were requested for ^{235}U, ^{238}U, ^{239}Pu, ^{240}Pu, ^{241}Pu, ^{242}Pu, ^{241}Am, ^{244}Cm and ^{245}Cm for the three fuel types. Results are provided in Figures 17-25 for the infinite grain lattice, Figures 26-34 for the pebble configuration and Figures 35-43 for the prismatic supercell. The following subsections provide a very brief and qualitative review of results by nuclide for each configuration type. The reader can review the plots and draw their own conclusions as to the overall performance.

Figure 17. ^{235}U mass vs burn-up for grain depletion

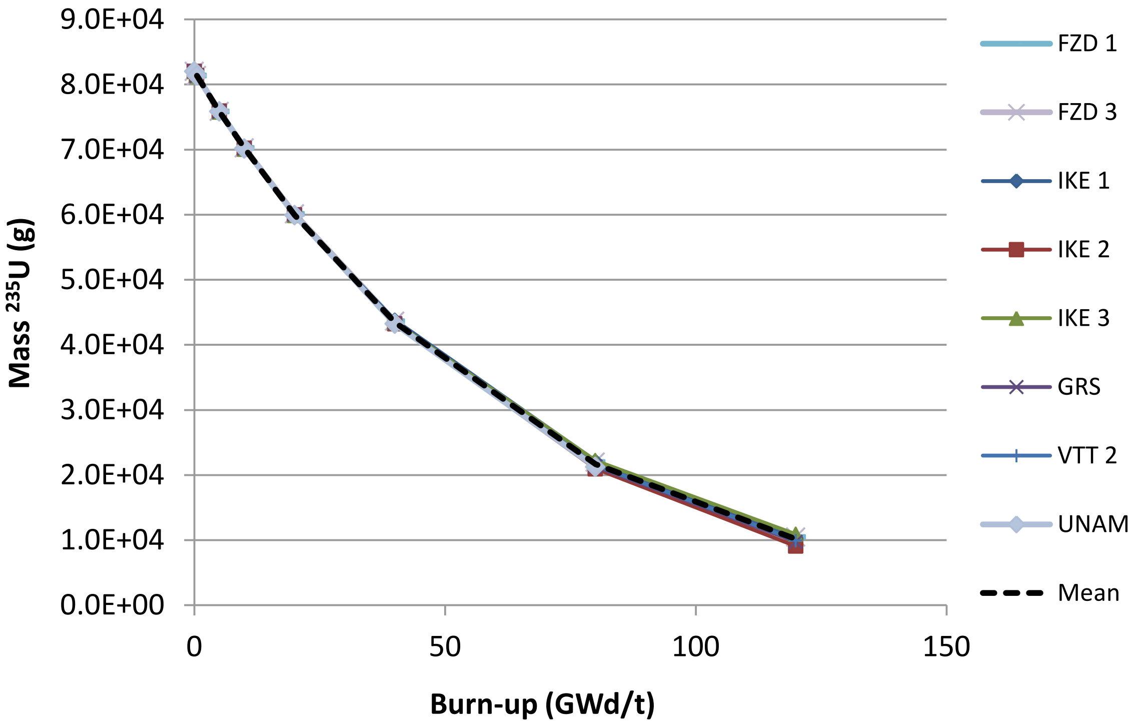

Figure 18. ^{238}U mass vs burn-up for grain depletion

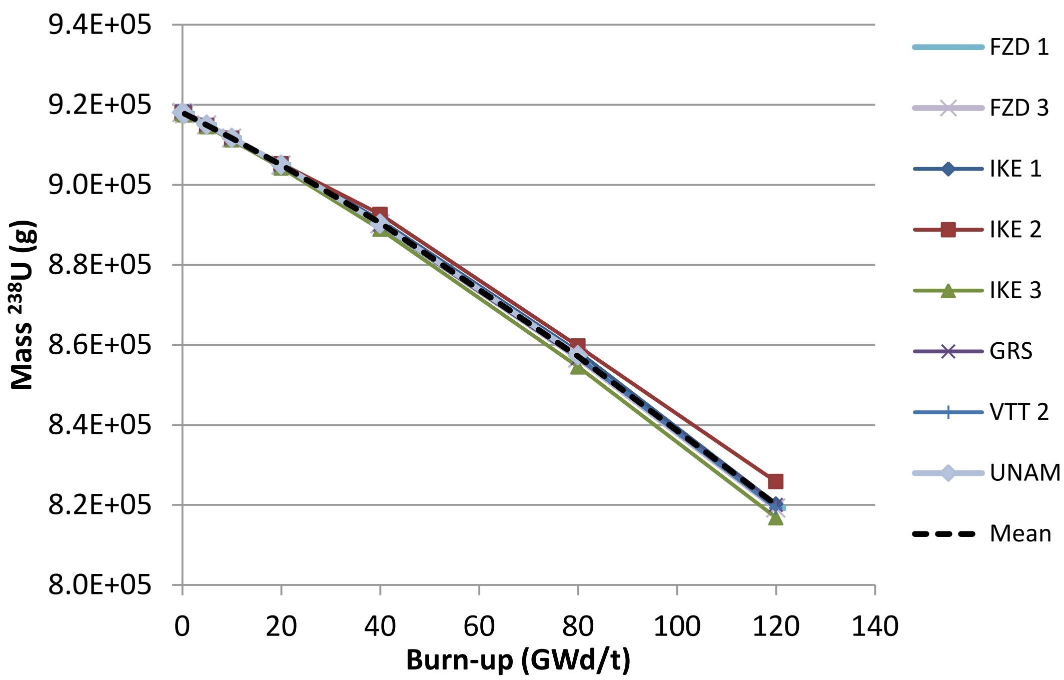

Figure 19. ^{239}Pu mass vs burn-up for grain depletion

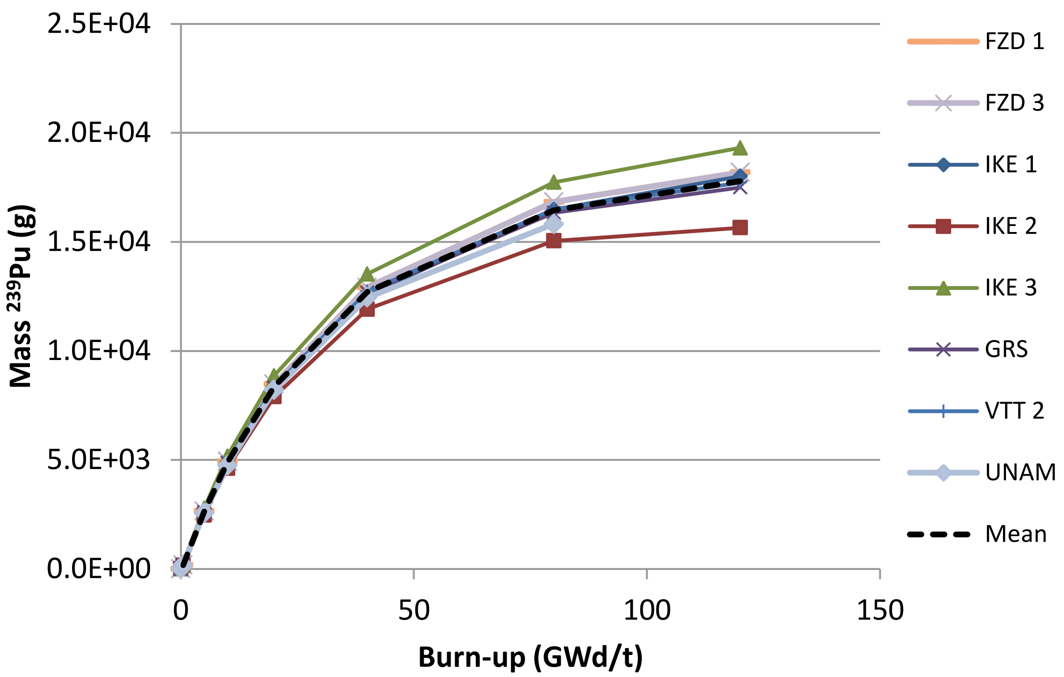

Figure 20. ^{240}Pu mass vs burn-up for grain depletion

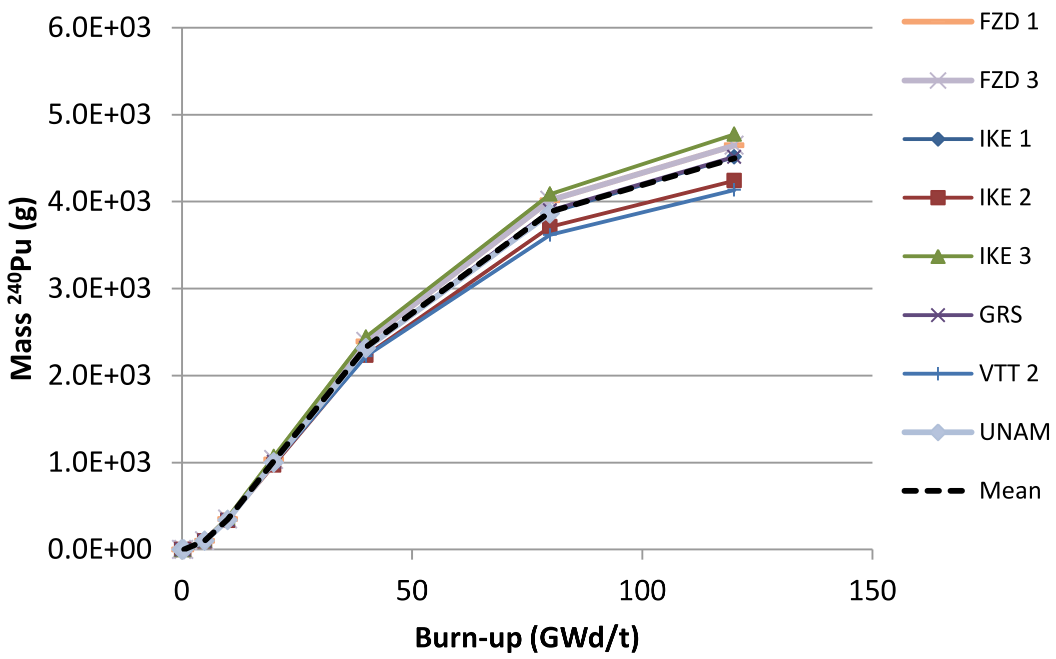

Figure 21. ^{241}Pu mass vs burn-up for grain depletion

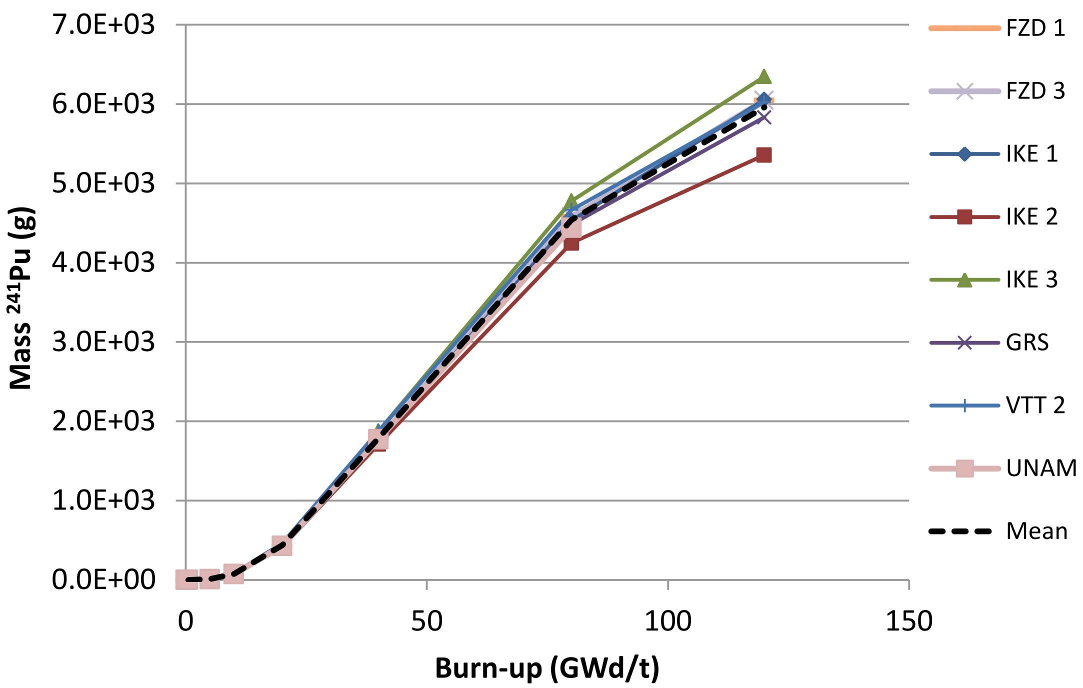

Figure 22. ^{242}Pu mass vs burn-up for grain depletion

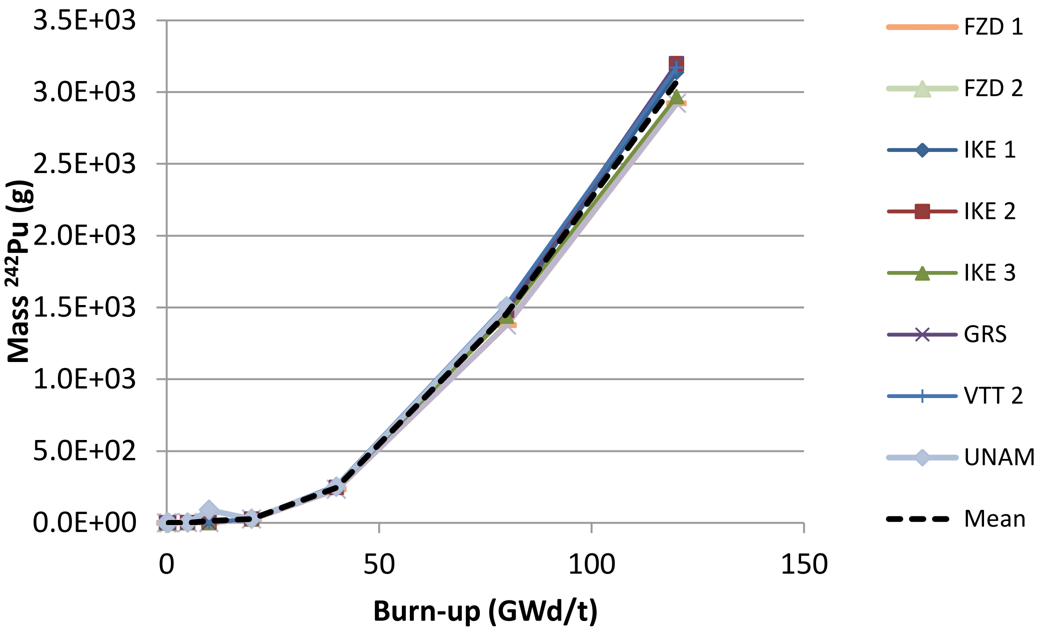

Figure 23. ^{241}Am mass vs burn-up for grain depletion

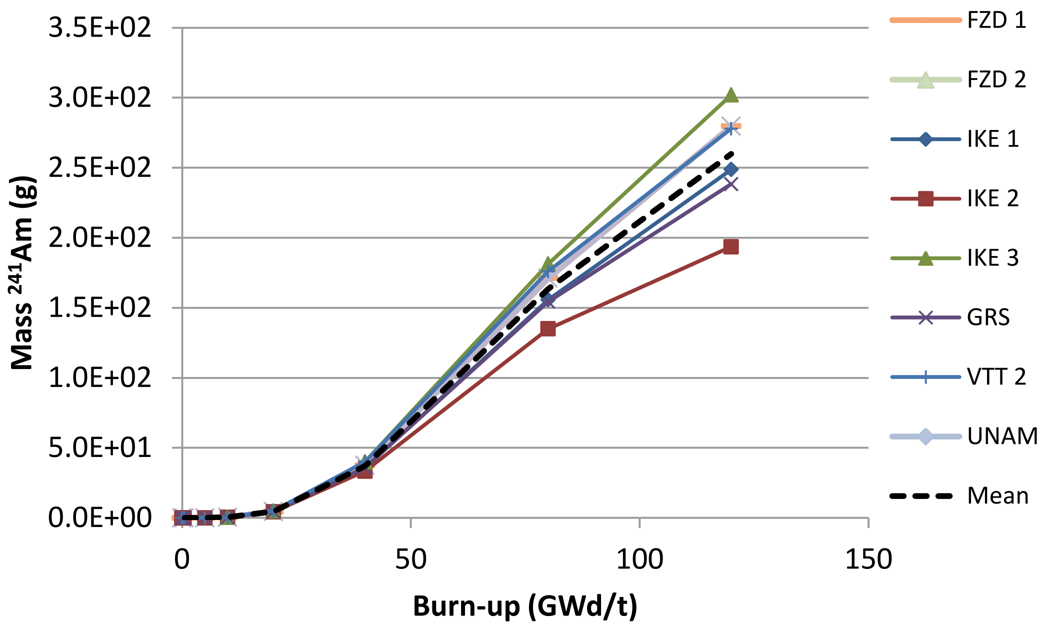

Figure 24. ^{244}Cm mass vs burn-up for grain depletion

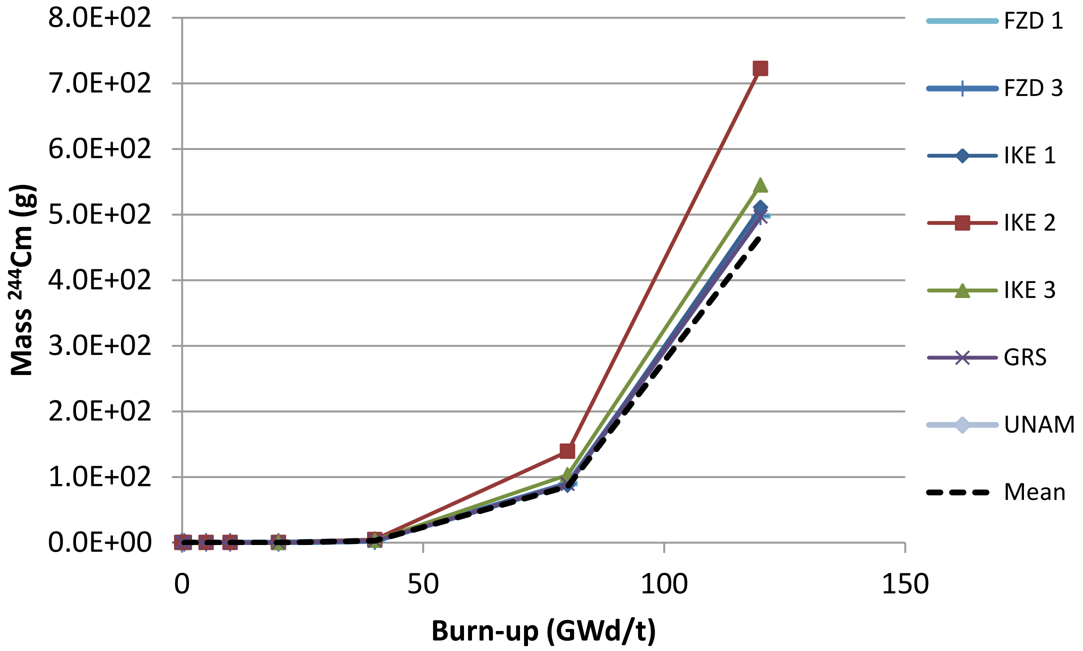

Figure 25. ^{245}Cm mass vs burn-up for grain depletion

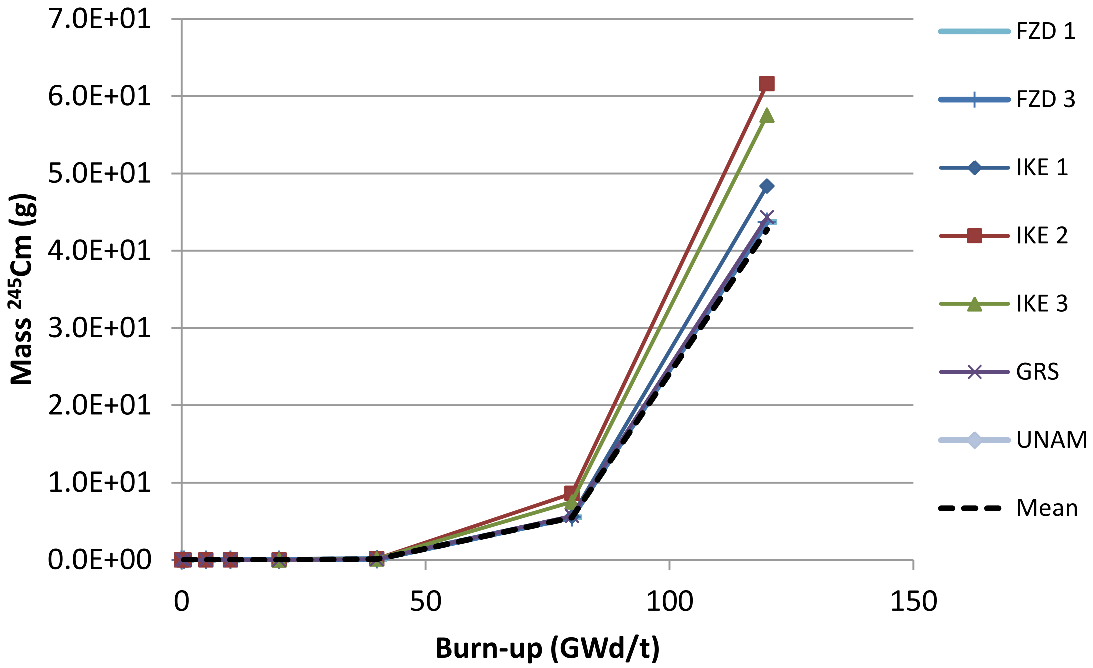

Figure 26. ^{235}U mass vs burn-up for pebble depletion

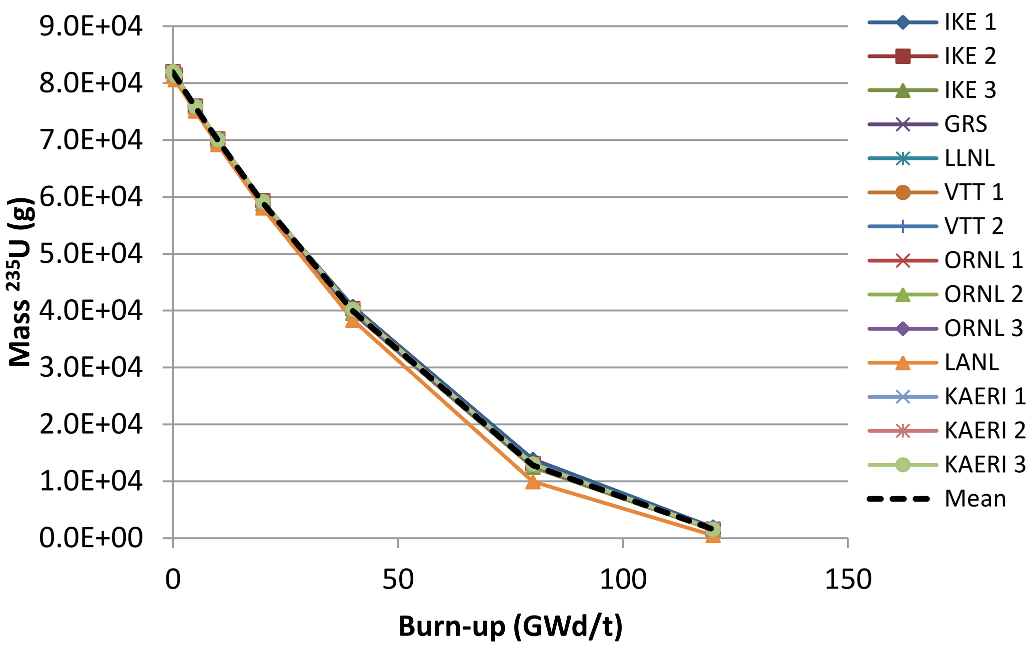

Figure 27. ^{238}U mass vs burn-up for pebble depletion

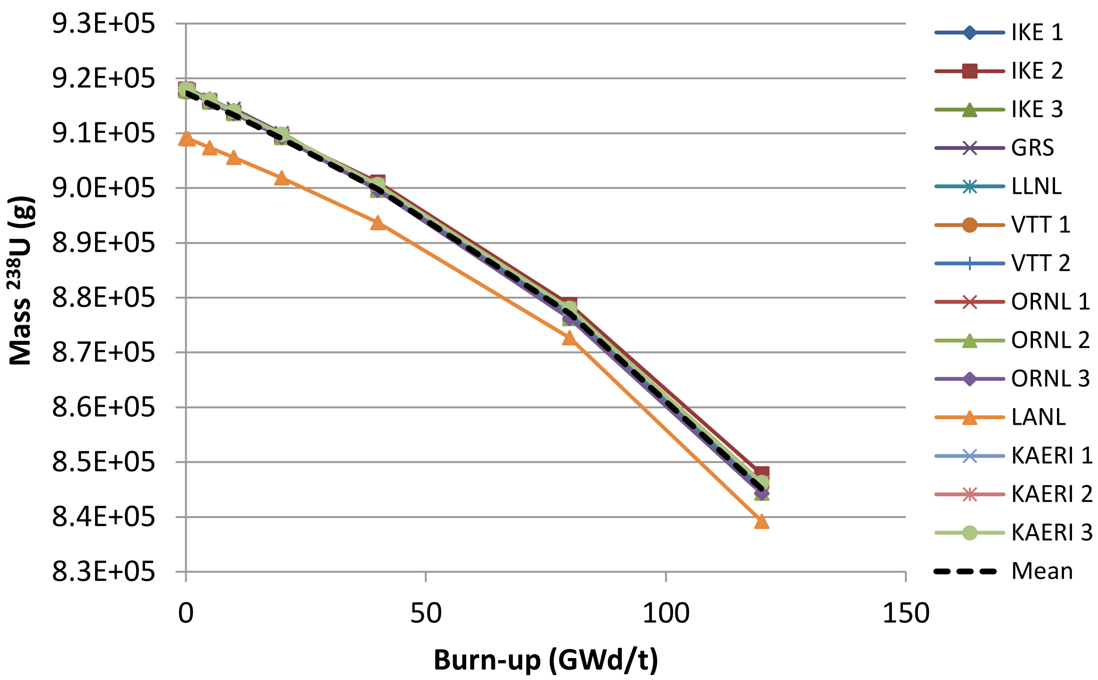

Figure 28. ^{239}Pu mass vs burn-up for pebble depletion

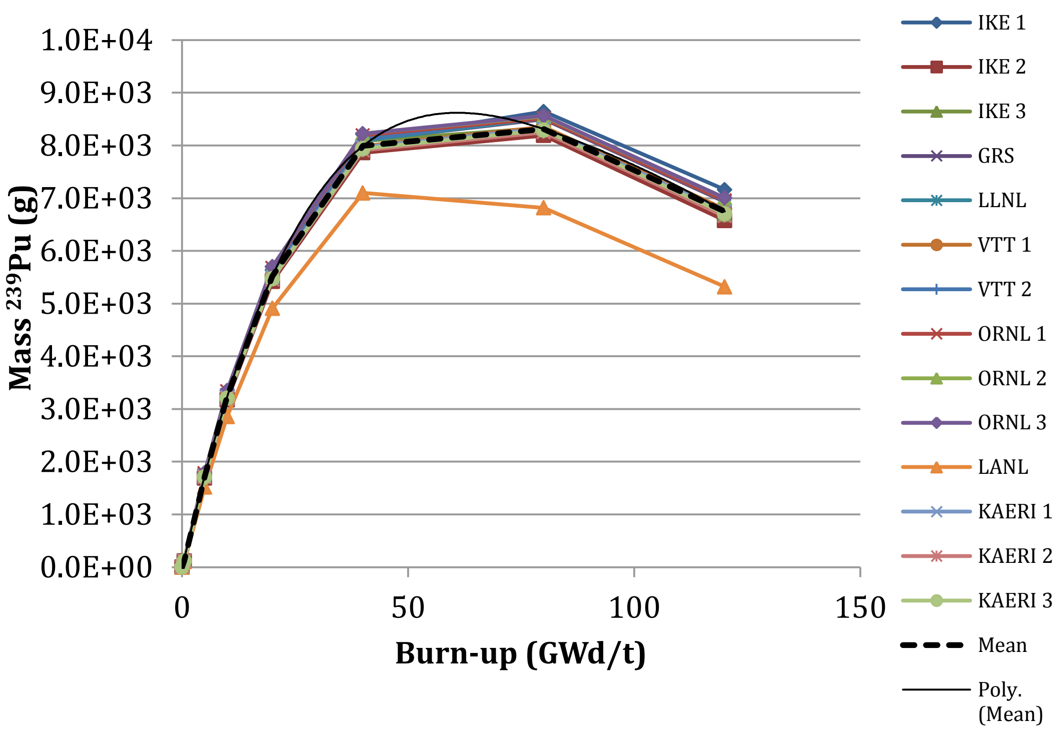

Figure 29. ^{240}Pu mass vs burn-up for pebble depletion

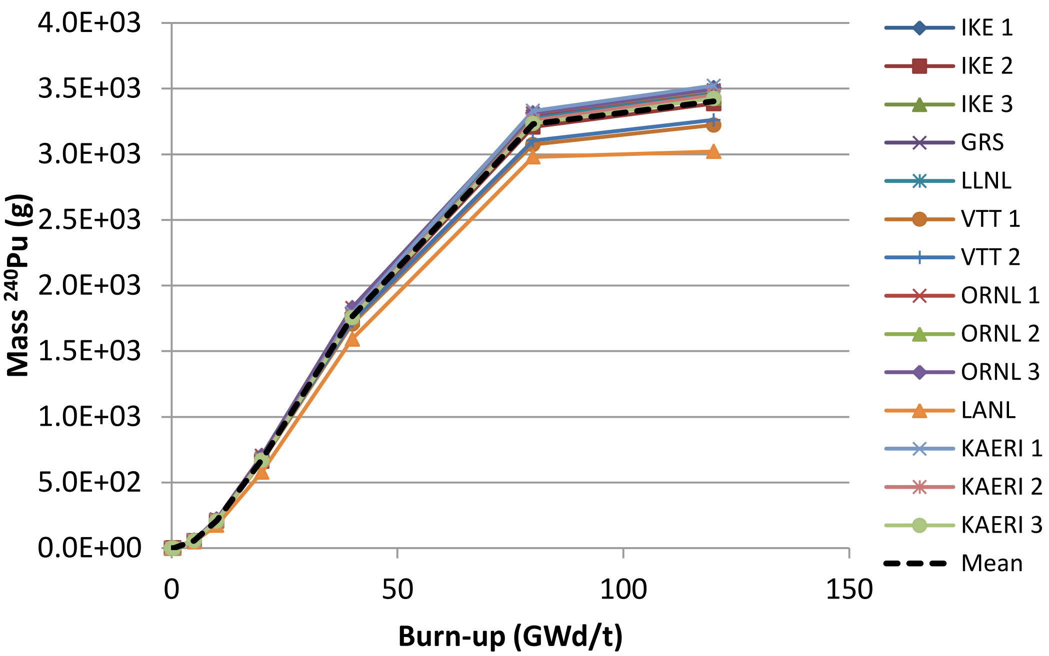

Figure 30. ^{241}**Pu mass vs burn-up for pebble depletion**

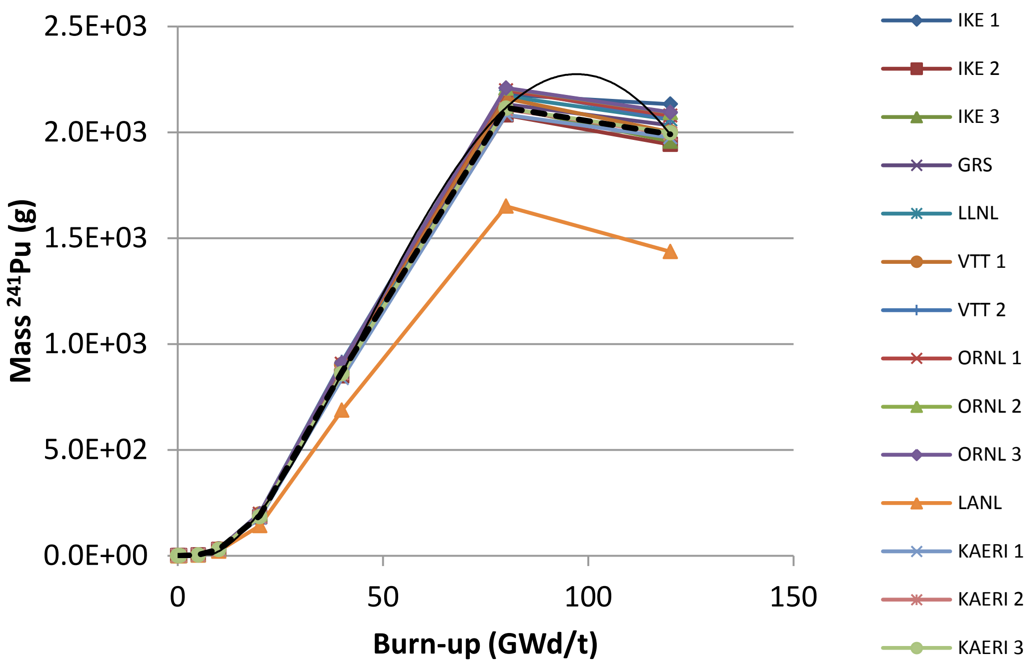

Figure 31. ^{242}**Pu mass vs burn-up for pebble depletion**

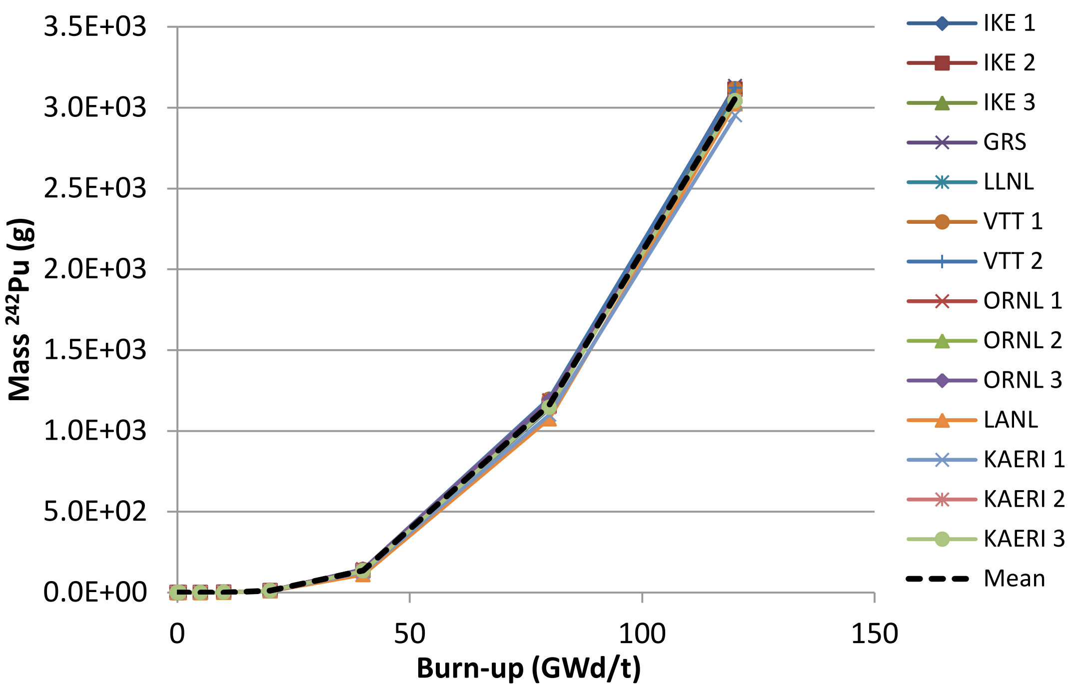

Figure 32. ^{241}Am mass vs burn-up for pebble depletion

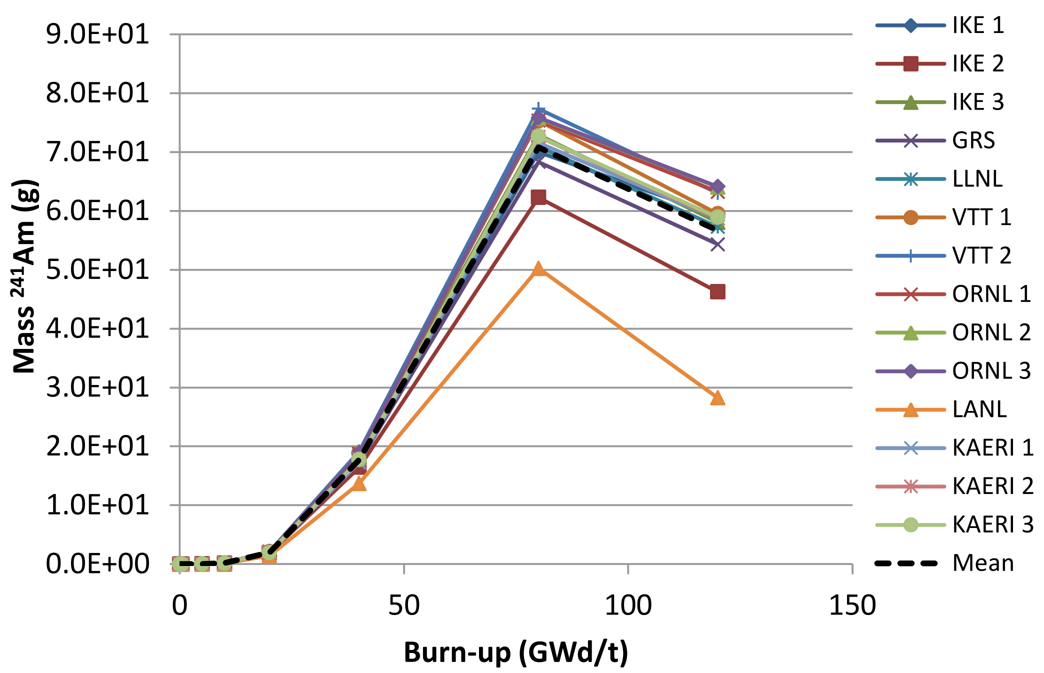

Figure 33. ^{244}Cm mass vs burn-up for pebble depletion

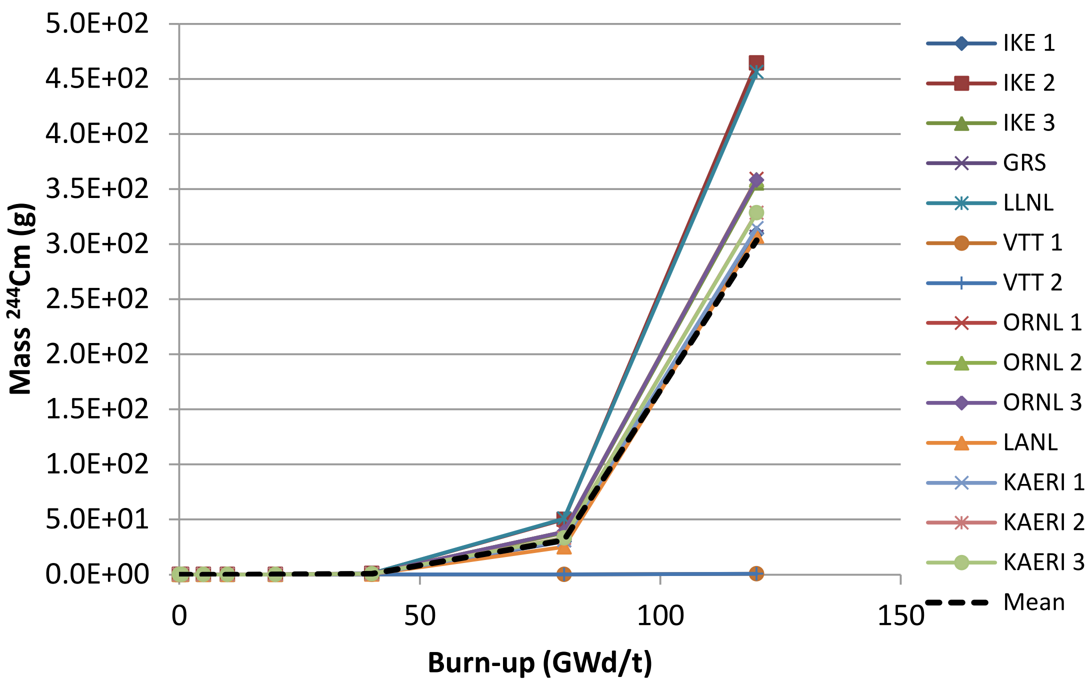

Figure 34. ^{245}Cm mass vs burn-up for pebble depletion

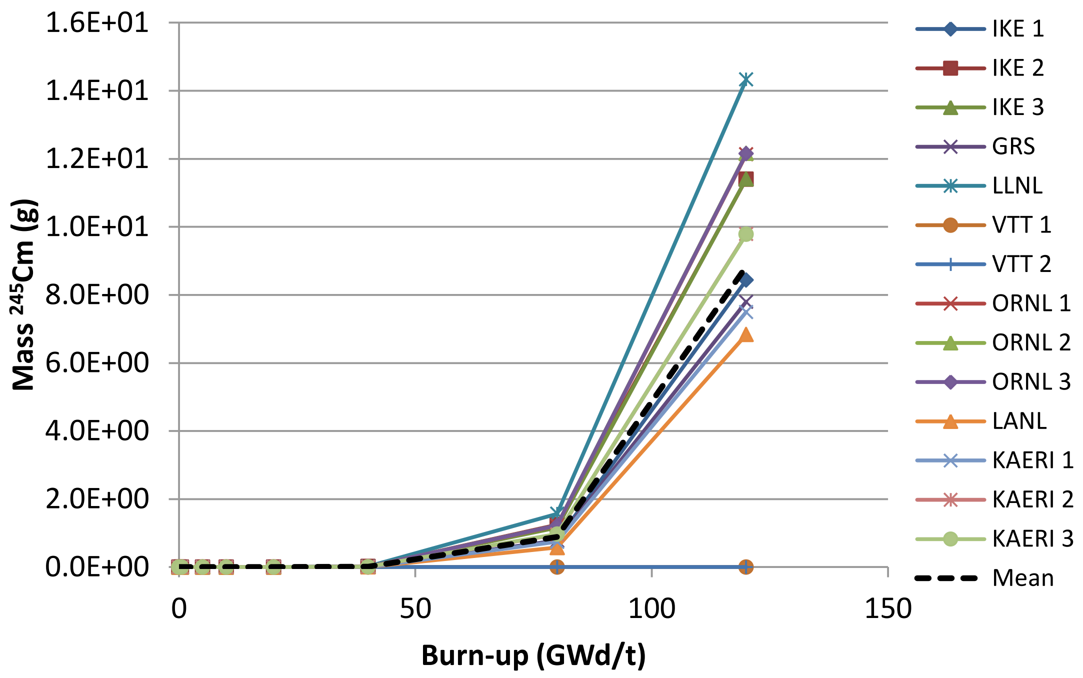

Figure 35. ^{235}U mass vs burn-up for prismatic depletion

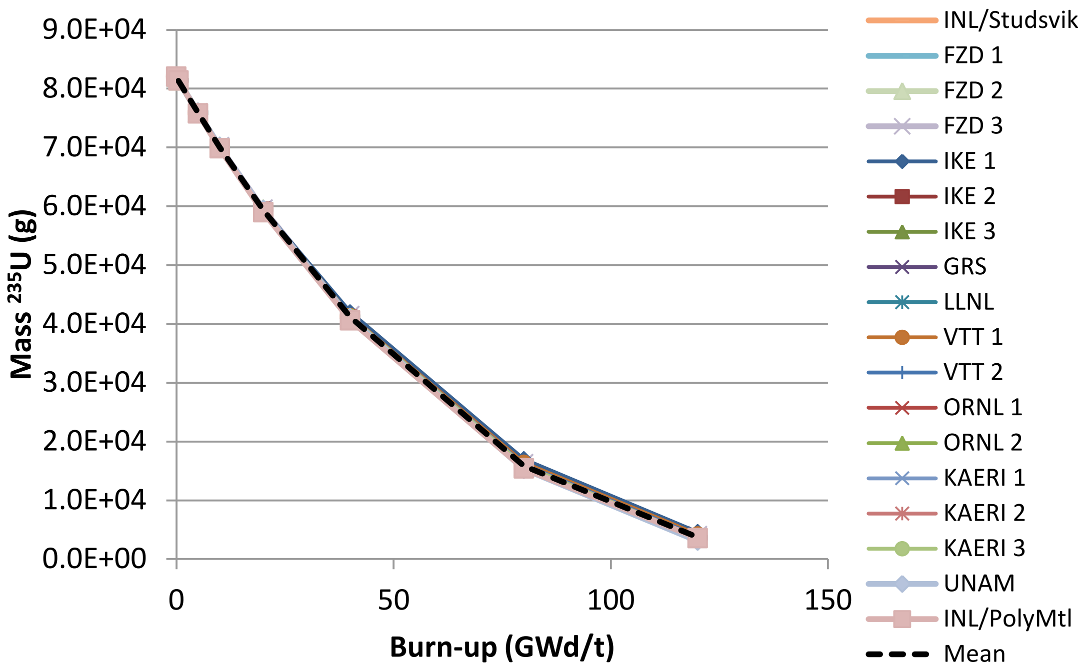

Figure 36. ^{238}**U mass vs burn-up for prismatic depletion**

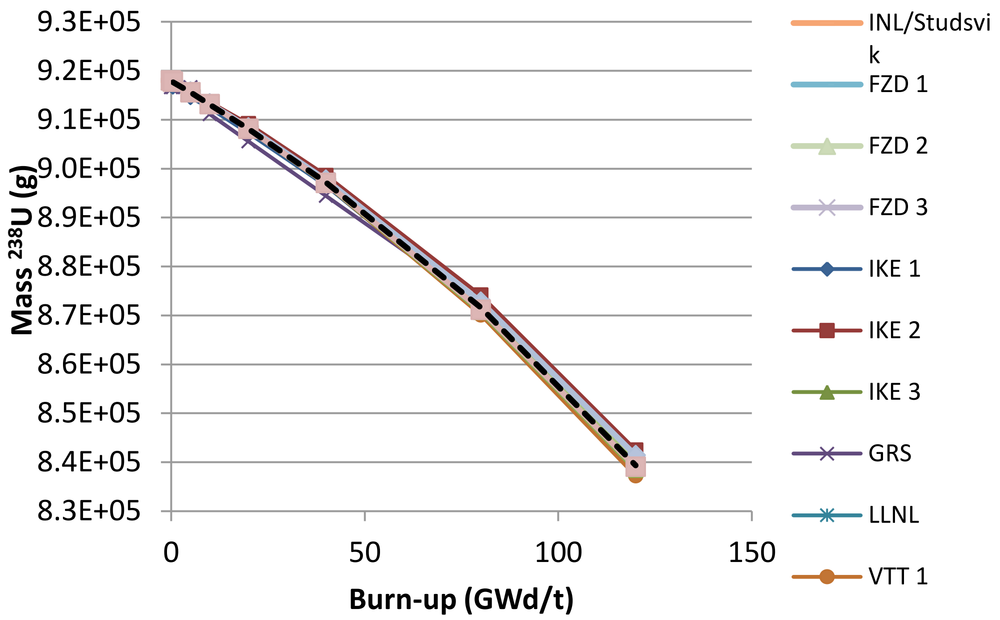

Figure 37. ^{239}**Pu mass vs burn-up for prismatic depletion**

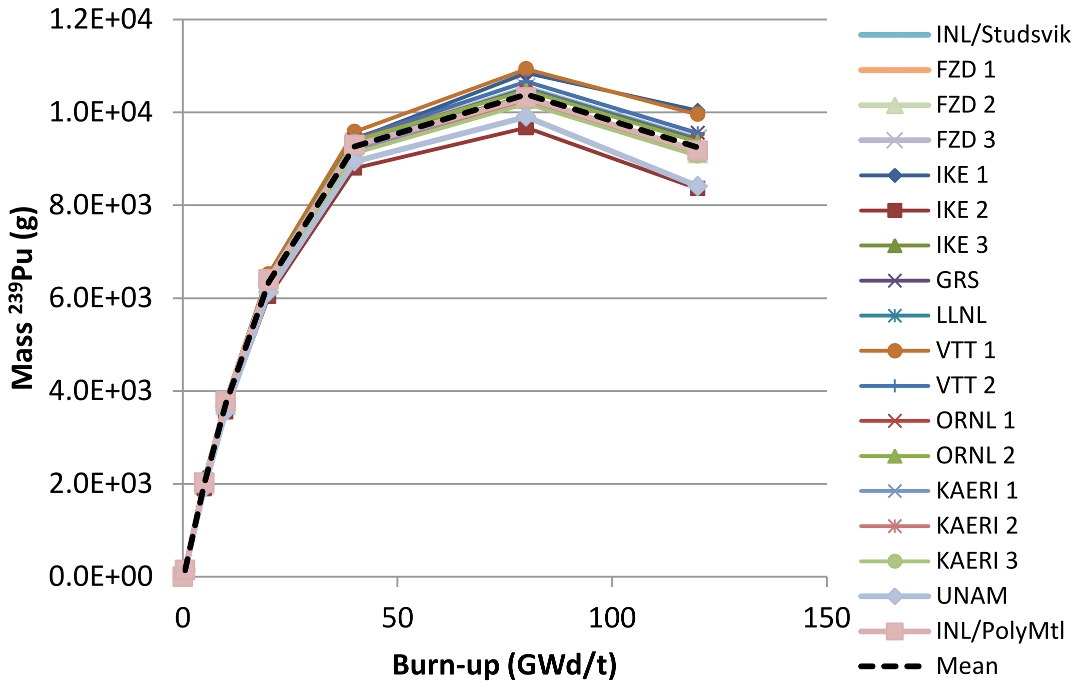

Figure 38. ^{240}Pu mass vs burn-up for prismatic depletion

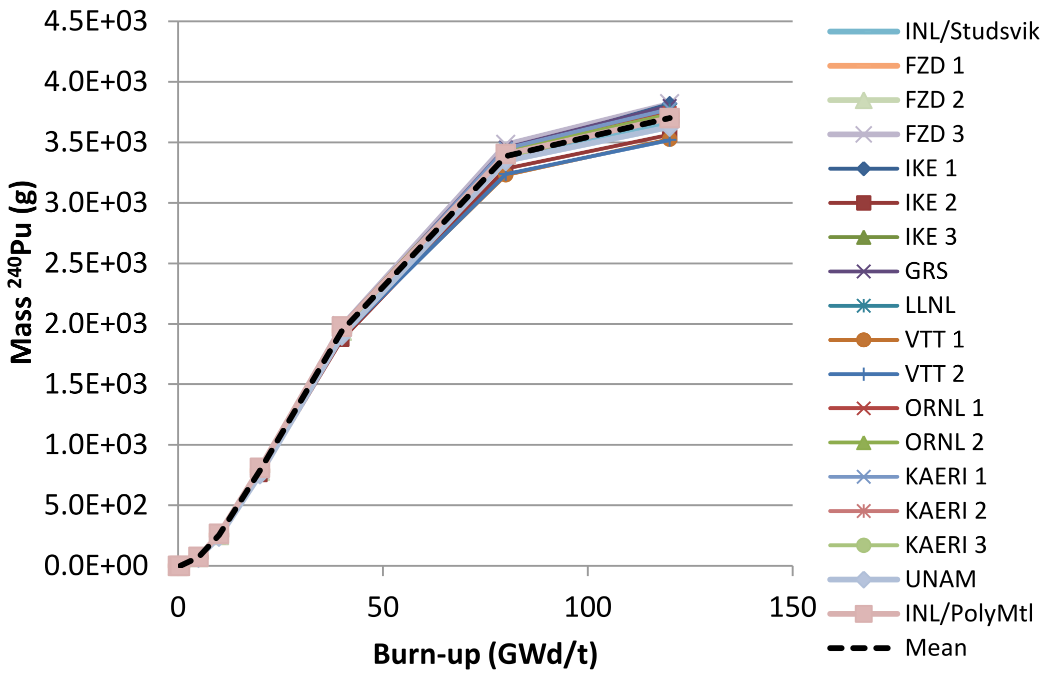

Figure 39. ^{241}Pu mass vs burn-up for prismatic depletion

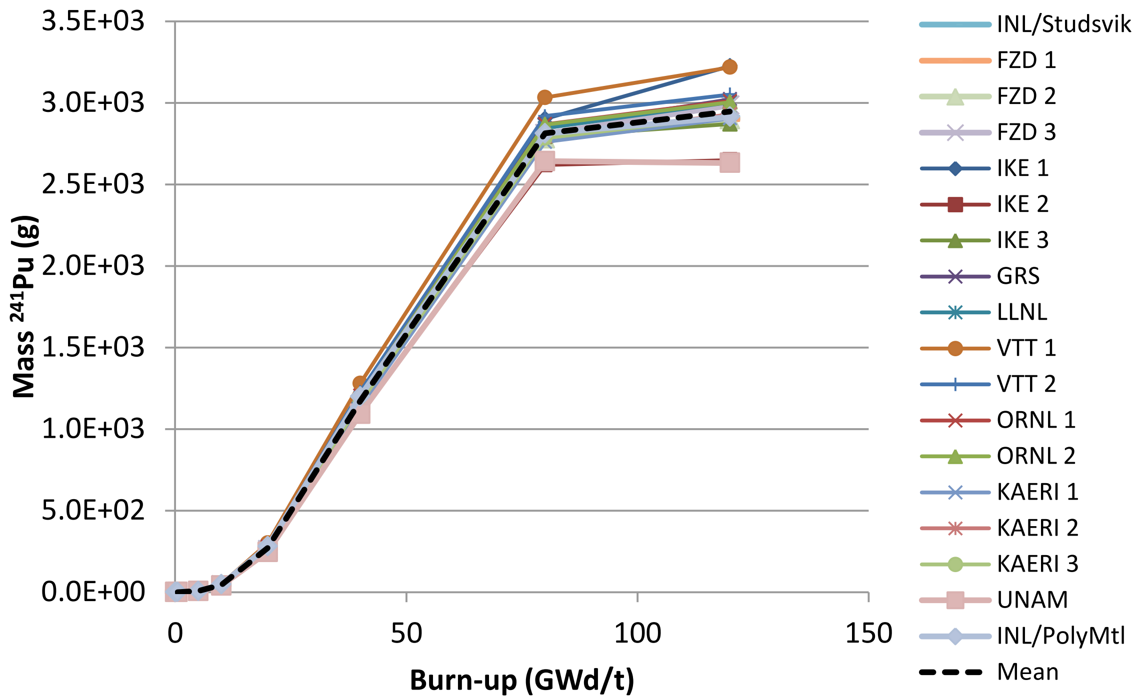

Figure 40. ^{242}Pu mass vs burn-up for prismatic depletion

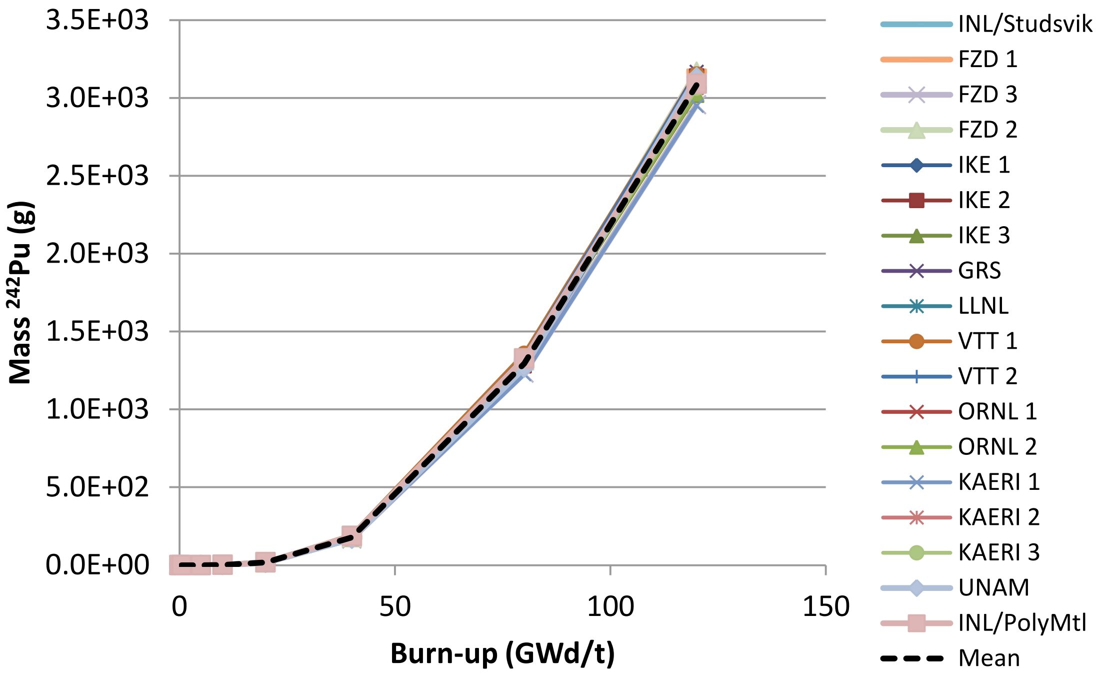

Figure 41. ^{241}Am mass vs burn-up for prismatic depletion

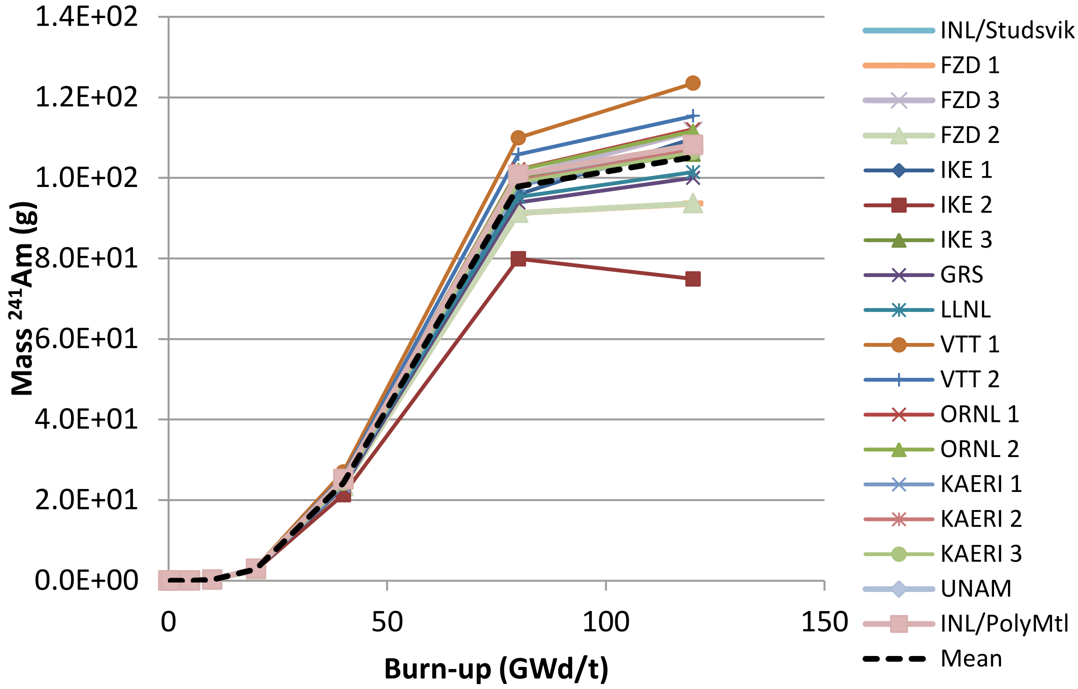

Figure 42. ^{244}**Cm mass vs burn-up for prismatic depletion**

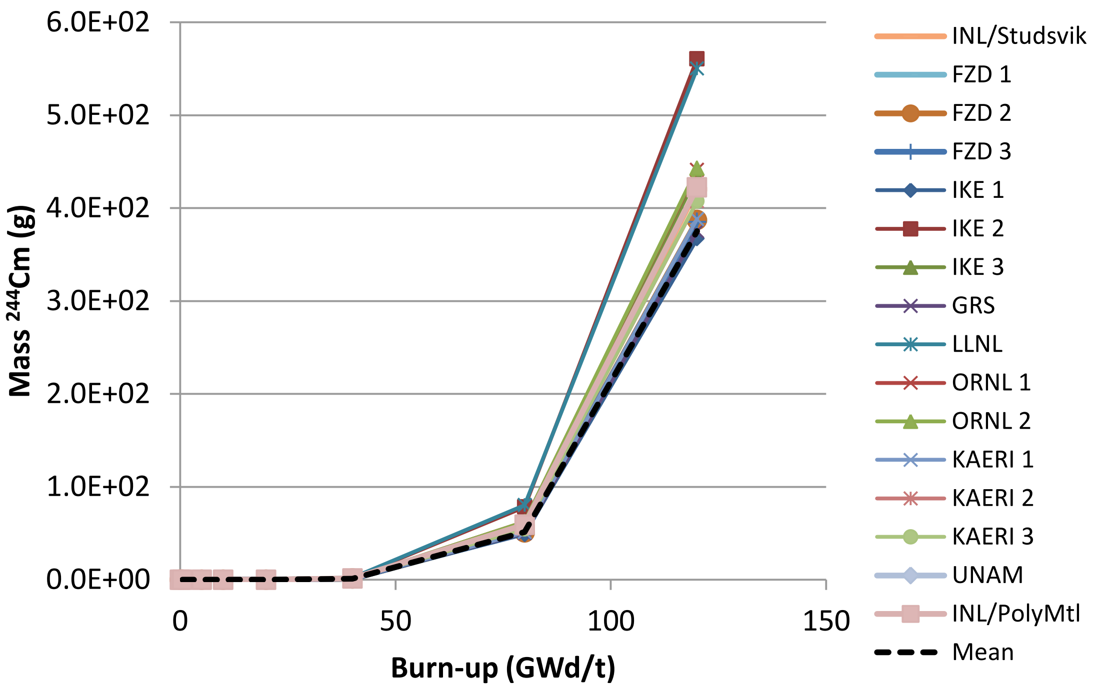

Figure 43. ^{245}**Cm mass vs burn-up for prismatic depletion**

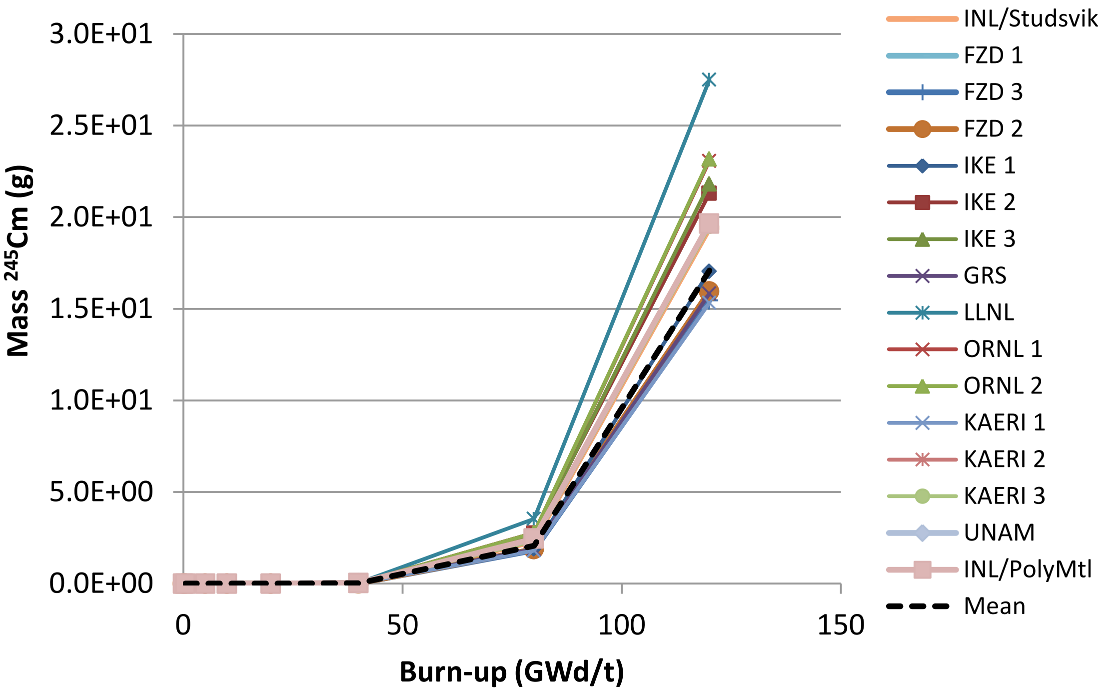

III.C.1 Actinides – Grain depletion

^{235}U – close agreement among all participants for the entire burn-up length. IKE 2 results set the lower bound on concentrations, but are not a statistical outlier.

^{238}U – close agreement for most participants. IKE 2 results are higher than the average, indicating the possibility of a slightly softer spectrum; IKE 3 results are slightly lower than the average, indicating a possibly harder spectrum.

^{239}Pu – not surprisingly, trends seen for ^{238}U are reversed and magnified for this nuclide. IKE 2 under-predicts ^{239}Pu inventories relative to the mean of the submitted values, while IKE 3 overestimates the mass of this nuclide compared to the mean.

^{240}Pu – more dispersion is seen among results – this dispersion results in the spectral differences noted earlier, but is magnified by the much smaller mass of ^{240}Pu produced by successive capture reactions. IKE 1 is low for this nuclide but has been consistent elsewhere, indicating a possible inconsistency in ^{239}Np branching fractions.

^{241}Pu – trends for this nuclide are consistent with the observations for ^{239}Pu, with not as much deviation from the average as was seen with ^{240}Pu.

^{242}Pu – results are generally consistent among all participants; however, two groups of results are seen. FZD 1, FZD 2, IKE 3, GRS and UNAM are in close agreement at EOL but slightly below the mean, while IKE 1, IKE 2, VTT 2 results are grouped together above the mean at the same burn-up. The lower group is more populated with joint evaluated fission and fusion (JEFF) 3.1 data, while the upper group tends to represent ENDF data. However, there are exceptions and no clear conclusions can be drawn. An inconsistency is seen in UNAM results at the 10 GWd/t burn-up point – this is possibly a data transcription error.

^{241}Am – a larger spread in results is seen for this nuclide, but this is primarily due to scale magnification since ^{241}Am inventories are more than an order of magnitude lower than Pu inventories. However, IKE3 remains high, and IKE2 low, relative to other participants.

^{244}Cm – results are in good agreement considering the small inventory of this nuclide. Here IKE3 is slightly high and IKE2 is significantly higher than the average. The average here is somewhat biased, as zero inventory was reported in UNAM results.

^{245}Cm – again, results are in good agreement considering the very small inventory of this nuclide. Here both IKE2 and IKE3 are significantly higher than other results, but the spread is perhaps not meaningful given the magnitude of the inventory. The average here is also biased by zero inventories.

III.C.2 Actinides – Pebble depletion

^{235}U – close agreement among all but one of the participants for the entire burn-up length; LANL results are somewhat low. This is consistent with differences seen in the spectral indices earlier.

^{238}U – Again, agreement is seen for all participants except for LANL. However, it is clear from this plot that the initial inventory in the LANL results was incorrect, causing the spectral differences seen earlier. Thus, no further comment will be made on LANL results – they are not expected to be consistent with other results. For other participants, better agreement is seen than for grain results. IKE2 results are slightly higher than other participants, but are in closer agreement than was seen for grain depletion.

^{239}Pu – Again, as with grain depletion, trends seen for ^{238}U are reversed and magnified for this nuclide. IKE2 comes in slightly low in prediction of ^{239}Pu inventories, while IKE3 overestimates the mass of this nuclide slightly relative to other participants. It is noted that in these results ^{239}Pu inventories peak between 40 and 120 GWd/t burn-up, decreasing for the last 1/3 to 1/2 of the burn period. This behaviour is not seen in the grain depletion results. A fourth order polynomial fit to the average indicates that the inventory is maximised around 60 GWd/t, although a more detailed depletion analysis would be necessary to identify the peak location more precisely.

^{240}Pu – Unlike ^{239}Pu, ^{240}Pu inventories are found to increase over the entire burn-up period. The outliers for this case are now VTT 1 and VTT 2, although the two are grouped together. This suggests a possible data difference.

^{241}Pu – Reasonable agreement is seen for all participants (excepting LANL), with a slightly increasing spread in data with burn-up. All results show the same trend, with inventory peaking around 100 GWd/t burn-up and then decreasing. This corresponds to the depletion of competing ^{235}U, and increased fissioning of ^{241}Pu.

^{242}Pu – Very good agreement is seen among all participants, all showing an exponential increase with burn-up.

^{241}Am – Trends here mimic ^{241}Pu, but with more spread in results. LANL results are the lowest outlier, but IKE 2 is also significantly lower than the average and GRS as the lowest of the clustered results.

^{244}Cm – Results are clustered in three groups: IKE 2 and GRS are above the average, the three ORNL results are in the next grouping, with remaining results clustered more closely together.

^{245}Cm – participants all show the same trend with inventories increasing exponentially with burn-up. There is a significant spread in participants' predictions, but this result at least in part from the small mass of the product.

III.C.3 Actinides – Prismatic depletion

^{235}U – extremely close agreement among all participants. The outlier from the pebble depletion case did not contribute to this calculation. Excepting that outlier, both pebble and prismatic results are in better agreement than the grain calculation. Given that the grain calculation is much more direct and simpler, it is unclear why the other two configurations are in better overall agreement. Offsetting effects are a possibility, but are unlikely to be consistent for all participants. More likely is simply differences in participants in each phase.

^{238}U – Again, reasonable agreement is seen for all participants, although not as good as was seen for ^{235}U. This may suggest the spectral differences; in fact, these results are consistent with spectral index ρ_{238} in Figure 13. Interestingly, GRS results take an unexpected dip beginning at around 15 GWd/t, but later become consistent with the nuclide average. The dip may be a result of the increase in time step size that occurs at this burn-up.

^{239}Pu – Again, as with the other depletion types, trends seen for ^{238}U are reversed and magnified for this nuclide. IKE 2 and UNAM come in slightly low in prediction of ^{239}Pu inventories, while VTT1 and VTT 2 both overestimate the mass of this nuclide slightly relative to other participants. It is noted that as in the pebble calculations, in these results ^{239}Pu inventories peak between 40 and 120 GWd/t burn-up, decreasing for the last 1/3 to 1/2 of the burn period. This behaviour is not seen in the grain depletion results.

^{240}Pu – Unlike ^{239}Pu, ^{240}Pu inventories are found to increase over the entire burn-up period. The outliers for the prismatic case are VTT 1 and VTT 2 as was seen for the pebble depletion results; again the two are grouped together. IKE 2 results are also observed to be slightly lower for this nuclide.

^{241}Pu – Unlike results for pebble depletion, a number of outliers are observed for this calculation. VTT 1 and VTT 2 are both high, although not showing the same trend with burn-up, while UNAM and IKE 2 are low. In general, however, all results show the same trend. Unlike pebble depletion, a peak inventory may be occurring but at a higher burn-up, perhaps greater than 120 MWd/t, with inventory peaking around 100 GWd/t burn-up and then decreasing. This corresponds to the depletion of competing ^{235}U (which does not deplete as fast as for the pebble case), and hence the corresponding increase in ^{241}Pu fission.

^{242}Pu – Very good agreement is seen among all participants, all showing an exponential increase with burn-up, as was seen with the other depletion types. Again, pebble and prismatic cases are in slightly better agreement than the grain depletion case.

^{241}Am – Trends here mimic ^{241}Pu, but with more spread in results. IKE 2 results are the lowest outlier, as seen in prismatic depletion, but in this case VTT 1 and VTT 2 are upper outliers.

^{244}Cm – Different trends are seen here relative to the pebble results. While most results are fairly closely clustered (spreading slightly with burn-up), IKE 2 and KAERI 1 results are outliers on the upper end.

^{245}Cm – participants all show the same trend with inventories increasing exponentially with burn-up. There is a significant spread in participants' predictions, but this result at least in part from the small mass of the product. KAERI 1 results are high as was seen with ^{244}Cm, but IKE 2 results are not.

III.D. Fission product depletion

Isotopic inventories were requested for seven fission products ^{85}Kr, ^{90}Sr, ^{110m}Ag, ^{137}Cs, ^{135}Xe, ^{149}Sm and ^{151}Sm for the three fuel types. These nuclides were selected as being the best indicators of depletion modelling in a graphite reactor. Results are provided in Figures 44-50 for the infinite grain lattice Figures 51-57 for the pebble configuration and Figures 58-64 for the prismatic supercell. As in the previous sections, the following subsections provide a very brief and qualitative review of results by nuclide for each configuration type. The reader can review the plots and draw their own conclusions as to the overall performance.

Figure 44. ^{85}Kr mass vs burn-up for grain depletion

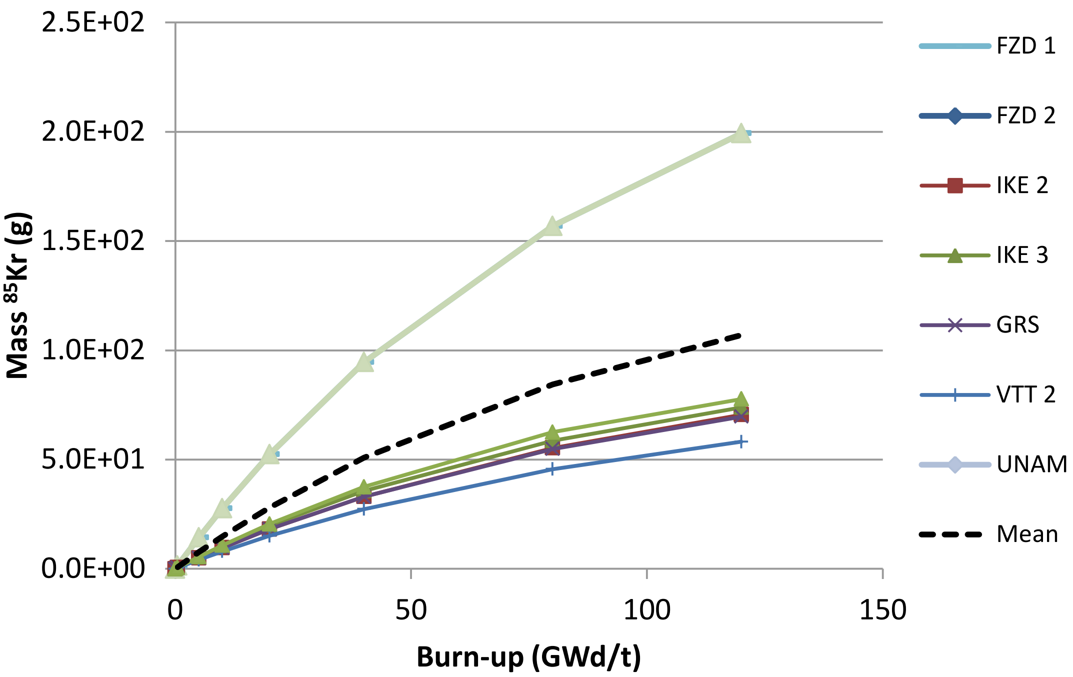

Figure 45. ^{90}Sr mass vs burn-up for grain depletion

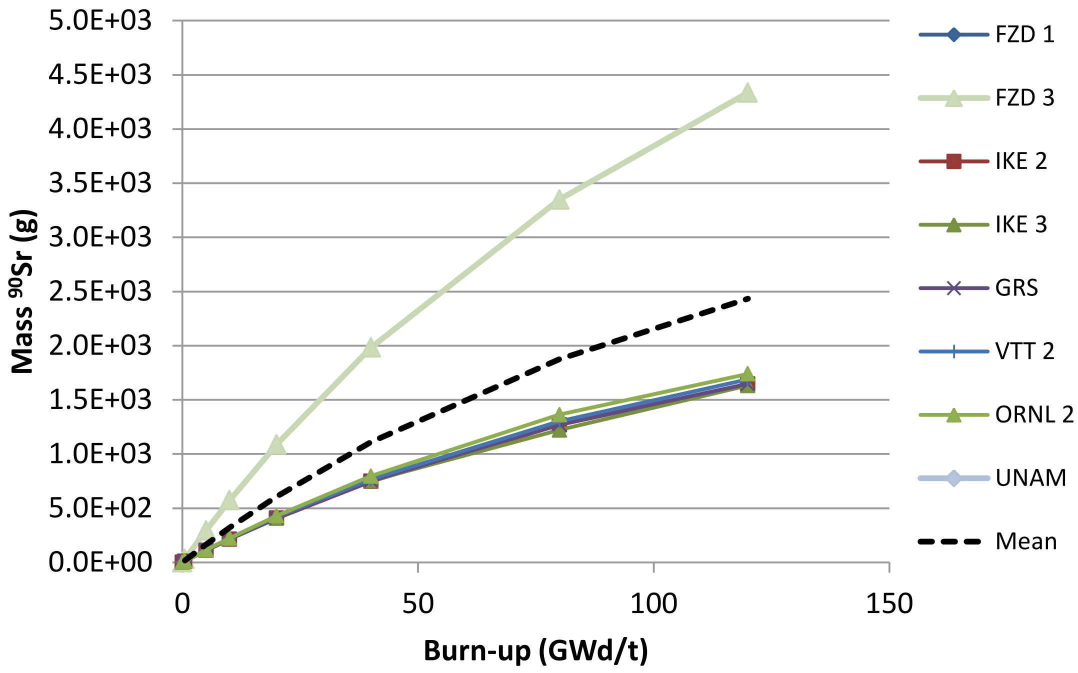

Figure 46. ^{110m}Ag mass vs burn-up for grain depletion

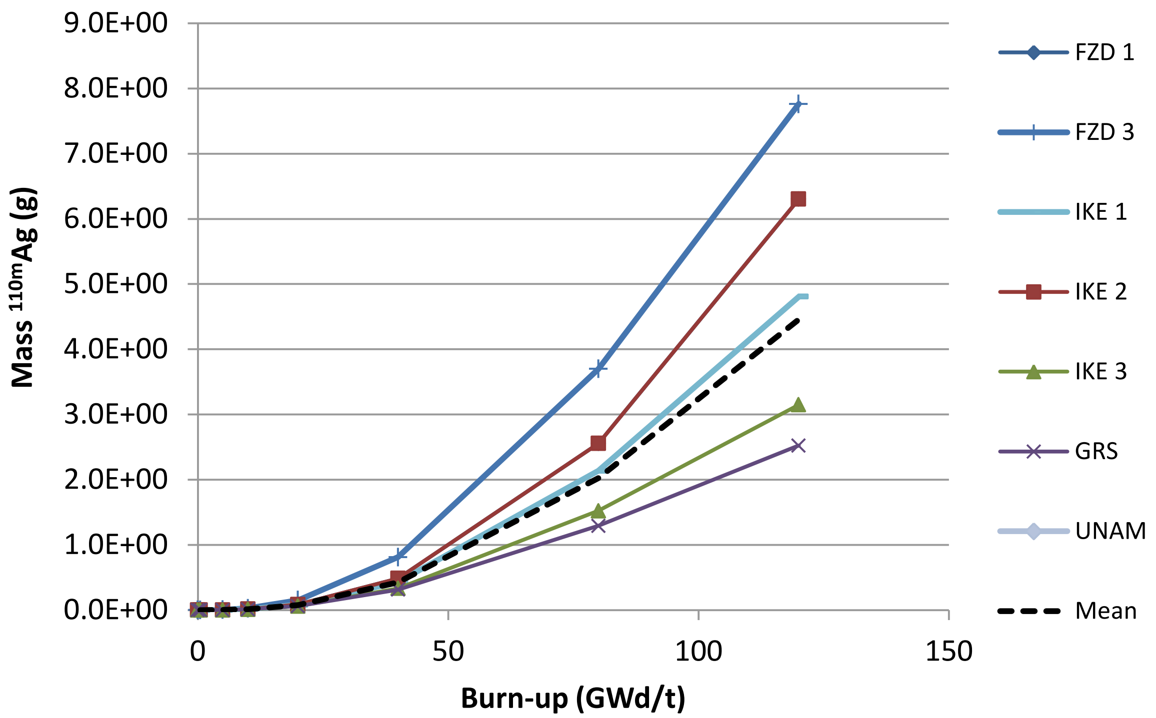

Figure 47. ^{137}Cs mass vs burn-up for grain depletion

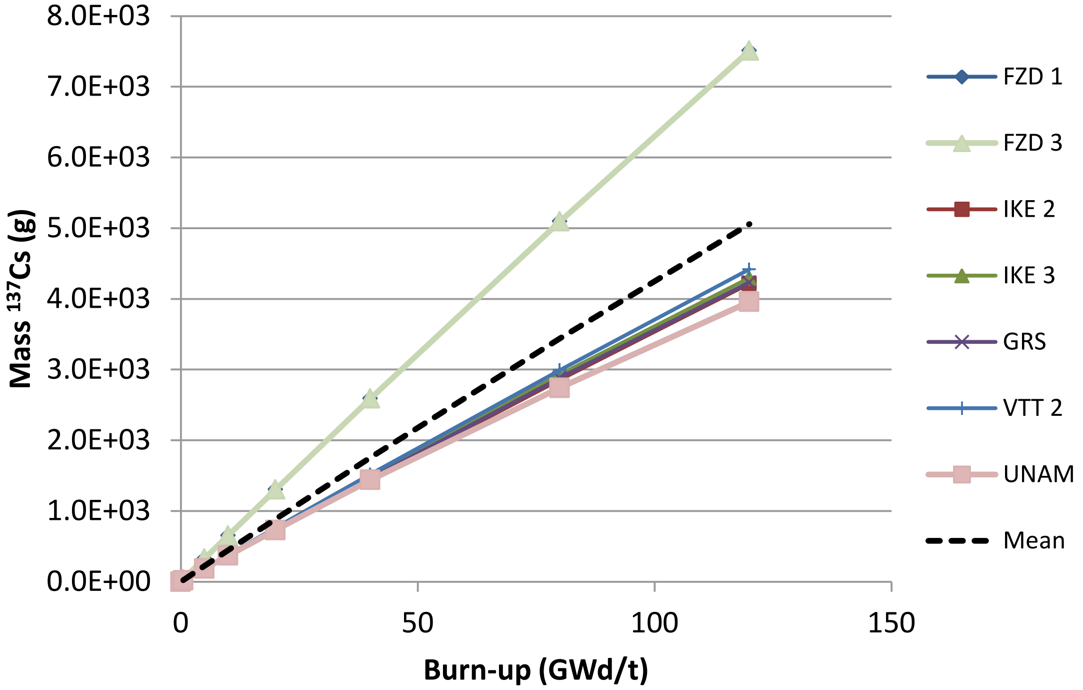

Figure 48. ^{135}Xe mass vs burn-up for grain depletion

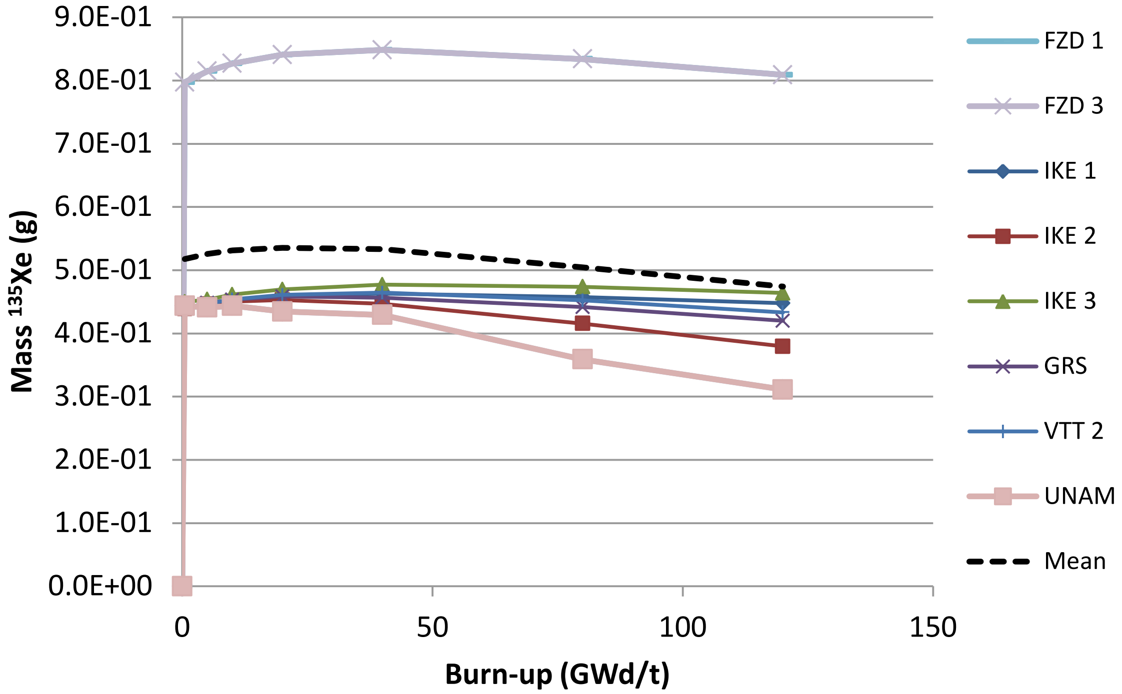

Figure 49. ^{149}Sm mass vs burn-up for grain depletion

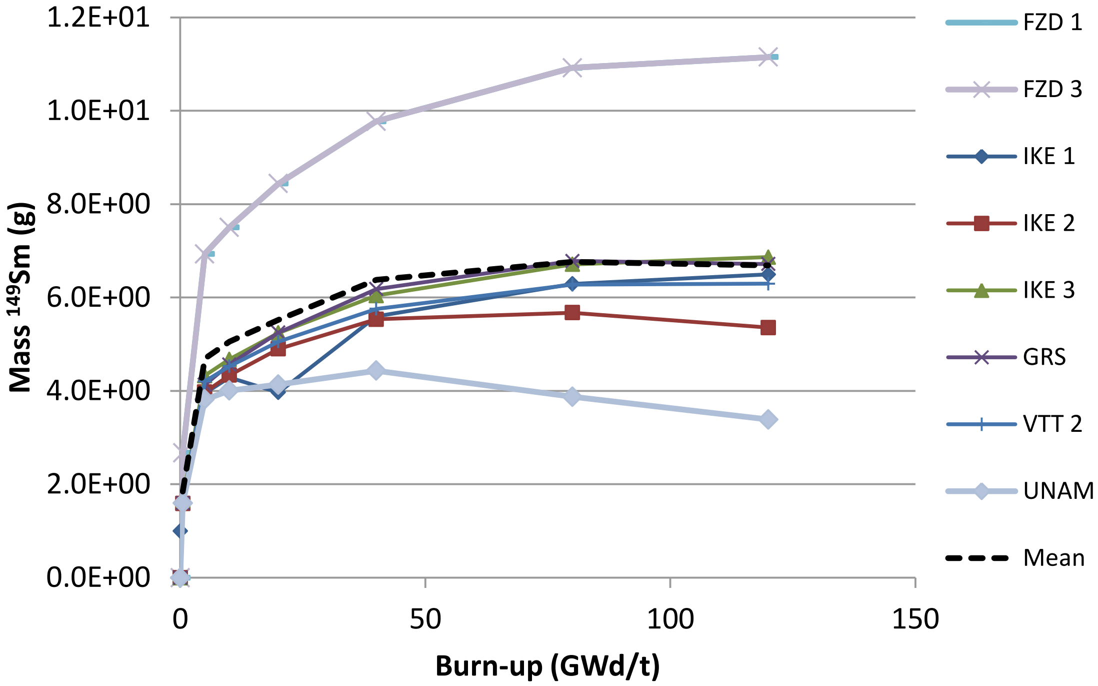

Figure 50. ^{151}Sm mass vs burn-up for grain depletion

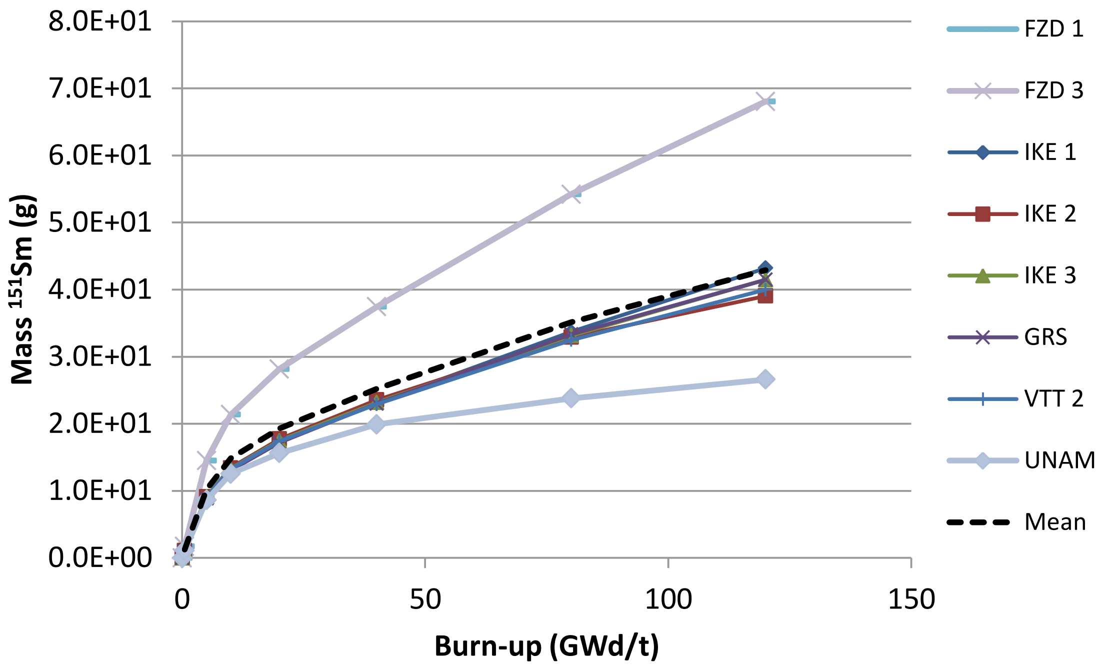

Figure 51. ^{85}Kr mass vs burn-up for pebble depletion

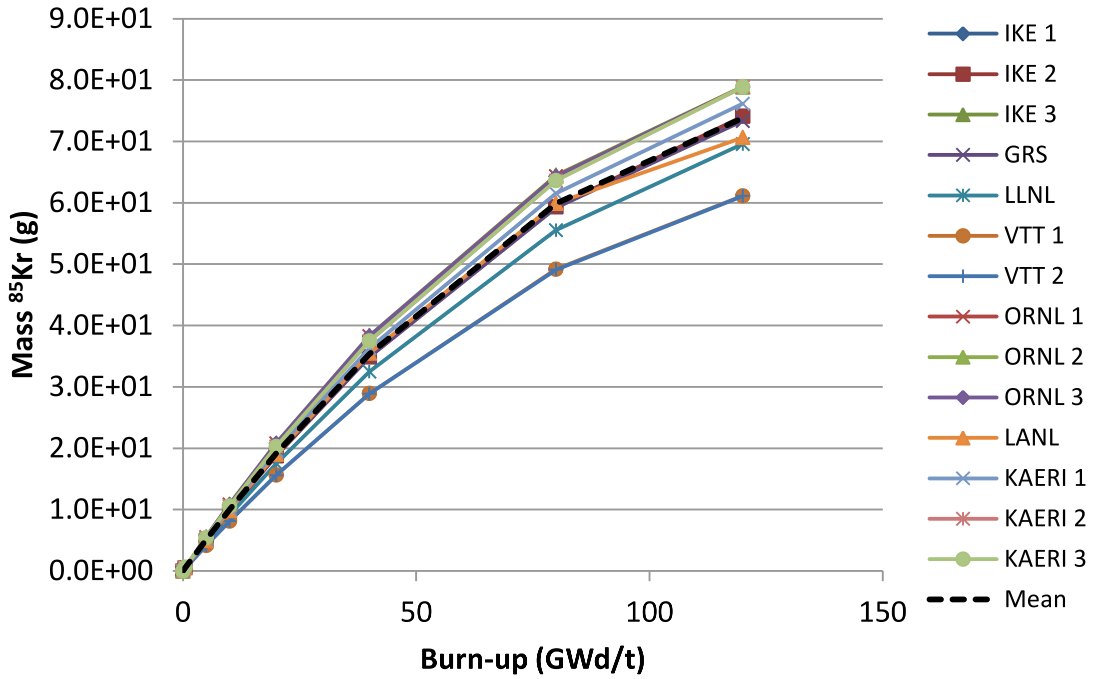

Figure 52. ^{90}Sr mass vs burn-up for pebble depletion

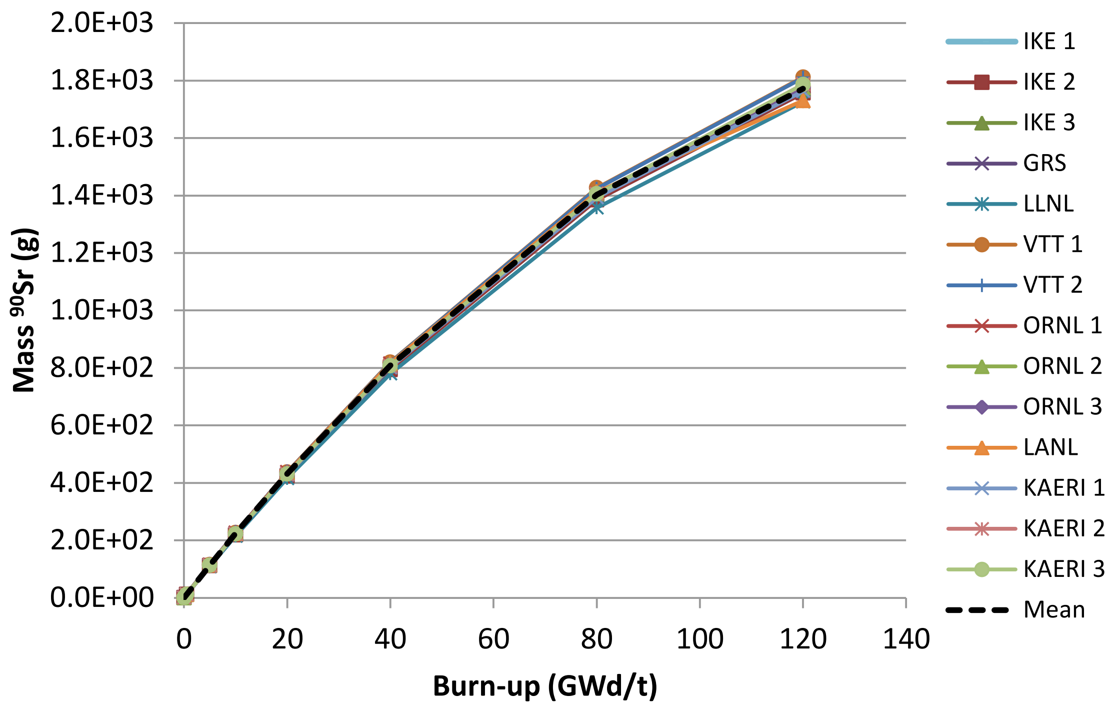

Figure 53. ^{110m}Ag mass vs burn-up for pebble depletion

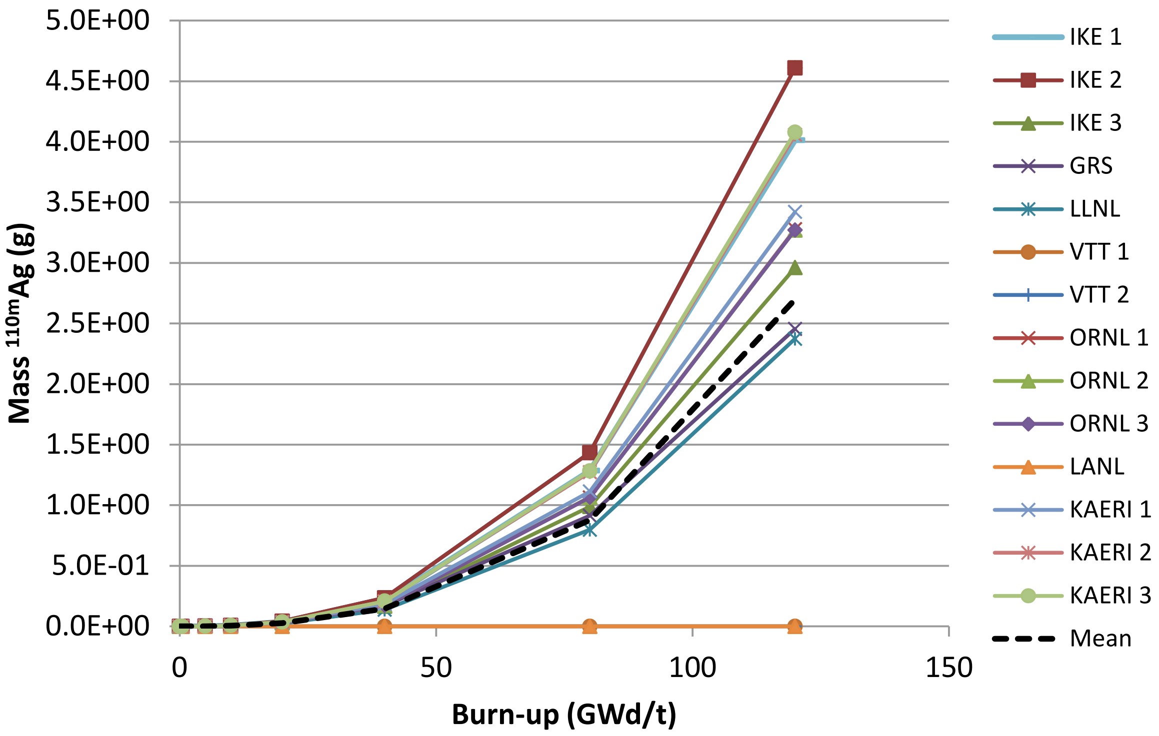

Figure 54. ^{137}Cs mass vs burn-up for pebble depletion

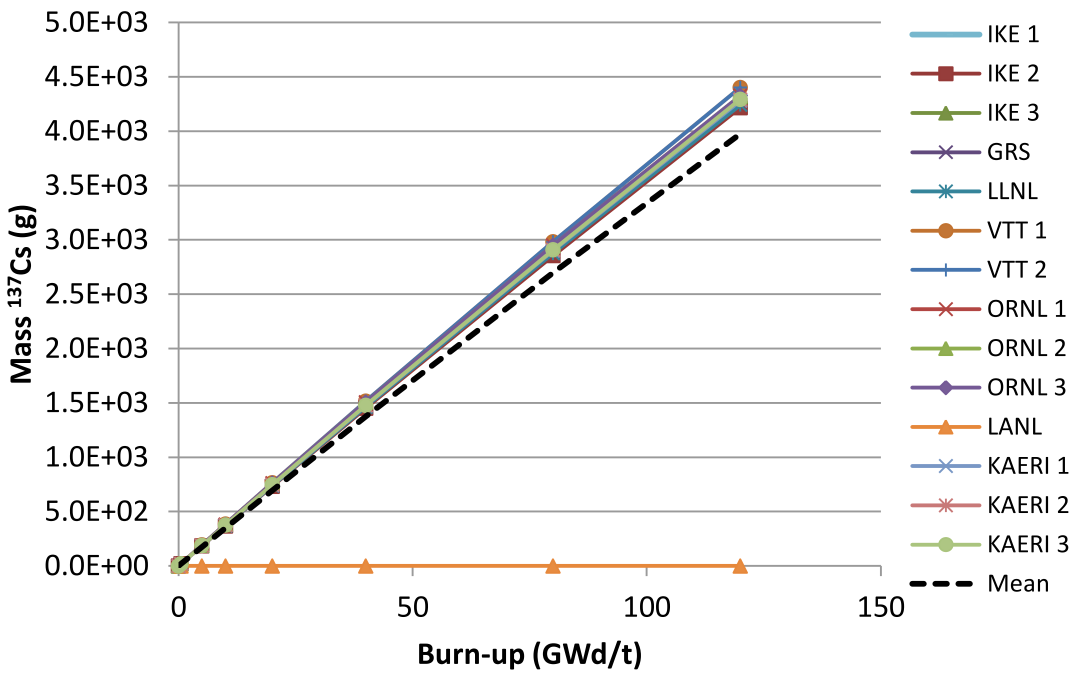

Figure 55. ^{135}Xe mass vs burn-up for pebble depletion

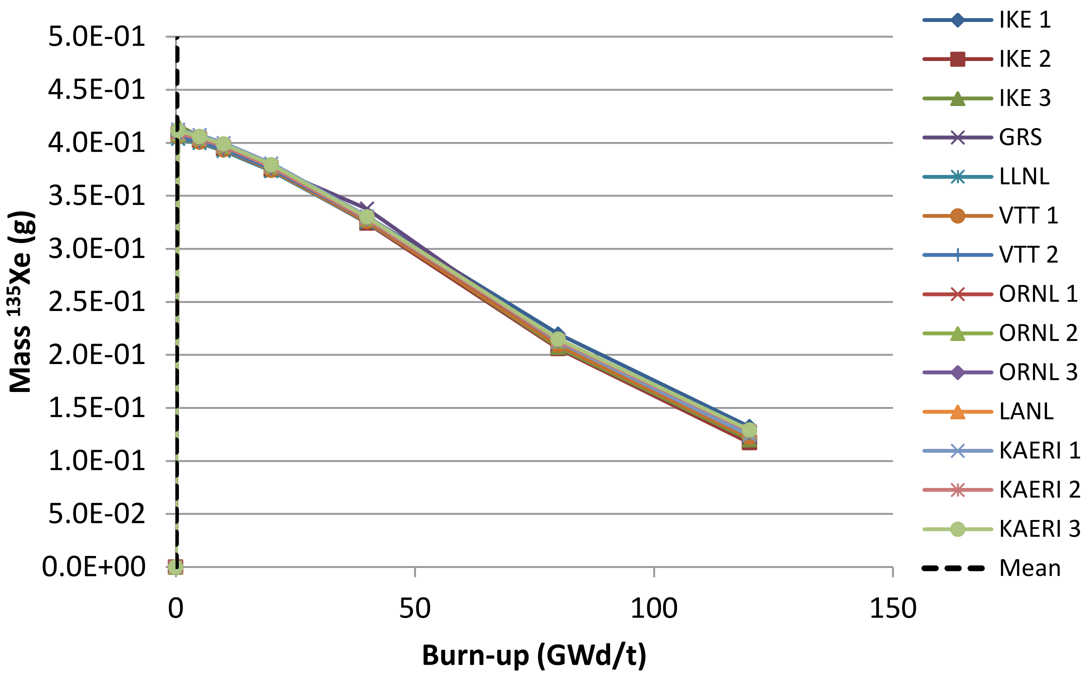

Figure 56. ^{149}Sm mass vs burn-up for pebble depletion

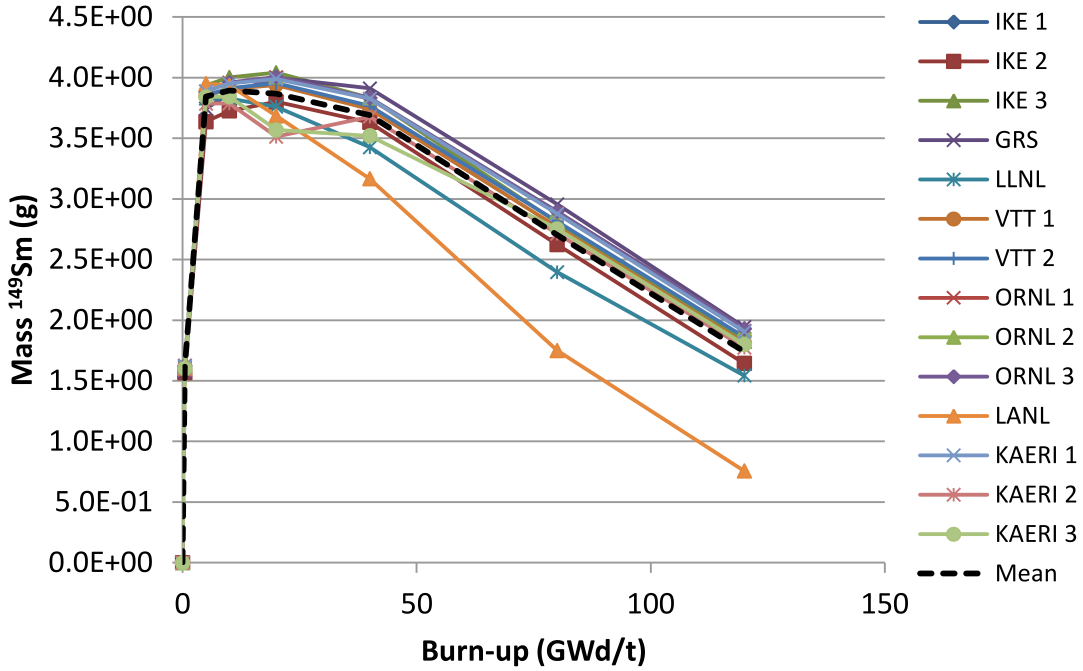

Figure 57. ^{151}Sm mass vs burn-up for pebble depletion

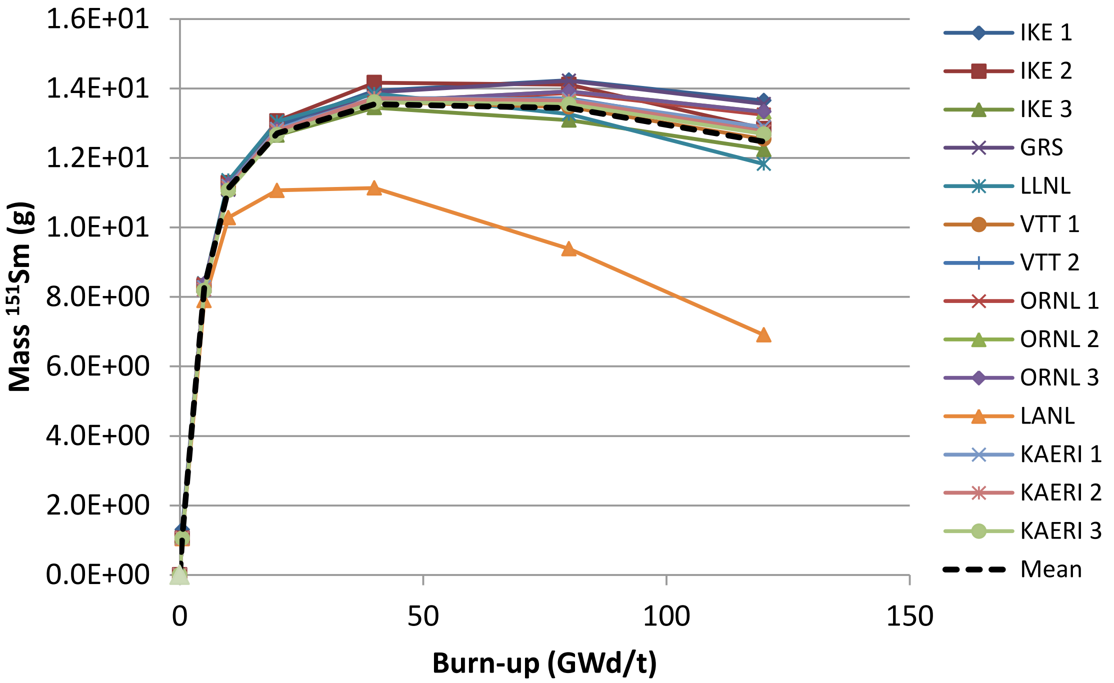

Figure 58. ^{85}Kr mass vs burn-up for prismatic depletion

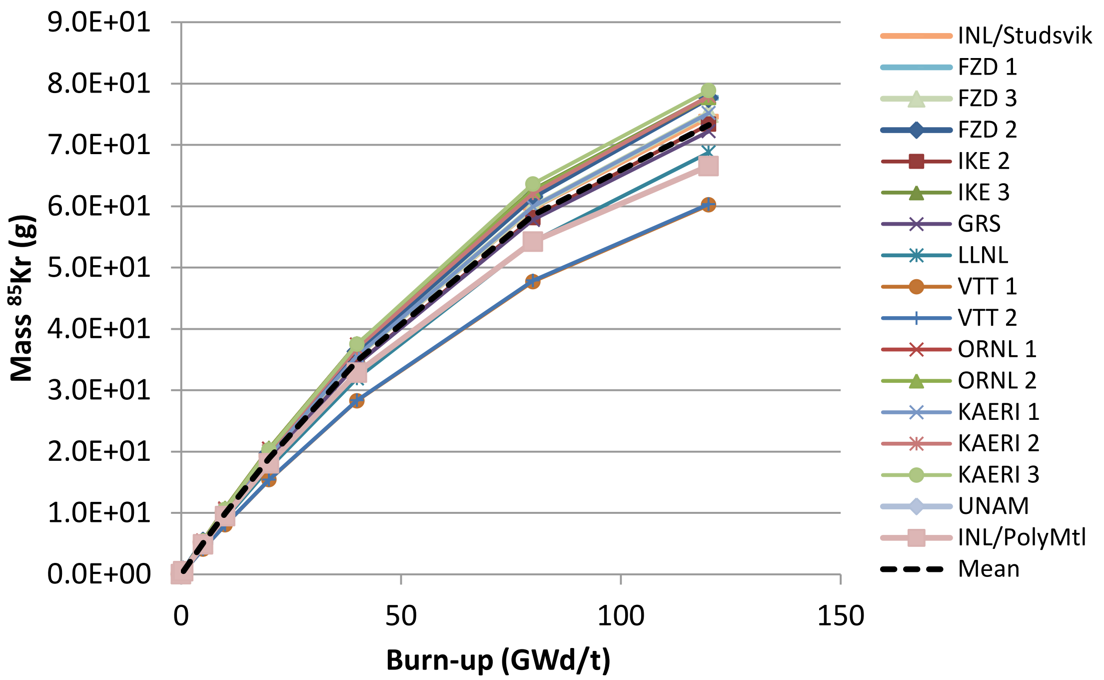

Figure 59. ^{90}Sr mass vs burn-up for prismatic depletion

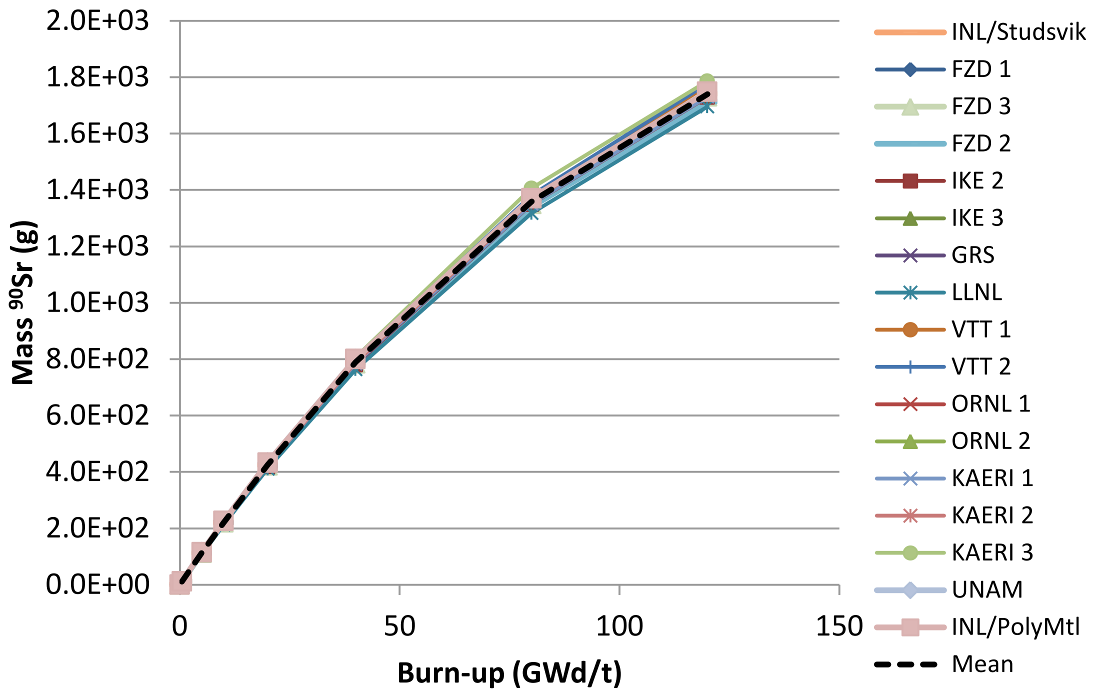

Figure 60. ^{110m}Ag mass vs burn-up for prismatic depletion

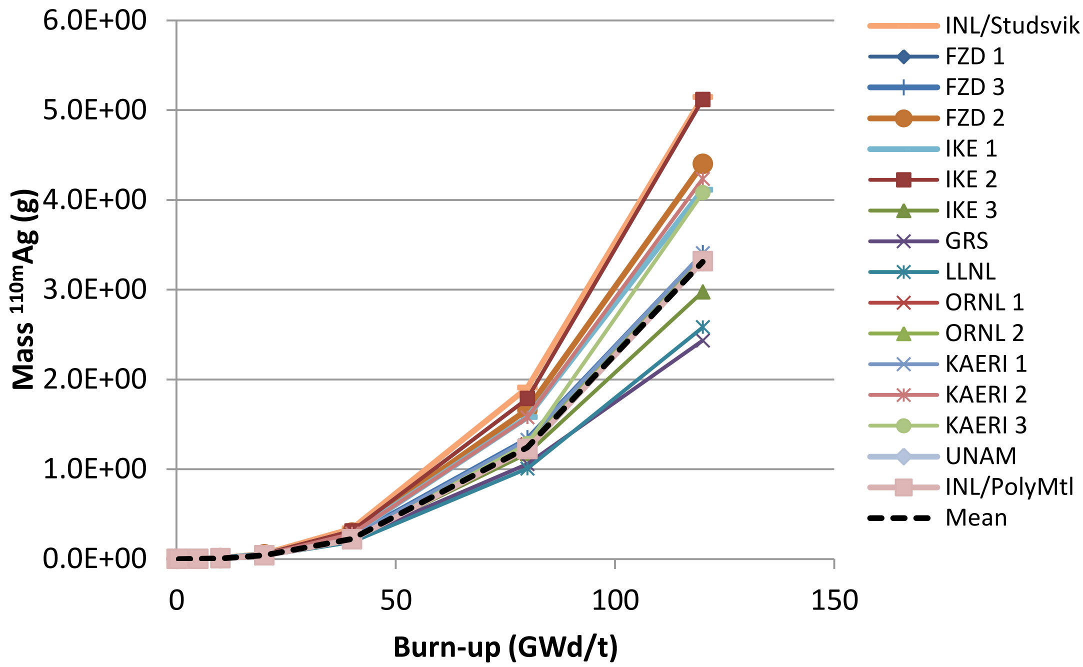

Figure 61. ^{137}Cs mass vs burn-up for prismatic depletion

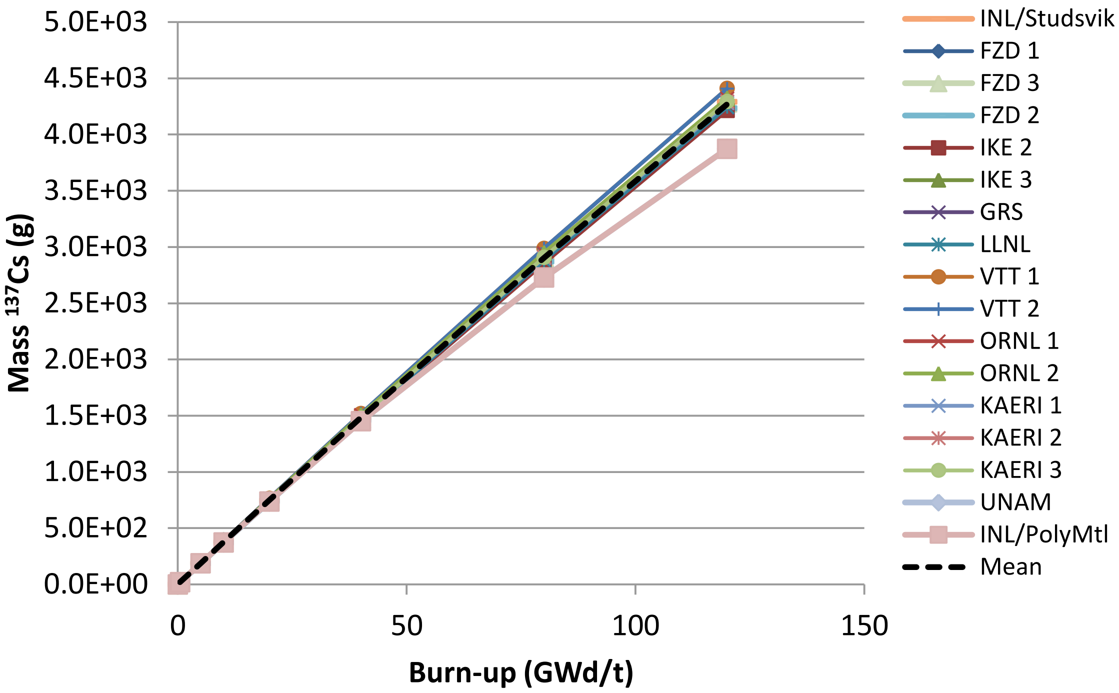

Figure 62. ^{135}Xe mass vs burn-up for prismatic depletion

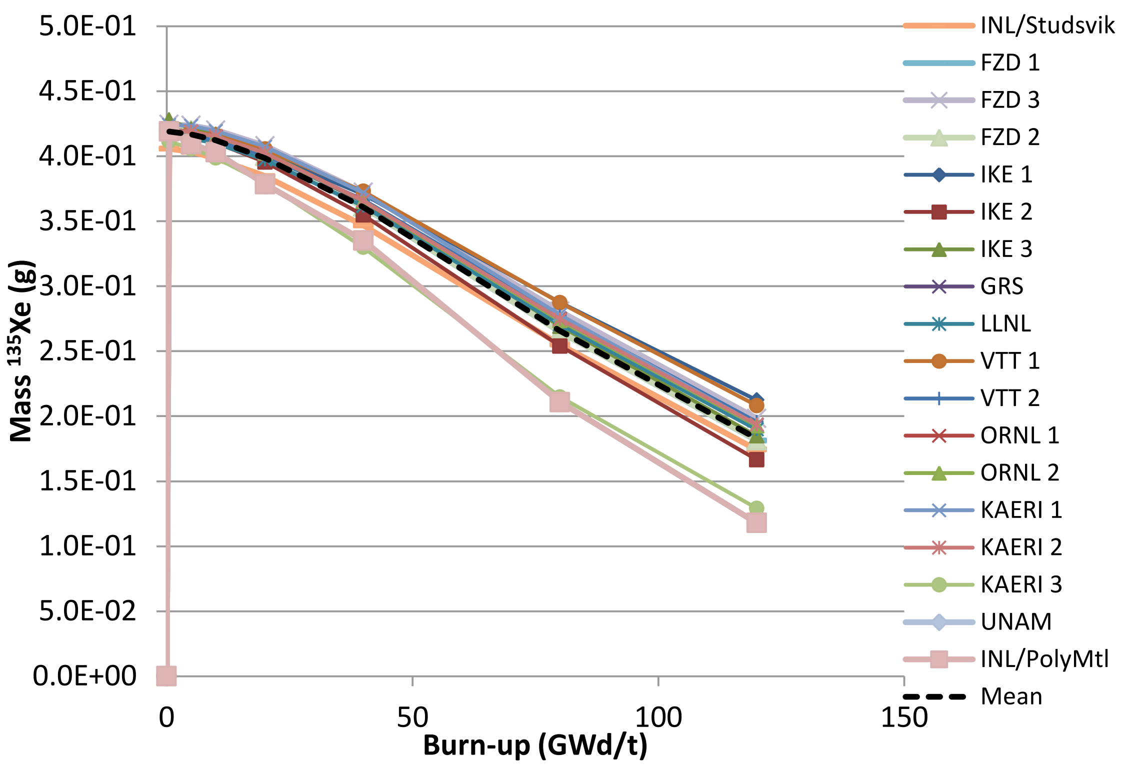

Figure 63. ^{149}Sm mass vs burn-up for prismatic depletion

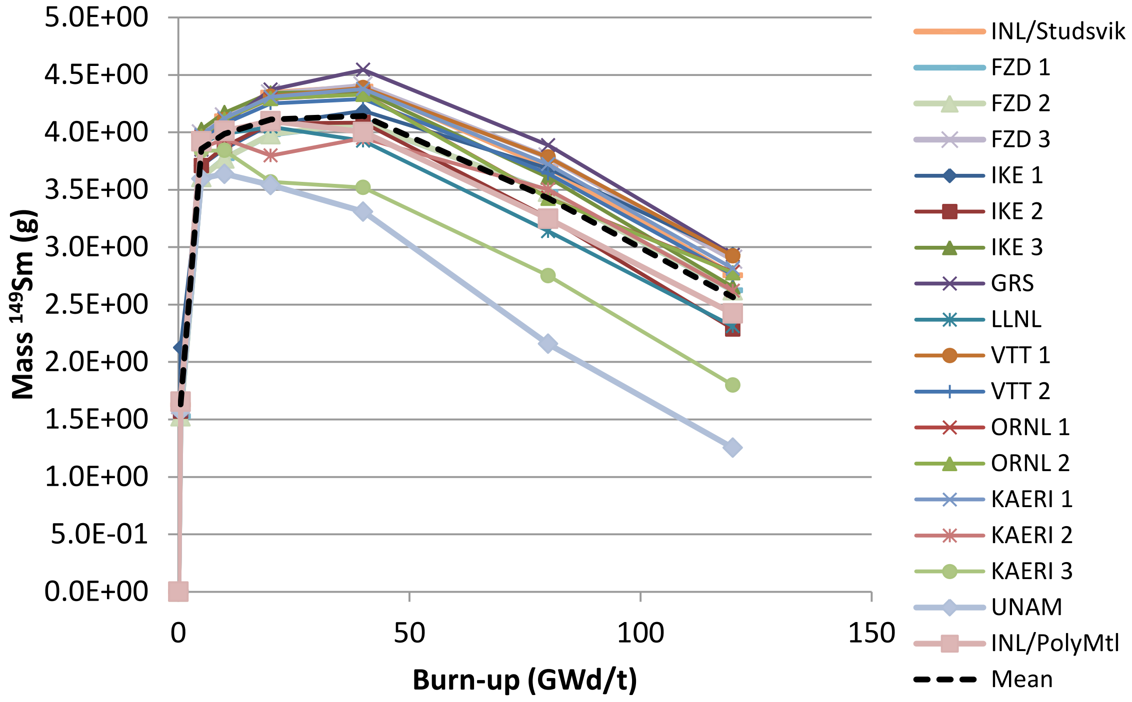

Figure 64. ^{151}Sm mass vs burn-up for prismatic depletion

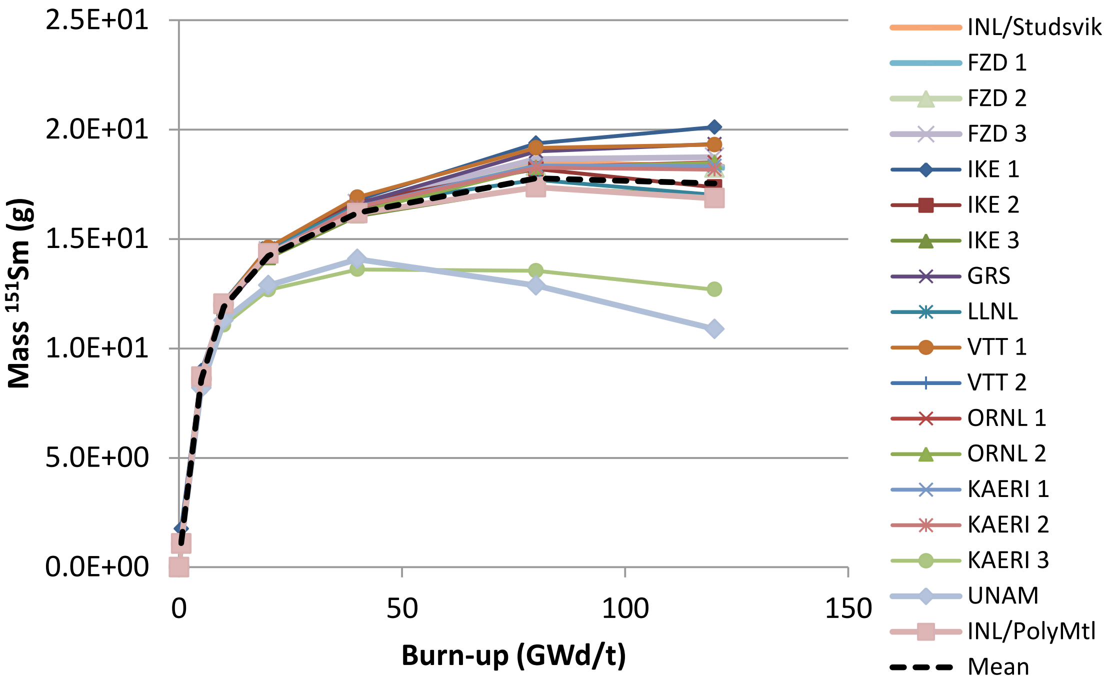

III.D.1 Fission products – Grain depletion

^{85}Kr – All submissions show the same general trends, and reasonable agreement, with the exception of FZD 3, which shows a predicted inventory about three times greater than that of the other results.

^{90}Sr – Better agreement is seen among participants for this nuclide; however, FZD 3 is also significantly higher than other submissions.

^{110m}Ag – Although all submissions show the same exponential growth with burn-up, there is no agreement among the participants. Results range from approximately 2.5 g to 8 g at the end of the depletion calculation. However, the disagreement likely results from the small mass of the fission product at EOL. While ^{85}Kr and ^{90}Sr masses were in the hundreds to thousands of grams inventory at full burn-up, ^{110m}Ag is predicted only in single digit gram quantities.

^{137}Cs – Results for this nuclide mirror those of ^{85}Kr and ^{90}Sr, with generally good agreement but with FZD 3 results significantly higher.

^{135}Xe – Here all results show a rapid generation of this fission product at BOL as would be expected. There is reasonable agreement for most participants with increasing disagreement with burn-up, with UNAM on the lower bound and IKE 3 the upper bound of the clustered results; once again, FZD 3 results are a significant outlier.

^{149}Sm – Results for this nuclide show similar trends in terms of the upper and lower bounds of the grouped results, with FZD 3 a major outlier. However, IKE 2 and UNAM show a peak value of this inventory in the 40-80 GWd/t burn-up range, while inventories computed by other participants are level to slowly increasing at the end of burn-up. IKE 1 shows an unexpected dip at 30 GWd/t, perhaps from a transcription error (although later pebble results indicate that there is perhaps a different explanation). As with Ag, the calculated inventories at 120 GWd/t are on the order of grams, which may partially explain the spread in results.

^{151}Sm – Closer agreement is seen for ^{151}Sm inventories, with an almost linear increase with burn-up after a rapid increase in the first 20 GWd/t. FZD 3 results are high as with other fission products, and UNAM results are slightly low.

III.D.2 Fission products – Pebble depletion

^{85}Kr – All submission show the same general trends, and reasonable agreement, with FZD 3 now consistent with other results. VTT 1 and VTT 2 are self-consistent, but slightly lower than the other reported results.

^{90}Sr – As with grain depletion, much better agreement is seen among participants for this nuclide; all results are clustered closely together over the full burn-up range, with only a small spread with increasing burn-up.

^{110m}Ag – As with grain depletion, all submissions show the same exponential growth with burn-up, there is no agreement among the participants. Again, the disagreement likely results from the small mass of the fission product at EOL. LANL results are too low by four orders of magnitude.

^{137}Cs – Results for this nuclide are in very good agreement, except for LANL results, which are again several orders of magnitude too low. This value artificially lowers the overall average. Excepting LANL results, agreement is slightly better among all participants than that of the grain results.

^{135}Xe – Behaviour is similar to that of the grain results, but with much more consistency among participants. There appears to be some structure to the shape of the Xe inventory. Again, there is a rapid build-up, but then the inventory decreases with what appears to be a concave down shape. After about 40 GWd/t burn-up, the shape of the depletion curve has a clear concave up shape, with inventory decreasing with burn-up. Interestingly, although the magnitude of the inventory ranges from 0.4 to 0.1 g/t, the agreement is much better than other low-inventory results.

^{149}Sm – The shape of the depletion curve for this nuclide is significantly different for pebble depletion than that of the grain depletion case. For the grain case, the inventory increases rapidly early in the cycle, but continues to increase at a slower rate for the remainder of the depletion case. For this case, after the initial increase, the mass of this nuclide decreases with burn-up. LANL results are significantly low; LLNL results are somewhat low as well. Remaining participants are in agreement on the shape but vary by a constant bias after 5 GWd/t. It appears that there is significant disagreement in the magnitude of the initial increase, resulting in a bias. After the first 5 GWd/t burn-up, all participants' results decrease at the same rate. Interestingly, while IKE 1 results showed an inconsistent dip in the ^{149}Sm at 20 GWd/t for grain depletion, that dip is not seen for IKE1 here. However, KAERI 2 and KAERI 3 results now show this dip. It is noted that the 20 GWd/t burn-up point is the first following a larger time step of 10 GWd/t; it is possible that the dip is a numerical error introduced by the change in the time step size; however, this behaviour is not seen when time step sizes are later increased.

^{151}Sm – Consistent with ^{149}Sm behaviour, while grain depletion shows an increase in ^{151}Sm inventory with increasing burn-up, pebble depletion shows an initial build-up that flattens out between 40 and 80 GWd/t, after this burn-up the mass of ^{151}Sm begins to decrease with burn-up. Unlike ^{149}Sm, however, predicted inventories diverge somewhat with burn-up. As with ^{149}Sm, LANL is a low outlier, but not by the orders of magnitude seen for other nuclides.

III.D.3 Fission products – Prismatic depletion

^{85}Kr – As with pebble depletion, all results show the same general trends, with increasing differences with burn-up, but overall reasonable agreement. Again, VTT 1 and VTT 2 are self-consistent, but slightly lower than the other reported results.

^{90}Sr – As with both grain and pebble depletion, very good agreement is seen among participants for this nuclide; all results are clustered closely together over the full burn-up range, with only a small spread with increasing burn-up.

^{110m}Ag – As with grain depletion, all submissions show the same exponential growth with burn-up, and again, for the most part there is little agreement/clustering among the participants.

^{137}Cs – Results for this nuclide are in very good agreement, except for INL/PolyMtl results, which depart from the average after approximately 40 GWd/t and come in lower than other submissions.

^{135}Xe – Grain results for this isotope showed a significant spread among submissions, while pebble depletion results much more consistency among participants. Prismatic results are not as closely grouped, with slightly more spread from the average. For this case, both INL/PolyMtl and KAERI 3 are low (although in good agreement). Relative to pebble depletion, there is a similar structure to the shape of the Xe inventory, although not as pronounced.

^{149}Sm – As with the pebble depletion case, the shape of the depletion curve for this nuclide is significantly different for prismatic depletion than that of the grain depletion case. As with pebble depletion, after the initial increase, the mass of this nuclide decreases with burn-up. However, here UNAM and KAERI 3 are lower than the average grouping. Remaining participants are in agreement on the shape but vary by a constant bias after 5 GWd/t. It appears that there is significant disagreement in the magnitude of the initial increase, resulting in a bias. After the first 5 GWd/t burn-up, all participants' results decrease at the same rate. While IKE1 results showed an inconsistent dip in the ^{149}Sm at 20 GWd/t for grain depletion, with KAERI 1 and KAERI 3 showing a dip in pebble depletion, here ORNL 1 and KAERI 3 now show this dip. Again it is noted that the 20 GWd/t burn-up point is the first following a larger time step of 10 GWd/t; it is possible that the dip is a numerical error introduced by the change in the time step size; however, this behaviour is not seen when time step sizes are later increased.

^{151}Sm – Consistent with ^{149}Sm behaviour, while grain depletion shows an increase in ^{151}Sm inventory with increasing burn-up, both prismatic and pebble depletion show an initial build-up that flattens out (on average) between 40 and 80 GWd/t, after this burn-up the average participant reported mass of ^{151}Sm begins to decrease with burn-up. As noted for pebble depletion, unlike ^{149}Sm, predicted inventories diverge somewhat with burn-up. As a result of trends in ^{149}Sm, UNAM and KAERI 3 are lower than the average grouping.

IV. Summary of results

Due to technical difficulties and funding source changes, this report has been significantly delayed in its release. The results contained herein may be somewhat dated. This has also resulted in the inability of many of the participants to review the compiled results and make comments.

Results provided by participants are largely consistent. The UNAM submission does not use a DH treatment that is important in the *non-grain* depletion calculations and thus is a bit of an outlier for prismatic calculations (pebble depletion calculations were not reported). This provides useful information on the effect of this approximation. Calculated eigenvalues in the prismatic depletion are higher than from the other contributions; however, the approximation has little effect on spectral indices and hence on depletion results by isotopes. UNAM isotopic results are consistently grouped, well within upper and lower bounds for each nuclide. Hence, uncertainties in data or other modelling approximations appear to be more significant due to the homogeneous treatment of grains within fuel blocks for isotopic predictions as a function of burn-up. The LANL submission was found to contain an error in the initial composition, so that set of results stands at odds with other submission; however, the results are included here for completeness.

In review of the grain depletion, it was found that these results are less consistent than those of the pebble and prismatic depletion. This was somewhat surprising; it was expected that the other depletion problems would show more variation due to differing treatments to account for self-shielding in the DH configurations. However, the most significant differences occurred in reported spectral indices. Nuclide predictions showed roughly the same spread as other depletion cases. Cases where there is a significant spread in reported results as a function of burn-up (e.g. ^{110m}Ag) perhaps indicate differences in fission product distributions and/or decay branching. It was interesting to note that the shape of the depletion inventory curves were significantly different between grain and the other depletion cases for some of the activation and fission products, as was noted in previous sections.

For calculation of the depletion of the infinite lattice of pebbles there were significantly more participants than the grain calculation (14 submissions from 7 organisations) and surprisingly, provided the best overall agreement. It was determined that the LANL submission had an error in the initial fuel composition and is the only significant outlier for all pebble calculations. For the spectral indices, ρ^{238} is consistent for all participants. However, δ^{235} [$^{235}U_{fis}$(fast)/$^{235}U_{fis}$(thermal)] shows a bias between some participants at zero burn-up, indicating potential differences in data. Other indices are in close agreement, with a slight divergence between 80 and 120 GWd/t. This divergence may be a result in differences in time step sizes (numerical issues) rather that methods or data. Actinide concentrations are in good agreement, but with increasing spread in data with higher actinides. For fission products, ^{90}Sr, ^{137}Cs and ^{135}Xe are in agreement among all participants. Significant differences are seen with increasing burn-up for ^{85}Kr, ^{110m}Ag, ^{149}Sm and ^{151}Sm. These differences may result from spectral differences, consistent with predictions of ^{239}Pu and ^{241}Pu differences among participants with increasing burn-up.

Finally, calculations were performed for a supercell representation of prismatic fuel. This benchmark had the most interest based on the number of contributions (18 submissions from nine organisations). Eigenvalue results were found to be tightly clustered for the full depletion history, with the exception of the UNAM results, which were an outlier on most results due to lack of a double heterogeneity treatment, as discussed earlier. ρ^{238} and δ^{235} both show a spread among participants, but that spread it available at zero burn and does not change by much for the full depletion. The other indices are in good overall agreement, with small differences growing between the last two depletion points. This may be due to different time steps used over this rather long 40 GWd/t period. In general, trends in isotopic depletion follow those observed in the pebble depletion, with a slightly higher deviation in results.

Direct comparison of trends between the three different scenarios may be somewhat misleading. Different numbers of participants contributed to the various scenarios, using different codes and data. Even with a given configuration, not all participants provided a complete set of results; often the spectral indices were omitted. Thus, some of the uncertainty seen within a given set of results is a consequence of the particular submissions.

V. References

Hosking, G. and T.D. Newton (2005), "Benchmark specification for an HTR fuelled with reactor grade-plutonium (or reactor-grade Pu/Th and U/Th): Proposal", NEA/NSC/DOC(2003)22.

Kim, Y., C. Cho and F. Venneri (2007), "Long-Cycle and High-Burnup Fuel Assembly for the VHTR," *Journal of Nucl. Sci. and Tech*., pp 294-302, Vol. 44, No. 3.

Appendix A. Participant's submissions – Basic information and analysis environment

INL-Studsvik (Prismatic Only)

Basic information	
Date	10/27/09
Organisation	Idaho National Laboratory / Studsvik Scandpower
Contact person	William F. Skerjanc
Contact e-mail	william.skerjanc@inl.gov
Computer code(s) used	HELIOS Code Package
Analysis environment	
Neutron data library/source	HELIOS Cross-Section Library based on ENDF/B-VII.0
Group structure	177 Group
Data processing method	ZENITH (part of HELIOS code package)
Convergence limit or statistical error on eigenvalues	Eigenvalue Iteration Convergence = 2.0E-5
Other related information	Geometry model consisted of a centre fuel compact with three one-sixth coolant channel holes. Reflective boundry condition applied to all three sides

FZD 1 (Grain and Prismatic)

Basic information	
Date	10/19/09
Organisation	Forschungszentrum Dresden-Rossendorf (FZD)
Contact person	Emil Fridman
Contact e-mail	e.fridman@fzd.de
Computer code(s) used	BGCore (MCNP + MG depletion). Refs: 1. Fridman E., Shwageraus E., and Galperin A., "Implementation of MG Cross-Section Methodology in BGcore Monte Carlo Depletion Code", Proc. PHYSOR-2008, International Conference on Reactor Physics, Kursaal Conference Centre, Interlaken, Switzerland, September 14-19, (2008). 2. Fridman, E., Shwageraus, E., Galperin, A., "Efficient generation of 1-g cross-sections for coupled Monte Carlo depletion calculations", Nucl. Sci. Eng. 159, 37-47, (2008).
Analysis environment	
Neutron data library/source	MCNP: ZZ-MCJEFF3.1NEA
Group structure	
Data processing method	NJOY99.90
Convergence limit or statistical error on eigenvalues	σ k-inf < 0.0004
Other related information	Grain: 3D model of spherical TRISO fuel particle embedded into the cubic graphite matrix. Prismatic: Explicit description of TRISO particles. TRISO particles distributed using hexagonal lattice. Single burnable (fuel) material

FZD 2 (Prismatic Only)

Basic information	
Date	10/19/09
Organisation	Forschungszentrum Dresden-Rossendorf (FZD)
Contact person	Emil Fridman
Contact e-mail	e.fridman@fzd.de
Computer code(s) used	BGCore 3D (MCNP + MG depletion). Refs: 1. Fridman E., Shwageraus E., and Galperin A., “Implementation of MG Cross-Section Methodology in BGcore Monte Carlo Depletion Code”, Proc. PHYSOR-2008, International Conference on Reactor Physics, Kursaal Conference Centre, Interlaken, Switzerland, September 14-19, (2008). 2. Fridman, E., Shwageraus, E., Galperin, A., “Efficient generation of 1-g cross-sections for coupled Monte Carlo depletion calculations”, Nucl. Sci. Eng. 159, 37-47, (2008).
Analysis environment	
Neutron data library/source	MCNP ACE: ZZ-MCJEFF3.1NEA
Group structure	
Data processing method	NJOY99.90
Convergence limit or statistical error on eigenvalues	
Other related information	TRISO particles were smeared using RPT [Ref.: Y.H. Kim, W. S. Park, “RPT for Elimination of Double Heterogeneity,” Transaction of American Nuclear Society, 93, pp. 959-960 (2005).]

FZD 3 (Grain and Prismatic)

Basic information	
Date	10/19/09
Organisation	Forschungszentrum Dresden-Rossendorf (FZD)
Contact person	Emil Fridman
Contact e-mail	e.fridman@fzd.de
Computer code(s) used	HELIOS 1.9
Analysis environment	
Neutron data library/source	ENDF/B-VI.8
Group structure	190 groups
Data processing method	
Convergence limit or statistical error on eigenvalues	
Other related information	Grain: 2D equivalent cylinder model of TRISO fuel particle was used. The transformation from sphere to cylinder was done by preserving: (1) the average chord length of the fuel region, and (2) volume fractions of all regions in the model. Prismatic: TRISO particles were smeared using RPT [Ref.: Y.H. Kim, W. S. Park, “RPT for Elimination of Double Heterogeneity,” Transaction of American Nuclear Society, 93, pp. 959-960 (2005).]

IKE 1 (Grain, Pebble and Prismatic)

Basic information	
Date	10/8/09
Organisation	Institut fuer Kernenergetik und Energiesysteme (IKE), Universitaet Stuttgart,Germany
Contact person	A. Meier, J. Bader, W. Bernnat
Contact e-mail	astrid.meier@ike.uni-stuttgart.de johannes.bader@ike.uni-stuttgart.de wolfgang.bernnat@ike.uni-stuttgart.de
Computer code(s) used	MCNP coupled with module Abbrand (simplified burn-up model with 85 fission products and 20 actinides)
Analysis environment	
Neutron data library/source	JEFF 3.1
Group structure	CE
Data processing method	NJOY
Convergence limit or statistical error on eigenvalues	keff with an estimated standard deviation < 0.002
Other related information	Fluxes are in arbitrary units / Kr-85,Sr-90, Cs-137 and Sm-149 are not considered in the burn-up model

IKE 2 (Grain, Pebble and Prismatic)

Basic information	
Date	10/8/09
Organisation	IKE, Universitaet Stuttgart,Germany
Contact person	A. Meier, J. Bader, W. Bernnat
Contact e-mail	astrid.meier@ike.uni-stuttgart.de johannes.bader@ike.uni-stuttgart.de wolfgang.bernnat@ike.uni-stuttgart.de
Computer code(s) used	Microx2.2 coupled with Origen2.2
Analysis environment	
Neutron data library/source	JEFF 3.1
Group structure	193 groups (92 fast groups – 101 thermal groups (boundary at 2.38 eV))
Data processing method	NJOY
Convergence limit or statistical error on eigenvalues	Thermal section convergence criterion: 0.0001
Other related information	Fluxes are in arbitrary units

IKE 3 (Grain, Pebble and Prismatic)

Basic information	
Date	10/25/09
Organisation	IKE, Universitaet Stuttgart,Germany
Contact person	Janis Lapins
Contact e-mail	janis.lapins@ike.uni-stuttgart.de
Computer code(s) used	Grain: SCALE 6, TRITON t6-depl sequence (KENO-VI) Pebble and Prismatic: SCALE 6, TRITON t5-depl sequence (KENO V.a)
Analysis environment	
Neutron data library/source	ENDF/B-VII
Group structure	238 groups thermal boundary at 0.625 eV
Data processing method	Pointwise-weighted (CENTRM)
Convergence limit or statistical error on eigenvalues	
Other related information	

GRS (Grain, Pebble and Prismatic)

Basic information	
Date	9/28/09
Organisation	Gesellschaft fuer Anlagen- und Reaktorsicherheit (GRS) mbH
Contact person	Winfried Zwermann
Contact e-mail	Winfried.Zwermann@grs.de
Computer code(s) used	MONTEBURNS 2.0 (MCNP5 + ORIGEN2.2)
Analysis environment	
Neutron data library/source	JEFF-3.1 based, available from NEA Data Bank as package ZZ-MCJEFF3.1NEA
Group structure	CE
Data processing method	
Convergence limit or statistical error on eigenvalues	1 sigma = 0.0003-0.0004
Other related information	No HTGR specific ORIGEN XS libraries were available; therefore, generic thermal XS were used

LLNL (Grain, Pebble and Prismatic)

Basic information	
Date	10/1/09
Organisation	Lawrence Livermore National Laboratory
Contact person	Massimiliano Fratoni
Contact e-mail	fratoni1@llnl.gov
Computer code(s) used	MOCUP, MCNP5 Version 1.40 + ORIGEN2.2
Analysis environment	
Neutron data library/source	ENDF/B-VII.0
Group structure	Continous energy
Data processing method	none
Convergence limit or statistical error on eigenvalues	< 0.00030
Other related information	double heterogeneity was fully modelled

VTT 1 (Pebble and Prismatic)

Basic information	
Date	11/3/09
Organisation	VTT Technical Research Centre of Finland
Contact person	Jaakko Leppänen
Contact e-mail	Jaakko.Leppanen@vtt.fi
Computer code(s) used	Serpent Monte Carlo reactor physics burn-up calculation code, version 1.1.2
Analysis environment	
Neutron data library/source	ENDF/B-VII, no probability table treatment for unresolved resonances
Group structure	CE
Data processing method	ACE format XS libraries generated using NJOY. Decay and fission yield data from standard ENDF format files
Convergence limit or statistical error on eigenvalues	2 million neutron histories run per transport cycle. Statistical error in keff ~ 30-50 pcm.
Other related information	Explicit particle fuel model used inside pebbles and compacts (single-grain results omitted). 44 burn-up steps with predictor-corrector calculation, 1 500 nuclide concentrations traced (300 with cross-sections). Overall calculation time 50 (pebble) / 38 (prism) hours on a 3 GHz single-processor Intel Xeon PC.

VTT 2 (Grain, Pebble and Prismatic)

Basic information	
Date	11/3/09
Organisation	VTT Technical Research Centre of Finland
Contact person	Jaakko Leppänen
Contact e-mail	Jaakko.Leppanen@vtt.fi
Computer code(s) used	Serpent Monte Carlo reactor physics burn-up calculation code, version 1.1.2
Analysis environment	
Neutron data library/source	ENDF/B-VII, no probability table treatment for unresolved resonances
Group structure	CE
Data processing method	ACE format XS libraries generated using NJOY. Decay and fission yield data from standard ENDF format files
Convergence limit or statistical error on eigenvalues	2 million neutron histories run per transport cycle. Statistical error in keff ~ 30-50 pcm.
Other related information	Fuel particles inside pebbles and compacts arranged in a regular cubical lattice. 44 burn-up steps with predictor-corrector calculation, 1 500 nuclide concentrations traced (300 with cross-sections). Overall calculation time 27 (grain) / 38 (pebble) / 37 (prism) hours on a 3 GHz single-processor Intel Xeon PC.

ORNL 1 (Pebble and Prismatic)

Basic information	
Date	9/9/09
Organisation	Oak Ridge National Laboratory
Contact person	Mark DeHart
Contact e-mail	dehamd@ornl.gov
Computer code(s) used	SCALE 6.1ß, TRITON t-depl sequence (NEWT)
Analysis environment	
Neutron data library/source	ENDF/B-VII.0
Group structure	SCALE 238g
Data processing method	CENTRM/PMC (pointwise-weighted shielded MG cross-sections), double-het treatment
Convergence limit or statistical error on eigenvalues	k_{eff} and flux convergence criterion of 10^{-5}
Other related information	Pebble: pebble lattice approximated by a 2D cylinder with volumes conserved Prismatic: prismatic lattice modelled explicitly.

ORNL 2 (Grain, Pebble and Prismatic)

Basic information	
Date	9/9/09
Organisation	Oak Ridge National Laboratory
Contact person	Mark DeHart
Contact e-mail	dehamd@ornl.gov
Computer code(s) used	SCALE 6.1ß, TRITON t5-depl sequence (KENO V.a)
Analysis environment	
Neutron data library/source	ENDF/B-VII.0
Group structure	SCALE 238g
Data processing method	CENTRM/PMC (pointwise-weighted shielded MG cross-sections), double-het treatment
Convergence limit or statistical error on eigenvalues	k_{eff} with less that +/- 0.0005 error (1 σ)
Other related information	2 100 generations, 1 000 neutrons/generation, first 100 generations skipped

ORNL 3 (Pebble Only)

Basic information	
Date	9/9/09
Organisation	Oak Ridge National Laboratory
Contact person	Mark DeHart
Contact e-mail	dehamd@ornl.gov
Computer code(s) used	SCALE 6.1ß, TRITON t-depl-1d sequence (XSDRN)
Analysis environment	
Neutron data library/source	ENDF/B-VII.0
Group structure	SCALE 238g
Data processing method	CENTRM/PMC (pointwise-weighted shielded MG cross-sections), double-het treatment
Convergence limit or statistical error on eigenvalues	10^{-6} overall convergence
Other related information	One-dimensional spherical solution with Wigner-Seitz boundary condition

ORNL 4 (Pebble Only)

Basic information	
Date	9/9/09
Organisation	Oak Ridge National Laboratory
Contact person	Mark DeHart
Contact e-mail	dehamd@ornl.gov
Computer code(s) used	SCALE 6.1ß, TRITON t-depl-1d sequence (XSDRN)
Analysis environment	
Neutron data library/source	ENDF/B-VII.0
Group structure	SCALE 238g
Data processing method	CENTRM/PMC (pointwise-weighted shielded MG cross-sections)
Convergence limit or statistical error on eigenvalues	10^{-6} overall convergence
Other related information	TRISO particles homogenised within pebble using RPT

LANL (Grain and Prismatic)

Basic information	
Date	11/13/09
Organisation	Los Alamos National Laboratory
Contact person	Sang-Yoon Lee
Contact e-mail	sang@lanl.gov
Computer code(s) used	MCNPX2.7b
Analysis environment	
Neutron data library/source	ENDF-7
Group structure	CE
Data processing method	N/A
Convergence limit or statistical error on eigenvalues	0.001
Other related information	

KAERI 1 (Pebble and Prismatic)

Basic information	
Date	11/26/09
Organisation	Korea Atomic Energy Research Institute
Contact person	Yong Hee Kim
Contact e-mail	yhkim@kaeri.re.kr
Computer code(s) used	HELIOS
Analysis environment	
Neutron data library/source	ENDF/B-VI.8
Group structure	190 groups
Data processing method	
Convergence limit or statistical error on eigenvalues	
Other related information	

KAERI 2 (Pebble and Prismatic)

Basic information	
Date	11/26/09
Organisation	Korea Atomic Energy Research Institute
Contact person	Yong Hee Kim
Contact e-mail	yhkim@kaeri.re.kr
Computer code(s) used	MCCARD
Analysis environment	
Neutron data library/source	ENDF/B-VII
Group structure	CE
Data processing method	RPT
Convergence limit or statistical error on eigenvalues	
Other related information	

KAERI 3 (Pebble and Prismatic)

Basic information	
Date	11/26/09
Organisation	Korea Atomic Energy Research Institute
Contact person	Yong Hee Kim
Contact e-mail	yhkim@kaeri.re.kr
Computer code(s) used	MCCARD
Analysis environment	
Neutron data library/source	ENDF/B-VII
Group structure	CE
Data processing method	DH treatment
Convergence limit or statistical error on eigenvalues	
Other related information	

UNAM (Grain and Prismatic)

Basic Information	
Date	12/28/09
Organisation	National Autonomous University of Mexico (UNAM) - College of Engineering
Contact person	Juan-Luis Francois
Contact e-mail	juan.luis.francois@gmail.com
Computer code(s) used	MCNPX version 2.6.0
Analysis environment	
Neutron data library/source	ENDF/B-VI and JEFF 3.1
Group structure	CE
Data processing method	Data obtained directly from MCNPX output
Convergence limit or statistical error on eigenvalues	
Other related information	Heterogeneous calculation. NO approximation in treating the double heterogeinity

INL/ PolyMtl (Prismatic Only)

Basic Information	
Date	12/20/09
Organisation	Idaho National Laboratory and Polytechnique Montreal
Contact person	Michael A. Pope (INL), Alain Hebert (Poly. Mont.) and Guy Marleau (Poly. Mont)
Contact e-mail	michael.pope@inl.gov
Computer code(s) used	DRAGON 4.03
Analysis environment	
Neutron data library/source	ENDF/B-VII
Group structure	SHEM-361
Data processing method	SHEM-361 library produced in DRAGLIB format using NJOY (modified by Montreal Polytechnique). GROUPR subroutine was used to collapse to SHEM-361 energy structure with weighting function from VHTR lattice cell
Convergence limit or statistical error on eigenvalues	Convergence limit 1.0E-5
Other related information	Collision probability solution with treatment of microstructure given by : Hebert, A, "A Collision Probability Analysis of the Double Heterogeneity Problem," Nuclear Science and Engineering, 115, pp.177 (1993)

Appendix B. Results of grain depletion calculations

Figure B.1. k_{inf} vs burn-up for grain depletion

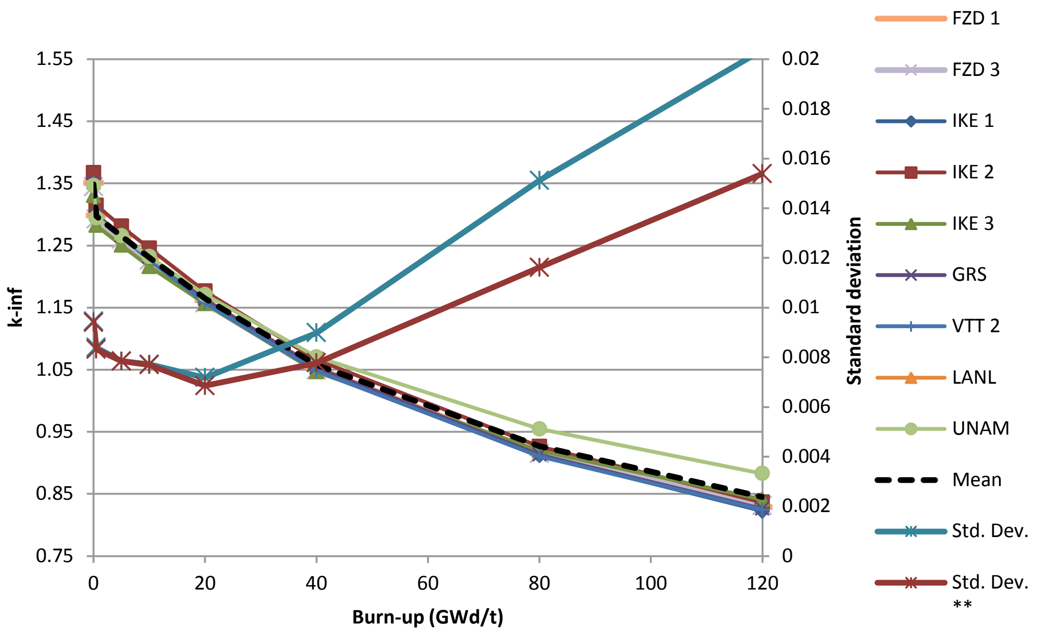

Figure B.2. p_{238} for grain depletion

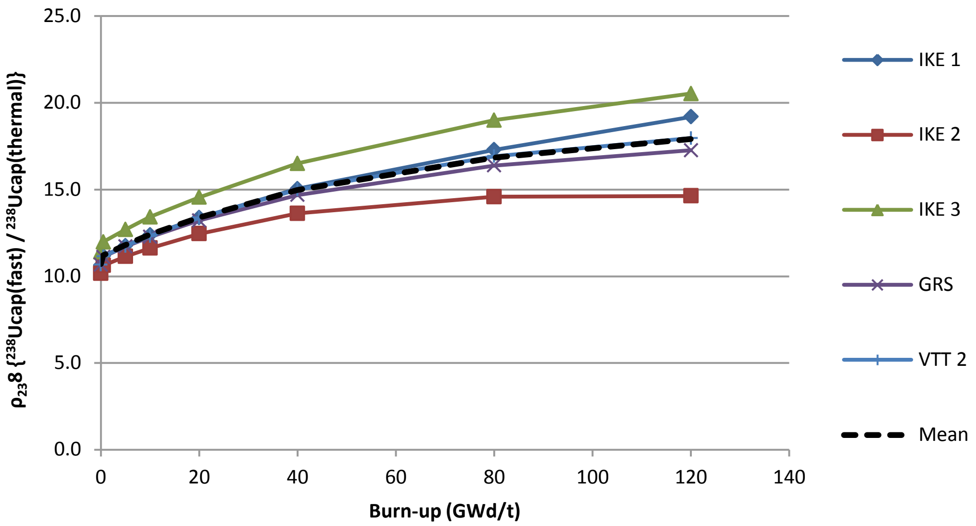

Figure B.3. δ_{235} for grain depletion

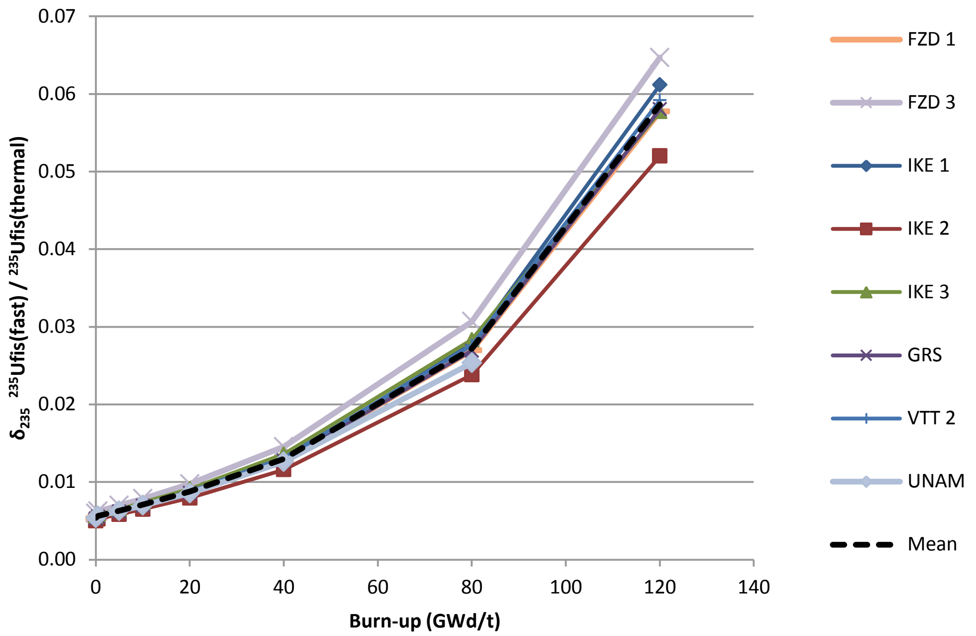

Figure B.4. δ_{238} for grain depletion

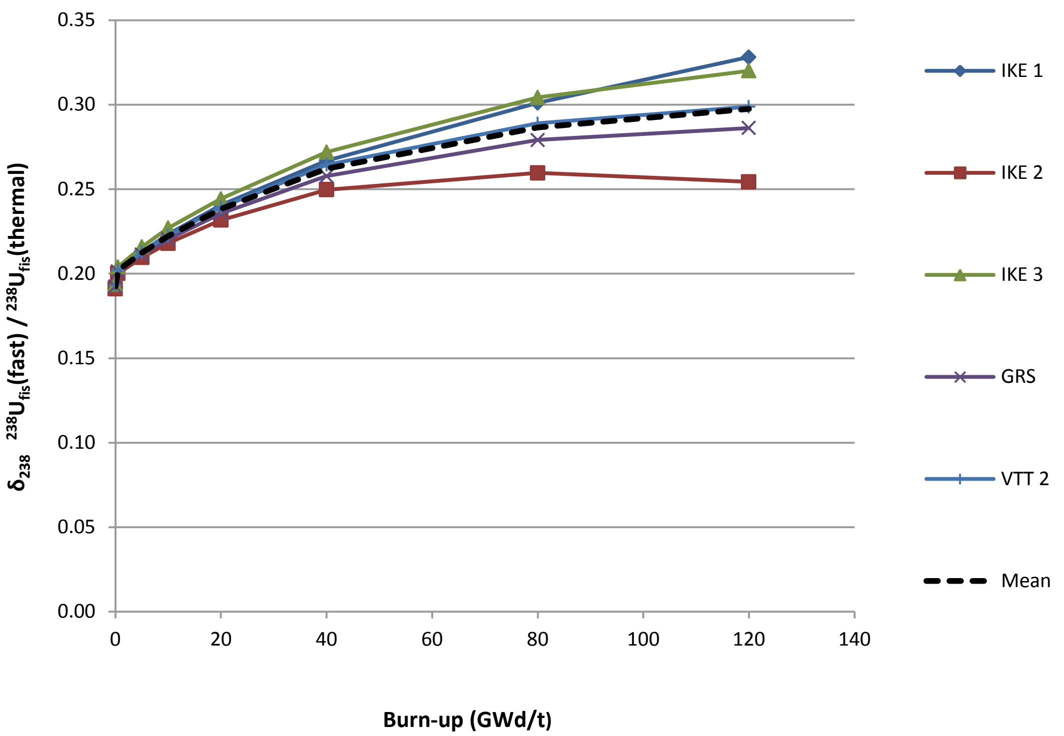

Figure B.5. c/f$_{235}$ for grain depletion

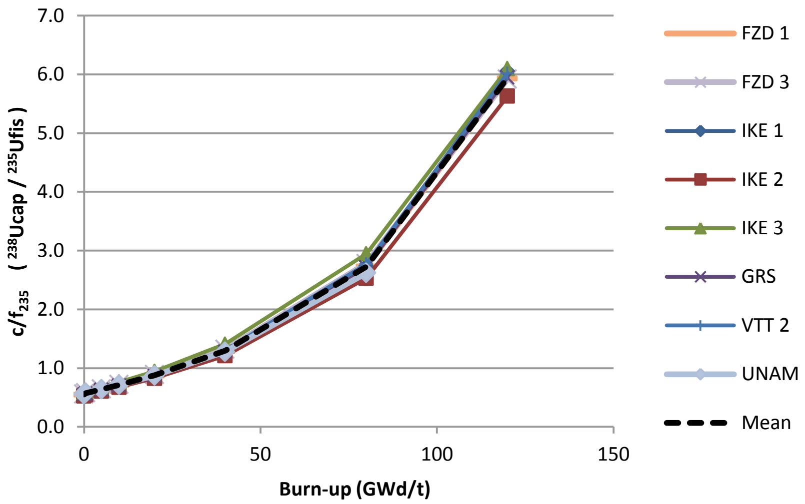

Figure B.6. ^{235}U mass vs burn-up for grain depletion

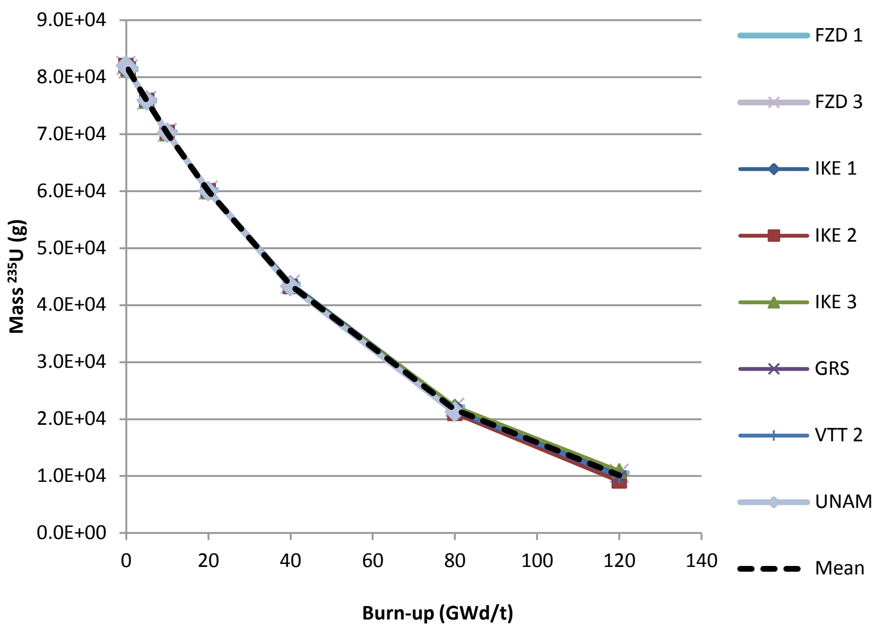

Figure B.7. ^{238}U mass vs burn-up for grain depletion

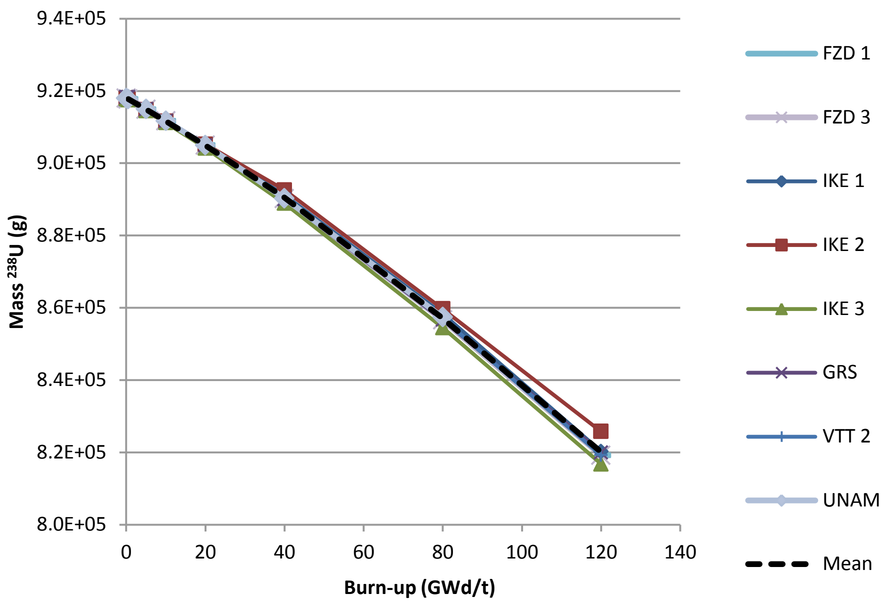

Figure B.8. ^{239}Pu mass vs burn-up for grain depletion

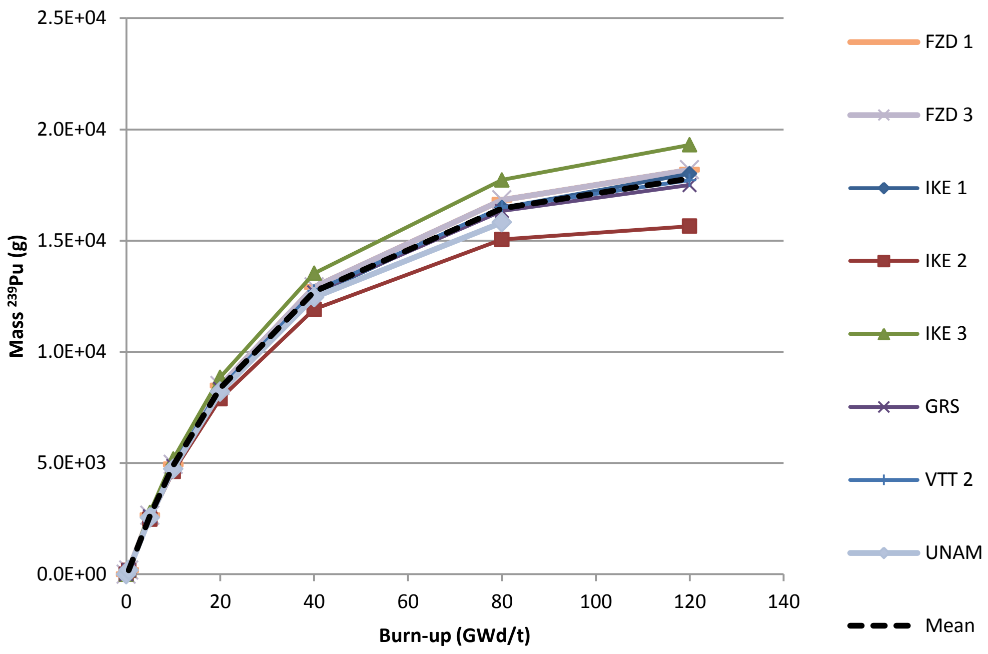

Figure B.9. ^{240}Pu mass vs burn-up for grain depletion

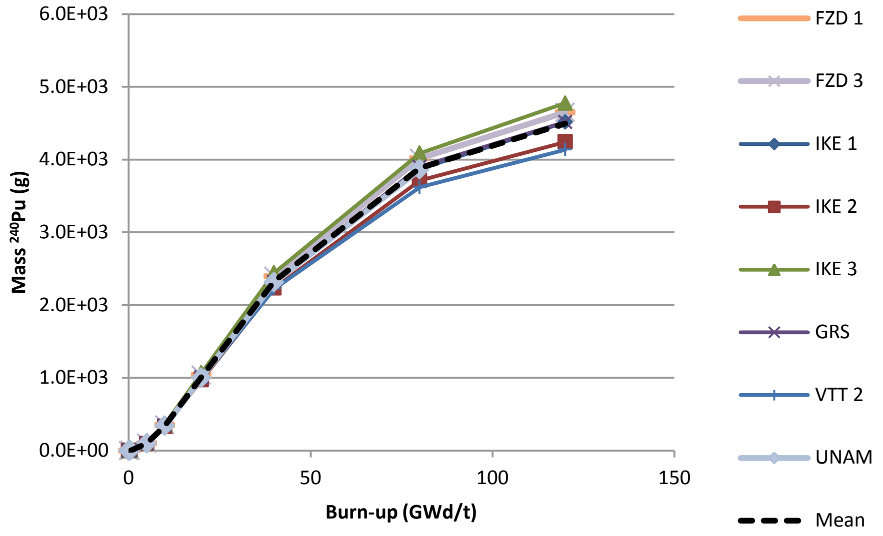

Figure B.10. ^{241}Pu mass vs burn-up for grain depletion

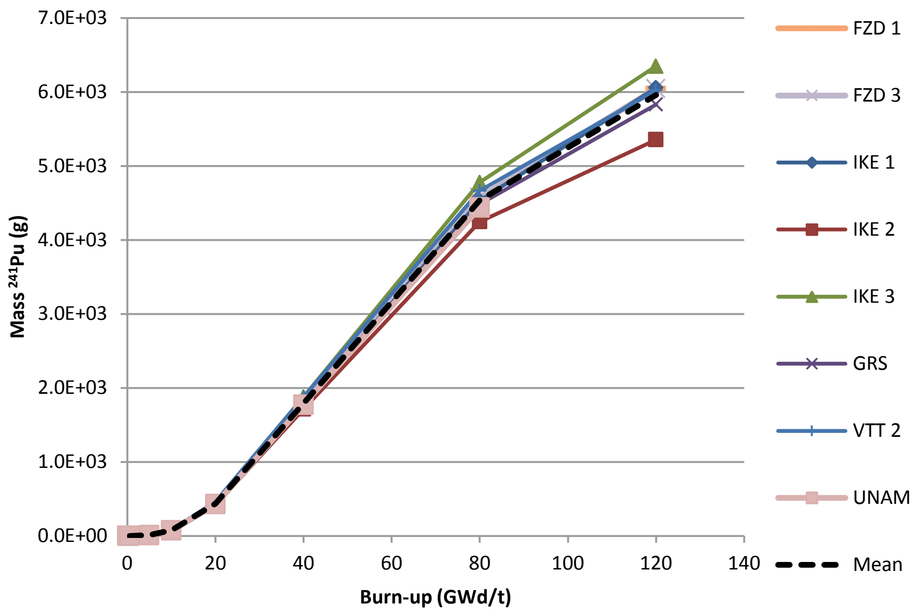

Figure B.11. ^{242}Pu mass vs burn-up for grain depletion

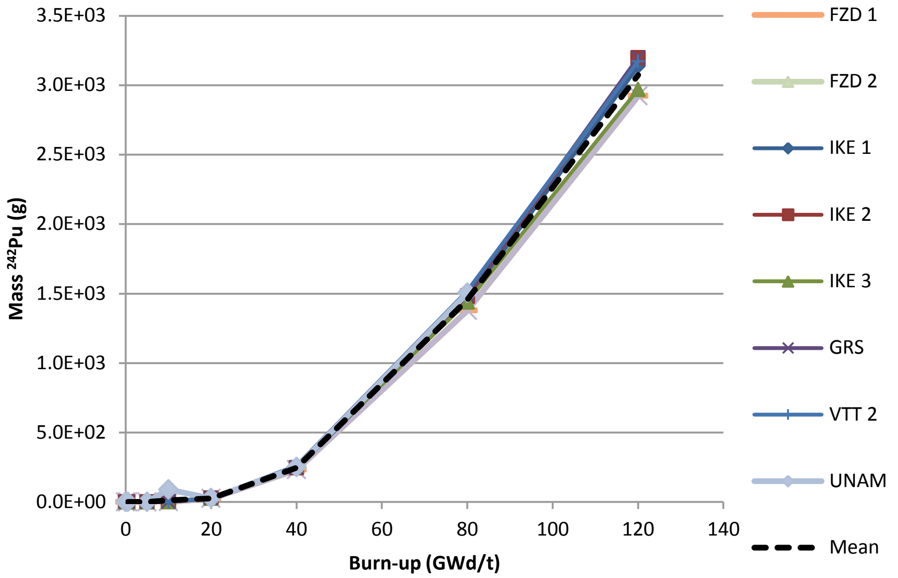

Figure B.12. ^{241}Am mass vs burn-up for grain depletion

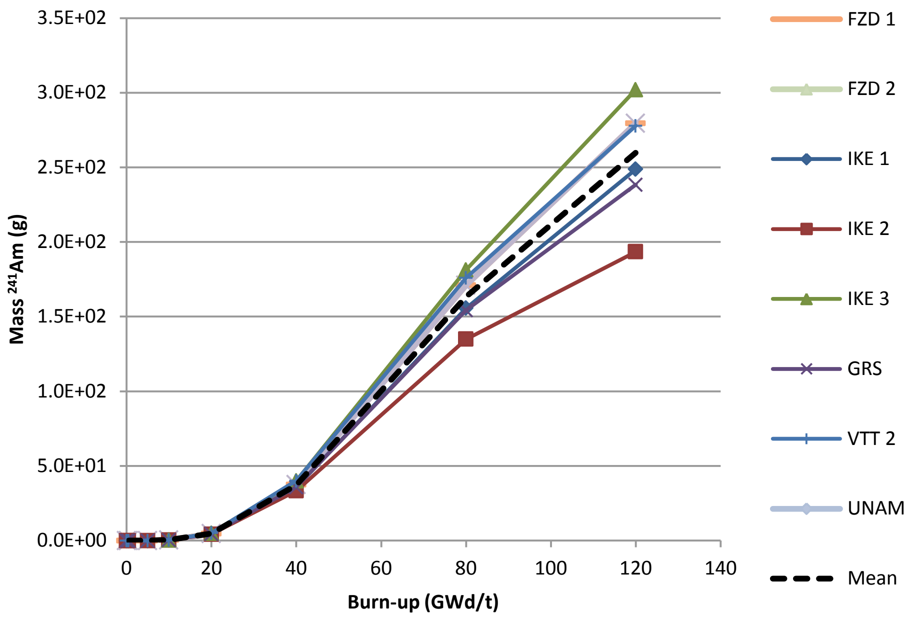

Figure B.13. ^{244}Cm mass vs burn-up for grain depletion

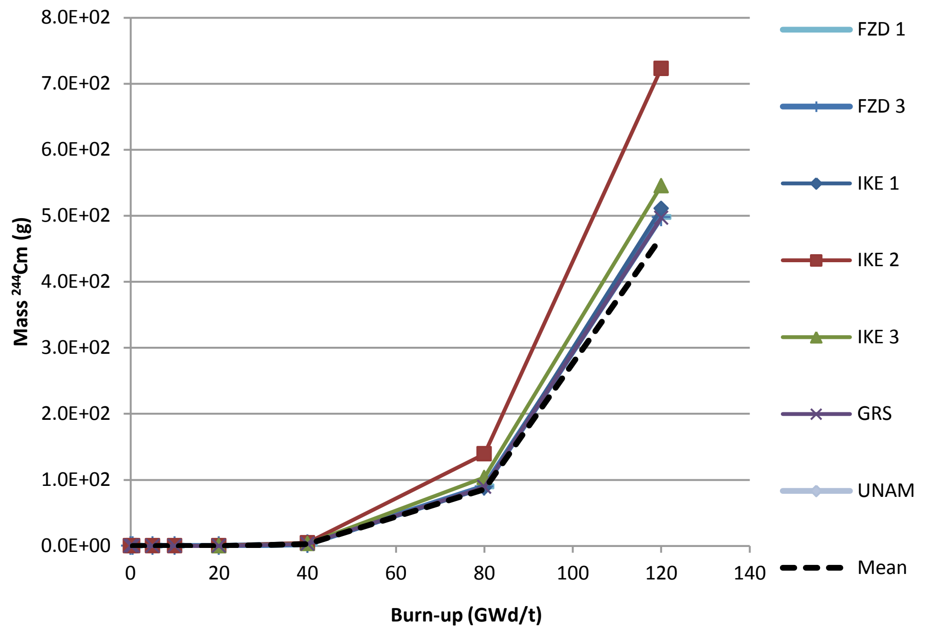

Figure B.14. ^{245}Cm mass vs burn-up for grain depletion

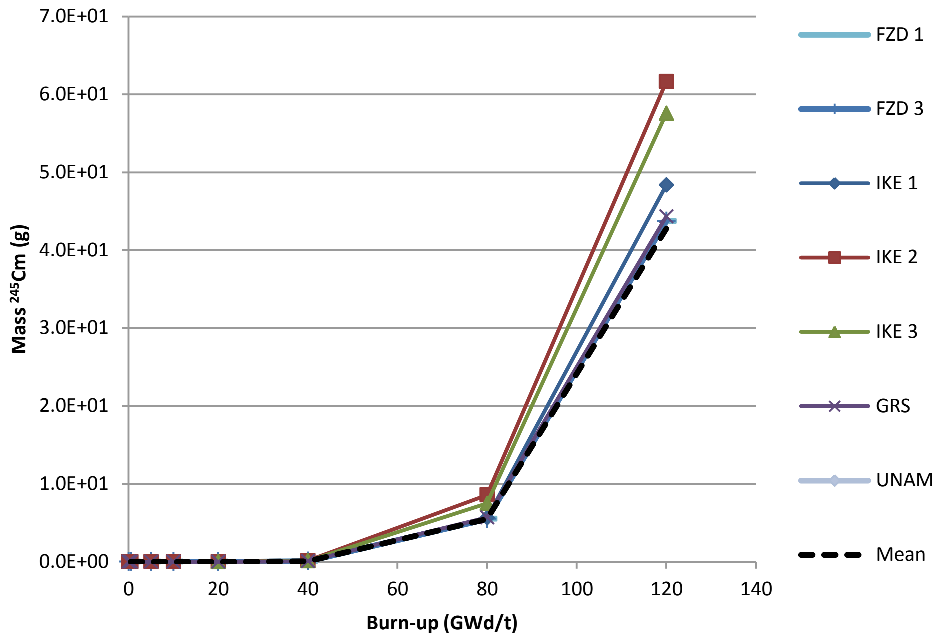

Figure B.15. ^{85}**Kr mass vs burn-up for grain depletion**

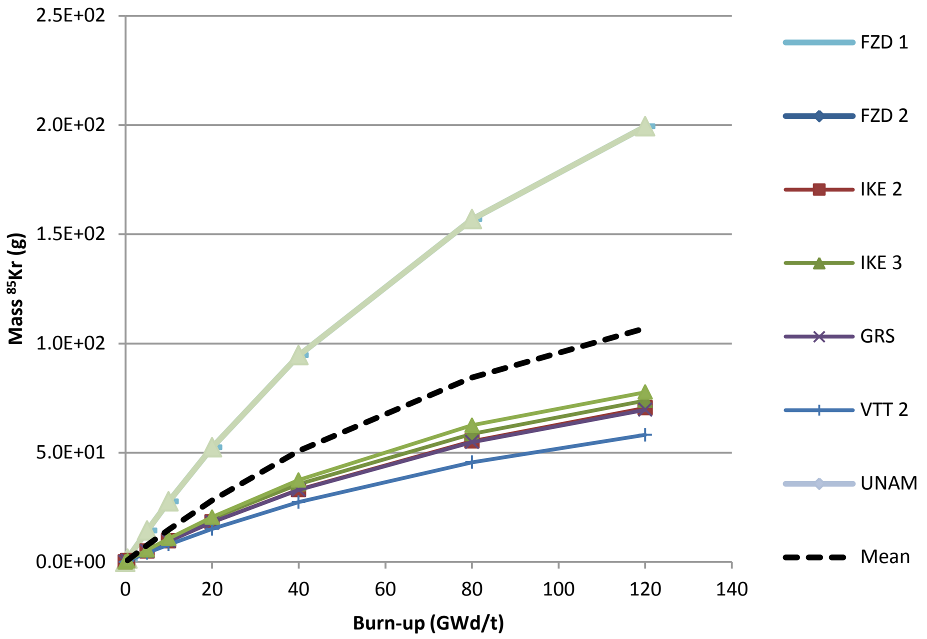

Figure B.16. ^{90}**Sr mass vs burn-up for grain depletion**

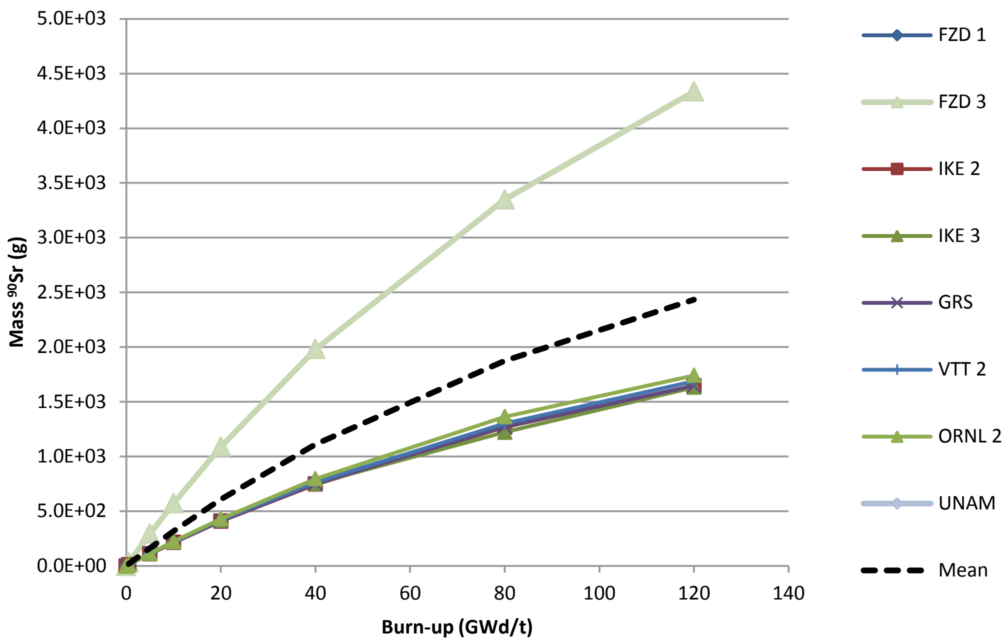

Figure B.17. ^{110m}Ag mass vs burn-up for grain depletion

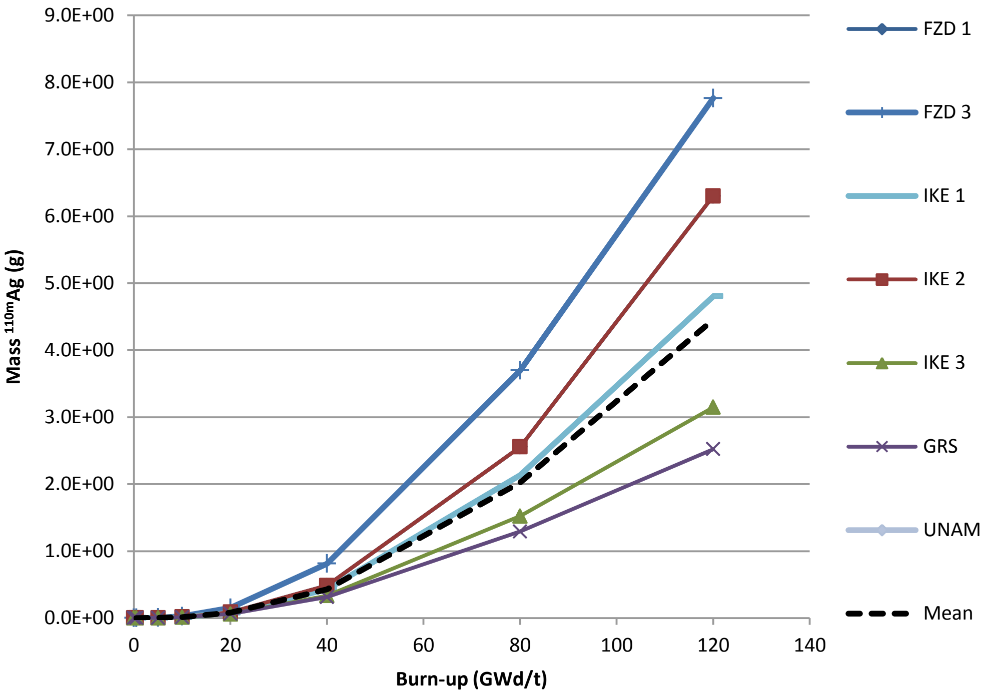

Figure B.18. ^{137}Cs mass vs burn-up for grain depletion

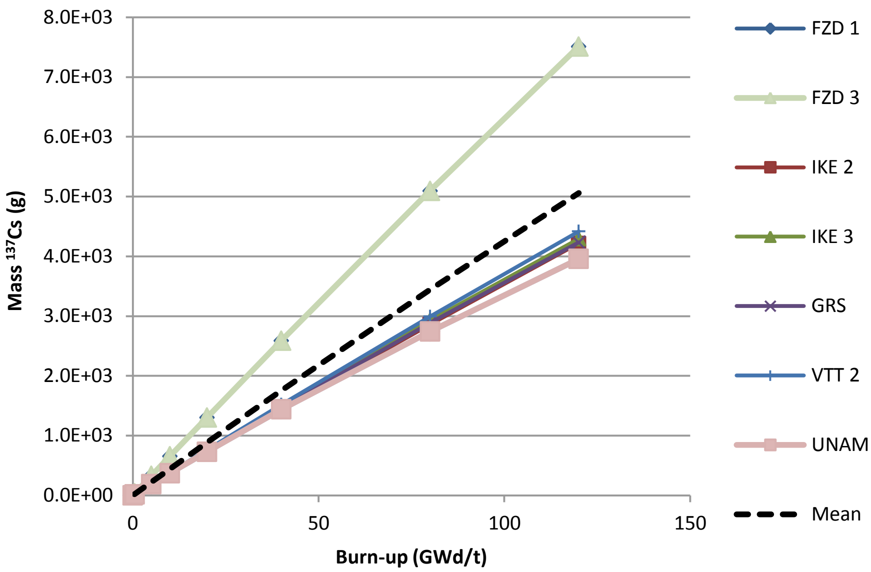

Figure B.19. ^{135}Xe mass vs burn-up for grain depletion

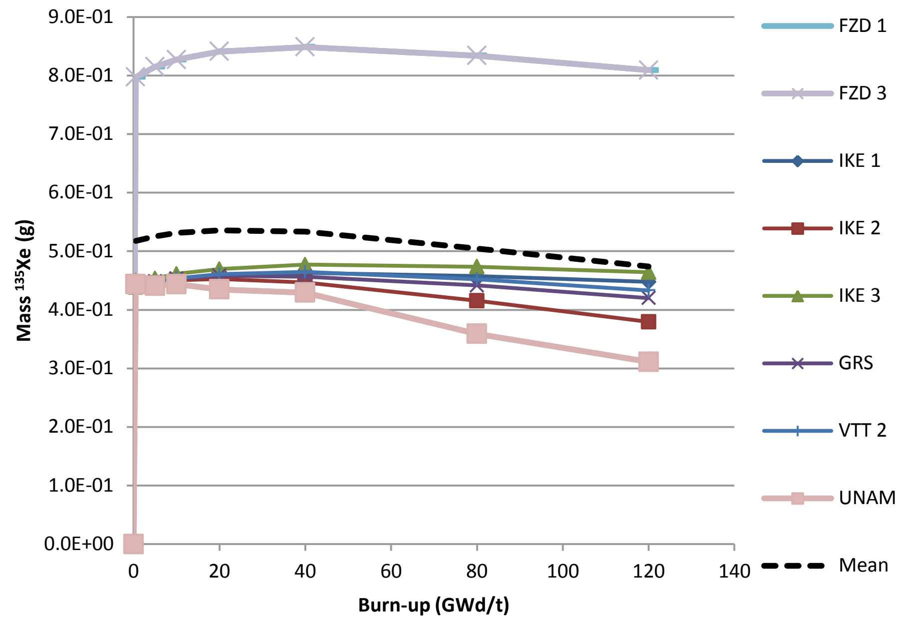

Figure B.20. ^{149}Sm mass vs burn-up for grain depletion

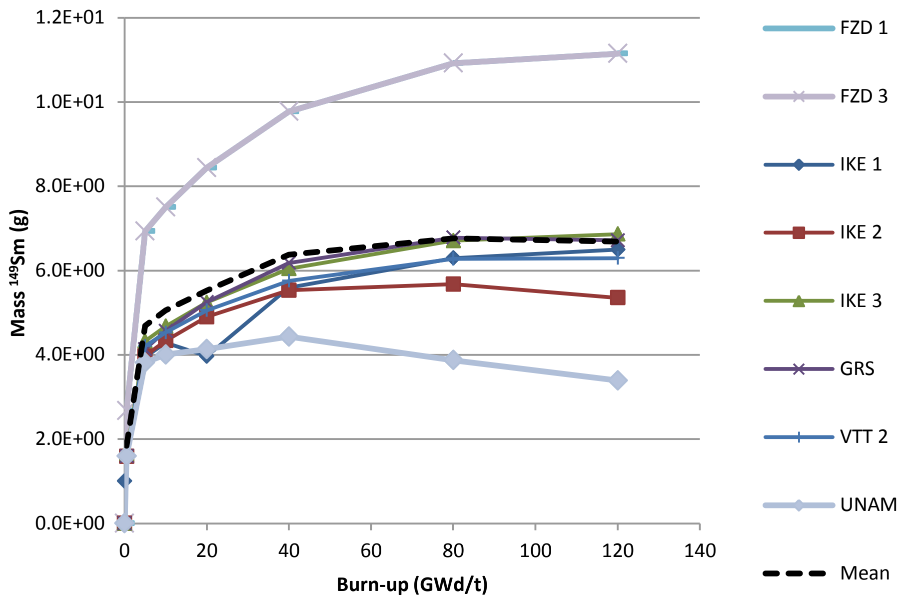

Figure B.21. ^{151}Sm mass vs burn-up for grain depletion

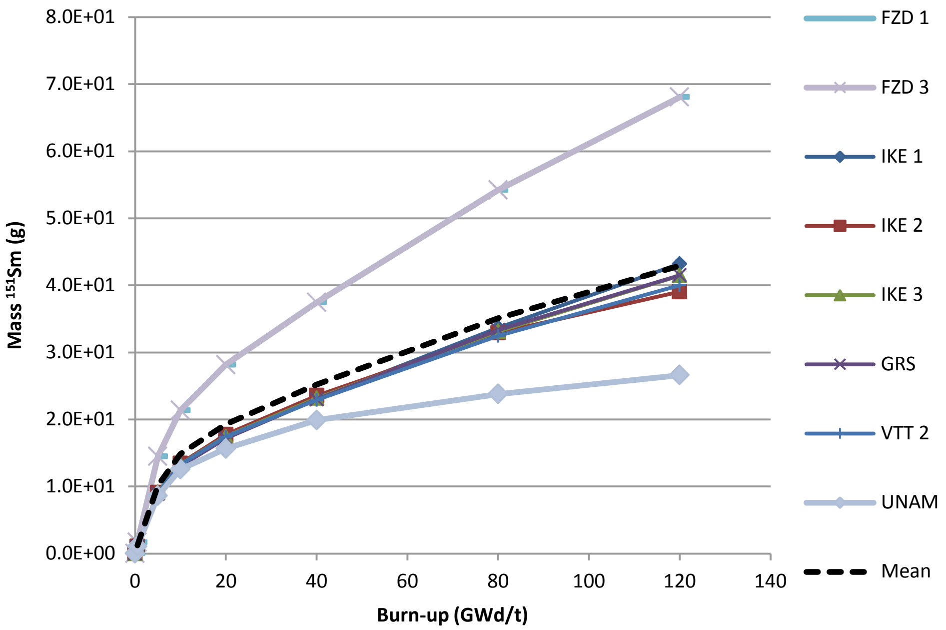

Appendix C. Results of pebble depletion calculations

Figure C.1. k_{-inf} vs burn-up for pebble depletion

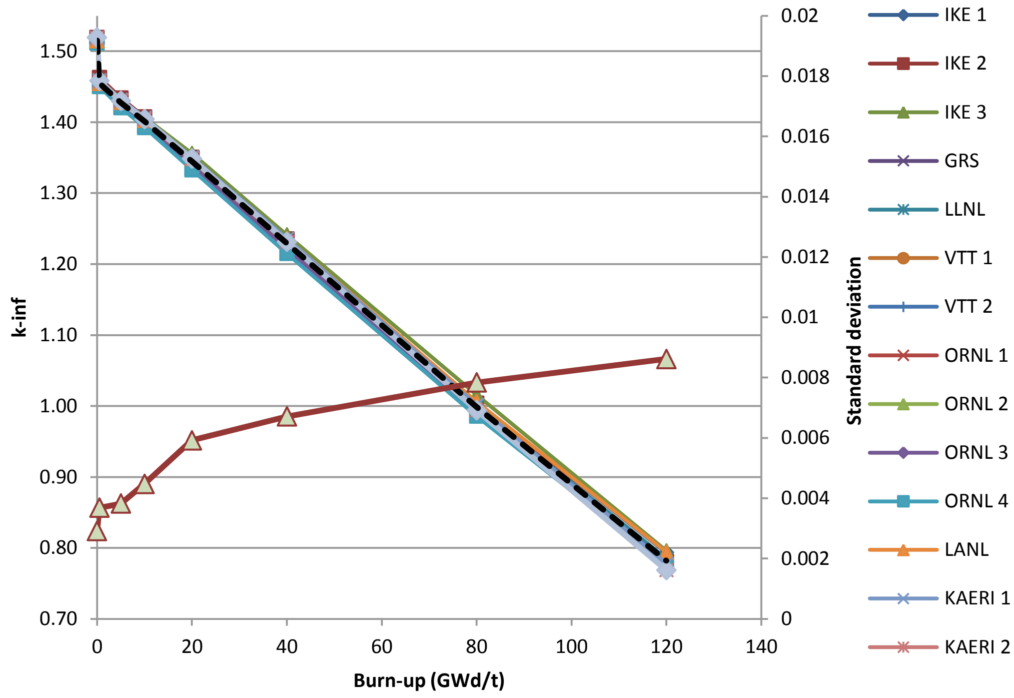

Figure C.2. ρ_{238} for pebble depletion

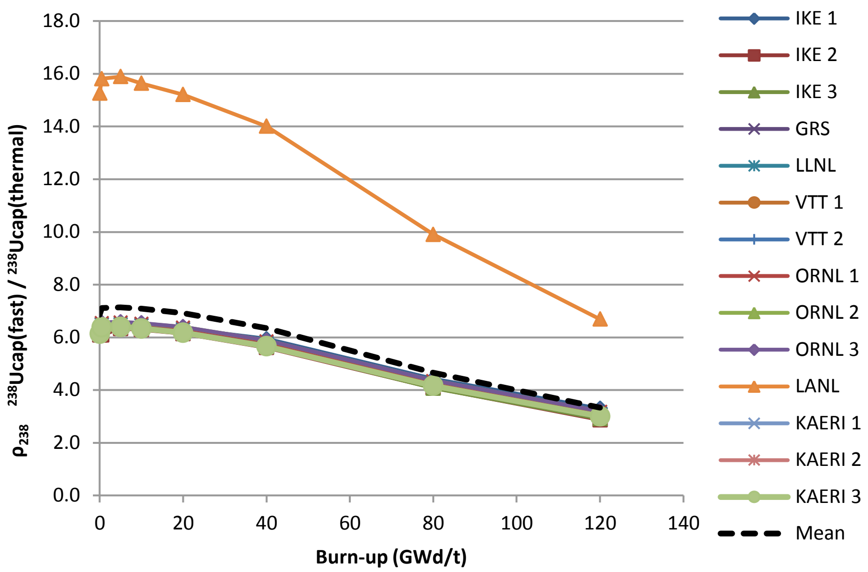

Figure C.3. δ_{235} for pebble depletion

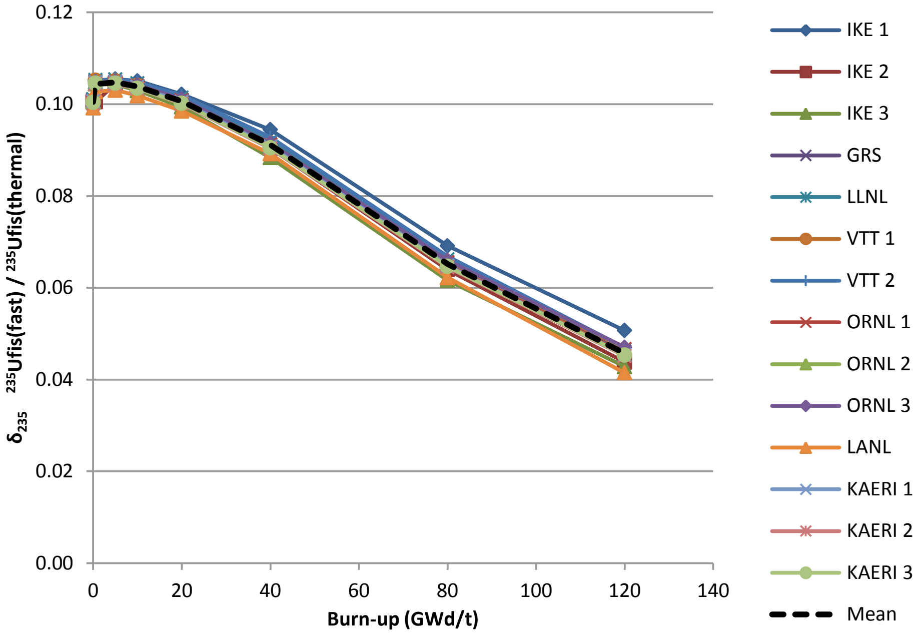

Figure C.4. δ_{238} for pebble depletion

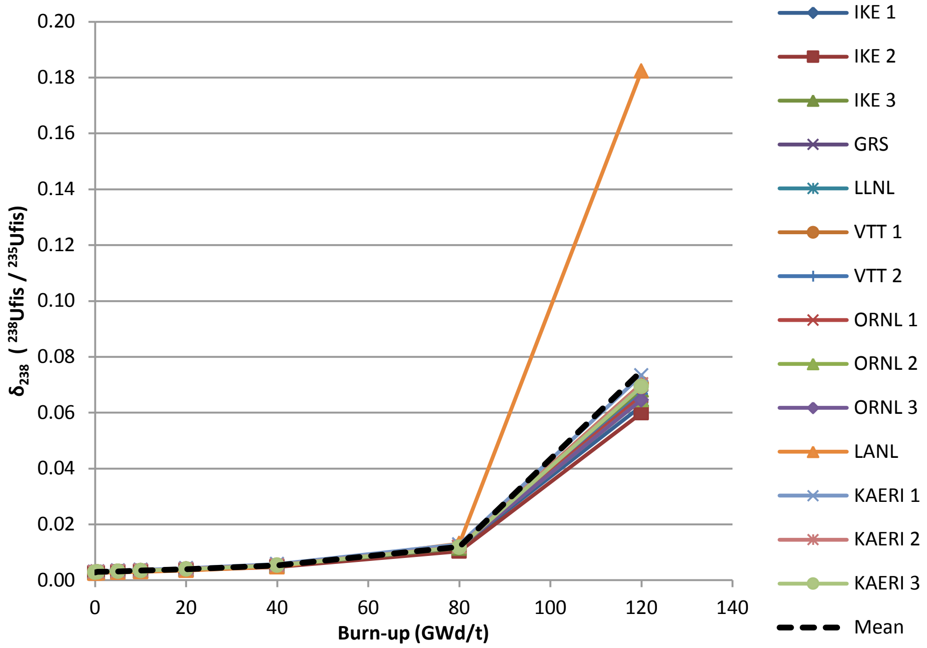

Figure C.5. c/f_{235} for pebble depletion

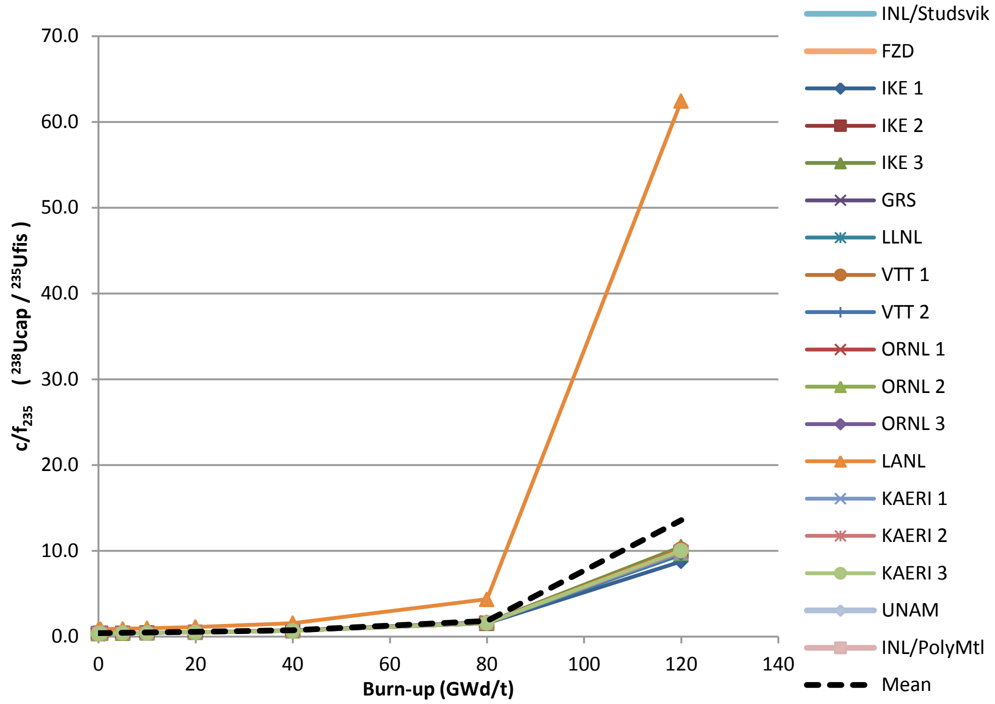

Figure C.6. ^{235}U mass vs burn-up for pebble depletion

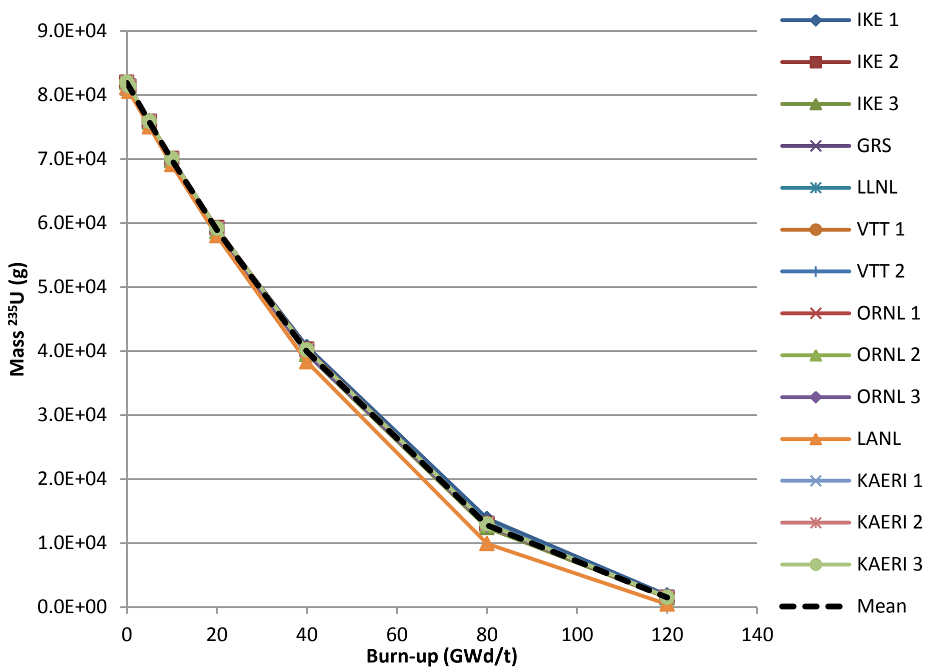

Figure C.7. ^{238}U mass vs burn-up for pebble depletion

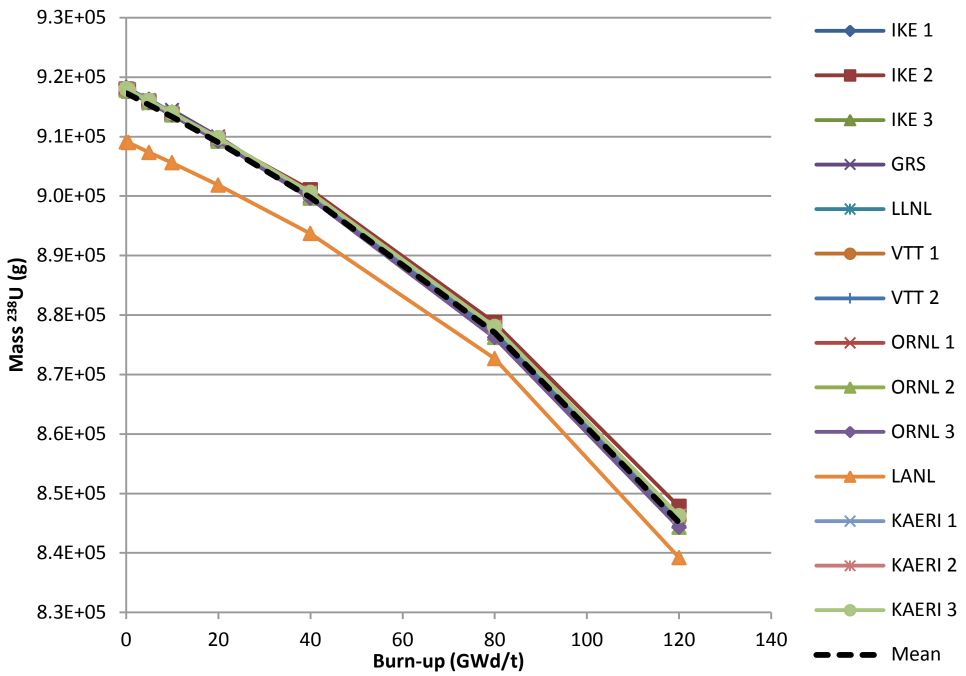

Figure C.8. ^{239}Pu mass vs burn-up for pebble depletion

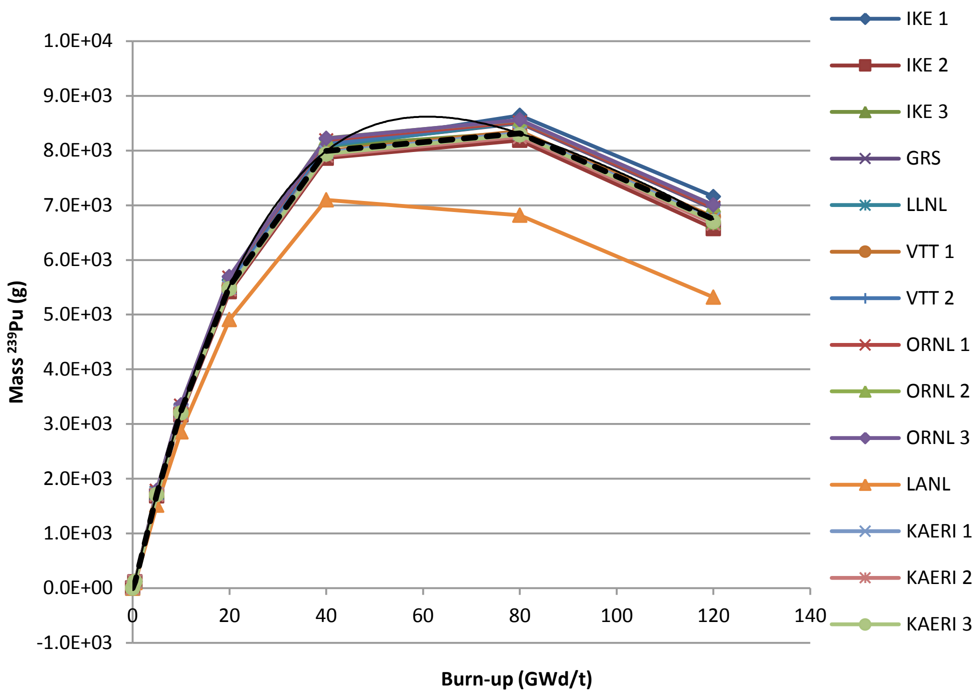

Figure C.9. ^{240}**Pu mass vs burn-up for pebble depletion**

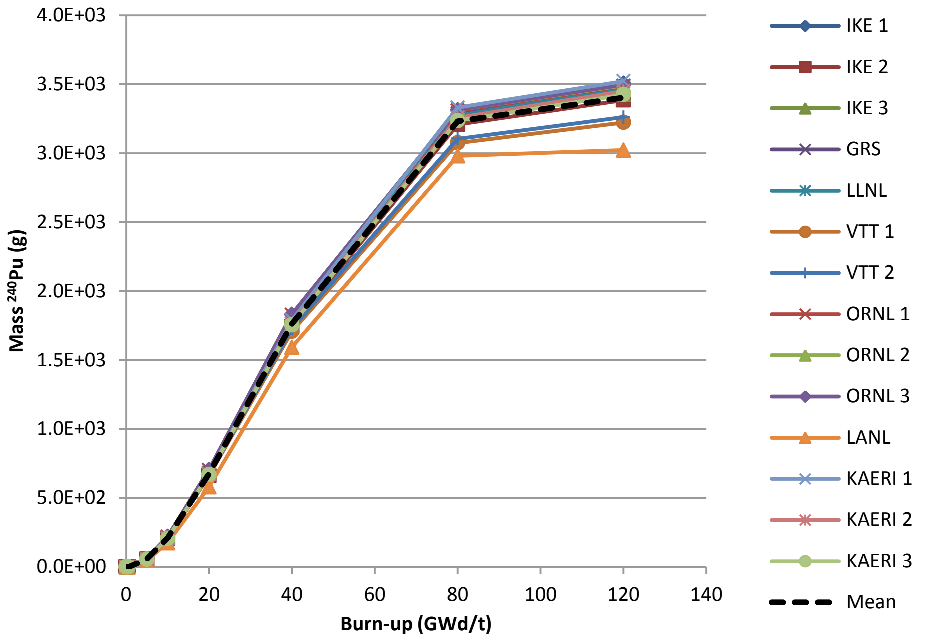

Figure C.10. ^{241}**Pu mass vs burn-up for pebble depletion**

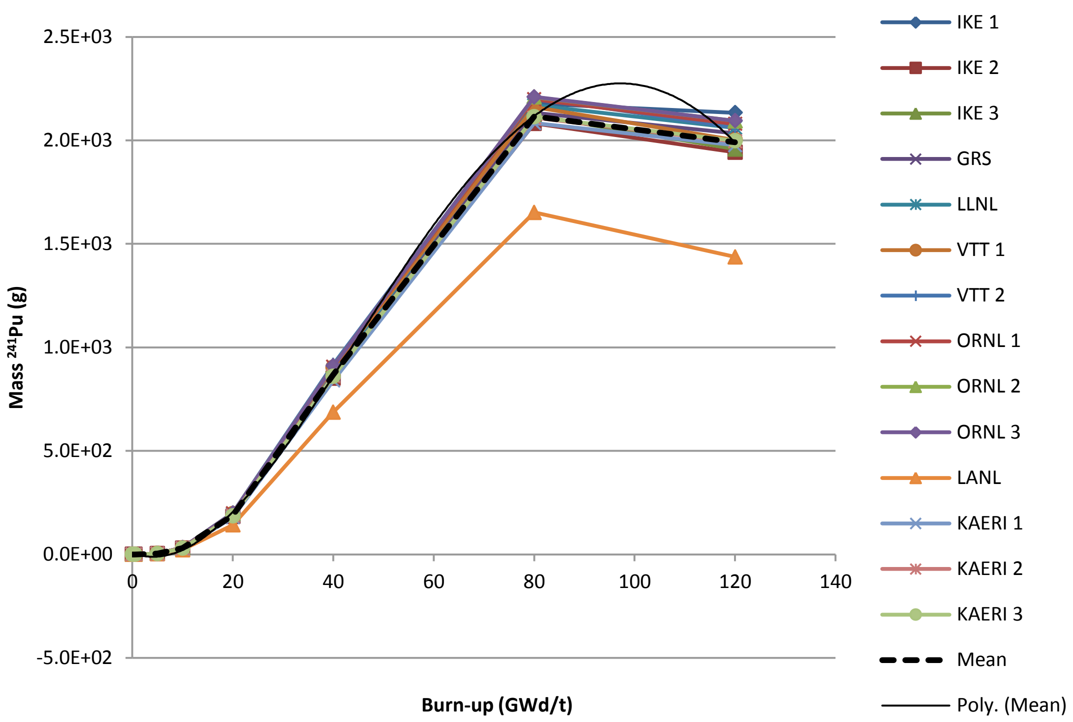

Figure C.11. ^{242}Pu mass vs burn-up for pebble depletion

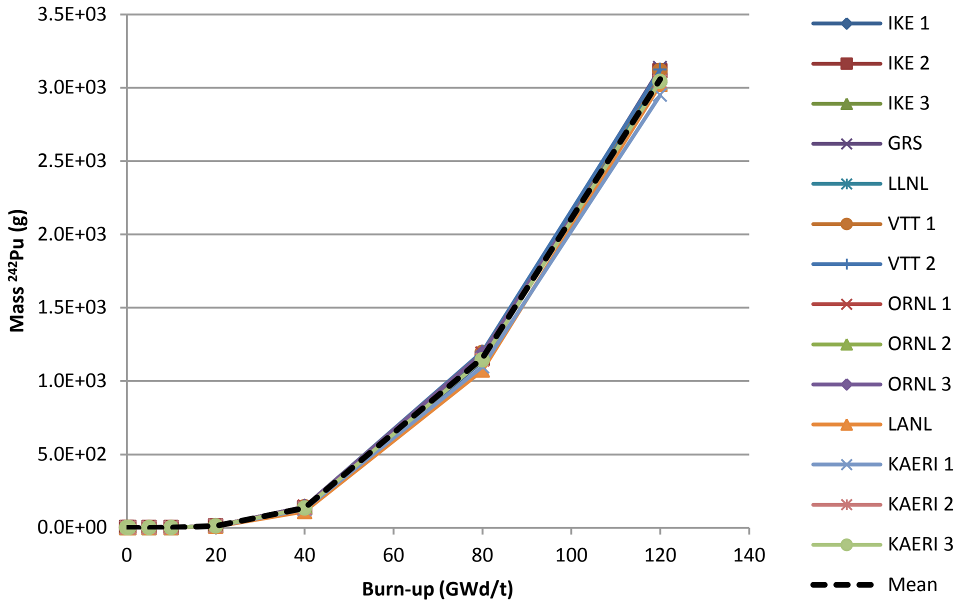

Figure C.12. ^{241}Am mass vs burn-up for pebble depletion

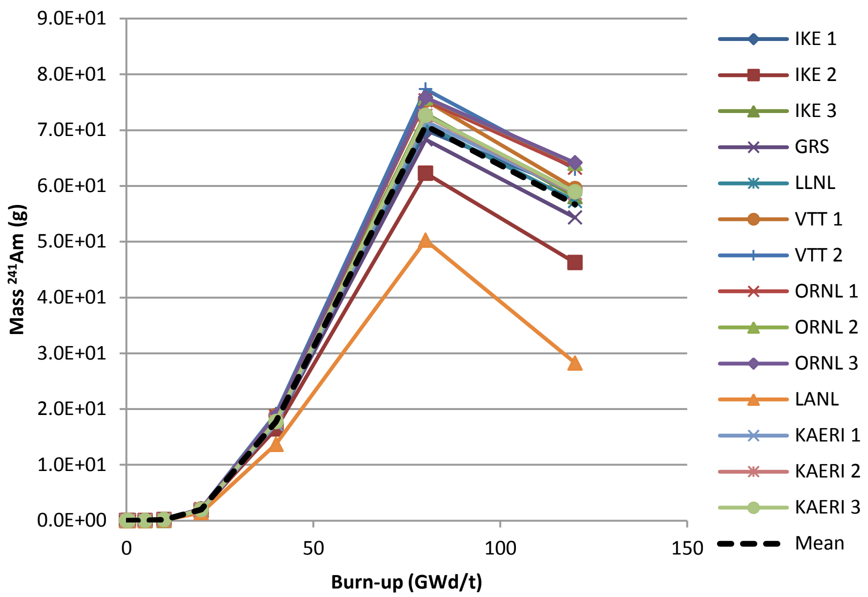

Figure C.13. ^{244}**Cm mass vs burn-up for pebble depletion**

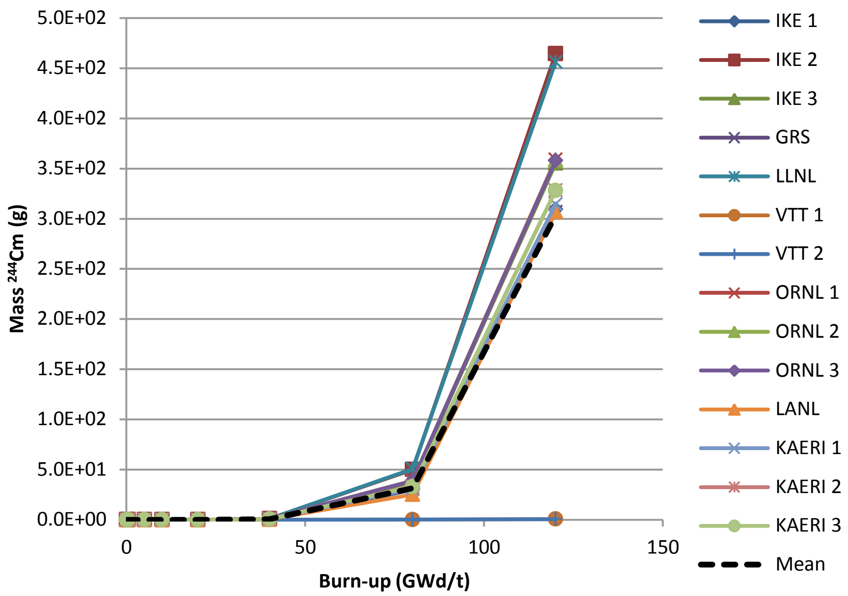

Figure C.14. ^{245}**Cm mass vs burn-up for pebble depletion**

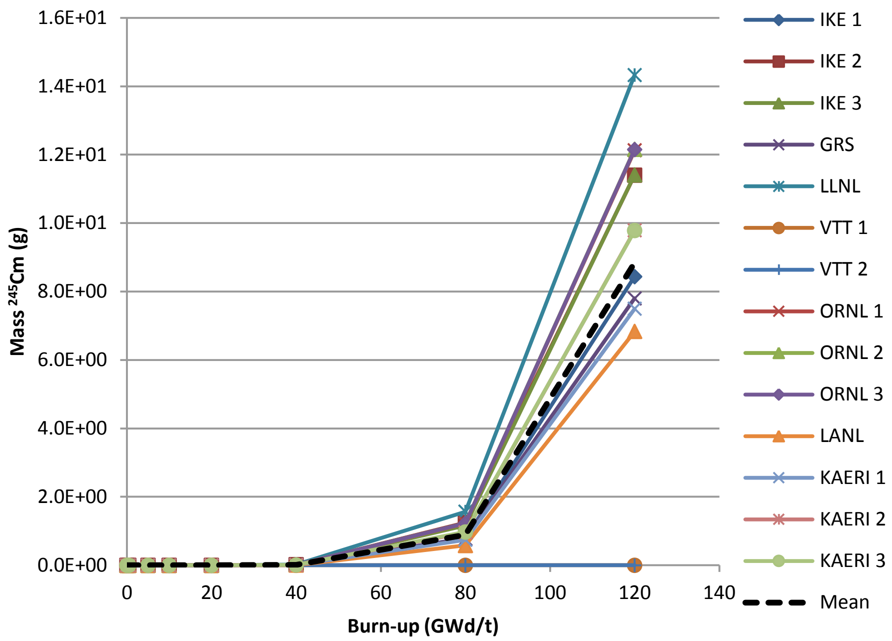

Figure C.15. ^{85}**Kr mass vs burn-up for pebble depletion**

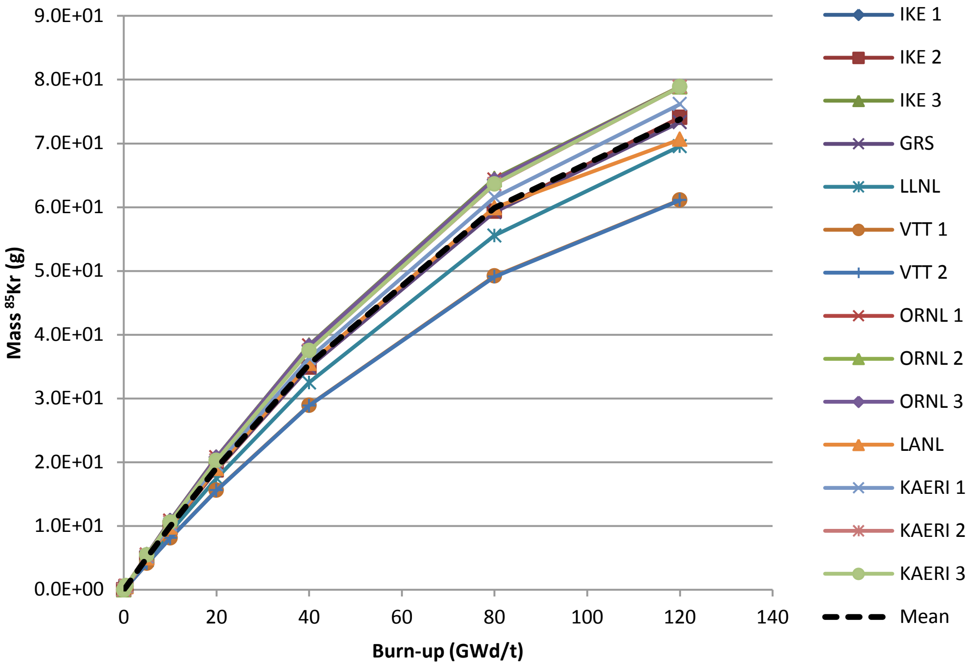

Figure C.16. ^{90}**Sr mass vs burn-up for pebble depletion**

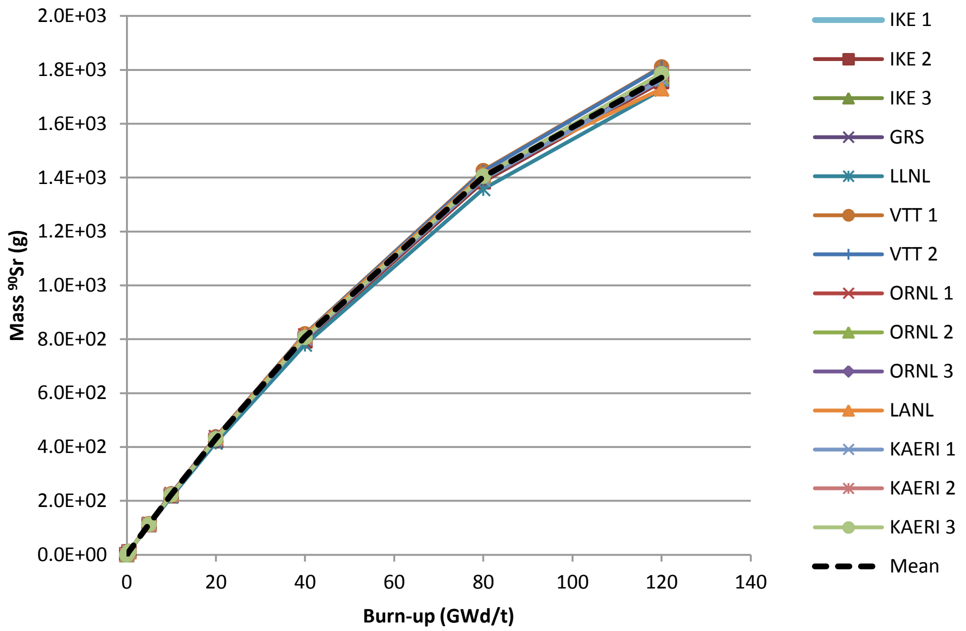

Figure C.17. ^{110m}Ag mass vs burn-up for pebble depletion

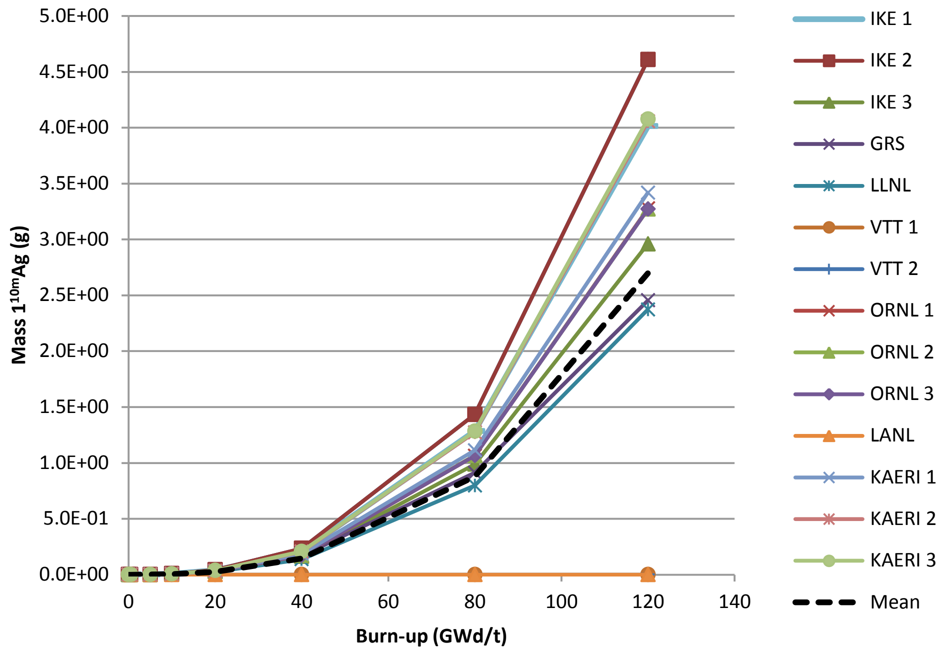

Figure C.18. ^{137}Cs mass vs burn-up for pebble depletion

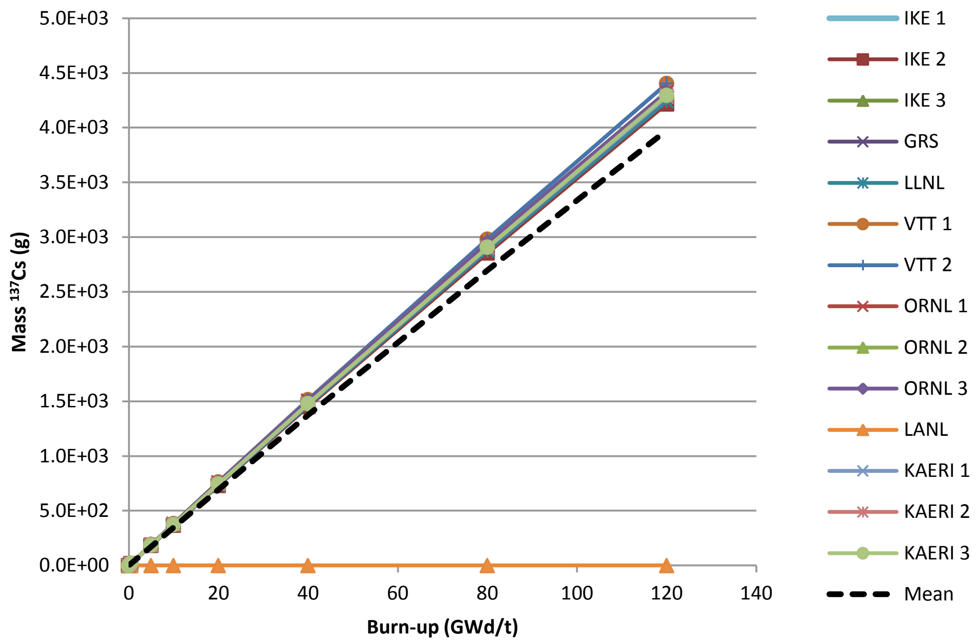

Figure C.19. ^{135}**Xe mass vs burn-up for pebble depletion**

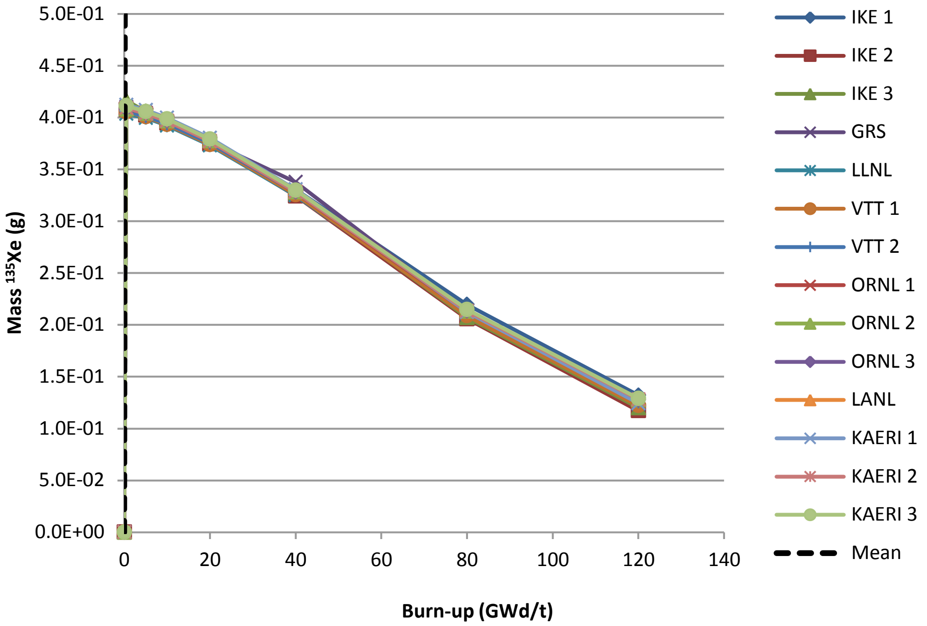

Figure C.20. ^{149}**Sm mass vs burn-up for pebble depletion**

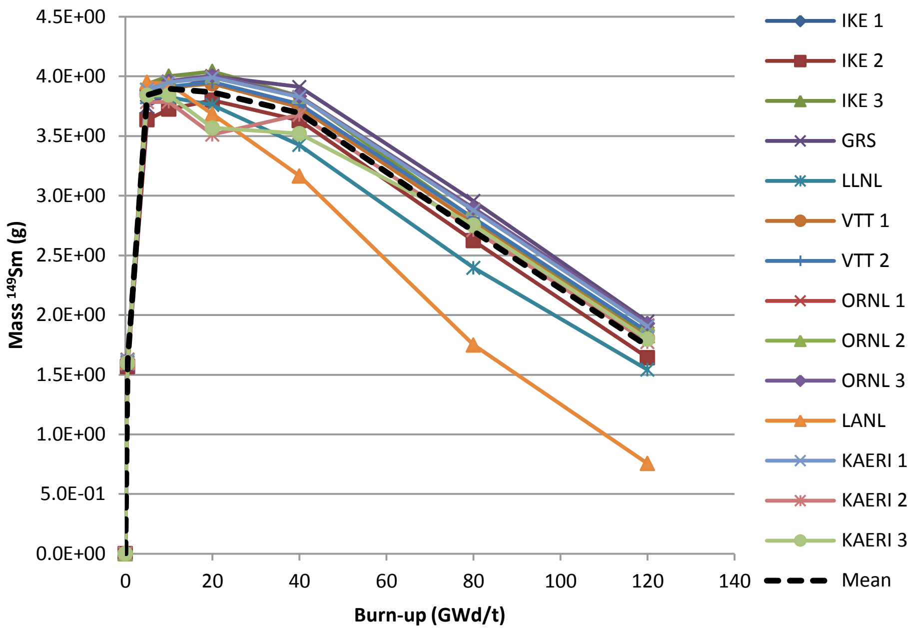

Figure C.21. ^{151}Sm mass vs burn-up for pebble depletion

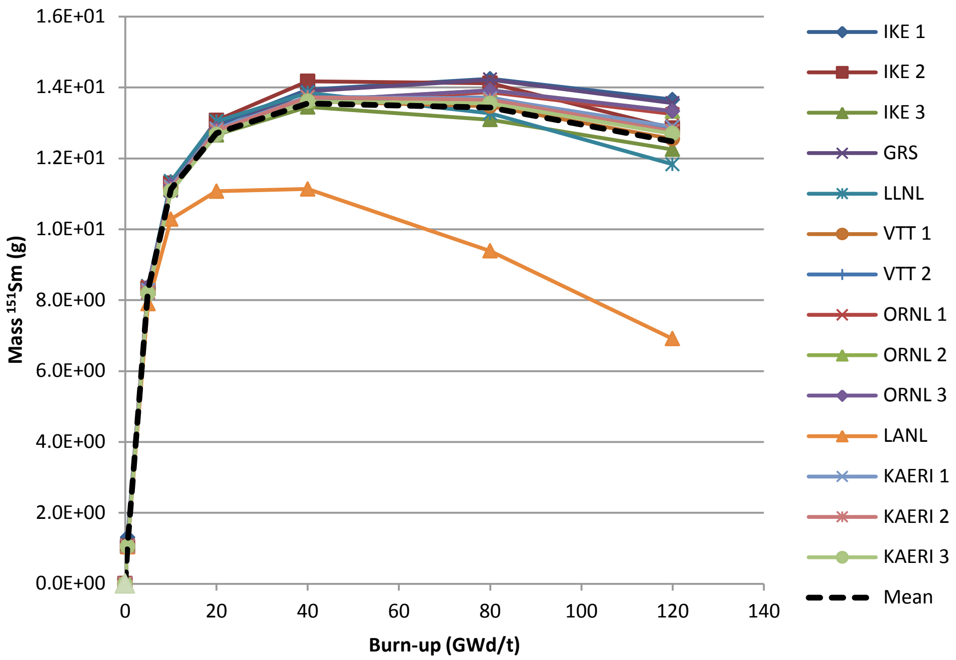

Appendix D. Results of prismatic supercell depletion calculations

Figure D.1. k_{-inf} vs burn-up for prismatic depletion

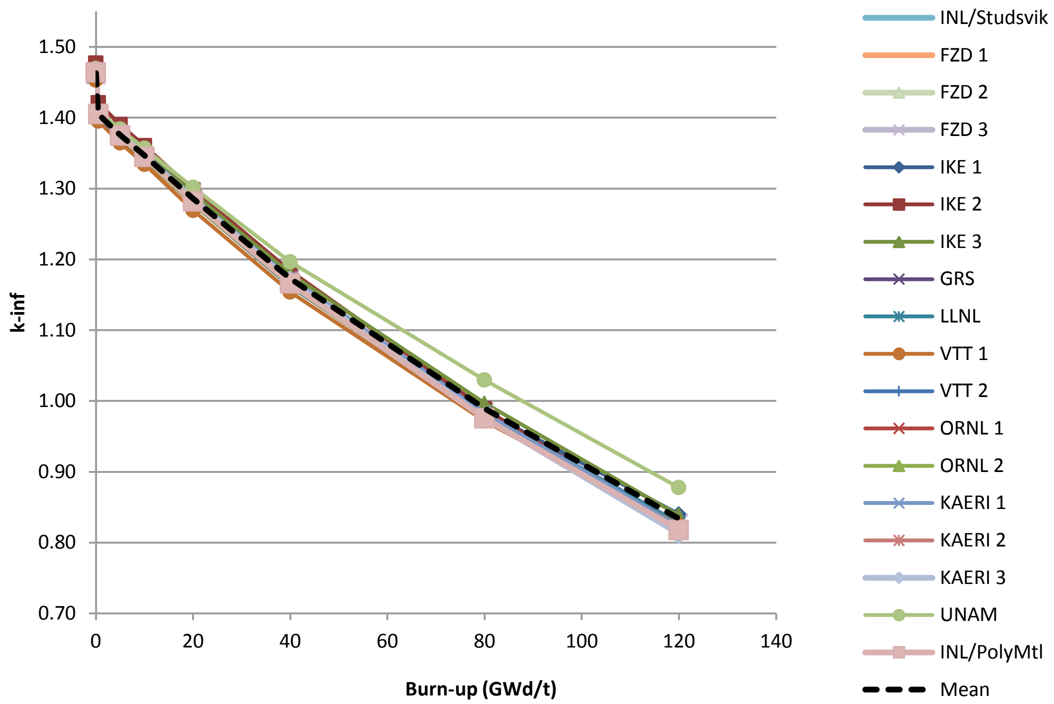

Figure D.2. ρ_{238} for prismatic depletion

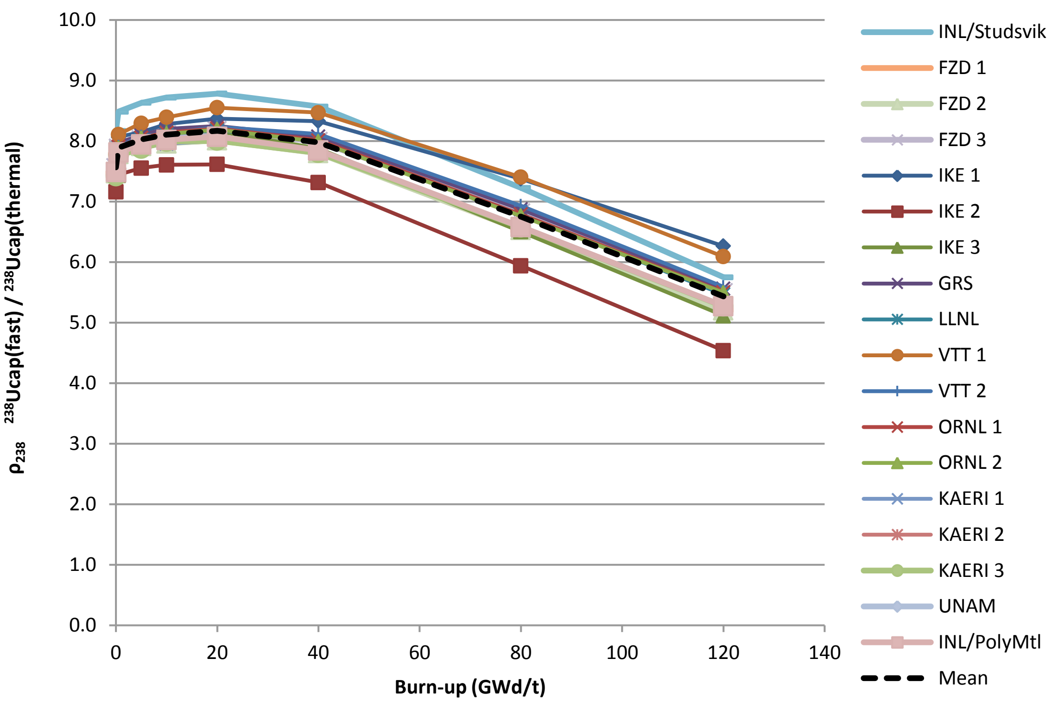

Figure D.3. δ_{235} for prismatic depletion

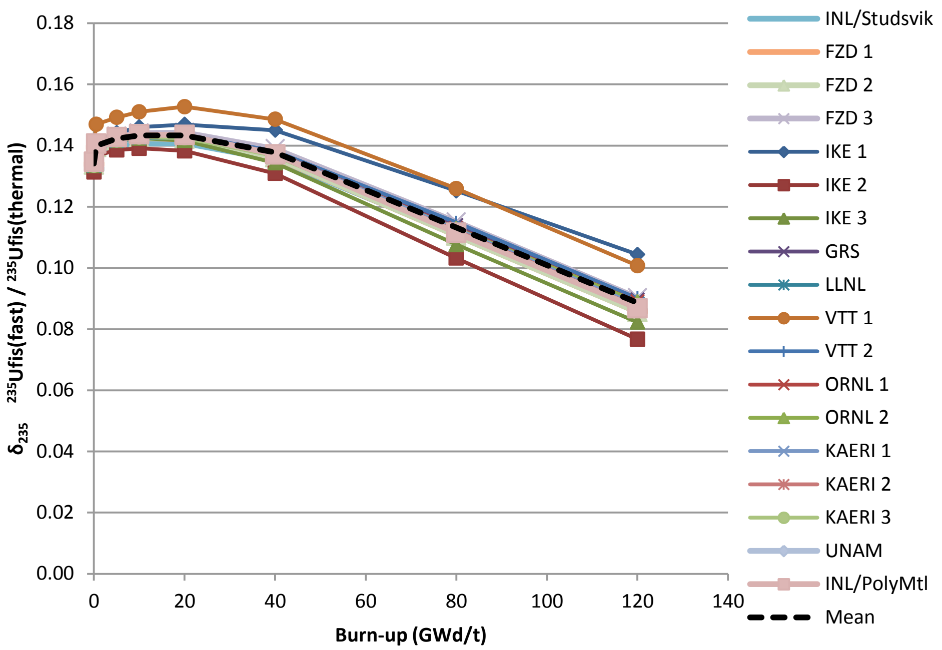

Figure D.4. δ_{238} for prismatic depletion

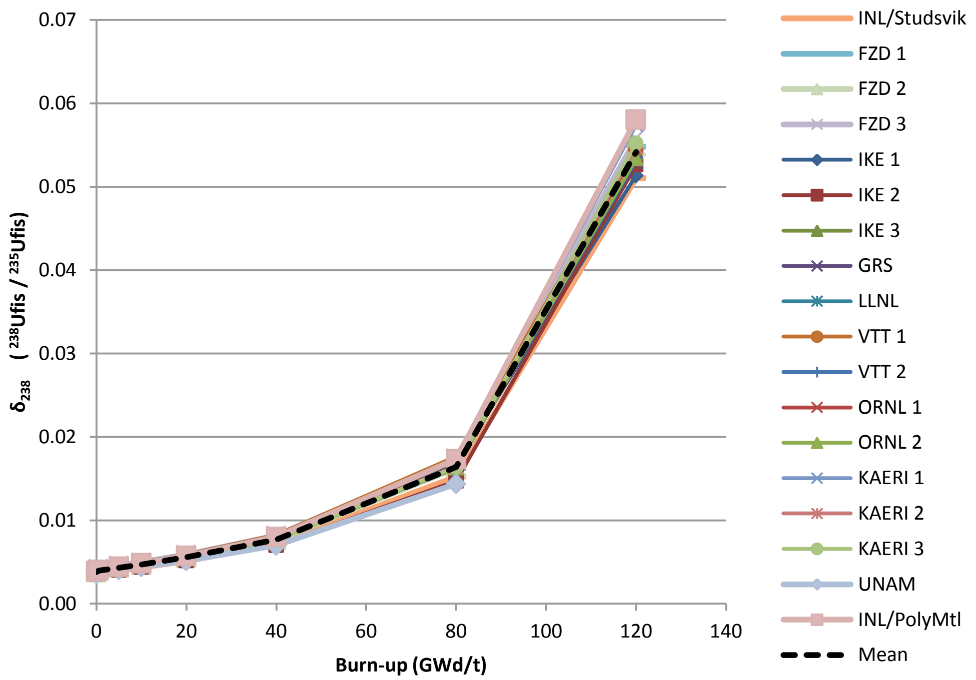

Figure D.5. c/f$_{235}$ for prismatic depletion

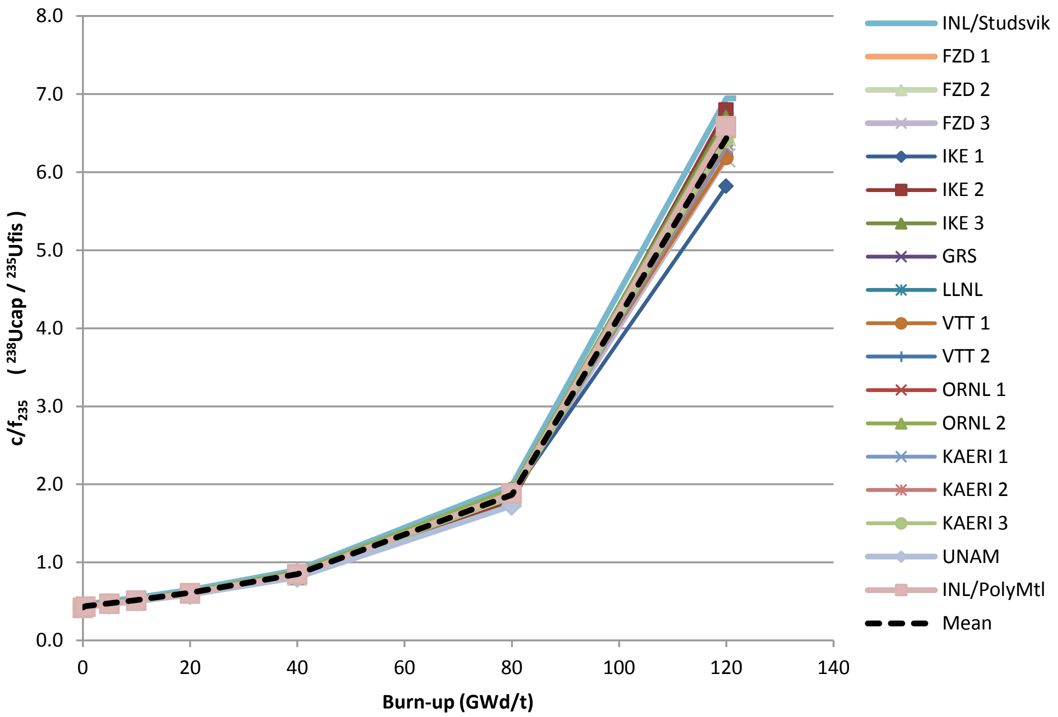

Figure D.6. ^{235}U mass vs burn-up for prismatic depletion

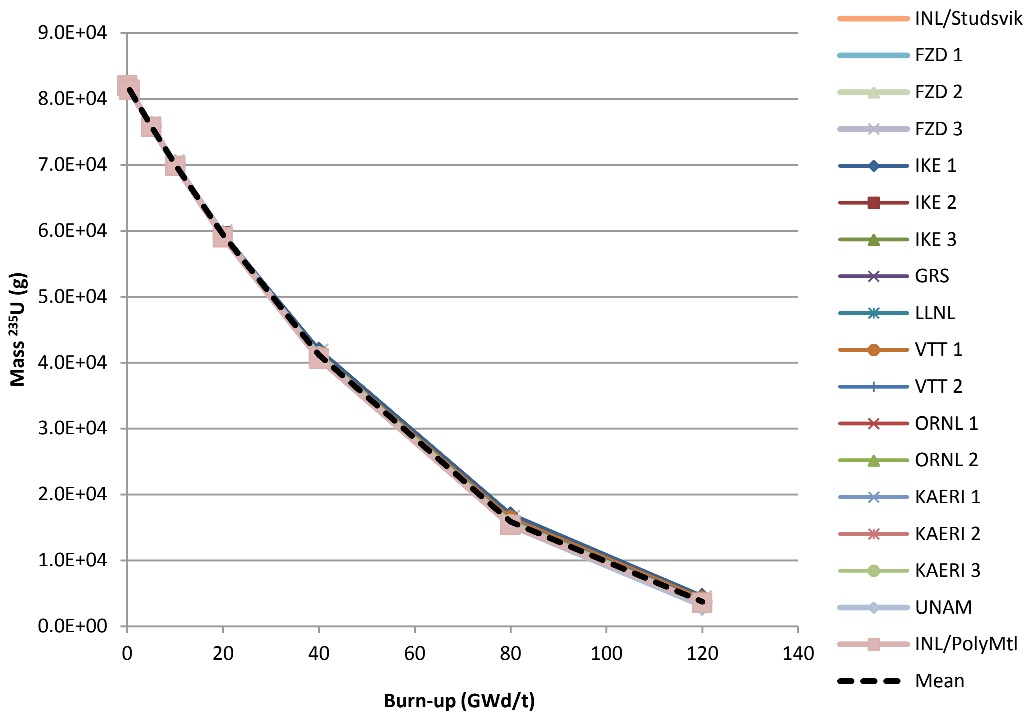

Figure D.7. ^{238}U mass vs burn-up for prismatic depletion

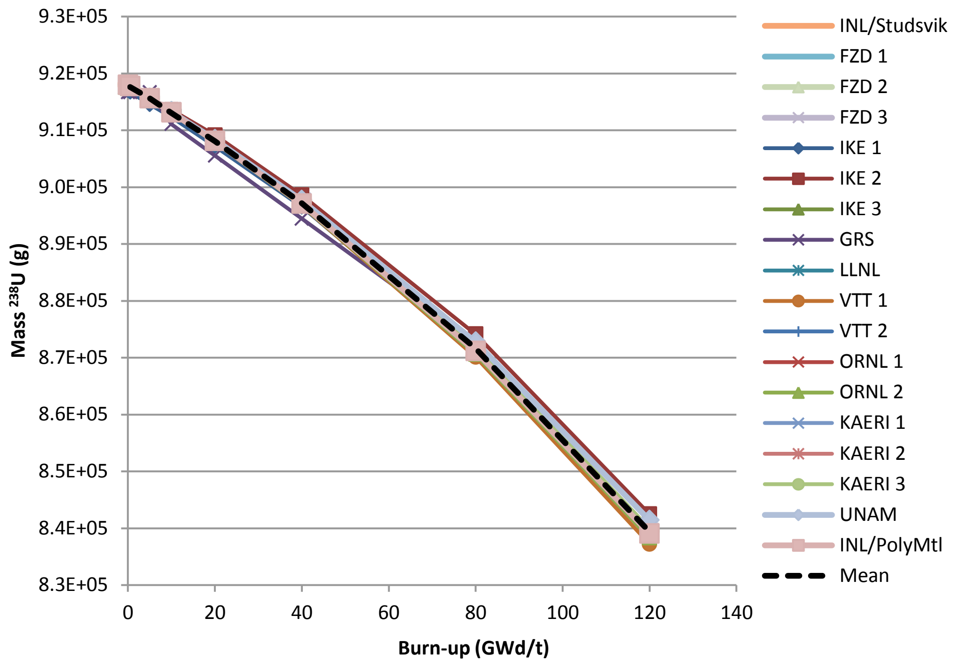

Figure D.8. ^{239}Pu mass vs burn-up for prismatic depletion

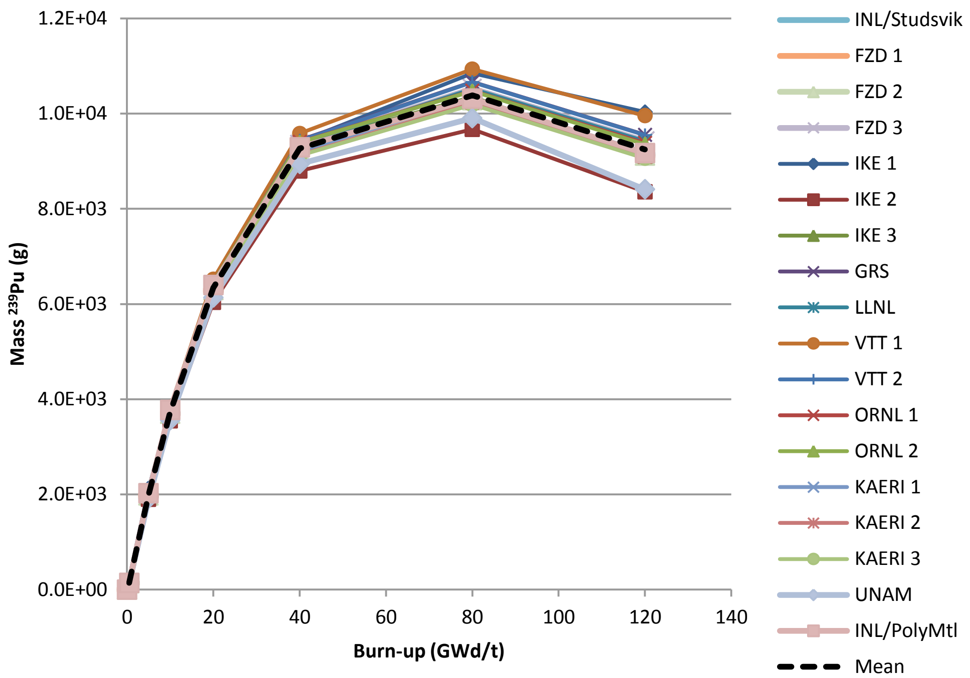

Figure D.9. ^{240}Pu mass vs burn-up for prismatic depletion

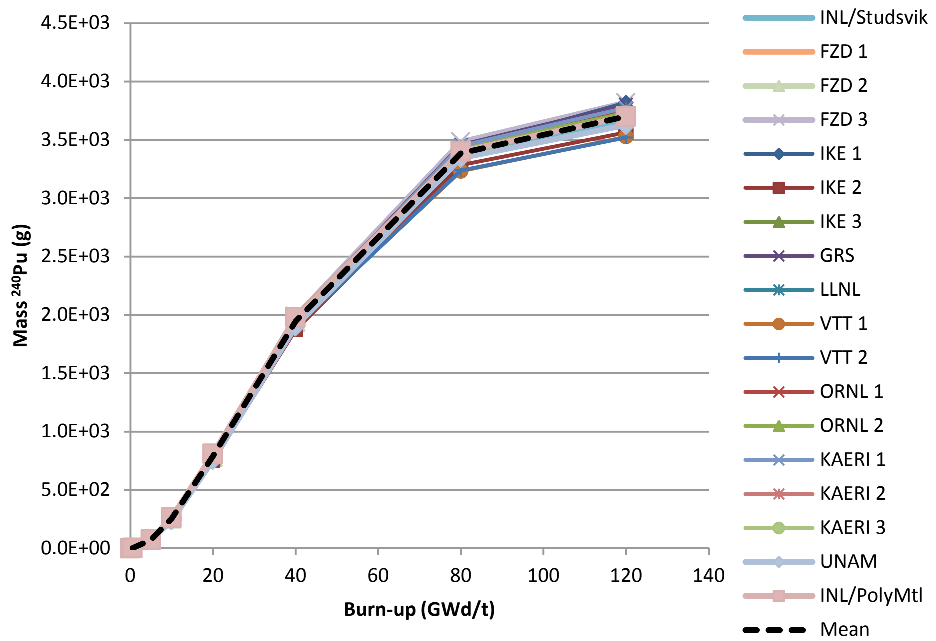

Figure D.10. ^{241}Pu mass vs burn-up for prismatic depletion

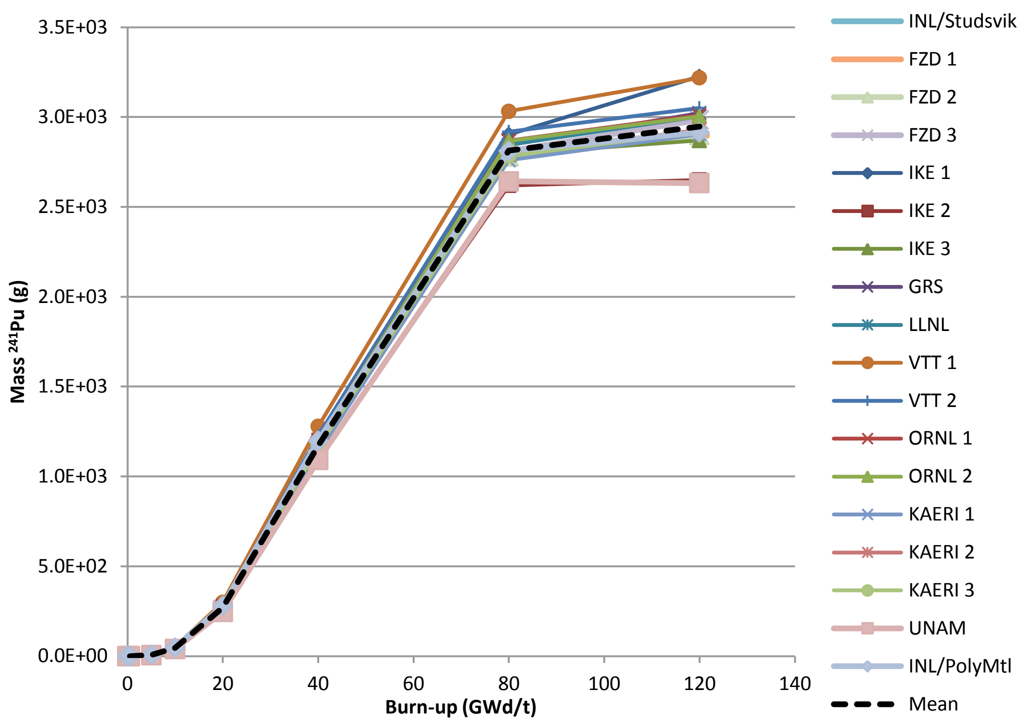

Figure D.11. ^{242}Pu mass vs burn-up for prismatic depletion

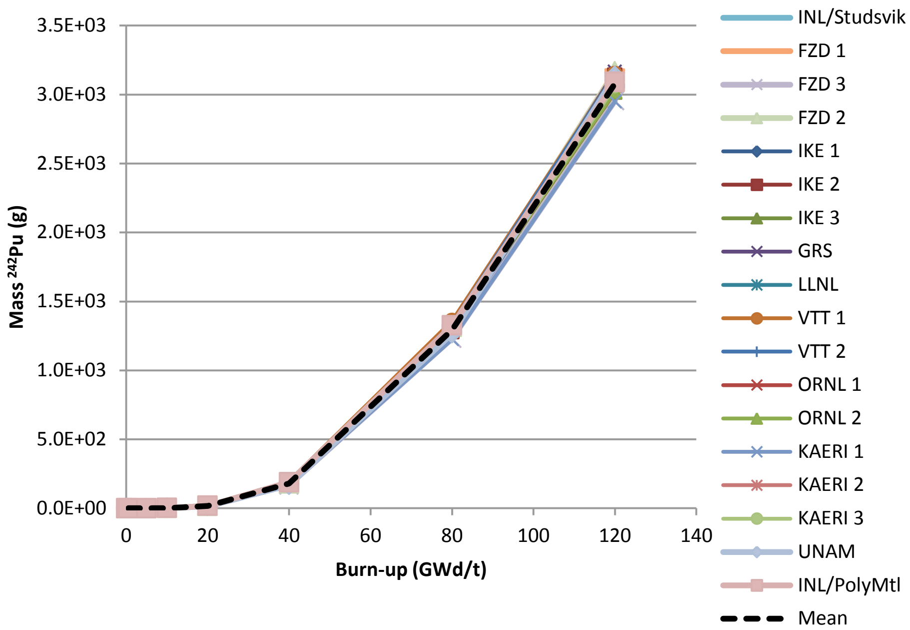

Figure D.12. ^{241}Am mass vs burn-up for prismatic depletion

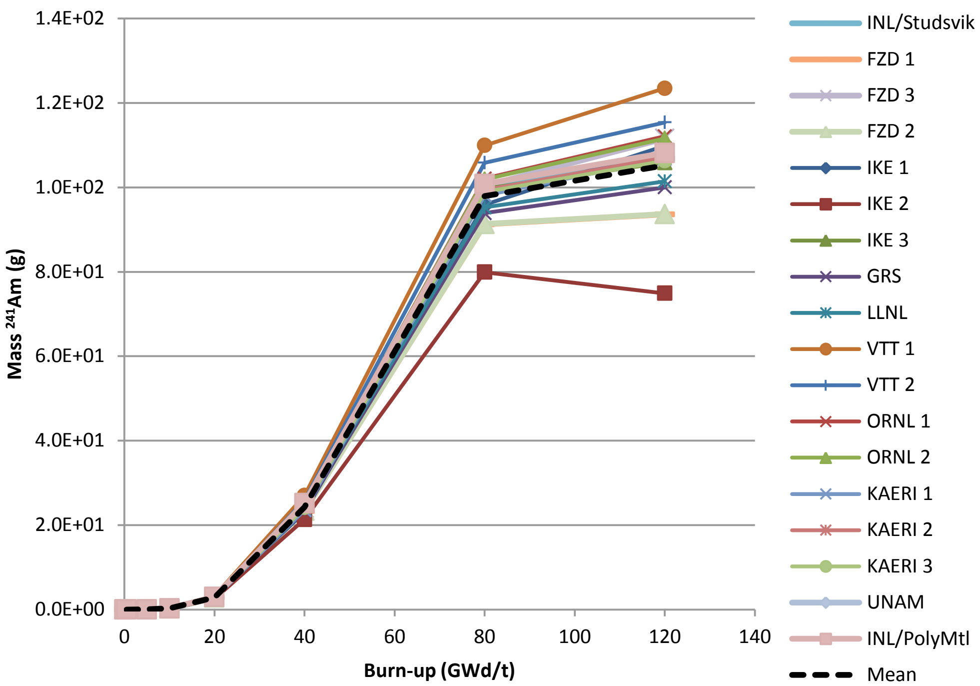

Figure D.13. ^{244}Cm mass vs burn-up for prismatic depletion

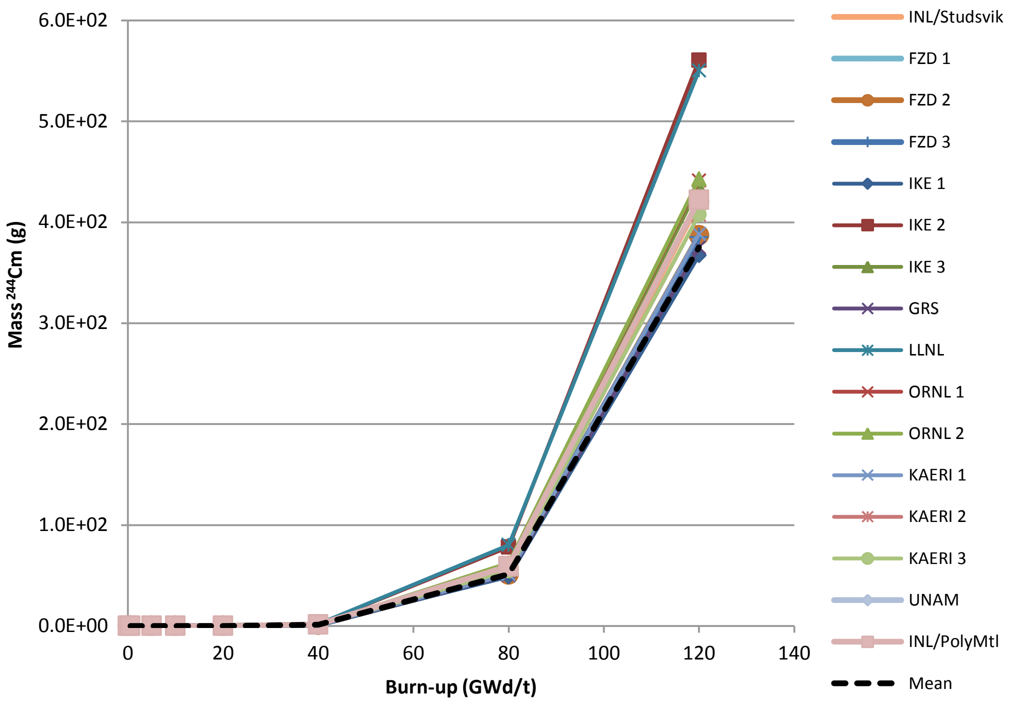

Figure D.14. ^{245}Cm mass vs burn-up for prismatic depletion

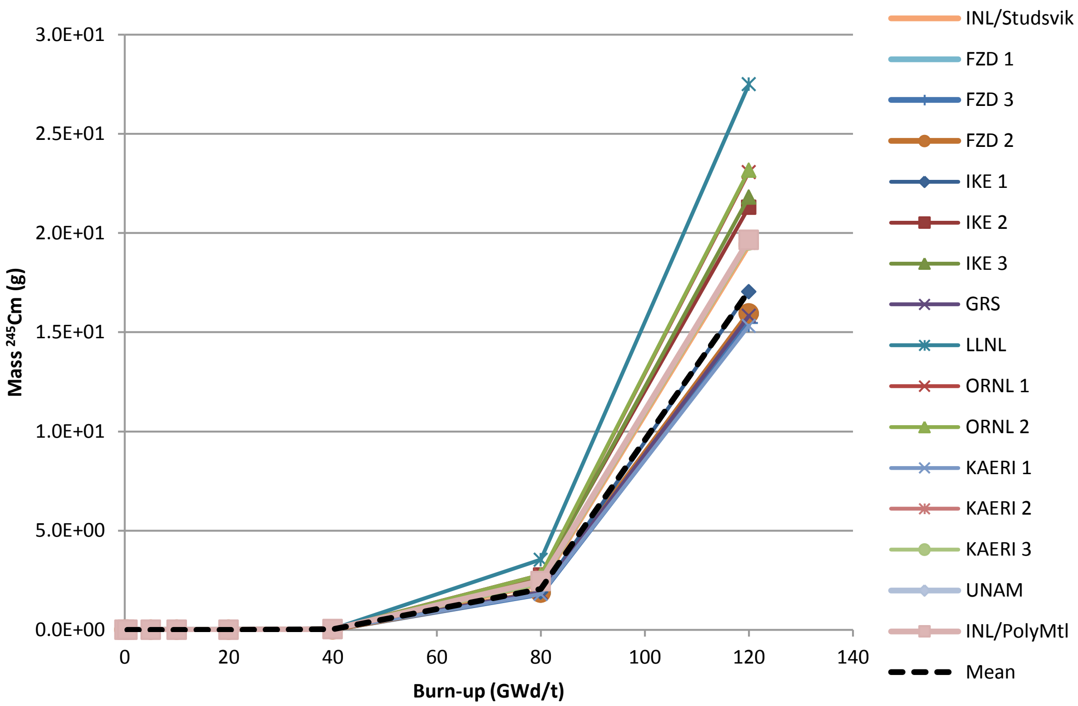

Figure D.15. ^{85}Kr mass vs burn-up for prismatic depletion

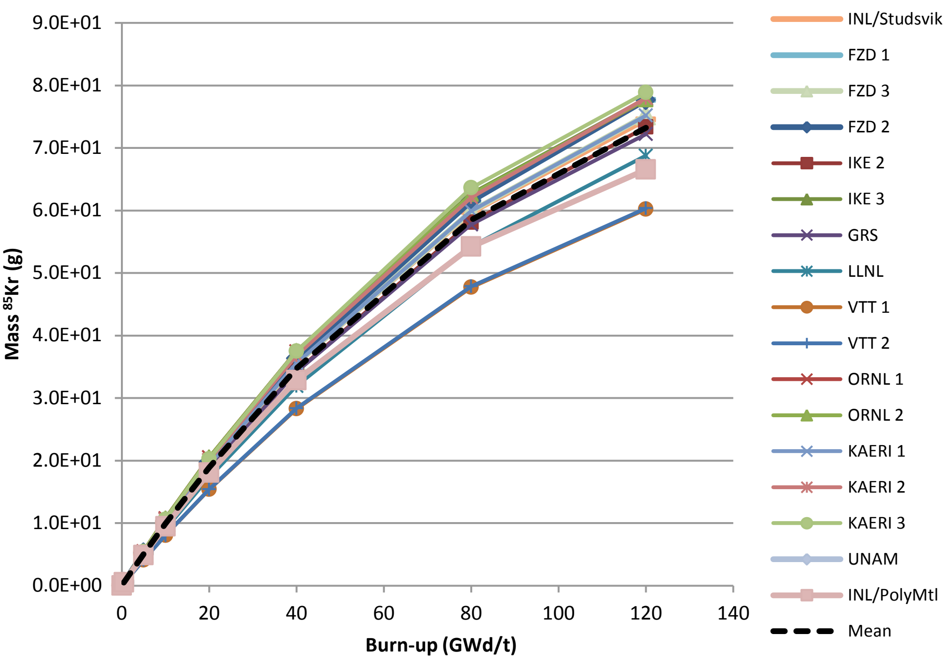

Figure D.16. ^{90}Sr mass vs burn-up for prismatic depletion

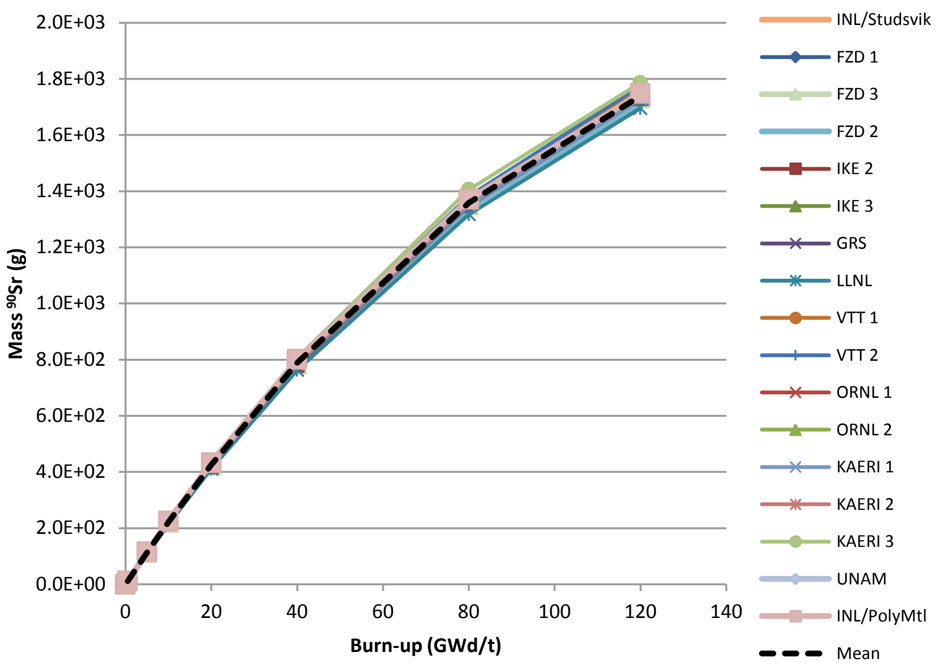

Figure D.17. ^{110m}Ag mass vs burn-up for prismatic depletion

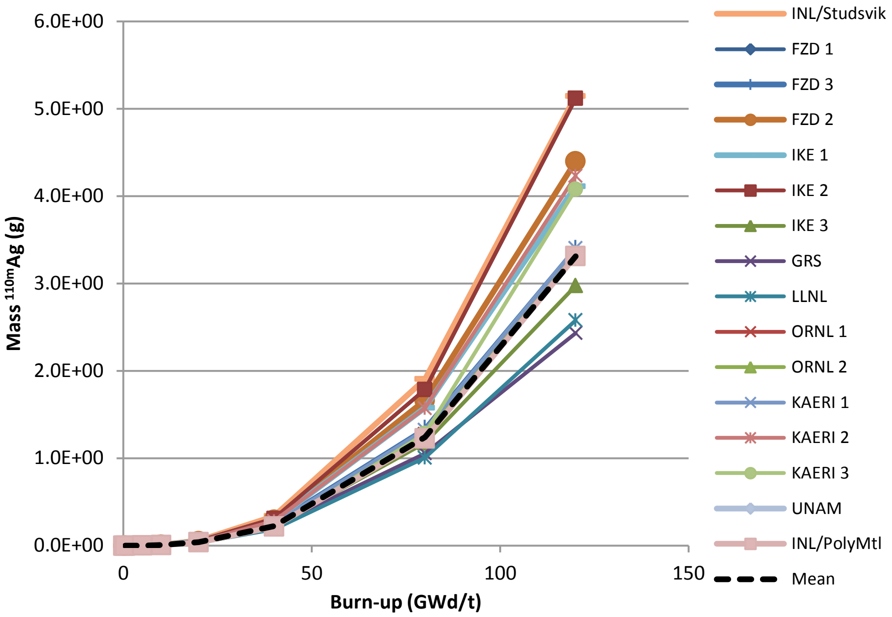

Figure D.18. ^{137}Cs mass vs burn-up for prismatic depletion

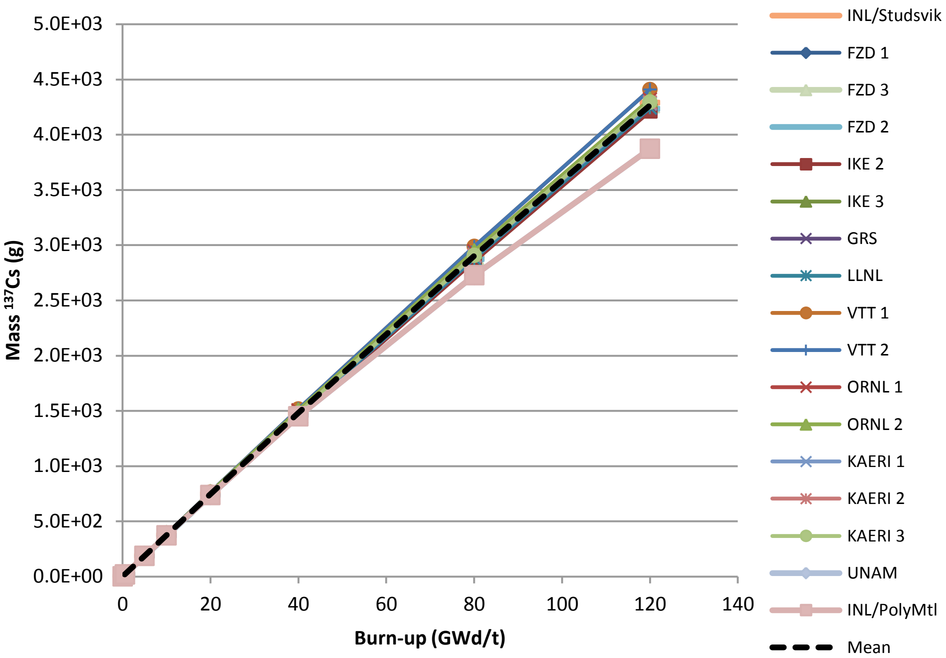

Figure D.19. ^{135}Xe mass vs burn-up for prismatic depletion

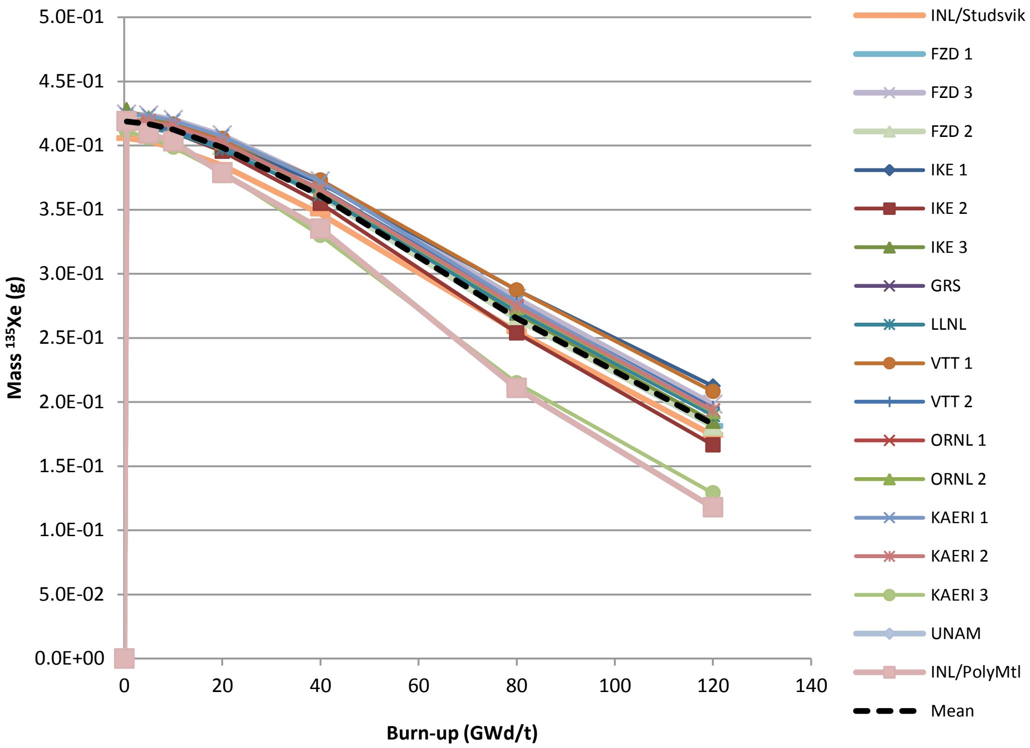

Figure D.20. ^{149}Sm mass vs burn-up for prismatic depletion

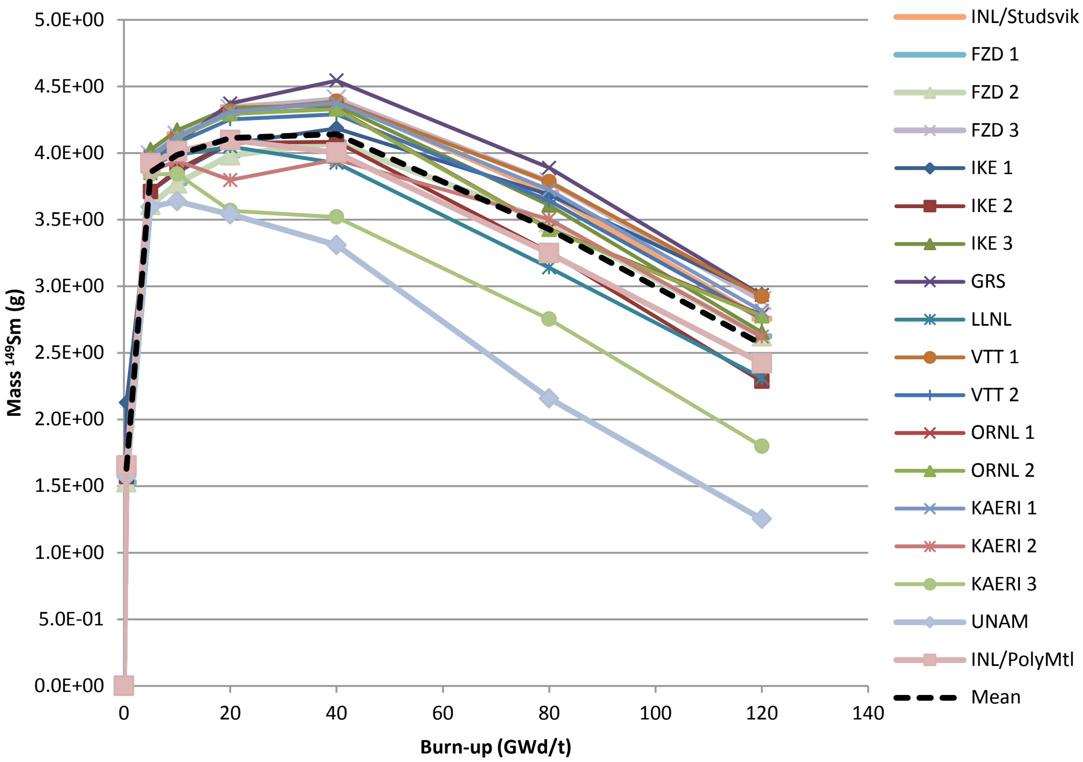

Figure D.21. ^{151}Sm mass vs burn-up for prismatic depletion

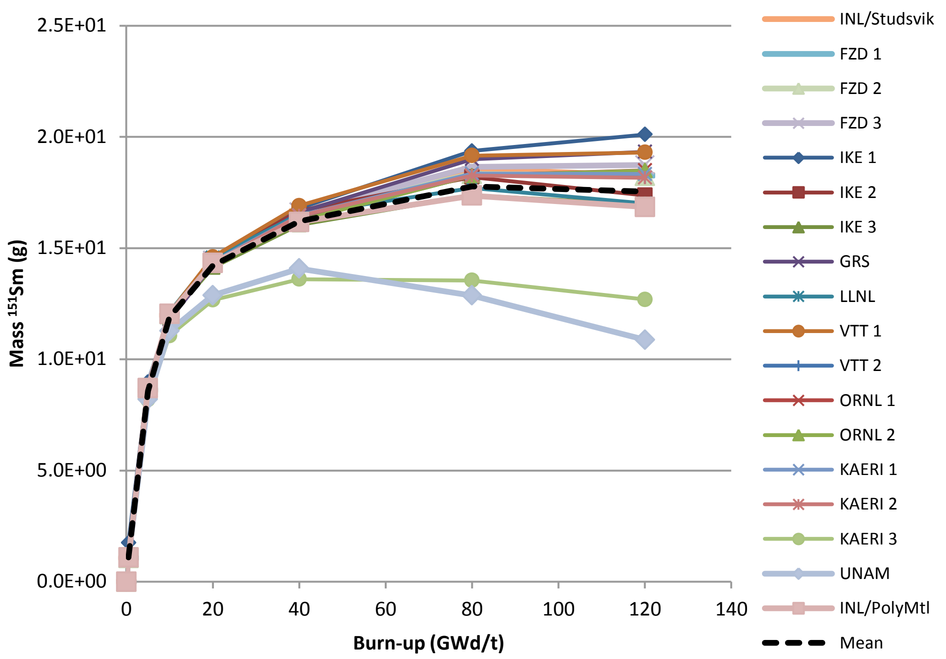

Appendix E. Raw data submissions

Grain – FZD1

GRAIN Results								
Burn-up (GWd/t)	**0**	**0.5**	**5**	**10**	**20**	**40**	**80**	**120**
k-inf	1.34444	1.29246	1.25967	1.22558	1.15719	1.04922	0.91473	0.83116
□^{238}	2.55E+00	2.58E+00	2.59E+00	2.60E+00	2.61E+00	2.62E+00	2.66E+00	2.70E+00
□^{235}	4.59E-02	4.64E-02	4.66E-02	4.65E-02	4.63E-02	4.59E-02	4.52E-02	4.46E-02
□^{238}	5.94E-03	6.23E-03	6.98E-03	7.84E-03	9.75E-03	1.45E-02	3.07E-02	6.47E-02
c/f^{235}	5.59E-01	5.83E-01	6.49E-01	7.25E-01	8.93E-01	1.32E+00	2.78E+00	5.92E+00
Actinide masses (g/t initial U)								
U-235	8.20E+04	8.14E+04	7.59E+04	7.02E+04	6.01E+04	4.36E+04	2.20E+04	1.05E+04
U-238	9.18E+05	9.18E+05	9.15E+05	9.12E+05	9.05E+05	8.90E+05	8.57E+05	8.19E+05
Pu-239	4.33E-13	1.86E+02	2.65E+03	4.94E+03	8.47E+03	1.29E+04	1.68E+04	1.82E+04
Pu-240	4.35E-13	6.08E-01	9.98E+01	3.50E+02	1.03E+03	2.39E+03	4.02E+03	4.65E+03
Pu-241	4.37E-13	5.34E-03	1.04E+01	7.36E+01	4.25E+02	1.78E+03	4.58E+03	6.05E+03
Pu-242	4.38E-13	5.64E-06	1.38E-01	2.04E+00	2.51E+01	2.32E+02	1.38E+03	2.92E+03
Am-241	4.37E-13	1.11E-06	2.67E-02	3.87E-01	4.54E+00	3.75E+01	1.71E+02	2.80E+02
Cm-244	4.42E-13	1.71E-12	1.48E-05	9.88E-04	5.75E-02	2.76E+00	8.99E+01	4.98E+02
Cm-245	4.44E-13	4.44E-13	4.95E-08	6.88E-06	8.29E-04	8.32E-02	5.51E+00	4.37E+01
Fission product masses (g/t initial U)								
Kr-85	4.26E-13	1.47E+00	1.43E+01	2.77E+01	5.24E+01	9.46E+01	1.57E+02	1.99E+02
Sr-90	4.31E-13	3.03E+01	2.95E+02	5.73E+02	1.09E+03	1.98E+03	3.35E+03	4.34E+03
Ag-110m	4.33E-13	2.58E-05	4.65E-03	2.63E-02	1.51E-01	8.13E-01	3.70E+00	7.76E+00
Cs-137	4.35E-13	3.28E+01	3.28E+02	6.55E+02	1.30E+03	2.59E+03	5.09E+03	7.51E+03
Xe-135	4.37E-13	7.97E-01	8.15E-01	8.27E-01	8.41E-01	8.49E-01	8.34E-01	8.09E-01
Sm-149	4.38E-13	2.67E+00	6.94E+00	7.50E+00	8.44E+00	9.77E+00	1.09E+01	1.11E+01
Sm-151	4.37E-13	1.70E+00	1.45E+01	2.14E+01	2.82E+01	3.74E+01	5.42E+01	6.81E+01

Grain – FZD3

GRAIN Results								
Burn-up (GWd/t)	**0**	**0.5**	**5**	**10**	**20**	**40**	**80**	**120**
k-inf	1.34444	1.29246	1.25967	1.22558	1.15719	1.04922	0.91473	0.83116
[illegible]^{238}	2.55E+00	2.58E+00	2.59E+00	2.60E+00	2.61E+00	2.62E+00	2.66E+00	2.70E+00
[illegible]^{235}	4.59E-02	4.64E-02	4.66E-02	4.65E-02	4.63E-02	4.59E-02	4.52E-02	4.46E-02
[illegible]^{238}	5.94E-03	6.23E-03	6.98E-03	7.84E-03	9.75E-03	1.45E-02	3.07E-02	6.47E-02
c/f^{235}	5.59E-01	5.83E-01	6.49E-01	7.25E-01	8.93E-01	1.32E+00	2.78E+00	5.92E+00
Actinide masses (g/t initial U)								
U-235	8.20E+04	8.14E+04	7.59E+04	7.02E+04	6.01E+04	4.36E+04	2.20E+04	1.05E+04
U-238	9.18E+05	9.18E+05	9.15E+05	9.12E+05	9.05E+05	8.90E+05	8.57E+05	8.19E+05
Pu-239	4.33E-13	1.86E+02	2.65E+03	4.94E+03	8.47E+03	1.29E+04	1.68E+04	1.82E+04
Pu-240	4.35E-13	6.08E-01	9.98E+01	3.50E+02	1.03E+03	2.39E+03	4.02E+03	4.65E+03
Pu-241	4.37E-13	5.34E-03	1.04E+01	7.36E+01	4.25E+02	1.78E+03	4.58E+03	6.05E+03
Pu-242	4.38E-13	5.64E-06	1.38E-01	2.04E+00	2.51E+01	2.32E+02	1.38E+03	2.92E+03
Am-241	4.37E-13	1.11E-06	2.67E-02	3.87E-01	4.54E+00	3.75E+01	1.71E+02	2.80E+02
Cm-244	4.42E-13	1.71E-12	1.48E-05	9.88E-04	5.75E-02	2.76E+00	8.99E+01	4.98E+02
Cm-245	4.44E-13	4.44E-13	4.95E-08	6.88E-06	8.29E-04	8.32E-02	5.51E+00	4.37E+01
Fission product masses (g/t initial U)								
Kr-85	4.26E-13	1.47E+00	1.43E+01	2.77E+01	5.24E+01	9.46E+01	1.57E+02	1.99E+02
Sr-90	4.31E-13	3.03E+01	2.95E+02	5.73E+02	1.09E+03	1.98E+03	3.35E+03	4.34E+03
Ag-110m	4.33E-13	2.58E-05	4.65E-03	2.63E-02	1.51E-01	8.13E-01	3.70E+00	7.76E+00
Cs-137	4.35E-13	3.28E+01	3.28E+02	6.55E+02	1.30E+03	2.59E+03	5.09E+03	7.51E+03
Xe-135	4.37E-13	7.97E-01	8.15E-01	8.27E-01	8.41E-01	8.49E-01	8.34E-01	8.09E-01
Sm-149	4.38E-13	2.67E+00	6.94E+00	7.50E+00	8.44E+00	9.77E+00	1.09E+01	1.11E+01
Sm-151	4.37E-13	1.70E+00	1.45E+01	2.14E+01	2.82E+01	3.74E+01	5.42E+01	6.81E+01

Grain – IKE 1

GRAIN Results								
Burn-up (GWd/t)	**0**	**0.5**	**5**	**10**	**20**	**40**	**80**	**120**
k-inf	1.34948	1.29758	1.26541	1.22725	1.15763	1.04882	0.91183	0.82235
ρ238	1.063E+01	1.117E+01	1.175E+01	1.238E+01	1.338E+01	1.505E+01	1.729E+01	1.919E+01
δ235	1.922E-01	2.021E-01	2.127E-01	2.233E-01	2.405E-01	2.668E-01	3.011E-01	3.282E-01
δ238	5.301E-03	5.541E-03	6.217E-03	7.037E-03	8.746E-03	1.295E-02	2.778E-02	6.116E-02
c/f235	5.476E-01	5.733E-01	6.368E-01	7.155E-01	8.816E-01	1.295E+00	2.737E+00	6.055E+00
Actinide masses (g/t initial U)								
U-235	82018.9270	8.14E+04	7.60E+04	7.01E+04	5.98E+04	4.38E+04	2.21E+04	1.03E+04
U-238	9.1821E+05	9.1791E+05	9.1520E+05	9.1192E+05	9.0522E+05	8.9121E+05	8.5831E+05	8.2026E+05
Pu-239	0.00E+00	1.78E+02	2.57E+03	4.90E+03	8.37E+03	1.26E+04	1.65E+04	1.80E+04
Pu-240	0.00E+00	7.62E-01	9.82E+01	3.55E+02	1.03E+03	2.30E+03	3.87E+03	4.51E+03
Pu-241	0.00E+00	7.51E-03	1.05E+01	7.92E+01	4.47E+02	1.76E+03	4.53E+03	6.06E+03
Pu-242	0.00E+00	9.77E-06	1.48E-01	2.37E+00	2.85E+01	2.43E+02	1.45E+03	3.14E+03
Am-241	0.00E+00	1.84E-06	2.72E-02	4.25E-01	4.80E+00	3.56E+01	1.56E+02	2.49E+02
Cm-244	0.00E+00	8.72E-12	1.47E-05	1.11E-03	6.25E-02	2.64E+00	8.77E+01	5.11E+02
Cm-245	0.00E+00	0.00E+00	5.00E-08	7.94E-06	9.32E-04	8.09E-02	5.63E+00	4.84E+01
Fission product masses (g/t initial U)								
Kr-85								
Sr-90								
Ag-110m	0.00E+00	1.15E-05	2.17E-03	1.35E-02	8.03E-02	4.31E-01	2.14E+00	4.81E+00
Cs-137								
Xe-135	0.00E+00	4.37E-01	4.46E-01	4.52E-01	4.60E-01	4.63E-01	4.58E-01	4.48E-01
Sm-149	1.00E+00	1.58E+00	3.95E+00	4.29E+00	3.97E+00	5.60E+00	6.29E+00	6.49E+00
Sm-151	0.00E+00	1.31E+00	9.11E+00	1.35E+01	1.76E+01	2.31E+01	3.37E+01	4.32E+01

Grain – IKE 2

GRAIN Results								
Burn-up (GWd/t)	**0**	**0.5**	**5**	**10**	**20**	**40**	**80**	**120**
k-inf	1.367	1.315	1.281	1.246	1.176	1.066	0.926	0.836
□^{238}	1.02E+01	1.06E+01	1.11E+01	1.16E+01	1.25E+01	1.36E+01	1.46E+01	1.46E+01
□^{235}	1.91E-01	2.00E-01	2.10E-01	2.18E-01	2.32E-01	2.50E-01	2.60E-01	2.54E-01
□^{238}	4.53E-04	4.71E-04	4.89E-04	5.06E-04	5.33E-04	5.68E-04	5.88E-04	5.80E-04
c/f^{235}	4.76E-02	4.92E-02	5.11E-02	5.27E-02	5.55E-02	5.94E-02	6.26E-02	6.28E-02
Actinide masses (g/t initial U)								
U-235	8.20E+04	8.14E+04	7.59E+04	7.02E+04	6.00E+04	4.32E+04	2.10E+04	9.09E+03
U-238	9.18E+05	9.18E+05	9.15E+05	9.12E+05	9.05E+05	8.93E+05	8.60E+05	8.26E+05
Pu-239	0.00E+00	1.71E+02	2.48E+03	4.62E+03	7.90E+03	1.19E+04	1.50E+04	1.56E+04
Pu-240	0.00E+00	8.21E-01	9.69E+01	3.33E+02	9.72E+02	2.23E+03	3.71E+03	4.24E+03
Pu-241	0.00E+00	8.46E-03	1.06E+01	7.35E+01	4.17E+02	1.71E+03	4.25E+03	5.36E+03
Pu-242	0.00E+00	1.14E-05	1.52E-01	2.18E+00	2.65E+01	2.46E+02	1.48E+03	3.20E+03
Am-241	0.00E+00	2.10E-06	2.73E-02	3.80E-01	4.28E+00	3.33E+01	1.35E+02	1.94E+02
Cm-244	0.00E+00	1.30E-11	2.81E-05	1.80E-03	1.01E-01	4.65E+00	1.39E+02	7.23E+02
Cm-245	0.00E+00	4.14E-15	9.61E-08	1.26E-05	1.47E-03	1.42E-01	8.59E+00	6.16E+01
Fission product masses (g/t initial U)								
Kr-85	0.00E+00	4.88E-01	4.91E+00	9.57E+00	1.82E+01	3.31E+01	5.53E+01	7.06E+01
Sr-90	0.00E+00	1.13E+01	1.10E+02	2.15E+02	4.09E+02	7.47E+02	1.27E+03	1.65E+03
Ag-110m	0.00E+00	1.54E-05	2.81E-03	1.52E-02	8.62E-02	4.86E-01	2.56E+00	6.30E+00
Cs-137	0.00E+00	1.84E+01	1.84E+02	3.68E+02	7.33E+02	1.45E+03	2.86E+03	4.22E+03
Xe-135	0.00E+00	4.39E-01	4.46E-01	4.50E-01	4.53E-01	4.47E-01	4.16E-01	3.79E-01
Sm-149	0.00E+00	1.59E+00	3.97E+00	4.34E+00	4.90E+00	5.53E+00	5.68E+00	5.35E+00
Sm-151	0.00E+00	1.06E+00	9.10E+00	1.34E+01	1.77E+01	2.36E+01	3.29E+01	3.91E+01

Grain – IKE 3\

GRAIN Results								
Burn-up (GWd/t)	0	0.5	5	10	20	40	80	120
k-inf	1.33031	1.28228	1.25047	1.21611	1.1565	1.0464	0.9195	0.84105
ρ^{238}	1.14064E+01	1.19781E+01	1.26932E+01	1.34223E+01	1.45624E+01	1.65099E+01	1.90001E+01	2.05311E+01
δ^{235}	1.93818E-01	2.04016E-01	2.15810E-01	2.26979E-01	2.44287E-01	2.71961E-01	3.04249E-01	3.20128E-01
δ^{238}	4.99509E-04	5.20093E-04	5.43658E-04	5.73201E-04	6.11286E-04	6.72403E-04	7.45408E-04	7.80256E-04
c/f^{235}	5.25704E-02	5.46241E-02	5.70983E-02	5.95953E-02	6.34078E-02	6.97349E-02	7.76035E-02	8.24482E-02
Actinide masses (g/t initial U)								
U-235	8.20E+04	8.13E+04	7.58E+04	7.00E+04	5.99E+04	4.34E+04	2.22E+04	1.09E+04
U-238	9.18E+05	9.18E+05	9.15E+05	9.11E+05	9.04E+05	8.89E+05	8.55E+05	8.17E+05
Pu-239	4.33E-13	1.94E+02	2.78E+03	5.18E+03	8.86E+03	1.35E+04	1.77E+04	1.93E+04
Pu-240	4.35E-13	8.08E-01	1.07E+02	3.67E+02	1.07E+03	2.44E+03	4.09E+03	4.78E+03
Pu-241	4.37E-13	8.10E-03	1.18E+01	8.14E+01	4.60E+02	1.88E+03	4.78E+03	6.35E+03
Pu-242	4.38E-13	1.07E-05	1.67E-01	2.40E+00	2.86E+01	2.55E+02	1.44E+03	2.97E+03
Am-241				4.32E-01	4.95E+00	4.00E+01	1.81E+02	3.02E+02
Cm-244					7.45E-02	3.42E+00	1.04E+02	5.45E+02
Cm-245					1.24E-03	1.20E-01	7.50E+00	5.76E+01
Fission product masses (g/t initial U)								
Kr-85	0.00E+00	5.44E-01	5.43E+00	1.05E+01	1.99E+01	3.57E+01	5.87E+01	7.39E+01
Sr-90	0.00E+00	1.17E+01	1.13E+02	2.20E+02	4.16E+02	7.54E+02	1.22E+03	1.63E+03
Ag-110m	0.00E+00	7.618E-06	1.750E-03	1.031E-02	6.102E-02	3.347E-01	1.522E+00	3.149E+00
Cs-137	2.48E-13	1.91E+01	1.91E+02	3.81E+02	7.57E+02	1.50E+03	2.93E+03	4.30E+03
Xe-135	2.45E-13	4.50E-01	4.54E-01	4.61E-01	4.70E-01	4.77E-01	4.74E-01	4.64E-01
Sm-149	1.62E-22	1.66E+00	4.33E+00	4.68E+00	5.24E+00	6.04E+00	6.71E+00	6.86E+00
Sm-151	2.74E-13	1.08E+00	9.11E+00	1.33E+01	1.75E+01	2.32E+01	3.32E+01	4.15E+01

Grain – GRS

GRAIN Results								
Burn-up (GWd/t)	**0**	**0.5**	**5**	**10**	**20**	**40**	**80**	**120**
k-inf	1.3509	1.29949	1.26592	1.23198	1.1635	1.05323	0.91308	0.8261
ρ^{238}	1.067E+01	1.112E+01	1.172E+01	1.227E+01	1.322E+01	1.469E+01	1.639E+01	1.726E+01
δ^{235}	1.923E-01	2.013E-01	2.113E-01	2.204E-01	2.357E-01	2.577E-01	2.792E-01	2.862E-01
δ^{238}	5.300E-03	5.539E-03	6.198E-03	6.944E-03	8.594E-03	1.275E-02	2.691E-02	5.803E-02
c/f^{235}	5.475E-01	5.695E-01	6.342E-01	7.073E-01	8.696E-01	1.284E+00	2.722E+00	5.948E+00
Actinide masses (g/t initial U)								
U-235	8.20E+04	8.13E+04	7.58E+04	7.02E+04	6.00E+04	4.33E+04	2.13E+04	9.75E+03
U-238	9.18E+05	9.18E+05	9.15E+05	9.12E+05	9.05E+05	8.90E+05	8.57E+05	8.20E+05
Pu-239	0.00E+00	1.82E+02	2.60E+03	4.87E+03	8.33E+03	1.27E+04	1.63E+04	1.75E+04
Pu-240	0.00E+00	7.98E-01	9.97E+01	3.43E+02	1.01E+03	2.32E+03	3.90E+03	4.52E+03
Pu-241	0.00E+00	8.22E-03	1.09E+01	7.53E+01	4.30E+02	1.77E+03	4.48E+03	5.83E+03
Pu-242	0.00E+00	1.12E-05	1.54E-01	2.22E+00	2.70E+01	2.48E+02	1.49E+03	3.20E+03
Am-241	0.00E+00	2.08E-06	2.80E-02	3.95E-01	4.50E+00	3.58E+01	1.54E+02	2.38E+02
Cm-244	0.00E+00	8.32E-12	1.63E-05	1.05E-03	6.03E-02	2.88E+00	8.93E+01	4.97E+02
Cm-245	0.00E+00	0.00E+00	5.65E-08	7.47E-06	8.88E-04	8.88E-02	5.68E+00	4.43E+01
Fission product masses (g/t initial U)								
Kr-85	0.00E+00	4.92E-01	4.93E+00	9.60E+00	1.82E+01	3.30E+01	5.48E+01	6.97E+01
Sr-90	0.00E+00	1.15E+01	1.12E+02	2.17E+02	4.13E+02	7.53E+02	1.27E+03	1.65E+03
Ag-110m	0.00E+00	1.34E-05	2.92E-03	1.22E-02	6.23E-02	3.14E-01	1.29E+00	2.52E+00
Cs-137	0.00E+00	1.85E+01	1.85E+02	3.70E+02	7.37E+02	1.46E+03	2.88E+03	4.23E+03
Xe-135	0.00E+00	4.40E-01	4.48E-01	4.53E-01	4.58E-01	4.57E-01	4.42E-01	4.20E-01
Sm-149	0.00E+00	1.60E+00	4.13E+00	4.57E+00	5.25E+00	6.18E+00	6.78E+00	6.72E+00
Sm-151	0.00E+00	1.05E+00	8.88E+00	1.30E+01	1.72E+01	2.30E+01	3.33E+01	4.15E+01

Grain – VTT 2

GRAIN Results								
Burn-up (GWd/t)	0	0.5	5	10	20	40	80	120
k-inf	1.35079	1.2979	1.26407	1.22865	1.15779	1.04798	0.91058	0.82426
ρ^{238}	1.07E+01	1.11E+01	1.17E+01	1.23E+01	1.34E+01	1.50E+01	1.69E+01	1.80E+01
δ^{235}	1.93E-01	2.02E-01	2.13E-01	2.23E-01	2.39E-01	2.64E-01	2.89E-01	2.99E-01
δ^{238}	5.35E-03	5.58E-03	6.27E-03	7.03E-03	8.79E-03	1.31E-02	2.76E-02	5.92E-02
c/f^{235}	5.49E-01	5.72E-01	6.37E-01	7.11E-01	8.79E-01	1.30E+00	2.77E+00	6.02E+00
Actinide masses (g/t initial U)								
U-235	8.20E+04	8.14E+04	7.59E+04	7.02E+04	6.00E+04	4.33E+04	2.15E+04	9.94E+03
U-238	9.18E+05	9.18E+05	9.15E+05	9.12E+05	9.05E+05	8.90E+05	8.57E+05	8.19E+05
Pu-239	0.00E+00	1.82E+02	2.61E+03	4.87E+03	8.36E+03	1.27E+04	1.65E+04	1.77E+04
Pu-240	0.00E+00	7.86E-01	1.00E+02	3.43E+02	9.90E+02	2.22E+03	3.62E+03	4.14E+03
Pu-241	0.00E+00	8.51E-03	1.18E+01	8.17E+01	4.62E+02	1.88E+03	4.67E+03	6.02E+03
Pu-242	0.00E+00	1.12E-05	1.67E-01	2.41E+00	2.90E+01	2.63E+02	1.52E+03	3.17E+03
Am-241	0.00E+00	2.10E-06	3.08E-02	4.36E-01	4.99E+00	4.01E+01	1.76E+02	2.78E+02
Cm-244	0.00E+00	2.75E-12	7.53E-07	2.46E-05	6.90E-04	1.60E-02	2.39E-01	8.36E-01
Cm-245	0.00E+00	2.92E-16	8.60E-11	2.81E-09	7.98E-08	1.91E-06	3.13E-05	1.19E-04
Fission product masses (g/t initial U)								
Kr-85	0.00E+00	4.10E-01	4.09E+00	7.96E+00	1.51E+01	2.74E+01	4.56E+01	5.81E+01
Sr-90	0.00E+00	1.17E+01	1.14E+02	2.21E+02	4.21E+02	7.68E+02	1.30E+03	1.69E+03
Ag-110m	0.00E+00	5.54E-12	5.84E-11	5.34E-10	1.69E-08	4.60E-07	8.67E-06	4.14E-05
Cs-137	0.00E+00	1.92E+01	1.92E+02	3.84E+02	7.65E+02	1.52E+03	2.99E+03	4.42E+03
Xe-135	0.00E+00	4.38E-01	4.47E-01	4.54E-01	4.61E-01	4.64E-01	4.52E-01	4.33E-01
Sm-149	0.00E+00	1.62E+00	4.21E+00	4.53E+00	5.06E+00	5.76E+00	6.28E+00	6.30E+00
Sm-151	0.00E+00	1.06E+00	9.05E+00	1.33E+01	1.74E+01	2.29E+01	3.25E+01	4.00E+01

Grain – LANL

GRAIN Results								
Burn-up (GWd/t)	0	0.5	5	10	20	40	80	120
k-inf	1.351	1.298	1.265	1.231	1.165	1.055	0.922	0.838
ρ^{238}	2.2174E+01	2.3203E+01	2.4387E+01	2.5555E+01	2.7439E+01	3.0244E+01	3.1629E+01	3.1261E+01
δ^{235}	1.9079E-01	2.0034E-01	2.0980E-01	2.1943E-01	2.3484E-01	2.5604E-01	2.6357E-01	2.5774E-01
δ^{238}	4.5856E-04	4.7837E-04	4.9760E-04	5.2034E-04	5.5417E-04	5.9949E-04	6.2379E-04	6.1609E-04
c/f^{235}	9.8697E-02	1.0245E-01	1.0666E-01	1.1069E-01	1.1701E-01	1.2621E-01	1.3048E-01	1.2915E-01
Actinide masses (g/t initial U)								
U-235	8.1187E+04	8.0544E+04	7.5018E+04	6.9322E+04	5.9115E+04	4.2497E+04	2.0545E+04	8.9355E+03
U-238	9.0882E+05	9.0852E+05	9.0581E+05	9.0259E+05	8.9596E+05	8.8149E+05	8.4844E+05	8.1117E+05
Pu-239	0.0000E+00	1.8034E+02	2.5991E+03	4.8355E+03	8.2684E+03	1.2488E+04	1.5452E+04	1.6075E+04
Pu-240	0.0000E+00	7.9238E-01	1.0228E+02	3.5083E+02	1.0217E+03	2.3308E+03	3.7655E+03	4.2879E+03
Pu-241	0.0000E+00	8.0243E-03	1.1363E+01	7.8565E+01	4.4316E+02	1.8074E+03	4.3733E+03	5.4624E+03
Pu-242	0.0000E+00	0.0000E+00	1.6175E-01	2.3479E+00	2.8231E+01	2.5659E+02	1.4899E+03	3.1094E+03
Am-241	0.0000E+00	0.0000E+00	2.9045E-02	4.1262E-01	4.6938E+00	3.7223E+01	1.5472E+02	2.2705E+02
Cm-244	0.0000E+00	0.0000E+00	0.0000E+00	1.0901E-03	6.3957E-02	3.0703E+00	9.4710E+01	4.9540E+02
Cm-245	0.0000E+00	0.0000E+00	0.0000E+00	0.0000E+00	1.0971E-03	1.1021E-01	6.8769E+00	4.9912E+01
Fission product masses (g/t initial U)								
Kr-85		4.9651E-01	4.9329E+00	9.5996E+00	1.8205E+01	3.2913E+01	5.4302E+01	6.8036E+01
Sr-90		1.1443E+01	1.1202E+02	2.1761E+02	4.1232E+02	7.4888E+02	1.2578E+03	1.6115E+03
Ag-110m		5.8572E-10	4.4296E-07	1.7039E-06	4.8817E-06	2.0545E-05	6.9875E-05	1.2669E-04
Cs-137		4.3402E-01	4.3974E-01	4.4758E-01	4.4356E-01	4.4477E-01	4.1021E-01	3.5083E-01
Xe-135		1.8717E+01	1.8777E+02	3.7434E+02	7.4345E+02	1.4708E+03	2.8633E+03	4.1744E+03
Sm-149		1.6014E+00	4.0930E+00	4.3834E+00	4.5190E+00	4.8998E+00	4.7350E+00	4.0689E+00
Sm-151		1.0529E+00	8.9385E+00	1.3020E+01	1.6497E+01	2.1279E+01	2.7618E+01	3.0713E+01

Grain – UNAM

GRAIN Results								
Burn-up (GWd/t)	0	1	5	10	20	40	80	120
k-inf	1.34617	1.29411	1.26538	1.23223	1.17085	1.07036	0.95456	0.88292
ρ^{238}								
δ^{235}								
δ^{238}	5.365E-03	5.624E-03	6.264E-03	6.959E-03	8.556E-03	1.259E-02	2.533E-02	
c/f^{235}	5.586E-01	5.804E-01	6.436E-01	7.164E-01	8.753E-01	1.279E+00	2.621E+00	
Actinide masses (g/t initial U)								
U-235	8.200E+04	8.136E+04	7.584E+04	7.016E+04	5.994E+04	4.324E+04	2.123E+04	
U-238	9.180E+05	9.177E+05	9.150E+05	9.117E+05	9.050E+05	8.903E+05	8.574E+05	
Pu-239	0.000E+00	1.859E+02	2.554E+03	4.742E+03	8.205E+03	1.245E+04	1.582E+04	
Pu-240	0.000E+00	8.743E-01	9.800E+01	3.388E+02	1.001E+03	2.313E+03	3.864E+03	
Pu-241	0.000E+00	9.048E-03	1.054E+01	7.472E+01	4.286E+02	1.774E+03	4.439E+03	
Pu-242	0.000E+00	0.000E+00	1.485E-01	9.000E+01	2.695E+01	2.507E+02	1.505E+03	
Am-241								
Cm-244								
Cm-245								
Fission product masses (g/t initial U)								
Kr-85								
Sr-90								
Ag-110m								
Cs-137	0.000E+00	1.885E+01	1.864E+02	3.711E+02	7.320E+02	1.441E+03	2.743E+03	3.958E+03
Xe-135	0.000E+00	4.436E-01	4.410E-01	4.438E-01	4.347E-01	4.293E-01	3.589E-01	3.111E-01
Sm-149	0.000E+00	1.595E+00	3.815E+00	4.007E+00	4.136E+00	4.432E+00	3.873E+00	3.389E+00
Sm-151	0.000E+00	1.064E+00	8.610E+00	1.255E+01	1.563E+01	1.990E+01	2.379E+01	2.660E+01

Pebble – IKE 1

PEBBLE Results								
Burn-up (GWd/t)	**0**	**0.5**	**5**	**10**	**20**	**40**	**80**	**120**
k-inf	1.5127	1.4523	1.4264	1.3984	1.3430	1.2284	1.0051	0.7933
ρ^{238}	6.23E+00	6.50E+00	6.49E+00	6.49E+00	6.34E+00	5.95E+00	4.43E+00	3.30E+00
δ^{235}	1.01E-01	1.05E-01	1.05E-01	1.05E-01	1.02E-01	9.44E-02	6.91E-02	5.07E-02
δ^{238}	2.58E-04	2.69E-04	2.69E-04	2.69E-04	2.66E-04	2.48E-04	1.88E-04	1.41E-04
c/f^{235}	3.27E-02	3.38E-02	3.37E-02	3.37E-02	3.30E-02	3.13E-02	2.48E-02	1.98E-02
Actinide masses (g/t initial U)								
U-235	8.20E+04	8.14E+04	7.60E+04	6.99E+04	5.90E+04	4.07E+04	1.39E+04	1.89E+03
U-238	9.18E+05	9.18E+05	9.16E+05	9.14E+05	9.10E+05	9.01E+05	8.78E+05	8.46E+05
Pu-239	0.00E+00	1.18E+02	1.72E+03	3.31E+03	5.63E+03	8.09E+03	8.64E+03	7.16E+03
Pu-240	0.00E+00	3.99E-01	5.62E+01	2.17E+02	6.95E+02	1.76E+03	3.27E+03	3.51E+03
Pu-241	0.00E+00	2.59E-03	3.98E+00	3.16E+01	1.96E+02	8.64E+02	2.18E+03	2.13E+03
Pu-242	0.00E+00	3.07E-06	5.21E-02	8.99E-01	1.24E+01	1.32E+02	1.14E+03	3.09E+03
Am-241	0.00E+00	6.28E-07	1.02E-02	1.68E-01	2.07E+00	1.72E+01	7.00E+01	5.92E+01
Cm-244	0.00E+00	1.53E-12	2.12E-06	1.69E-04	1.05E-02	5.46E-01	2.99E+01	3.09E+02
Cm-245	0.00E+00	0.00E+00	4.27E-09	6.99E-07	8.79E-05	8.63E-03	7.83E-01	8.44E+00
Fission product masses (g/t initial U)								
Kr-85	-	-	-	-	-	-	-	-
Sr-90	-	-	-	-	-	-	-	-
Ag-110m	0.00E+00	7.54E-06	1.15E-03	6.64E-03	3.79E-02	2.09E-01	1.28E+00	4.01E+00
Cs-137	-	-	-	-	-	-	-	-
Xe-135	0.00E+00	4.06E-01	4.01E-01	3.94E-01	3.76E-01	3.31E-01	2.20E-01	1.32E-01
Sm-149	-	-	-	-	-	-	-	-
Sm-151	0.00E+00	1.30E+00	8.33E+00	1.13E+01	1.29E+01	1.39E+01	1.42E+01	1.37E+01

Pebble – IKE 2

PEBBLE Results								
Burn-up (GWd/t)	**0**	**0.5**	**5**	**10**	**20**	**40**	**80**	**120**
k-inf	1.520	1.463	1.434	1.407	1.351	1.236	1.004	0.781
ρ^{238}	6.09E+00	6.09E+00	6.34E+00	6.29E+00	6.14E+00	5.61E+00	4.08E+00	2.87E+00
δ^{235}	1.00E-01	1.00E-01	1.04E-01	1.03E-01	1.00E-01	9.04E-02	6.39E-02	4.38E-02
δ^{238}	2.40E-04	2.40E-04	2.48E-04	2.46E-04	2.39E-04	2.17E-04	1.57E-04	1.09E-04
c/f^{235}	3.20E-02	3.20E-02	3.30E-02	3.28E-02	3.22E-02	2.99E-02	2.33E-02	1.79E-02
Actinide masses (g/t initial U)								
U-235	8.20E+04	8.14E+04	7.59E+04	7.01E+04	5.93E+04	4.03E+04	1.31E+04	1.52E+03
U-238	9.18E+05	9.18E+05	9.16E+05	9.14E+05	9.09E+05	9.01E+05	8.79E+05	8.48E+05
Pu-239	0.00E+00	1.15E+02	1.69E+03	3.17E+03	5.42E+03	7.86E+03	8.19E+03	6.58E+03
Pu-240	0.00E+00	4.34E-01	5.63E+01	2.05E+02	6.62E+02	1.74E+03	3.21E+03	3.39E+03
Pu-241	0.00E+00	2.93E-03	4.04E+00	2.95E+01	1.84E+02	8.50E+02	2.08E+03	1.94E+03
Pu-242	0.00E+00	3.59E-06	5.37E-02	8.28E-01	1.14E+01	1.33E+02	1.15E+03	3.11E+03
Am-241	0.00E+00	7.22E-07	1.03E-02	1.51E-01	1.87E+00	1.64E+01	6.23E+01	4.62E+01
Cm-244	0.00E+00	1.70E-12	4.08E-06	2.75E-04	1.72E-02	9.84E-01	5.00E+01	4.64E+02
Cm-245	0.00E+00	3.16E-16	8.19E-09	1.12E-06	1.39E-04	1.54E-02	1.25E+00	1.14E+01
Fission product masses (g/t initial U)								
Kr-85	0.00E+00	4.89E-01	4.95E+00	9.73E+00	1.87E+01	3.49E+01	5.93E+01	7.41E+01
Sr-90	0.00E+00	1.13E+01	1.11E+02	2.19E+02	4.23E+02	7.94E+02	1.38E+03	1.76E+03
Ag-110m	0.00E+00	9.99E-06	1.56E-03	7.86E-03	4.19E-02	2.34E-01	1.43E+00	4.61E+00
Cs-137	0.00E+00	1.84E+01	1.84E+02	3.67E+02	7.32E+02	1.45E+03	2.85E+03	4.22E+03
Xe-135	0.00E+00	4.08E-01	4.02E-01	3.95E-01	3.75E-01	3.24E-01	2.06E-01	1.17E-01
Sm-149	0.00E+00	1.57E+00	3.64E+00	3.73E+00	3.80E+00	3.63E+00	2.62E+00	1.64E+00
Sm-151	0.00E+00	1.05E+00	8.33E+00	1.13E+01	1.31E+01	1.42E+01	1.41E+01	1.28E+01

Pebble – IKE 3

PEBBLE Results								
Burn-up (GWd/t)	**0**	**0.5**	**5**	**10**	**20**	**40**	**80**	**120**
k-inf	1.51441	1.4592	1.43056	1.40684	1.35605	1.24127	1.01569	0.79593
ρ^{238}	6.27117E+00	6.52764E+00	6.53133E+00	6.45096E+00	6.27899E+00	5.65082E+00	4.07286E+00	2.91421E+00
δ^{235}	1.00418E-01	1.04427E-01	1.04260E-01	1.02982E-01	9.93787E-02	8.83586E-02	6.16120E-02	4.28386E-02
δ^{238}	2.58113E-04	2.66634E-04	2.67459E-04	2.63712E-04	2.55053E-04	2.31322E-04	1.65343E-04	1.17450E-04
c/f^{235}	3.27687E-02	3.38383E-02	3.38319E-02	3.34652E-02	3.27188E-02	3.00227E-02	2.32031E-02	1.80800E-02
Actinide masses (g/t initial U)								
U-235	8.20E+04	8.14E+04	7.57E+04	6.98E+04	5.87E+04	3.95E+04	1.24E+04	1.44E+03
U-238	9.18E+05	9.18E+05	9.16E+05	9.14E+05	9.09E+05	9.00E+05	8.77E+05	8.45E+05
Pu-239	4.33E-13	1.22E+02	1.76E+03	3.30E+03	5.61E+03	8.08E+03	8.33E+03	6.69E+03
Pu-240	4.35E-13	4.12E-01	5.89E+01	2.15E+02	6.92E+02	1.80E+03	3.27E+03	3.43E+03
Pu-241	4.37E-13	2.77E-03	4.30E+00	3.14E+01	1.95E+02	8.89E+02	2.12E+03	1.96E+03
Pu-242	4.38E-13	3.38E-06	5.80E-02	8.98E-01	1.24E+01	1.41E+02	1.18E+03	3.02E+03
Am-241					2.05E+00	1.84E+01	7.30E+01	5.81E+01
Cm-244						7.26E-01	3.78E+01	3.55E+02
Cm-245						1.34E-02	1.16E+00	1.14E+01
Fission product masses (g/t initial U)								
Kr-85	0.00E+00	5.48E-01	5.52E+00	1.08E+01	2.08E+01	3.84E+01	6.45E+01	7.89E+01
Sr-90	0.00E+00	1.17E+01	1.15E+02	2.27E+02	4.37E+02	8.16E+02	1.41E+03	1.77E+03
Ag-110m	0	0	9.21E-04	5.01E-03	2.86E-02	1.65E-01	9.88E-01	2.96E+00
Cs-137	0.00E+00	1.92E+01	1.92E+02	3.83E+02	7.62E+02	1.51E+03	2.95E+03	4.32E+03
Xe-135	0.00E+00	4.17E-01	4.06E-01	3.98E-01	3.78E-01	3.27E-01	0.2072	1.20E-01
Sm-149	0	1.64E+00	3.94E+00	4.00E+00	4.04E+00	3.83E+00	2.81E+00	1.83E+00
Sm-151	0	1.08E+00	8.33E+00	1.11E+01	1.27E+01	1.35E+01	1.31E+01	1.23E+01

Pebble – GRS

PEBBLE Results								
Burn-up (GWd/t)	0	0.5	5	10	20	40	80	120
k-inf	1.51321	1.45398	1.42748	1.40139	1.34543	1.22858	0.99708	0.77894
ρ^{238}	6.254E+00	6.488E+00	6.491E+00	6.456E+00	6.294E+00	5.791E+00	4.267E+00	3.091E+00
δ^{235}	1.010E-01	1.050E-01	1.049E-01	1.040E-01	1.008E-01	9.122E-02	6.539E-02	4.600E-02
δ^{238}	2.868E-03	2.993E-03	3.209E-03	3.442E-03	3.968E-03	5.320E-03	1.180E-02	6.616E-02
c/f^{235}	3.614E-01	3.749E-01	4.012E-01	4.316E-01	4.979E-01	6.784E-01	1.595E+00	9.716E+00
Actinide masses (g/t initial U)								
U-235	8.20E+04	8.13E+04	7.59E+04	7.00E+04	5.91E+04	4.01E+04	1.31E+04	1.62E+03
U-238	9.18E+05	9.18E+05	9.16E+05	9.14E+05	9.10E+05	9.00E+05	8.78E+05	8.46E+05
Pu-239	0.00E+00	1.20E+02	1.74E+03	3.27E+03	5.58E+03	8.10E+03	8.50E+03	6.93E+03
Pu-240	0.00E+00	4.18E-01	5.72E+01	2.10E+02	6.76E+02	1.78E+03	3.29E+03	3.48E+03
Pu-241	0.00E+00	2.81E-03	4.10E+00	3.00E+01	1.88E+02	8.68E+02	2.13E+03	2.03E+03
Pu-242	0.00E+00	3.47E-06	5.43E-02	8.42E-01	1.17E+01	1.36E+02	1.17E+03	3.13E+03
Am-241	0.00E+00	7.02E-07	1.06E-02	1.57E-01	1.94E+00	1.73E+01	6.83E+01	5.43E+01
Cm-244	0.00E+00	1.03E-12	2.20E-06	1.50E-04	9.50E-03	5.61E-01	3.07E+01	3.07E+02
Cm-245	0.00E+00	1.77E-16	4.51E-09	6.19E-07	7.81E-05	8.86E-03	7.78E-01	7.80E+00
Fission product masses (g/t initial U)								
Kr-85	0.00E+00	4.93E-01	4.99E+00	9.79E+00	1.89E+01	3.49E+01	5.92E+01	7.33E+01
Sr-90	0.00E+00	1.16E+01	1.13E+02	2.22E+02	4.30E+02	8.04E+02	1.40E+03	1.77E+03
Ag-110m	0.00E+00	8.13E-06	1.44E-03	6.98E-03	3.16E-02	1.68E-01	9.13E-01	2.45E+00
Cs-137	0.00E+00	1.86E+01	1.86E+02	3.70E+02	7.38E+02	1.47E+03	2.88E+03	4.24E+03
Xe-135	0.00E+00	4.10E-01	4.04E-01	3.97E-01	3.77E-01	3.38E-01	2.11E-01	1.23E-01
Sm-149	0.00E+00	1.58E+00	3.74E+00	3.87E+00	4.00E+00	3.91E+00	2.96E+00	1.94E+00
Sm-151	0.00E+00	1.05E+00	8.21E+00	1.11E+01	1.28E+01	1.39E+01	1.42E+01	1.36E+01

Pebble – LLNL

<u>**PEBBLE Results**</u>								
Burn-up (GWd/t)	**0**	**0.5**	**5**	**10**	**20**	**40**	**80**	**120**
k-inf	1.51436	1.45409	1.42565	1.39896	1.34246	1.22765	0.99846	0.78509
ρ^{238}	6.225833352	6.473527551	6.500525348	6.461224737	6.318181201	5.800069234	4.311215696	3.115597279
δ^{235}	0.101095744	0.105235121	0.105397365	0.104552112	0.10145697	0.091861871	0.066219358	0.046536269
δ^{238}	0.002894947	0.003025714	0.003248627	0.003492928	0.004022983	0.005387255	0.011950263	0.065607488
c/f^{235}	0.360666959	0.374845231	0.402345076	0.432501701	0.500158365	0.679500552	1.599860694	9.526431616
Actinide masses (g/t initial U)								
U-235	82000.65101	81387.23943	75886.00542	70047.58271	59154.70213	40178.35103	13147.9041	1665.362093
U-238	918002.537	917939.4265	916113.9729	914049.8264	909724.3151	900358.9316	877302.8047	845356.4302
Pu-239	0	118.2906837	1735.321918	3259.439673	5568.424357	8089.019017	8515.023335	6950.058463
Pu-240	0	0.415309524	57.87850571	211.6051373	681.9918402	1784.499735	3272.372929	3469.868406
Pu-241	0	0.002756403	4.177278141	30.66117795	191.3312659	885.3666574	2170.058951	2060.830983
Pu-242	0	3.31807E-06	0.055525022	0.861889694	11.94194904	138.0091481	1168.570309	3064.044853
Am-241	0	6.70697E-07	0.010789001	0.160002849	1.997545556	17.86893016	70.90729179	57.28032193
Cm-244	0	1.35328E-12	4.02939E-06	0.000273886	0.017208368	0.993037321	50.7362166	456.2995081
Cm-245	0	6.60973E-16	1.10857E-08	1.4211E-06	0.000172174	0.01897939	1.568533799	14.33146951
Fission product masses (g/t initial U)								
Kr-85	0	0.456369569	4.620172247	9.076001061	17.49181552	32.49648187	55.54294374	69.56803849
Sr-90	0	11.14321791	109.6575307	215.4387605	416.4448676	779.9814081	1357.103227	1726.026552
Ag-110m	0	5.91561E-06	0.000934548	0.00469646	0.024945332	0.136874306	0.797572684	2.373418556
Cs-137	0	18.57299414	185.4859821	370.2603345	737.5537191	1462.867532	2876.637382	4242.143585
Xe-135	0	0.403623622	0.399710458	0.392266327	0.373195079	0.324909762	0.210375812	0.124035876
Sm-149	0	1.605725242	3.826073946	3.826822694	3.759787609	3.4251442	2.396465346	1.542767727
Sm-151	0	1.064208888	8.392102355	11.35761788	13.04774569	13.85215124	13.26817798	11.83138515

Pebble – VTT 1

PEBBLE Results								
Burn-up (GWd/t)	0	0.5	5	10	20	40	80	120
k-inf	1.51836	1.45805	1.4304	1.40426	1.34611	1.22922	0.99545	0.77522
ρ^{238}	6.15E+00	6.39E+00	6.40E+00	6.35E+00	6.22E+00	5.70E+00	4.19E+00	3.01E+00
δ^{235}	1.01E-01	1.05E-01	1.05E-01	1.04E-01	1.01E-01	9.15E-02	6.53E-02	4.54E-02
δ^{238}	2.88E-03	3.01E-03	3.24E-03	3.48E-03	4.02E-03	5.40E-03	1.20E-02	7.04E-02
c/f^{235}	3.57E-01	3.71E-01	3.97E-01	4.26E-01	4.94E-01	6.72E-01	1.60E+00	1.02E+01
Actinide masses (g/t initial U)								
U-235	8.20E+04	8.14E+04	7.59E+04	7.00E+04	5.91E+04	4.01E+04	1.29E+04	1.52E+03
U-238	9.18E+05	9.18E+05	9.16E+05	9.14E+05	9.10E+05	9.00E+05	8.78E+05	8.46E+05
Pu-239	0.00E+00	1.18E+02	1.72E+03	3.22E+03	5.51E+03	7.99E+03	8.35E+03	6.79E+03
Pu-240	0.00E+00	4.07E-01	5.66E+01	2.06E+02	6.60E+02	1.71E+03	3.07E+03	3.22E+03
Pu-241	0.00E+00	2.85E-03	4.35E+00	3.18E+01	1.97E+02	9.03E+02	2.16E+03	2.00E+03
Pu-242	0.00E+00	3.43E-06	5.78E-02	8.94E-01	1.23E+01	1.42E+02	1.19E+03	3.12E+03
Am-241	0.00E+00	6.98E-07	1.13E-02	1.68E-01	2.10E+00	1.88E+01	7.53E+01	5.95E+01
Cm-244	0.00E+00	3.48E-13	1.07E-07	3.63E-06	1.15E-04	3.39E-03	9.38E-02	6.41E-01
Cm-245	0.00E+00	3.65E-17	1.24E-11	4.37E-10	1.49E-08	5.33E-07	2.48E-05	3.20E-04
Fission product masses (g/t initial U)								
Kr-85	0.00E+00	4.11E-01	4.13E+00	8.10E+00	1.56E+01	2.89E+01	4.92E+01	6.11E+01
Sr-90	0.00E+00	1.17E+01	1.15E+02	2.26E+02	4.37E+02	8.20E+02	1.43E+03	1.81E+03
Ag-110m	0.00E+00	5.52E-12	5.16E-11	2.25E-10	5.93E-09	1.88E-07	4.60E-06	2.96E-05
Cs-137	0.00E+00	1.92E+01	1.92E+02	3.83E+02	7.64E+02	1.52E+03	2.98E+03	4.40E+03
Xe-135	0.00E+00	4.06E-01	4.01E-01	3.93E-01	3.74E-01	3.26E-01	2.09E-01	1.22E-01
Sm-149	0.00E+00	1.60E+00	3.85E+00	3.91E+00	3.94E+00	3.74E+00	2.77E+00	1.81E+00
Sm-151	0.00E+00	1.05E+00	8.29E+00	1.12E+01	1.28E+01	1.36E+01	1.35E+01	1.25E+01

Pebble – VTT 2

PEBBLE Results								
Burn-up (GWd/t)	**0**	**0.5**	**5**	**10**	**20**	**40**	**80**	**120**
k-inf	1.51346	1.45368	1.42577	1.3994	1.34126	1.22537	0.99506	0.77967
ρ^{238}	6.25E+00	6.49E+00	6.51E+00	6.48E+00	6.35E+00	5.85E+00	4.36E+00	3.15E+00
δ^{235}	1.01E-01	1.05E-01	1.05E-01	1.05E-01	1.02E-01	9.28E-02	6.68E-02	4.70E-02
δ^{238}	2.90E-03	3.02E-03	3.26E-03	3.47E-03	4.03E-03	5.43E-03	1.20E-02	6.67E-02
c/f^{235}	3.62E-01	3.76E-01	4.03E-01	4.33E-01	5.02E-01	6.85E-01	1.61E+00	9.68E+00
Actinide masses (g/t initial U)								
U-235	8.20E+04	8.14E+04	7.59E+04	7.01E+04	5.92E+04	4.02E+04	1.31E+04	1.65E+03
U-238	9.18E+05	9.18E+05	9.16E+05	9.14E+05	9.10E+05	9.00E+05	8.77E+05	8.45E+05
Pu-239	0.00E+00	1.20E+02	1.74E+03	3.27E+03	5.59E+03	8.12E+03	8.54E+03	6.97E+03
Pu-240	0.00E+00	4.14E-01	5.75E+01	2.09E+02	6.70E+02	1.73E+03	3.10E+03	3.26E+03
Pu-241	0.00E+00	2.96E-03	4.43E+00	3.24E+01	2.00E+02	9.18E+02	2.21E+03	2.06E+03
Pu-242	0.00E+00	3.56E-06	5.87E-02	9.09E-01	1.25E+01	1.44E+02	1.20E+03	3.12E+03
Am-241	0.00E+00	7.25E-07	1.15E-02	1.71E-01	2.13E+00	1.92E+01	7.74E+01	6.30E+01
Cm-244	0.00E+00	3.68E-13	1.09E-07	3.76E-06	1.17E-04	3.47E-03	9.44E-02	6.28E-01
Cm-245	0.00E+00	3.85E-17	1.27E-11	4.51E-10	1.51E-08	5.42E-07	2.45E-05	3.03E-04
Fission product masses (g/t initial U)								
Kr-85	0.00E+00	4.11E-01	4.13E+00	8.10E+00	1.56E+01	2.89E+01	4.91E+01	6.11E+01
Sr-90	0.00E+00	1.17E+01	1.15E+02	2.26E+02	4.37E+02	8.19E+02	1.42E+03	1.81E+03
Ag-110m	0.00E+00	5.52E-12	5.17E-11	2.27E-10	6.02E-09	1.90E-07	4.61E-06	2.92E-05
Cs-137	0.00E+00	1.92E+01	1.92E+02	3.83E+02	7.64E+02	1.52E+03	2.98E+03	4.40E+03
Xe-135	0.00E+00	4.06E-01	4.01E-01	3.94E-01	3.75E-01	3.28E-01	2.13E-01	1.26E-01
Sm-149	0.00E+00	1.60E+00	3.85E+00	3.91E+00	3.95E+00	3.77E+00	2.81E+00	1.86E+00
Sm-151	0.00E+00	1.05E+00	8.29E+00	1.12E+01	1.28E+01	1.37E+01	1.37E+01	1.28E+01

Pebble – ORNL 1

PEBBLE Results	NEWT							
Burn-up (GWd/t)	**0**	**0.5**	**5**	**10**	**20**	**40**	**80**	**120**
k-inf	1.51315407	1.45192124	1.42334857	1.39667636	1.33927904	1.22248363	0.98945644	0.77422005
ρ^{238}	6.28E+00	6.54E+00	6.56E+00	6.52E+00	6.37E+00	5.85E+00	4.33E+00	3.17E+00
δ^{235}	1.00E-01	1.05E-01	1.05E-01	1.04E-01	1.01E-01	9.12E-02	6.56E-02	4.67E-02
δ^{238}	2.87E-03	3.00E-03	3.22E-03	3.46E-03	4.00E-03	5.38E-03	1.21E-02	6.60E-02
c/f^{235}	3.63E-01	3.78E-01	4.06E-01	4.37E-01	5.06E-01	6.93E-01	1.66E+00	9.86E+00
Actinide masses (g/t initial U)								
U-235	8.20E+04	8.14E+04	7.57E+04	6.98E+04	5.88E+04	3.96E+04	1.27E+04	1.63E+03
U-238	9.18E+05	9.18E+05	9.16E+05	9.14E+05	9.09E+05	9.00E+05	8.76E+05	8.44E+05
Pu-239	0.00E+00	1.24E+02	1.78E+03	3.34E+03	5.68E+03	8.19E+03	8.52E+03	6.96E+03
Pu-240	0.00E+00	4.20E-01	6.00E+01	2.19E+02	7.03E+02	1.83E+03	3.31E+03	3.49E+03
Pu-241	0.00E+00	2.81E-03	4.38E+00	3.20E+01	1.99E+02	9.07E+02	2.20E+03	2.08E+03
Pu-242	0.00E+00	3.43E-06	5.93E-02	9.18E-01	1.26E+01	1.44E+02	1.19E+03	3.03E+03
Am-241	0.00E+00	6.81E-07	1.13E-02	1.68E-01	2.10E+00	1.87E+01	7.53E+01	6.32E+01
Cm-244	0.00E+00	1.26E-12	3.01E-06	2.05E-04	1.29E-02	7.43E-01	3.88E+01	3.59E+02
Cm-245	0.00E+00	9.06E-16	7.15E-09	9.75E-07	1.22E-04	1.37E-02	1.22E+00	1.21E+01
Fission product masses (g/t initial U)								
Kr-85	0.00E+00	5.48E-01	5.52E+00	1.08E+01	2.08E+01	3.83E+01	6.43E+01	7.89E+01
Sr-90	0.00E+00	1.17E+01	1.15E+02	2.26E+02	4.37E+02	8.15E+02	1.41E+03	1.78E+03
Ag-110m	0.00E+00	5.07E-06	9.31E-04	5.10E-03	2.94E-02	1.72E-01	1.06E+00	3.28E+00
Cs-137	0.00E+00	1.92E+01	1.92E+02	3.83E+02	7.62E+02	1.51E+03	2.95E+03	4.33E+03
Xe-135	0.00E+00	4.08E-01	4.04E-01	3.97E-01	3.77E-01	3.28E-01	2.12E-01	1.27E-01
Sm-149	0.00E+00	1.63E+00	3.89E+00	3.96E+00	4.00E+00	3.83E+00	2.88E+00	1.91E+00
Sm-151	0.00E+00	1.08E+00	8.37E+00	1.12E+01	1.28E+01	1.36E+01	1.39E+01	1.33E+01

Pebble – ORNL 2

PEBBLE Results	KENOVA							
Burn-up (GWd/t)	**0**	**0.5**	**5**	**10**	**20**	**40**	**80**	**120**
k-inf	1.512	1.4508	1.4222	1.3955	1.3381	1.2215	0.9895	0.7755
ρ^{238}	6.30E+00	6.56E+00	6.58E+00	6.54E+00	6.39E+00	5.88E+00	4.37E+00	3.20E+00
δ^{235}	1.00E-01	1.05E-01	1.05E-01	1.04E-01	1.01E-01	9.15E-02	6.59E-02	4.70E-02
δ^{238}	2.85E-03	2.98E-03	3.20E-03	3.44E-03	3.98E-03	5.36E-03	1.20E-02	6.47E-02
c/f^{235}	3.64E-01	3.79E-01	4.07E-01	4.38E-01	5.08E-01	6.96E-01	1.66E+00	9.74E+00
Actinide masses (g/t initial U)								
U-235	8.20E+04	8.14E+04	7.57E+04	6.98E+04	5.88E+04	3.96E+04	1.28E+04	1.66E+03
U-238	9.18E+05	9.18E+05	9.16E+05	9.14E+05	9.09E+05	9.00E+05	8.76E+05	8.44E+05
Pu-239	4.33E-13	1.24E+02	1.79E+03	3.35E+03	5.70E+03	8.23E+03	8.55E+03	7.00E+03
Pu-240	4.35E-13	4.21E-01	6.02E+01	2.20E+02	7.05E+02	1.83E+03	3.32E+03	3.49E+03
Pu-241	4.37E-13	2.81E-03	4.39E+00	3.21E+01	1.99E+02	9.10E+02	2.21E+03	2.09E+03
Pu-242	4.38E-13	3.44E-06	5.95E-02	9.20E-01	1.26E+01	1.44E+02	1.19E+03	3.03E+03
Am-241	4.37E-13	6.82E-07	1.14E-02	1.69E-01	2.10E+00	1.88E+01	7.58E+01	6.41E+01
Cm-244	4.42E-13	1.27E-12	3.02E-06	2.06E-04	1.29E-02	7.46E-01	3.88E+01	3.58E+02
Cm-245	9.13E-37	9.07E-16	7.19E-09	9.80E-07	1.23E-04	1.38E-02	1.22E+00	1.22E+01
Fission product masses (g/t initial U)								
Kr-85	1.54E-13	5.48E-01	5.52E+00	1.08E+01	2.08E+01	3.83E+01	6.43E+01	7.88E+01
Sr-90	1.63E-13	1.17E+01	1.15E+02	2.26E+02	4.37E+02	8.15E+02	1.41E+03	1.77E+03
Ag-110m	7.04E-33	5.07E-06	9.33E-04	5.11E-03	2.95E-02	1.72E-01	1.07E+00	3.27E+00
Cs-137	2.48E-13	1.92E+01	1.92E+02	3.83E+02	7.62E+02	1.51E+03	2.95E+03	4.33E+03
Xe-135	2.45E-13	4.08E-01	4.04E-01	3.97E-01	3.78E-01	3.29E-01	2.13E-01	1.28E-01
Sm-149	2.70E-13	1.63E+00	3.89E+00	3.96E+00	4.01E+00	3.83E+00	2.90E+00	1.93E+00
Sm-151	2.74E-13	1.08E+00	8.38E+00	1.12E+01	1.28E+01	1.36E+01	1.39E+01	1.33E+01

Pebble – ORNL 3

PEBBLE Results	XSDRN							
Burn-up (GWd/t)	**0**	**0.5**	**5**	**10**	**20**	**40**	**80**	**120**
k-inf	1.511951	1.450771	1.4222	1.395524	1.338127	1.221453	0.989518	0.775463
ρ^{238}	6.30E+00	6.57E+00	6.59E+00	6.55E+00	6.40E+00	5.88E+00	4.37E+00	3.20E+00
δ^{235}	1.00E-01	1.05E-01	1.05E-01	1.04E-01	1.01E-01	9.15E-02	6.60E-02	4.70E-02
δ^{238}	2.85E-03	2.98E-03	3.20E-03	3.44E-03	3.97E-03	5.35E-03	1.20E-02	6.46E-02
c/f^{235}	3.64E-01	3.79E-01	4.07E-01	4.39E-01	5.08E-01	6.96E-01	1.66E+00	9.73E+00
Actinide masses (g/t initial U)								
U-235	8.20E+04	8.14E+04	7.57E+04	6.98E+04	5.88E+04	3.96E+04	1.28E+04	1.66E+03
U-238	9.18E+05	9.18E+05	9.16E+05	9.14E+05	9.09E+05	9.00E+05	8.76E+05	8.44E+05
Pu-239	4.33E-13	1.24E+02	1.79E+03	3.35E+03	5.70E+03	8.22E+03	8.56E+03	7.01E+03
Pu-240	4.35E-13	4.21E-01	6.02E+01	2.20E+02	7.05E+02	1.83E+03	3.32E+03	3.50E+03
Pu-241	4.37E-13	2.82E-03	4.40E+00	3.22E+01	1.99E+02	9.11E+02	2.21E+03	2.10E+03
Pu-242	4.38E-13	3.45E-06	5.95E-02	9.21E-01	1.26E+01	1.44E+02	1.19E+03	3.03E+03
Am-241	4.37E-13	6.84E-07	1.14E-02	1.69E-01	2.10E+00	1.88E+01	7.59E+01	6.41E+01
Cm-244	4.42E-13	1.27E-12	3.03E-06	2.06E-04	1.29E-02	7.45E-01	3.88E+01	3.58E+02
Cm-245	9.14E-37	9.07E-16	7.19E-09	9.80E-07	1.23E-04	1.38E-02	1.22E+00	1.22E+01
Fission product masses (g/t initial U)								
Kr-85	1.54E-13	5.48E-01	5.52E+00	1.08E+01	2.08E+01	3.83E+01	6.43E+01	7.88E+01
Sr-90	1.63E-13	1.17E+01	1.15E+02	2.26E+02	4.37E+02	8.15E+02	1.41E+03	1.77E+03
Ag-110m	7.04E-33	5.07E-06	9.33E-04	5.11E-03	2.95E-02	1.72E-01	1.07E+00	3.27E+00
Cs-137	2.48E-13	1.92E+01	1.92E+02	3.83E+02	7.62E+02	1.51E+03	2.95E+03	4.33E+03
Xe-135	2.45E-13	4.08E-01	4.04E-01	3.97E-01	3.78E-01	3.29E-01	2.14E-01	1.28E-01
Sm-149	2.70E-13	1.63E+00	3.89E+00	3.96E+00	4.01E+00	3.83E+00	2.90E+00	1.93E+00
Sm-151	2.74E-13	1.08E+00	8.38E+00	1.12E+01	1.28E+01	1.36E+01	1.39E+01	1.33E+01

Pebble – ORNL 4 (k_{eff} Only)

PEBBLE Results	XSDRN/RET							
Burn-up (GWd/t)	**0**	**0.5**	**5**	**10**	**20**	**40**	**80**	**120**
k-inf	1.5117	1.4503	1.4207	1.3927	1.3331	1.215	0.9857	0.7752
ρ^{238}								
δ^{235}								
δ^{238}								
c/f^{235}								
Actinide masses (g/t initial U)								
U-235								
U-238								
Pu-239								
Pu-240								
Pu-241								
Pu-242								
Am-241								
Cm-244								
Cm-245								
Fission product masses (g/t initial U)								
Kr-85								
Sr-90								
Ag-110m								
Cs-137								
Xe-135								
Sm-149								
Sm-151								

Pebble – LANL

PEBBLE Results								
Burn-up (GWd/t)	0	0.5	5	10	20	40	80	120
k-inf	1.515	1.455	1.428	1.403	1.349	1.236	1.006	0.794
ρ^{238}	1.5261E+01	1.5812E+01	1.5893E+01	1.5640E+01	1.5210E+01	1.4010E+01	9.9052E+00	6.6918E+00
δ^{235}	9.9182E-02	1.0275E-01	1.0306E-01	1.0185E-01	9.8514E-02	8.9204E-02	6.2242E-02	4.1467E-02
δ^{238}	2.2827E-04	2.3613E-04	2.3680E-04	2.3491E-04	2.2863E-04	2.1074E-04	1.5185E-04	1.0400E-04
c/f^{235}	7.3440E-02	7.5759E-02	7.6056E-02	7.4913E-02	7.3017E-02	6.7847E-02	4.9943E-02	3.5606E-02
Actinide masses (g/t initial U)								
U-235	8.1203E+04	8.0587E+04	7.5063E+04	6.9164E+04	5.8039E+04	3.8329E+04	9.9306E+03	4.7254E+02
U-238	9.0910E+05	9.0899E+05	9.0733E+05	9.0557E+05	9.0183E+05	8.9369E+05	8.7267E+05	8.3922E+05
Pu-239	0.0000E+00	1.0384E+02	1.5208E+03	2.8590E+03	4.9092E+03	7.0991E+03	6.8174E+03	5.3197E+03
Pu-240	0.0000E+00	3.2992E-01	4.7067E+01	1.7475E+02	5.7940E+02	1.5924E+03	2.9801E+03	3.0219E+03
Pu-241	0.0000E+00	5.6476E-04	2.9570E+00	2.2262E+01	1.4207E+02	6.8735E+02	1.6518E+03	1.4372E+03
Pu-242	0.0000E+00	7.8265E-07	3.5908E-02	6.0856E-01	8.6772E+00	1.0998E+02	1.0738E+03	3.0219E+03
Am-241	0.0000E+00	1.6210E-07	6.2253E-03	1.0827E-01	1.4383E+00	1.3690E+01	5.0258E+01	2.8249E+01
Cm-244	0.0000E+00	0.0000E+00	8.5704E-07	8.3701E-05	5.6685E-03	3.7284E-01	2.5091E+01	3.0714E+02
Cm-245	0.0000E+00	0.0000E+00	1.5528E-09	3.1969E-07	4.6847E-05	5.7279E-03	5.7830E-01	6.8350E+00
Fission product masses (g/t initial U)								
Kr-85	0.0000E+00	4.9664E-01	5.0005E+00	9.8448E+00	1.9038E+01	3.5490E+01	5.9920E+01	7.0639E+01
Sr-90	0.0000E+00	1.1445E+01	1.1379E+02	2.2383E+02	4.3391E+02	8.1622E+02	1.4119E+03	1.7299E+03
Ag-110m	0.0000E+00	1.6067E-10	1.7629E-07	6.4784E-07	2.0546E-06	8.2205E-06	4.3799E-05	1.1555E-04
Cs-137	0.0000E+00	4.0442E-01	3.9496E-01	3.8571E-01	3.5633E-01	2.9834E-01	1.5726E-01	6.5775E-02
Xe-135	0.0000E+00	1.8675E+01	1.8785E+02	3.7460E+02	7.4480E+02	1.4735E+03	2.8623E+03	4.0761E+03
Sm-149	0.0000E+00	1.6056E+00	3.9496E+00	3.9353E+00	3.6844E+00	3.1660E+00	1.7497E+00	7.5657E-01
Sm-151	0.0000E+00	1.0390E+00	7.8969E+00	1.0286E+01	1.1071E+01	1.1137E+01	9.3881E+00	6.9109E+00

Pebble – KAERI 1

PEBBLE Results								
Burn-up (GWd/t)	**0**	**0.5**	**5**	**10**	**20**	**40**	**80**	**120**
k-inf	1.51903	1.45913	1.43185	1.40632	1.35081	1.23595	1.00160	0.77781
ρ^{238}	6.11160	6.35592	6.36715	6.32058	6.16160	5.64258	4.14510	2.97365
δ^{235}	0.10067	0.10480	0.10483	0.10380	0.10055	0.09078	0.06482	0.04529
δ^{238}	0.00312	0.00326	0.00349	0.00375	0.00432	0.00579	0.01286	0.07344
c/f^{235}	0.35751	0.37156	0.39794	0.42727	0.49277	0.66852	1.57445	9.78533
Actinide masses (g/t initial U)								
U-235	82000.3	81377.0	75900.1	70085.6	59220.1	40240.0	13077.8	1583.4
U-238	918000	917804	916012	913977	909741	900507	877883	846179
Pu-239	0	119.340	1718.06	3220.71	5499.66	7971.98	8319.93	6747.22
Pu-240	0	0.32094	55.7411	206.864	673.837	1788.51	3330.85	3522.66
Pu-241	0	0.00181	3.81034	28.4433	179.418	839.065	2083.37	1976.49
Pu-242	0	0	0.04814	0.76427	10.7302	126.090	1098.89	2950.38
Am-241	0	0	0.00969	0.14854	1.88751	17.3032	71.5985	58.6999
Cm-244	0	0	0	0.000146613	0.00946	0.56155	31.048	314.485
Cm-245	0	0	0	0	0	0.00854	0.74446	7.49935
Fission product masses (g/t initial U)								
Kr-85	0	0.53110	5.21119	10.2085	19.6181	36.2973	61.5434	76.1592
Sr-90	0	11.4715	112.834	221.646	428.386	802.088	1393.17	1762.93
Ag-110m	0	0	0.00112	0.00591	0.03274	0.18509	1.11219	3.41913
Cs-137	0	18.7420	187.085	373.416	743.764	1475.07	2900.78	4280.57
Xe-135	0	0.41236	0.40742	0.39988	0.38050	0.33077	0.21239	0.12442
Sm-149	0	1.62106	3.88814	3.95062	3.98985	3.82643	2.87677	1.90597
Sm-151	0	1.05318	8.28429	11.1918	12.8313	13.7250	13.6918	12.8881

Pebble – KAERI 2

PEBBLE Results								
Burn-up (GWd/t)	**0**	**0.5**	**5**	**10**	**20**	**40**	**80**	**120**
k-inf	1.51914	1.45752	1.42985	1.40408	1.34869	1.23148	0.99392	0.76861
□^{238}	6.11040	6.37389	6.37694	6.33108	6.16825	5.65833	4.16066	2.98902
□^{235}	0.10013	0.10439	0.10431	0.10341	0.10009	0.09035	0.06449	0.04515
□^{238}	0.00293	0.00307	0.00329	0.00353	0.00405	0.00541	0.01202	0.07018
c/f^{235}	0.35562	0.37054	0.39640	0.42561	0.49056	0.66606	1.57291	9.94888
Actinide masses (g/t initial U)								
U-235	82000.3	81377.2	75902.3	70080.3	59212.1	40240.3	13037.1	1550.7
U-238	918000	917805	916026	913998	909785	900600	878038	846270
Pu-239	0	117.979	1707.43	3200.08	5459.94	7907.16	8249.55	6662.61
Pu-240	0	0.40788	56.5587	208.815	672.344	1762.96	3256.41	3450.48
Pu-241	0	0.00260	4.05399	29.9352	186.745	861.646	2109.53	1994.44
Pu-242	0	0	0.05356	0.83516	11.5813	133.710	1144.31	3041.24
Am-241	0	0	0.01047	0.15648	1.96748	17.8080	72.5867	58.7194
Cm-244	0	0	0	0	0.01015	0.61259	33.258	328.383
Cm-245	0	0	0	0	0	0.01089	0.96029	9.78976
Fission product masses (g/t initial U)								
Kr-85	0	0.60911	5.42517	10.5801	20.2808	37.4768	63.6165	78.8822
Sr-90	0	11.5039	113.210	222.640	430.491	806.526	1405.34	1786.25
Ag-110m	0	0	0.00118	0.00641	0.03586	0.20536	1.27259	4.05641
Cs-137	0	18.7808	187.521	374.672	746.186	1478.83	2908.08	4293.99
Xe-135	0	0.40922	0.40371	0.39674	0.37727	0.32821	0.21357	0.12815
Sm-149	0	1.59311	3.78448	3.78704	3.51244	3.67848	2.71318	1.77406
Sm-151	0	1.05015	8.22127	11.1429	12.7808	13.7261	13.6482	12.7651

Pebble – KAERI 3

PEBBLE Results								
Burn-up (GWd/t)	**0**	**0.5**	**5**	**10**	**20**	**40**	**80**	**120**
k-inf	1.51918	1.45825	1.42982	1.40433	1.34875	1.23140	0.99399	0.76874
ρ^{238}	6.13137	6.37568	6.39330	6.33637	6.17867	5.66257	4.16706	3.00556
δ^{235}	0.10035	0.10454	0.10455	0.10343	0.10020	0.09049	0.06464	0.04531
δ^{238}	0.00289	0.00302	0.00324	0.00347	0.00399	0.00533	0.01186	0.06938
c/f^{235}	0.35588	0.36985	0.39643	0.42510	0.49039	0.66563	1.57549	10.00290
Actinide masses (g/t initial U)								
U-235	82000.3	81377.1	75900.0	70074.6	59198.3	40210.5	13007.0	1546.0
U-238	918000	917805	916025	913998	909784	900597	878028	846248
Pu-239	0	118.001	1709.37	3204.31	5471.47	7937.83	8290.38	6704.39
Pu-240	0	0.40568	56.1931	207.475	668.789	1754.86	3235.39	3424.56
Pu-241	0	0.00268	4.01730	29.6924	185.680	859.537	2113.53	1997.86
Pu-242	0	0	0.05295	0.82623	11.4842	133.032	1143.84	3042.20
Am-241	0	0	0.01040	0.15520	1.95440	17.7423	72.6720	58.9187
Cm-244	0	0	0	0.000157604	0.01035	0.60843	33.044	328.215
Cm-245	0	0	0	0	0	0.01085	0.97248	9.78002
Fission product masses (g/t initial U)								
Kr-85	0	0.60915	5.42565	10.5816	20.2851	37.4870	63.6230	78.8757
Sr-90	0	11.5042	113.218	222.671	430.584	806.758	1405.49	1786.06
Ag-110m	0	4.74042E-06	0.00123	0.00650	0.03616	0.20715	1.28249	4.07799
Cs-137	0	18.7808	187.520	374.671	746.183	1478.83	2908.07	4294.00
Xe-135	0	0.41139	0.40583	0.39879	0.37925	0.32999	0.21484	0.12909
Sm-149	0	1.60045	3.84002	3.84312	3.56843	3.51933	2.75299	1.79888
Sm-151	0	1.04970	8.18694	11.0661	12.6718	13.6069	13.5482	12.6918

Prism – INL/Studsvik

PRISM Results								
Burn-up (GWd/t)	**0**	**0.5**	**5**	**10**	**20**	**40**	**80**	**120**
k-inf	1.46403	1.40926	1.37913	1.34888	1.28594	1.17023	0.97905	0.81816
ρ^{238}	8.16933	8.48795	8.63334	8.71965	8.78657	8.57166	7.22806	5.75211
δ^{235}	0.13225	0.13757	0.13970	0.14070	0.14080	0.13534	0.11097	0.08599
δ^{238}	0.00351	0.00366	0.00399	0.00434	0.00513	0.00713	0.01526	0.05103
c/f^{235}	0.44792	0.46535	0.50444	0.54865	0.64696	0.90237	1.98818	6.94532
Actinide masses (g/t initial U)								
U-235	8.19988E+04	8.13695E+04	7.58676E+04	7.00795E+04	5.94010E+04	4.11716E+04	1.57940E+04	3.62497E+03
U-238	9.18001E+05	9.17777E+05	9.15694E+05	9.13327E+05	9.08372E+05	8.97561E+05	8.71898E+05	8.39637E+05
Pu-239	0.00000E+00	1.37715E+02	1.97980E+03	3.69869E+03	6.29966E+03	9.21590E+03	1.03110E+04	9.14371E+03
Pu-240	0.00000E+00	5.28000E-01	7.07142E+01	2.52638E+02	7.81739E+02	1.93200E+03	3.36760E+03	3.67471E+03
Pu-241	0.00000E+00	4.06358E-03	6.18896E+00	4.43889E+01	2.66191E+02	1.16183E+03	2.79259E+03	2.90718E+03
Pu-242	0.00000E+00	3.94186E-06	8.45739E-02	1.28096E+00	1.68507E+01	1.77859E+02	1.29018E+03	3.06001E+03
Am-241	0.00000E+00	7.72161E-07	1.60824E-02	2.34868E-01	2.83918E+00	2.43416E+01	9.99087E+01	1.06877E+02
Cm-244	0.00000E+00	1.48128E-11	5.83624E-06	3.96346E-04	2.39760E-02	1.28130E+00	5.62416E+01	4.20267E+02
Cm-245	0.00000E+00	0.00000E+00	1.64258E-08	2.30633E-06	2.83225E-04	2.98985E-02	2.30642E+00	1.94172E+01
Fission product masses (g/t initial U)								
Kr-85	0.00000E+00	5.31327E-01	5.19852E+00	1.01541E+01	1.94126E+01	3.55989E+01	5.97482E+01	7.45580E+01
Sr-90	0.00000E+00	1.14726E+01	1.12512E+02	2.20355E+02	4.23689E+02	7.86592E+02	1.35587E+03	1.74035E+03
Ag-110m	0.00000E+00	1.18711E-05	1.87760E-03	1.02309E-02	5.87042E-02	3.37628E-01	1.90690E+00	5.14559E+00
Cs-137	0.00000E+00	1.87571E+01	1.87271E+02	3.73864E+02	7.44901E+02	1.47806E+03	2.90803E+03	4.29029E+03
Xe-135	0.00000E+00	4.05796E-01	4.03364E-01	3.98259E-01	3.84656E-01	3.46820E-01	2.55053E-01	1.74265E-01
Sm-149	0.00000E+00	1.62600E+00	3.98498E+00	4.13978E+00	4.34356E+00	4.39654E+00	3.69782E+00	2.75544E+00
Sm-151	0.00000E+00	1.05771E+00	8.58348E+00	1.19697E+01	1.44275E+01	1.66405E+01	1.85475E+01	1.82770E+01

Prism – FZD 1

PRISM Results								
Burn-up (GWd/t)	**0**	**0.5**	**5**	**10**	**20**	**40**	**80**	**120**
k-inf	1.46469	1.40711	1.37776	1.34895	1.28714	1.17254	0.98240	0.82090
ρ^{238}	7.47E+00	7.78E+00	7.90E+00	7.97E+00	8.01E+00	7.80E+00	6.53E+00	5.21E+00
δ^{235}	1.34E-01	1.39E-01	1.42E-01	1.42E-01	1.42E-01	1.36E-01	1.11E-01	8.56E-02
δ^{238}	3.79E-03	3.97E-03	4.31E-03	4.69E-03	5.51E-03	7.65E-03	1.63E-02	5.48E-02
c/f^{235}	4.14E-01	4.31E-01	4.67E-01	5.07E-01	5.97E-01	8.32E-01	1.83E+00	6.47E+00
Actinide masses (g/t initial U)								
U-235	8.20E+04	8.14E+04	7.59E+04	7.01E+04	5.94E+04	4.11E+04	1.57E+04	3.58E+03
U-238	9.18E+05	9.18E+05	9.16E+05	9.13E+05	9.08E+05	8.98E+05	8.72E+05	8.40E+05
Pu-239	0.00E+00	1.35E+02	1.98E+03	3.69E+03	6.29E+03	9.19E+03	1.03E+04	9.11E+03
Pu-240	0.00E+00	5.15E-01	7.09E+01	2.53E+02	7.85E+02	1.94E+03	3.40E+03	3.73E+03
Pu-241	0.00E+00	4.08E-03	6.17E+00	4.43E+01	2.66E+02	1.16E+03	2.78E+03	2.90E+03
Pu-242	0.00E+00	5.10E-06	8.49E-02	1.29E+00	1.69E+01	1.79E+02	1.31E+03	3.17E+03
Am-241	0.00E+00	9.93E-07	1.60E-02	2.32E-01	2.78E+00	2.33E+01	9.13E+01	9.36E+01
Cm-244	0.00E+00	2.11E-12	5.17E-06	3.47E-04	2.12E-02	1.15E+00	5.08E+01	3.87E+02
Cm-245	0.00E+00	5.92E-16	1.36E-08	1.83E-06	2.26E-04	2.43E-02	1.88E+00	1.59E+01
Fission product masses (g/t initial U)								
Kr-85	0.00E+00	5.20E-01	5.25E+00	1.03E+01	1.97E+01	3.63E+01	6.15E+01	7.77E+01
Sr-90	0.00E+00	1.14E+01	1.12E+02	2.19E+02	4.21E+02	7.80E+02	1.34E+03	1.71E+03
Ag-110m	0.00E+00	6.54E-06	1.41E-03	8.27E-03	4.98E-02	2.94E-01	1.67E+00	4.41E+00
Cs-137	0.00E+00	1.85E+01	1.85E+02	3.69E+02	7.35E+02	1.46E+03	2.87E+03	4.23E+03
Xe-135	0.00E+00	4.22E-01	4.20E-01	4.15E-01	4.00E-01	3.61E-01	2.65E-01	1.81E-01
Sm-149	0.00E+00	1.53E+00	3.61E+00	3.77E+00	3.98E+00	4.08E+00	3.48E+00	2.62E+00
Sm-151	0.00E+00	1.06E+00	8.63E+00	1.20E+01	1.45E+01	1.65E+01	1.83E+01	1.83E+01

Prism – FZD 2

PRISM Results								
Burn-up (GWd/t)	0	0.5	5	10	20	40	80	120
k-inf	1.46448	1.40658	1.37799	1.34853	1.28794	1.17269	0.98267	0.82132
ρ^{238}	7.47E+00	7.79E+00	7.92E+00	7.96E+00	8.01E+00	7.80E+00	6.53E+00	5.20E+00
δ^{235}	1.34E-01	1.39E-01	1.42E-01	1.42E-01	1.42E-01	1.36E-01	1.11E-01	8.56E-02
δ^{238}	3.80E-03	3.97E-03	4.31E-03	4.70E-03	5.54E-03	7.66E-03	1.63E-02	5.49E-02
c/f^{235}	4.15E-01	4.32E-01	4.68E-01	5.07E-01	5.97E-01	8.32E-01	1.83E+00	6.46E+00
Actinide masses (g/t initial U)								
U-235	8.20E+04	8.14E+04	7.59E+04	7.01E+04	5.94E+04	4.11E+04	1.57E+04	3.59E+03
U-238	9.18E+05	9.18E+05	9.16E+05	9.13E+05	9.08E+05	8.98E+05	8.72E+05	8.40E+05
Pu-239	0.00E+00	1.35E+02	1.98E+03	3.70E+03	6.29E+03	9.19E+03	1.03E+04	9.12E+03
Pu-240	0.00E+00	5.15E-01	7.08E+01	2.53E+02	7.84E+02	1.94E+03	3.40E+03	3.73E+03
Pu-241	0.00E+00	4.09E-03	6.18E+00	4.44E+01	2.66E+02	1.16E+03	2.78E+03	2.90E+03
Pu-242	0.00E+00	5.11E-06	8.50E-02	1.29E+00	1.70E+01	1.79E+02	1.31E+03	3.17E+03
Am-241	0.00E+00	9.95E-07	1.60E-02	2.32E-01	2.78E+00	2.33E+01	9.13E+01	9.37E+01
Cm-244	0.00E+00	2.11E-12	5.18E-06	3.48E-04	2.13E-02	1.16E+00	5.09E+01	3.87E+02
Cm-245	0.00E+00	5.92E-16	1.36E-08	1.84E-06	2.26E-04	2.44E-02	1.88E+00	1.60E+01
Fission product masses (g/t initial U)								
Kr-85	0.00E+00	5.20E-01	5.25E+00	1.03E+01	1.97E+01	3.63E+01	6.15E+01	7.77E+01
Sr-90	0.00E+00	1.14E+01	1.12E+02	2.19E+02	4.21E+02	7.80E+02	1.34E+03	1.71E+03
Ag-110m	0.00E+00	6.51E-06	1.41E-03	8.24E-03	4.96E-02	2.93E-01	1.66E+00	4.40E+00
Cs-137	0.00E+00	1.85E+01	1.85E+02	3.69E+02	7.35E+02	1.46E+03	2.87E+03	4.23E+03
Xe-135	0.00E+00	4.22E-01	4.20E-01	4.15E-01	4.00E-01	3.61E-01	2.65E-01	1.82E-01
Sm-149	0.00E+00	1.53E+00	3.61E+00	3.77E+00	3.98E+00	4.08E+00	3.48E+00	2.62E+00
Sm-151	0.00E+00	1.06E+00	8.63E+00	1.20E+01	1.45E+01	1.65E+01	1.83E+01	1.82E+01

Prism – FZD 3

PRISM Results								
Burn-up (GWd/t)	**0**	**0.5**	**5**	**10**	**20**	**40**	**80**	**120**
k-inf	1.46039	1.40332	1.37411	1.34568	1.28545	1.17205	0.98396	0.82677
ρ^{238}	7.56E+00	7.88E+00	8.02E+00	8.10E+00	8.17E+00	7.99E+00	6.81E+00	5.49E+00
δ^{235}	1.35E-01	1.41E-01	1.43E-01	1.44E-01	1.44E-01	1.39E-01	1.15E-01	9.03E-02
δ^{238}	4.03E-03	4.21E-03	4.58E-03	5.00E-03	5.90E-03	8.21E-03	1.75E-02	5.58E-02
c/f^{235}	4.21E-01	4.38E-01	4.75E-01	5.17E-01	6.09E-01	8.49E-01	1.85E+00	6.18E+00
Actinide masses (g/t initial U)								
U-235	8.20E+04	8.14E+04	7.59E+04	7.01E+04	5.95E+04	4.14E+04	1.62E+04	3.94E+03
U-238	9.18E+05	9.18E+05	9.16E+05	9.13E+05	9.08E+05	8.97E+05	8.71E+05	8.39E+05
Pu-239	4.11E-12	1.40E+02	2.01E+03	3.75E+03	6.39E+03	9.35E+03	1.05E+04	9.43E+03
Pu-240	4.13E-12	4.14E-01	7.04E+01	2.55E+02	7.97E+02	1.98E+03	3.48E+03	3.82E+03
Pu-241	4.15E-12	2.46E-03	5.86E+00	4.28E+01	2.60E+02	1.15E+03	2.81E+03	2.98E+03
Pu-242	4.16E-12	1.27E-06	7.58E-02	1.18E+00	1.57E+01	1.68E+02	1.23E+03	2.95E+03
Am-241	4.15E-12	2.59E-07	1.50E-02	2.24E-01	2.75E+00	2.39E+01	1.00E+02	1.12E+02
Cm-244	4.20E-12	4.20E-12	4.90E-06	3.47E-04	2.15E-02	1.17E+00	5.13E+01	3.85E+02
Cm-245	4.22E-12	4.22E-12	1.20E-08	1.77E-06	2.23E-04	2.40E-02	1.83E+00	1.55E+01
Fission product masses (g/t initial U)								
Kr-85	1.46E-12	5.31E-01	5.20E+00	1.02E+01	1.94E+01	3.56E+01	5.99E+01	7.52E+01
Sr-90	1.55E-12	1.15E+01	1.12E+02	2.20E+02	4.23E+02	7.84E+02	1.35E+03	1.73E+03
Ag-110m	1.89E-12	9.26E-06	1.47E-03	7.96E-03	4.50E-02	2.50E-01	1.33E+00	3.39E+00
Cs-137	2.36E-12	1.88E+01	1.87E+02	3.74E+02	7.45E+02	1.48E+03	2.90E+03	4.28E+03
Xe-135	2.32E-12	4.25E-01	4.24E-01	4.20E-01	4.08E-01	3.72E-01	2.81E-01	1.98E-01
Sm-149	2.56E-12	1.63E+00	3.98E+00	4.13E+00	4.33E+00	4.40E+00	3.78E+00	2.89E+00
Sm-151	2.60E-12	1.06E+00	8.59E+00	1.20E+01	1.44E+01	1.66E+01	1.87E+01	1.87E+01

Prism – IKE 1

PRISM Results								
Burn-up (GWd/t)	**0**	**0.5**	**5**	**10**	**20**	**40**	**80**	**120**
k-inf	1.45466	1.3963	1.37209	1.34326	1.28227	1.16924	0.98562	0.84024
ρ^{238}	7.696E+00	8.069E+00	8.149E+00	8.281E+00	8.372E+00	8.331E+00	7.379E+00	6.268E+00
δ^{235}	1.357E-01	1.416E-01	1.442E-01	1.461E-01	1.469E-01	1.450E-01	1.252E-01	1.044E-01
δ^{238}	3.813E-03	4.009E-03	4.374E-03	4.765E-03	5.661E-03	7.887E-03	1.678E-02	5.135E-02
c/f^{235}	4.248E-01	4.458E-01	4.807E-01	5.220E-01	6.171E-01	8.579E-01	1.863E+00	5.821E+00
Actinide masses (g/t initial U)								
U-235	82018.8360	8.11E+04	7.55E+04	7.02E+04	5.95E+04	4.20E+04	1.70E+04	4.60E+03
U-238	9.1705E+05	9.1673E+05	9.1456E+05	9.1233E+05	9.0721E+05	8.9653E+05	8.7068E+05	8.3862E+05
Pu-239	0.00E+00	2.16E+02	2.13E+03	3.74E+03	6.44E+03	9.41E+03	1.08E+04	1.00E+04
Pu-240	0.00E+00	1.08E+00	8.04E+01	2.53E+02	7.99E+02	1.93E+03	3.43E+03	3.82E+03
Pu-241	0.00E+00	1.18E-02	7.41E+00	4.42E+01	2.73E+02	1.16E+03	2.90E+03	3.23E+03
Pu-242	0.00E+00	2.01E-05	1.08E-01	1.26E+00	1.73E+01	1.72E+02	1.27E+03	3.06E+03
Am-241	0.00E+00	3.94E-06	2.05E-02	2.29E-01	2.87E+00	2.31E+01	9.59E+01	1.10E+02
Cm-244	0.00E+00	2.07E-11	7.62E-06	3.38E-04	2.21E-02	1.10E+00	4.88E+01	3.67E+02
Cm-245	0.00E+00	4.37E-13	2.11E-08	1.77E-06	2.38E-04	2.34E-02	1.90E+00	1.71E+01
Fission product masses (g/t initial U)								
Kr-85	-	-	-	-	-	-	-	-
Sr-90	-	-	-	-	-	-	-	-
Ag-110m	0.00E+00	1.76E-05	1.78E-03	8.44E-03	5.06E-02	2.81E-01	1.58E+00	4.11E+00
Cs-137	-	-	-	-	-	-	-	-
Xe-135	0.00E+00	4.16E-01	4.16E-01	4.13E-01	4.02E-01	3.71E-01	2.87E-01	2.12E-01
Sm-149	0.00E+00	2.12E+00	3.71E+00	3.86E+00	4.07E+00	4.19E+00	3.69E+00	2.94E+00
Sm-151	0.00E+00	1.76E+00	8.97E+00	1.20E+01	1.45E+01	1.68E+01	1.94E+01	2.01E+01

Prism – IKE 2

PRISM Results								
Burn-up (GWd/t)	0	0.5	5	10	20	40	80	120
k-inf	1.477	1.421	1.390	1.360	1.298	1.184	0.989	0.818
ρ^{238}	7.16E+00	7.44E+00	7.56E+00	7.61E+00	7.62E+00	7.32E+00	5.94E+00	4.54E+00
δ^{235}	1.31E-01	1.37E-01	1.39E-01	1.39E-01	1.38E-01	1.31E-01	1.03E-01	7.67E-02
δ^{238}	3.62E-03	3.78E-03	4.08E-03	4.42E-03	5.16E-03	7.03E-03	1.47E-02	5.26E-02
c/f^{235}	4.10E-01	4.26E-01	4.61E-01	5.00E-01	5.86E-01	8.11E-01	1.78E+00	6.80E+00
Actinide masses (g/t initial U)								
U-235	8.20E+04	8.14E+04	7.59E+04	7.01E+04	5.95E+04	4.11E+04	1.54E+04	3.15E+03
U-238	9.18E+05	9.18E+05	9.16E+05	9.14E+05	9.09E+05	8.99E+05	8.74E+05	8.42E+05
Pu-239	0.00E+00	1.30E+02	1.90E+03	3.54E+03	6.04E+03	8.80E+03	9.67E+03	8.36E+03
Pu-240	0.00E+00	5.44E-01	6.81E+01	2.43E+02	7.53E+02	1.87E+03	3.28E+03	3.56E+03
Pu-241	0.00E+00	4.43E-03	5.90E+00	4.21E+01	2.52E+02	1.10E+03	2.62E+03	2.65E+03
Pu-242	0.00E+00	5.65E-06	8.12E-02	1.22E+00	1.61E+01	1.72E+02	1.28E+03	3.14E+03
Am-241	0.00E+00	1.09E-06	1.51E-02	2.17E-01	2.58E+00	2.13E+01	7.99E+01	7.49E+01
Cm-244	0.00E+00	3.95E-12	9.14E-06	6.05E-04	3.63E-02	1.91E+00	7.82E+01	5.61E+02
Cm-245	0.00E+00	9.16E-16	2.30E-08	3.09E-06	3.76E-04	3.92E-02	2.76E+00	2.13E+01
Fission product masses (g/t initial U)								
Kr-85	0.00E+00	4.89E-01	4.94E+00	9.69E+00	1.86E+01	3.43E+01	5.81E+01	7.34E+01
Sr-90	0.00E+00	1.13E+01	1.11E+02	2.18E+02	4.19E+02	7.80E+02	1.35E+03	1.73E+03
Ag-110m	0.00E+00	1.20E-05	1.98E-03	1.02E-02	5.55E-02	3.11E-01	1.79E+00	5.12E+00
Cs-137	0.00E+00	1.84E+01	1.84E+02	3.68E+02	7.32E+02	1.45E+03	2.85E+03	4.21E+03
Xe-135	0.00E+00	4.18E-01	4.15E-01	4.10E-01	3.96E-01	3.55E-01	2.54E-01	1.67E-01
Sm-149	0.00E+00	1.57E+00	3.71E+00	3.88E+00	4.08E+00	4.08E+00	3.26E+00	2.29E+00
Sm-151	0.00E+00	1.06E+00	8.60E+00	1.20E+01	1.45E+01	1.67E+01	1.82E+01	1.74E+01

Prism – IKE 3

PRISM Results								
Burn-up (GWd/t)	**0**	**0.5**	**5**	**10**	**20**	**40**	**80**	**120**
k-inf	1.46316	1.40781	1.37801	1.35028	1.29334	1.17978	0.99688	0.83841
ρ^{238}	7.60130E+00	7.94727E+00	8.08930E+00	8.14849E+00	8.16811E+00	7.88178E+00	6.50406E+00	5.11630E+00
δ^{235}	1.33437E-01	1.39772E-01	1.41718E-01	1.42467E-01	1.41652E-01	1.34369E-01	1.07621E-01	8.22994E-02
δ^{238}	3.84338E-03	4.02241E-03	4.37051E-03	4.75253E-03	5.59867E-03	7.71549E-03	1.62899E-02	5.40753E-02
c/f^{235}	4.30357E-01	4.49285E-01	4.87942E-01	5.30232E-01	6.24572E-01	8.69140E-01	1.90998E+00	6.70141E+00
Actinide masses (g/t initial U)								
U-235	8.20E+04	8.13E+04	7.57E+04	6.98E+04	5.90E+04	4.06E+04	1.54E+04	3.49E+03
U-238	9.18E+05	9.18E+05	9.15E+05	9.13E+05	9.08E+05	8.97E+05	8.71E+05	8.39E+05
Pu-239	4.33E-13	1.41E+02	2.03E+03	3.78E+03	6.42E+03	9.33E+03	1.04E+04	9.10E+03
Pu-240	4.35E-13	5.25E-01	7.29E+01	2.60E+02	8.02E+02	1.97E+03	3.40E+03	3.70E+03
Pu-241	4.37E-13	4.26E-03	6.47E+00	4.63E+01	2.75E+02	1.19E+03	2.79E+03	2.87E+03
Pu-242	4.38E-13	5.41E-06	9.02E-02	1.36E+00	1.77E+01	1.84E+02	1.30E+03	3.02E+03
Am-241	0	0	0	2.44E-01	2.93E+00	2.48E+01	9.97E+01	1.06E+02
Cm-244	0	0	0	0	2.79E-02	1.47E+00	6.10E+01	4.35E+02
Cm-245	0	0	0	0	3.40E-04	3.58E-02	2.65E+00	2.18E+01
Fission product masses (g/t initial U)								
Kr-85	0.00E+00	5.47E-01	5.50E+00	1.07E+01	2.05E+01	3.76E+01	6.27E+01	7.79E+01
Sr-90	0.00E+00	1.17E+01	1.15E+02	2.25E+02	4.31E+02	7.97E+02	1.36E+03	1.74E+03
Ag-110m	0	0	1.19E-03	6.69E-03	3.88E-02	2.19E-01	1.18E+00	2.98E+00
Cs-137	0.00E+00	1.92E+01	1.92E+02	3.82E+02	7.60E+02	1.51E+03	2.94E+03	4.31E+03
Xe-135	0.00E+00	4.28E-01	4.21E-01	4.17E-01	4.03E-01	3.65E-01	2.69E-01	1.85E-01
Sm-149	0	1.64E+00	4.03E+00	4.17E+00	4.34E+00	4.36E+00	3.61E+00	2.65E+00
Sm-151	0	1.08E+00	8.62E+00	1.19E+01	1.41E+01	1.61E+01	1.74E+01	1.70E+01

Prism – GRS

PRISM Results								
Burn-up (GWd/t)	0	0.5	5	10	20	40	80	120
k-inf	1.4572	1.4002	1.37168	1.34207	1.28038	1.16593	0.97849	0.82265
ρ238	7.653E+00	7.976E+00	8.100E+00	8.202E+00	8.248E+00	8.078E+00	6.876E+00	5.564E+00
δ235	1.341E-01	1.399E-01	1.421E-01	1.432E-01	1.432E-01	1.378E-01	1.140E-01	8.958E-02
δ238	3.792E-03	3.965E-03	4.312E-03	4.698E-03	5.542E-03	7.690E-03	1.640E-02	5.294E-02
c/f235	4.221E-01	4.395E-01	4.757E-01	5.185E-01	6.101E-01	8.528E-01	1.871E+00	6.313E+00
Actinide masses (g/t initial U)								
U-235	8.22E+04	8.11E+04	7.61E+04	7.00E+04	5.94E+04	4.12E+04	1.60E+04	3.86E+03
U-238	9.17E+05	9.17E+05	9.17E+05	9.11E+05	9.06E+05	8.94E+05	8.72E+05	8.39E+05
Pu-239	0.00E+00	1.41E+02	2.02E+03	3.78E+03	6.44E+03	9.44E+03	1.07E+04	9.56E+03
Pu-240	0.00E+00	5.42E-01	7.17E+01	2.56E+02	7.94E+02	1.97E+03	3.46E+03	3.80E+03
Pu-241	0.00E+00	4.44E-03	6.22E+00	4.46E+01	2.67E+02	1.17E+03	2.84E+03	3.02E+03
Pu-242	0.00E+00	5.72E-06	8.56E-02	1.29E+00	1.69E+01	1.79E+02	1.31E+03	3.17E+03
Am-241	0.00E+00	1.12E-06	1.61E-02	2.33E-01	2.78E+00	2.34E+01	9.39E+01	1.00E+02
Cm-244	0.00E+00	2.63E-12	5.32E-06	3.54E-04	2.16E-02	1.17E+00	5.03E+01	3.75E+02
Cm-245	0.00E+00	5.41E-16	1.38E-08	1.87E-06	2.30E-04	2.46E-02	1.88E+00	1.58E+01
Fission product masses (g/t initial U)								
Kr-85	0.00E+00	4.92E-01	4.97E+00	9.72E+00	1.86E+01	3.42E+01	5.78E+01	7.22E+01
Sr-90	0.00E+00	1.15E+01	1.13E+02	2.21E+02	4.24E+02	7.83E+02	1.35E+03	1.73E+03
Ag-110m	0.00E+00	1.01E-05	1.93E-03	8.69E-03	4.20E-02	2.20E-01	1.06E+00	2.43E+00
Cs-137	0.00E+00	1.86E+01	1.86E+02	3.70E+02	7.39E+02	1.46E+03	2.88E+03	4.24E+03
Xe-135	0.00E+00	4.21E-01	4.19E-01	4.15E-01	4.02E-01	3.65E-01	2.75E-01	1.93E-01
Sm-149	0.00E+00	1.58E+00	3.85E+00	4.07E+00	4.37E+00	4.54E+00	3.89E+00	2.93E+00
Sm-151	0.00E+00	1.05E+00	8.50E+00	1.18E+01	1.43E+01	1.66E+01	1.90E+01	1.93E+01

Prism – LLNL

PRISM Results								
Burn-up (GWd/t)	**0**	**0.5**	**5**	**10**	**20**	**40**	**80**	**120**
k-inf	1.46004	1.40216	1.37214	1.34224	1.28067	1.16686	0.98136	0.82741
ρ^{238}	7.566591616	7.89590723	8.032088154	8.115326082	8.182671845	8.007858003	6.787490417	5.468158259
δ^{235}	0.133303106	0.139270551	0.141453272	0.142519311	0.142599619	0.137068719	0.112907997	0.08834736
δ^{238}	0.003799832	0.003977941	0.00432312	0.004708483	0.005560756	0.007715472	0.016399095	0.053263973
c/f^{235}	0.419103113	0.436804329	0.473506971	0.515114893	0.607529397	0.848678623	1.859326978	6.314209995
Actinide masses (g/t initial U)								
U-235	82000.65101	81383.35168	75870.36228	70079.05708	59405.48487	41228.54988	15982.83338	3816.552263
U-238	918002.537	917899.7844	915796.6848	913416.136	908415.5522	897462.3006	871468.8329	839007.2605
Pu-239	0	136.7618211	2000.33441	3742.911065	6379.795952	9347.130612	10519.94657	9424.445214
Pu-240	0	0.531603085	71.79283335	256.6411755	793.8425094	1959.342139	3421.088993	3761.604107
Pu-241	0	0.004243593	6.245235771	45.0318687	270.1063154	1177.920042	2844.850651	3004.42689
Pu-242	0	5.32008E-06	0.085781511	1.301695647	17.10015929	179.9960887	1298.063462	3076.96462
Am-241	0	1.03566E-06	0.016150595	0.235511465	2.82833643	23.89707476	95.27176936	101.4563976
Cm-244	0	3.27633E-12	9.29282E-06	0.000623726	0.037566727	1.980995246	80.36826322	550.2861842
Cm-245	0	1.78355E-15	3.10085E-08	4.00122E-06	0.000476968	0.049371781	3.537444919	27.50566852
Fission product masses (g/t initial U)								
Kr-85	0	0.456142733	4.606168838	9.025338767	17.31770018	31.94310871	54.25332894	68.75982345
Sr-90	0	11.13661305	109.2529637	213.9551539	411.3487203	763.7198108	1317.713894	1695.753793
Ag-110m	0	7.37477E-06	0.001227258	0.00635626	0.034469112	0.188606766	1.005985274	2.58083517
Cs-137	0	18.57115604	185.4907454	370.3057351	737.7582768	1463.669142	2878.688116	4244.194648
Xe-135	0	0.41423897	0.413587646	0.409988583	0.397394268	0.361725999	0.270619605	0.189832008
Sm-149	0	1.609672624	3.909238816	3.985710939	4.049252243	3.926370176	3.139907559	2.31133384
Sm-151	0	1.06785622	8.683697776	12.12392548	14.56970825	16.52883814	17.70530611	17.00938205

Prism – VTT 1

PRISM Results								
Burn-up (GWd/t)	**0**	**0.5**	**5**	**10**	**20**	**40**	**80**	**120**
k-inf	1.45312	1.39538	1.3648	1.33448	1.26933	1.15398	0.97182	0.82482
ρ^{238}	7.78E+00	8.11E+00	8.30E+00	8.39E+00	8.55E+00	8.47E+00	7.40E+00	6.09E+00
δ^{235}	1.41E-01	1.47E-01	1.49E-01	1.51E-01	1.53E-01	1.49E-01	1.26E-01	1.01E-01
δ^{238}	4.00E-03	4.20E-03	4.54E-03	4.98E-03	5.92E-03	8.28E-03	1.77E-02	5.45E-02
c/f^{235}	4.28E-01	4.45E-01	4.85E-01	5.28E-01	6.27E-01	8.82E-01	1.93E+00	6.19E+00
Actinide masses (g/t initial U)								
U-235	8.20E+04	8.14E+04	7.59E+04	7.01E+04	5.94E+04	4.14E+04	1.64E+04	4.23E+03
U-238	9.18E+05	9.18E+05	9.16E+05	9.13E+05	9.08E+05	8.97E+05	8.70E+05	8.37E+05
Pu-239	0.00E+00	1.42E+02	2.05E+03	3.83E+03	6.52E+03	9.58E+03	1.09E+04	9.96E+03
Pu-240	0.00E+00	5.51E-01	7.36E+01	2.61E+02	7.92E+02	1.91E+03	3.23E+03	3.53E+03
Pu-241	0.00E+00	4.84E-03	7.13E+00	5.07E+01	3.00E+02	1.28E+03	3.03E+03	3.22E+03
Pu-242	0.00E+00	6.11E-06	9.86E-02	1.47E+00	1.91E+01	1.96E+02	1.36E+03	3.15E+03
Am-241	0.00E+00	1.19E-06	1.86E-02	2.69E-01	3.21E+00	2.70E+01	1.10E+02	1.23E+02
Cm-244	0.00E+00	9.91E-13	2.95E-07	9.82E-06	2.95E-04	7.69E-03	1.55E-01	7.24E-01
Cm-245	0.00E+00	1.05E-16	3.42E-11	1.16E-09	3.68E-08	1.09E-06	3.05E-05	2.11E-04
Fission product masses (g/t initial U)								
Kr-85	0.00E+00	4.11E-01	4.11E+00	8.05E+00	1.54E+01	2.83E+01	4.77E+01	6.02E+01
Sr-90	0.00E+00	1.17E+01	1.15E+02	2.24E+02	4.31E+02	7.99E+02	1.38E+03	1.77E+03
Ag-110m	0.00E+00	5.53E-12	5.40E-11	3.38E-10	1.01E-08	2.96E-07	6.24E-06	3.44E-05
Cs-137	0.00E+00	1.92E+01	1.92E+02	3.84E+02	7.65E+02	1.52E+03	2.99E+03	4.41E+03
Xe-135	0.00E+00	4.19E-01	4.19E-01	4.16E-01	4.06E-01	3.73E-01	2.87E-01	2.08E-01
Sm-149	0.00E+00	1.60E+00	3.96E+00	4.11E+00	4.31E+00	4.39E+00	3.78E+00	2.92E+00
Sm-151	0.00E+00	1.06E+00	8.63E+00	1.21E+01	1.46E+01	1.69E+01	1.92E+01	1.93E+01

Prism – VTT 2

PRISM Results								
Burn-up (GWd/t)	0	0.5	5	10	20	40	80	120
k-inf	1.45884	1.40171	1.37067	1.34225	1.27872	1.16214	0.97697	0.82224
ρ^{238}	7.61E+00	7.91E+00	8.08E+00	8.13E+00	8.24E+00	8.12E+00	6.93E+00	5.59E+00
δ^{235}	1.33E-01	1.39E-01	1.42E-01	1.43E-01	1.43E-01	1.38E-01	1.15E-01	9.01E-02
δ^{238}	3.78E-03	3.97E-03	4.33E-03	4.71E-03	5.59E-03	7.74E-03	1.66E-02	5.35E-02
c/f^{235}	4.21E-01	4.38E-01	4.76E-01	5.16E-01	6.11E-01	8.58E-01	1.88E+00	6.34E+00
Actinide masses (g/t initial U)								
U-235	8.20E+04	8.14E+04	7.59E+04	7.01E+04	5.94E+04	4.12E+04	1.60E+04	3.87E+03
U-238	9.18E+05	9.18E+05	9.16E+05	9.13E+05	9.08E+05	8.97E+05	8.71E+05	8.38E+05
Pu-239	0.00E+00	1.40E+02	2.02E+03	3.77E+03	6.43E+03	9.43E+03	1.07E+04	9.55E+03
Pu-240	0.00E+00	5.32E-01	7.15E+01	2.54E+02	7.79E+02	1.89E+03	3.24E+03	3.52E+03
Pu-241	0.00E+00	4.52E-03	6.68E+00	4.76E+01	2.84E+02	1.23E+03	2.92E+03	3.05E+03
Pu-242	0.00E+00	5.66E-06	9.17E-02	1.38E+00	1.80E+01	1.88E+02	1.34E+03	3.15E+03
Am-241	0.00E+00	1.11E-06	1.74E-02	2.53E-01	3.04E+00	2.58E+01	1.06E+02	1.15E+02
Cm-244	0.00E+00	8.64E-13	2.55E-07	8.52E-06	2.56E-04	6.80E-03	1.42E-01	6.96E-01
Cm-245	0.00E+00	9.12E-17	2.96E-11	1.01E-09	3.20E-08	9.78E-07	2.90E-05	2.15E-04
Fission product masses (g/t initial U)								
Kr-85	0.00E+00	4.11E-01	4.12E+00	8.05E+00	1.54E+01	2.84E+01	4.79E+01	6.03E+01
Sr-90	0.00E+00	1.17E+01	1.15E+02	2.24E+02	4.32E+02	8.01E+02	1.38E+03	1.78E+03
Ag-110m	0.00E+00	5.53E-12	5.36E-11	3.18E-10	9.36E-09	2.77E-07	5.93E-06	3.30E-05
Cs-137	0.00E+00	1.92E+01	1.92E+02	3.84E+02	7.64E+02	1.52E+03	2.99E+03	4.41E+03
Xe-135	0.00E+00	4.17E-01	4.16E-01	4.12E-01	4.01E-01	3.67E-01	2.77E-01	1.96E-01
Sm-149	0.00E+00	1.60E+00	3.94E+00	4.08E+00	4.25E+00	4.29E+00	3.64E+00	2.76E+00
Sm-151	0.00E+00	1.06E+00	8.58E+00	1.19E+01	1.43E+01	1.64E+01	1.83E+01	1.82E+01

Prism – ORNL 1

PRISM Results								
Burn-up (GWd/t)	**0**	**0.5**	**5**	**10**	**20**	**40**	**80**	**120**
k-inf	1.4619	1.4029	1.3719	1.3415	1.2786	1.1631	0.9739	0.8153
ρ^{238}	7.580E+00	7.908E+00	8.055E+00	8.142E+00	8.21E+00	8.016E+00	6.791E+00	5.507E+00
δ^{235}	1.337E-01	1.40E-01	1.42E-01	1.43E-01	1.43E-01	1.38E-01	1.13E-01	8.91E-02
δ^{238}	3.788E-03	3.97E-03	4.32E-03	4.71E-03	5.56E-03	7.75E-03	1.65E-02	5.36E-02
c/f^{235}	4.246E-01	4.43E-01	4.81E-01	5.24E-01	6.20E-01	8.68E-01	1.92E+00	6.53E+00
Actinide masses (g/t initial U)								
U-235	8.20E+04	8.13E+04	7.57E+04	6.99E+04	5.91E+04	4.08E+04	1.56E+04	3.75E+03
U-238	9.18E+05	9.18E+05	9.15E+05	9.13E+05	9.08E+05	8.97E+05	8.71E+05	8.38E+05
Pu-239	0.00E+00	1.42E+02	2.04E+03	3.81E+03	6.46E+03	9.41E+03	1.05E+04	9.38E+03
Pu-240	0.00E+00	5.33E-01	7.40E+01	2.64E+02	8.12E+02	1.99E+03	3.43E+03	3.74E+03
Pu-241	0.00E+00	4.32E-03	6.58E+00	4.71E+01	2.80E+02	1.20E+03	2.87E+03	3.01E+03
Pu-242	0.00E+00	5.50E-06	9.19E-02	1.38E+00	1.80E+01	1.86E+02	1.31E+03	3.02E+03
Am-241	0.00E+00	1.05E-06	1.71E-02	2.48E-01	2.97E+00	2.51E+01	1.02E+02	1.12E+02
Cm-244	0.00E+00	2.43E-12	7.08E-06	4.72E-04	2.85E-02	1.50E+00	6.23E+01	4.41E+02
Cm-245	0.00E+00	1.44E-15	2.12E-08	2.85E-06	3.47E-04	3.66E-02	2.76E+00	2.31E+01
Fission product masses (g/t initial U)								
Kr-85	0.00E+00	5.47E-01	5.49E+00	1.07E+01	2.05E+01	3.75E+01	6.25E+01	7.77E+01
Sr-90	0.00E+00	1.17E+01	1.15E+02	2.24E+02	4.31E+02	7.96E+02	1.36E+03	1.74E+03
Ag-110m	0.00E+00	6.11E-06	1.21E-03	6.80E-03	3.98E-02	2.30E-01	1.28E+00	3.34E+00
Cs-137	0.00E+00	1.92E+01	1.91E+02	3.82E+02	7.60E+02	1.50E+03	2.95E+03	4.32E+03
Xe-135	0.00E+00	4.19E-01	4.19E-01	4.15E-01	4.02E-01	3.66E-01	2.74E-01	1.93E-01
Sm-149	0.00E+00	1.63E+00	3.97E+00	4.12E+00	4.29E+00	4.33E+00	3.43E+00	2.79E+00
Sm-151	0.00E+00	1.08E+00	8.67E+00	1.20E+01	1.43E+01	1.63E+01	1.83E+01	1.85E+01

Prism – ORNL 2

PRISM Results								
Burn-up (GWd/t)	0	0.5	5	10	20	40	80	120
k-inf	1.4622	1.404	1.3722	1.342	1.2791	1.1635	0.9744	0.8149
ρ^{238}	7.576E+00	7.88E+00	8.05E+00	8.12E+00	8.19E+00	7.99E+00	6.76E+00	5.50E+00
δ^{235}	1.338E-01	1.39E-01	1.42E-01	1.43E-01	1.43E-01	1.37E-01	1.13E-01	8.89E-02
δ^{238}	3.751E-03	3.92E-03	4.26E-03	4.66E-03	5.49E-03	7.66E-03	1.64E-02	5.34E-02
c/f^{235}	4.304E-01	4.48E-01	4.87E-01	5.30E-01	6.27E-01	8.79E-01	1.94E+00	6.64E+00
Actinide masses (g/t initial U)								
U-235	8.20E+04	8.13E+04	7.57E+04	6.99E+04	5.90E+04	4.07E+04	1.56E+04	3.73E+03
U-238	9.18E+05	9.18E+05	9.15E+05	9.13E+05	9.08E+05	8.97E+05	8.71E+05	8.38E+05
Pu-239	0.00E+00	1.42E+02	2.04E+03	3.80E+03	6.45E+03	9.39E+03	1.05E+04	9.36E+03
Pu-240	0.00E+00	5.32E-01	7.40E+01	2.64E+02	8.12E+02	1.99E+03	3.43E+03	3.73E+03
Pu-241	0.00E+00	4.31E-03	6.58E+00	4.71E+01	2.80E+02	1.20E+03	2.87E+03	3.00E+03
Pu-242	0.00E+00	5.49E-06	9.20E-02	1.39E+00	1.80E+01	1.86E+02	1.31E+03	3.03E+03
Am-241	0.00E+00	1.05E-06	1.71E-02	2.48E-01	2.97E+00	2.51E+01	1.02E+02	1.12E+02
Cm-244	0.00E+00	2.42E-12	7.10E-06	4.72E-04	2.85E-02	1.51E+00	6.24E+01	4.43E+02
Cm-245	0.00E+00	1.44E-15	2.12E-08	2.85E-06	3.47E-04	3.67E-02	2.77E+00	2.32E+01
Fission product masses (g/t initial U)								
Kr-85	0.00E+00	5.47E-01	5.49E+00	1.07E+01	2.05E+01	3.75E+01	6.25E+01	7.77E+01
Sr-90	0.00E+00	1.17E+01	1.15E+02	2.25E+02	4.31E+02	7.97E+02	1.36E+03	1.74E+03
Ag-110m	0.00E+00	6.11E-06	1.21E-03	6.81E-03	3.99E-02	2.30E-01	1.28E+00	3.35E+00
Cs-137	0.00E+00	1.92E+01	1.92E+02	3.82E+02	7.60E+02	1.51E+03	2.95E+03	4.32E+03
Xe-135	0.00E+00	4.19E-01	4.19E-01	4.15E-01	4.02E-01	3.66E-01	2.74E-01	1.93E-01
Sm-149	0.00E+00	1.63E+00	3.97E+00	4.11E+00	4.30E+00	4.33E+00	3.43E+00	2.78E+00
Sm-151	0.00E+00	1.08E+00	8.67E+00	1.20E+01	1.43E+01	1.62E+01	1.83E+01	1.85E+01

Prism – KAERI 1

PRISM Results								
Burn-up (GWd/t)	0	0.5	5	10	20	40	80	120
k-inf	1.46624	1.40841	1.37883	1.34945	1.28798	1.17329	0.983179	0.823023
ρ^{238}	7.43799825	7.750879528	7.884318333	7.957020599	8.008098197	7.802609649	6.586158741	5.278573326
δ^{235}	0.134549445	0.140372675	0.142586841	0.143493661	0.1433914	0.137535677	0.112728603	0.08785475
δ^{238}	0.004012861	0.004196798	0.004562534	0.00497365	0.005869089	0.008143307	0.017388367	0.057428873
c/f^{235}	0.41501365	0.43195779	0.467837188	0.508725963	0.598983227	0.833937411	1.831231994	6.323627747
Actinide masses (g/t initial U)								
U-235	82002.14743	81372.16233	75932.37795	70111.86344	59462.37619	41280.45841	15943.82724	3735.81164
U-238	917997.8526	917778.7273	915724.4281	913314.0503	908383.7321	897564.4228	871954.159	839824.9189
Pu-239	0	138.3995092	1967.114778	3701.025506	6299.303182	9211.203874	10319.15593	9191.756508
Pu-240	0	0.408504251	68.32325357	251.6050925	786.6048733	1962.595319	3449.031466	3773.610746
Pu-241	0	0.002793025	5.636175388	42.21721886	256.4395433	1132.713209	2759.882549	2904.505215
Pu-242	0	0	0.072067556	1.161089929	15.51352003	165.9873784	1225.81405	2949.973705
Am-241	0	0	0.014230268	0.221083684	2.712195416	23.54336489	98.12976597	106.807126
Cm-244	0	0	0	0.000338302	0.021210503	1.160952976	51.1849198	388.2625559
Cm-245	0	0	0	0	0.000218876	0.023682509	1.807125953	15.32753747
Fission product masses (g/t initial U)								
Kr-85	0	0.530666579	5.151908581	10.14303401	19.39751512	35.60511438	59.94171268	75.19009116
Sr-90	0	11.46162021	111.5018845	220.0483171	422.939127	784.7423087	1350.907179	1730.979928
Ag-110m	0	9.21641E-06	0.001435216	0.007950686	0.044602945	0.247871746	1.324913446	3.404384696
Cs-137	0	18.73630467	185.5552634	373.3894294	743.8206679	1475.534666	2902.040056	4280.063985
Xe-135	0	0.424144316	0.423322596	0.419433123	0.407326453	0.371937725	0.277987773	0.193369818
Sm-149	0	1.624923306	3.976575511	4.123115523	4.309645894	4.377026909	3.723485845	2.815485582
Sm-151	0	1.056621965	8.540680603	11.9617736	14.373247	16.46835831	18.35393111	18.33037514

Prism – KAERI 2

PRISM Results								
Burn-up (GWd/t)	**0**	**0.5**	**5**	**10**	**20**	**40**	**80**	**120**
k-inf	1.46626	1.40698	1.37732	1.34723	1.28559	1.16937	0.97612	0.81369
ρ^{238}	7.43529	7.75677	7.89586	7.96710	8.01549	7.81263	6.59948	5.29233
δ^{235}	0.13365	0.13965	0.14178	0.14271	0.14254	0.13674	0.11211	0.08728
δ^{238}	0.00382	0.00400	0.00434	0.00473	0.00557	0.00770	0.01643	0.05475
c/f^{235}	0.41318	0.43049	0.46650	0.50716	0.59690	0.83090	1.82859	6.37492
Actinide masses (g/t initial U)								
U-235	82000.5	81372.7	75934	70109.2	59458.6	41278.9	15903	3689.29
U-238	918000	917772	915722	913338	908410	897659	872086	839878
Pu-239	0	136.993	1956.59	3678.55	6254.88	9132.05	10224.5	9092.16
Pu-240	0	0.526166	69.5875	254.385	785.619	1936.89	3381.38	3699.69
Pu-241	0	0	6.03142	44.584	267.294	1161.15	2792.36	2929.38
Pu-242	0	0	0.0820594	1.28228	16.8833	177.166	1284.92	3063.14
Am-241	0	0	0	0.23622	2.83384	24.207	99.3493	107.084
Cm-244	0	0	0	0	0	1.27185	54.852	407.427
Cm-245	0	0	0	0	0	0	2.32591	19.5174
Fission product masses (g/t initial U)								
Kr-85	0	0.609487	5.37193	10.5262	20.0837	36.8336	62.0804	77.9613
Sr-90	0	11.4799	111.759	220.764	424.538	788.37	1361.36	1750.71
Ag-110m	0	0	0.00159	0.00880	0.04971	0.28163	1.57521	4.23283
Cs-137	0	18.7749	186.036	374.677	746.428	1479.97	2910.42	4293.03
Xe-135	0	0.420231	0.418781	0.41531	0.402554	0.365831	0.27463	0.193679
Sm-149	0	1.59475	3.86269	3.9428	3.79763	3.95124	3.50298	2.62074
Sm-151	0	1.05301	8.47556	11.9077	14.3156	16.4535	18.2601	18.1676

Prism – KAERI 3

PRISM Results								
Burn-up (GWd/t)	**0**	**0.5**	**5**	**10**	**20**	**40**	**80**	**120**
k-inf	1.46599	1.40648	1.37788	1.34655	1.28555	1.16932	0.97603	0.81246
ρ^{238}	7.42328	7.75978	7.87913	7.99405	8.00887	7.80774	6.57703	5.27244
δ^{235}	0.13359	0.13972	0.14185	0.14273	0.14251	0.13659	0.11177	0.08695
δ^{238}	0.00382	0.00401	0.00435	0.00474	0.00559	0.00771	0.01644	0.05521
c/f^{235}	0.41262	0.43060	0.46564	0.50870	0.59649	0.83064	1.82758	6.40792
Actinide masses (g/t initial U)								
U-235	82000.3	81372.7	75933.4	70108.3	59456.4	41271.4	15870.2	3659.6
U-238	918000	917773	915724	913344	908419	897680	872156	839951
Pu-239	0	137.072	1952.59	3674.01	6246.27	9118.44	10189.9	9059.7
Pu-240	0	0.526722	69.4932	254.17	784.957	1936.17	3381.9	3702.1
Pu-241	0	0	6.03018	44.5363	267.039	1160.04	2783.51	2917.9
Pu-242	0	0	0.0820273	1.28166	16.8574	176.979	1284.16	3062.3
Am-241	0	0	0.0155396	0.233666	2.8272	24.1642	98.941	106.3
Cm-244	0	0	0	0	0.0235347	1.27145	54.7777	407.6
Cm-245	0	0	0	0	0	0.0308008	2.3222	19.5
Fission product masses (g/t initial U)								
Kr-85	0	0.60915	5.42565	10.5816	20.2851	37.4870	63.6230	78.8757
Sr-90	0	11.5042	113.218	222.671	430.584	806.758	1405.49	1786.06
Ag-110m	0	4.74042E-06	0.00123	0.00650	0.03616	0.20715	1.28249	4.07799
Cs-137	0	18.7808	187.520	374.671	746.183	1478.83	2908.07	4294.00
Xe-135	0	0.41139	0.40583	0.39879	0.37925	0.32999	0.21484	0.12909
Sm-149	0	1.60045	3.84002	3.84312	3.56843	3.51933	2.75299	1.79888
Sm-151	0	1.04970	8.18694	11.0661	12.6718	13.6069	13.5482	12.6918

Prism – UNAM

PRISM Results								
Burn-up (GWd/t)	**0**	**0.5**	**5**	**10**	**20**	**40**	**80**	**120**
k-inf	1.46949	1.4101	1.384	1.35679	1.3017	1.19641	1.02955	0.87787
ρ^{238}								
δ^{235}								
δ^{238}	3.596E-03	3.771E-03	4.069E-03	4.414E-03	5.154E-03	6.996E-03	1.437E-02	
c/f^{235}	4.121E-01	4.288E-01	4.620E-01	5.006E-01	5.861E-01	8.063E-01	1.728E+00	
Actinide masses (g/t initial U)								
U-235	8.200E+04	8.137E+04	7.587E+04	7.005E+04	5.931E+04	4.091E+04	1.529E+04	3.094E+03
U-238	9.180E+05	9.178E+05	9.157E+05	9.133E+05	9.084E+05	8.977E+05	8.728E+05	8.414E+05
Pu-239	0.000E+00	1.378E+02	1.910E+03	3.561E+03	6.134E+03	8.943E+03	9.906E+03	8.408E+03
Pu-240	0.000E+00	5.538E-01	6.624E+01	2.399E+02	7.558E+02	1.901E+03	3.345E+03	3.627E+03
Pu-241	0.000E+00	1.538E-03	5.469E+00	4.020E+01	2.462E+02	1.092E+03	2.642E+03	2.632E+03
Pu-242	0.000E+00	0.000E+00	6.498E-03	1.088E+00	1.543E+01	1.688E+02	1.267E+03	3.133E+03
Am-241								
Cm-244								
Cm-245								
Fission product masses (g/t initial U)								
Kr-85								
Sr-90								
Ag-110m								
Cs-137	0.000E+00	1.883E+01	1.864E+02	3.721E+02	7.360E+02	1.450E+03	2.727E+03	3.873E+03
Xe-135	0.000E+00	4.190E-01	4.093E-01	4.031E-01	3.785E-01	3.352E-01	2.109E-01	1.179E-01
Sm-149	0.000E+00	1.574E+00	3.596E+00	3.638E+00	3.540E+00	3.309E+00	2.158E+00	1.253E+00
Sm-151	0.000E+00	1.057E+00	8.192E+00	1.127E+01	1.288E+01	1.408E+01	1.287E+01	1.088E+01

Prism – INL/PolyMtl

PRISM Results								
Burn-up (GWd/t)	0	0.5	5	10	20	40	80	120
k-inf	1.46409	1.40518	1.37496	1.34496	1.28207	1.16625	0.97542	0.81785
ρ^{238}	7.491	7.812	7.948	8.022	8.073	7.848	6.582	5.275
δ^{235}	0.1347	0.1406	0.1428	0.1437	0.1434	0.1371	0.1115	0.0868
δ^{238}	0.00390	0.00408	0.00445	0.00485	0.00575	0.00802	0.01732	0.05806
c/f^{235}	0.415	0.432	0.469	0.511	0.604	0.846	1.883	6.587
Actinide masses (g/t initial U)								
U-235	8.200E+04	8.136E+04	7.573E+04	6.982E+04	5.897E+04	4.058E+04	1.537E+04	3.552E+03
U-238	9.180E+05	9.177E+05	9.156E+05	9.132E+05	9.081E+05	8.971E+05	8.712E+05	8.390E+05
Pu-239	0.000E+00	1.416E+02	2.028E+03	3.777E+03	6.400E+03	9.292E+03	1.031E+04	9.168E+03
Pu-240	0.000E+00	5.580E-01	7.415E+01	2.635E+02	8.088E+02	1.977E+03	3.403E+03	3.700E+03
Pu-241	0.000E+00	4.630E-03	6.650E+00	4.733E+01	2.802E+02	1.199E+03	2.812E+03	2.914E+03
Pu-242	0.000E+00	5.985E-06	9.350E-02	1.400E+00	1.818E+01	1.881E+02	1.327E+03	3.092E+03
Am-241	0.000E+00	1.143E-06	1.737E-02	2.510E-01	2.996E+00	2.519E+01	1.008E+02	1.082E+02
Cm-244	0.000E+00	3.183E-12	6.858E-06	4.563E-04	2.727E-02	1.432E+00	5.920E+01	4.224E+02
Cm-245	0.000E+00	9.078E-16	2.036E-08	2.742E-06	3.309E-04	3.434E-02	2.461E+00	1.966E+01
Fission product masses (g/t initial U)								
Kr-85	0.000E+00	5.005E-01	4.875E+00	9.495E+00	1.807E+01	3.285E+01	5.422E+01	6.653E+01
Sr-90	0.000E+00	1.181E+01	1.155E+02	2.258E+02	4.332E+02	8.011E+02	1.371E+03	1.748E+03
Ag-110m	0.000E+00	9.833E-06	1.377E-03	7.103E-03	3.880E-02	2.172E-01	1.225E+00	3.315E+00
Cs-137	0.000E+00	1.928E+01	1.919E+02	3.828E+02	7.617E+02	1.507E+03	2.946E+03	4.314E+03
Xe-135	0.000E+00	4.204E-01	4.187E-01	4.145E-01	4.011E-01	3.626E-01	2.672E-01	1.858E-01
Sm-149	0.000E+00	1.655E+00	3.921E+00	4.012E+00	4.098E+00	4.003E+00	3.248E+00	2.423E+00
Sm-151	0.000E+00	1.087E+00	8.707E+00	1.204E+01	1.433E+01	1.617E+01	1.736E+01	1.685E+01